UNIVERSITÀ DEGLI STUDI DI MILANO

PhD IN PHARMACOLOGICAL BIOMOLECULAR SCIENCES,
EXPERIMENTAL AND CLINICAL
35TH CYCLE

DEPARTMENT OF PHARMACOLOGICAL AND BIOMOLECULAR SCIENCES

BRAZILIAN PROPOLIS: A MULTIFACETED NATURAL PRODUCT WITH HEALING PROPERTIES

–

A COMPREHENSIVE STUDY ON THE ABILITY TO IMPROVE CUTANEOUS WOUND HEALING THROUGH HIF-1 MODULATION

SSD BIO/14

Andrea MAGNAVACCA
R12574

TUTOR: Prof. Mario DELL'AGLI
COORDINATOR: Prof. Giuseppe Danilo NORATA

ACADEMIC YEAR 2021-2022

TABLE OF CONTENTS

ABSTRACT

Cutaneous wound healing is a dynamic multi-step process, encompassing the four cascading, partially overlapping, phases of haemostasis, inflammation, proliferation, and remodelling, that occurs in response to injuries and requires a well-orchestrated intervention of cellular and non-cellular elements to regain tissue integrity and restore local homeostasis. The ultimate outcome of skin wound healing is most commonly repair, a form of incomplete regeneration implying fibrosis and the formation of scars proportional to the duration and severity of inflammation. An early condition of mild hypoxia can trigger cell survival. Apart from being master regulators of cellular responses under hypoxia, hypoxia-inducible factors (HIFs) play a key role in upregulating the expression of several genes that enhance wound healing. Recent evidence suggests that also the non-hypoxic pharmacological stabilisation of HIF-1α can evoke a regenerative phenotype, claiming a role for HIFs in tissue regeneration. Natural products able to elicit multifaceted activities on the wound microenvironment, modulating the HIF-1 pathway while counteracting the deleterious drawbacks of inflammation, are promising candidates to enhance repair, and possibly regeneration, of skin injuries. Propolis is a resinous, polyphenol-rich, product elaborated by honeybees from plant exudates, and traditionally used for wound healing due to its renowned anti-microbial, antioxidant, anti-inflammatory, and immunomodulatory properties. The biological activities depend on the chemical composition and vary according to geographic origin, environmental conditions, and botanical sources from which bees gather the resins. Numerous chemotypes of propolis have been classified, including several Brazilian varieties. The aim of this study was a comprehensive *in vitro* evaluation of green and red Brazilian propolis biological activities on human keratinocytes (HaCaT) and dermal fibroblasts (HDF), exploring the ability to modulate the HIF-1 pathway to substantiate their application as innovative healing agents. The preliminary chemical characterisation conducted through HPLC-UV, GC-MS, and HPLC-HRMS determined the presence of artepillin C and drupanin in green propolis, and vestitol/neovestitol and medicarpin in red propolis as major components. The ability of propolis to impair NF-κB-driven transcription was evaluated upon TNF-α or IL-1β stimulation, showing a greater activity of red propolis (IC_{50}s < 10 μg/mL in HaCaT cells, IC_{50} = 23.6 μg/mL in HDF cells), prominent also on TNF-α-induced IL-8 secretion (IC_{50} = 11.89 μg/mL in HaCaT cells, IC_{50} = 5.89 μg/mL in HDF cells). On the other hand, red propolis proved able to induce the overexpression of *IL6* gene,

encoding a pleiotropic cytokine with pro-resolving functions, and enhance IL-6 release under pro-inflammatory stimulation. The investigation of HIF-1a stabilisation and nuclear translocation suggested the activity of both propolis in HaCaT cells, while only red propolis was active in HDF cells. These results have been confirmed through immunocytochemistry, western blot, and qPCR of the HIF-1 target gene *VEGFA*. Finally, a bioguided fractionation has been performed to better clarify the chemical species responsible for the biological activities. Following an initial fractionation by partitioning between immiscible solvents, the biological activity was screened in a HIF-1 reporter assay. Active fractions were further subfractioned by Sephadex LH-20 column chromatography, enabling to the qualification of the putative molecules responsible for HIF-1 stabilisation. Taken together, the results of this study contribute to elucidate the molecular mechanisms behind the promising activity of Brazilian propolis in wound healing, shedding light on the possible exploitation of these natural products in skin regeneration.

RIASSUNTO

La guarigione delle ferite cutanee consiste in un processo dinamico e multifasico, comprendente le quattro fasi parzialmente sovrapposte di emostasi, infiammazione, proliferazione e rimodellamento, che si innesca in risposta ad un danno e richiede l'intervento orchestrato di elementi cellulari e non per ristabilire l'integrità tissutale e l'omeostasi locale. L'esito finale della guarigione è di norma la riparazione, una forma di incompleta rigenerazione che implica fibrosi e la formazione di cicatrici la cui estensione è proporzionale alla durata e intensità della fase infiammatoria. Una precoce condizione di lieve ipossia è in grado di stimolare la sopravvivenza cellulare. Infatti, oltre ad essere i principali responsabili delle risposte cellulari in scarsità di ossigeno, i fattori indotti da ipossia (HIF) svolgono un ruolo preminente nell'espressione di numerosi geni coinvolti nel processo di guarigione. Recenti scoperte suggeriscono inoltre che la stabilizzazione farmacologica di HIF-1a, indipendentemente dalla presenza di ipossia, possa evocare un fenotipo rigenerativo, attribuendo a HIF un ruolo nella rigenerazione tissutale. Prodotti di origine naturale in grado svolgere molteplici attività sul microambiente della ferita, modulando la via di segnalazione di HIF-1 e al contempo contrastando i deleteri effetti dell'infiammazione, sono candidati promettenti per migliorare il riparo, e possibilmente la rigenerazione, delle ferite cutanee. La propoli è un prodotto resinoso, ricco in sostanze polifenoliche, elaborato dalle api a partire da essudati vegetali e tradizionalmente impiegato per la guarigione

delle ferite grazie alle note proprietà antimicrobiche, antiossidanti, antinfiammatorie e immunomodulatorie. Le attività biologiche dipendono dalla composizione chimica e variano a seconda di origine geografica, condizioni ambientali e fonti botaniche da cui le api bottinano le resine. Numerosi chemotipi di propoli sono stati classificati, incluse numerose varietà brasiliane. Lo scopo di questo studio è la valutazione *in vitro* delle attività biologiche delle propoli brasiliane verde e rossa in cheratinociti (HaCaT) e fibroblasti dermici (HDF) umani, esplorando la capacità di modulare la via di segnalazione di HIF-1 per corroborarne l'applicazione come innovativi agenti di guarigione. La preliminare caratterizzazione chimica condotta mediante HPLC-UV, GC-MS e HPLC-HRMS ha determinato la presenza di artepillina C e drupanina in propoli verde, e vestitolo/neovestitolo e medicarpina in propoli rossa, come componenti principali. L'abilità delle propoli di inibire la trascrizione guidata da NF-κB è stata valutata a seguito di stimolazione con TNF-a o IL-1β, mostrando una maggiore attività della propoli rossa (IC_{50} < 10 µg/mL in HaCaT, IC_{50} = 23.6 µg/mL in HDF), prominente anche sulla secrezione di IL-8 indotta da TNF-a (IC_{50} = 11.89 µg/mL in HaCaT, IC_{50} = 5.89 µg/mL in HDF). La propoli rossa si è dimostrata in grado di indurre l'espressione del gene *IL6*, codificante una citochina pleiotropica con funzioni risolventi, e la secrezione di IL-6 sotto stimolo pro-infiammatorio. L'investigazione della stabilizzazione e della traslocazione nucleare di HIF-1a suggerisce l'attività di entrambe le propoli in cheratinociti HaCaT, mentre solo la propoli rossa risulta attiva in fibroblasti HDF. Tali risultati sono stati confermati mediante immunocitochimica, western blot e qPCR del gene target di HIF-1 *VEGFA*. Infine, è stato condotto un frazionamento bioguidato per meglio definire le entità chimiche responsabili dell'attività biologica. A seguito dell'iniziale frazionamento mediante partizione fra solventi immiscibili, l'attività biologica è stata determinata in un saggio reporter per HIF-1. Le frazioni attive sono state ulteriormente subfrazionate mediante cromatografia su colonna di Sephadex LH-20, permettendo la qualificazione delle molecole ipoteticamente responsabili della stabilizzazione di HIF-1. Complessivamente, i risultati di questo studio contribuiscono a delucidare i meccanismi molecolari alla base della promettente attività delle propoli brasiliane nella guarigione delle ferite, gettando luce sul possibile utilizzo di questi prodotti naturali nella rigenerazione cutanea.

1 INTRODUCTION

1.1 INTEGUMENTARY SYSTEM

«**Integument** [from Latin *integumentum* «a covering», from *integĕre* «to cover over»]. The outermost body layer of an animal, characteristically comprising a layer of living cells – the epidermis – together with a superficial protective coat, which may be a secreted hardened cuticle, as in arthropods, or dead keratinised cells, as in vertebrates» (Hine, 2019). The integumentary system comprises the cutis or skin, and differently organised structures with specific functions, the skin appendages, or adnexa (hair follicles, nails, sebaceous and sweat glands).

Cutis is the outer tissue covering the body of vertebrate animals and in humans, with an average surface area of around 1.5-2 m^2, constitutes the largest organ of the integumentary system, with a weight equal to 17% of body weight. It is a resistant, elastic, and extensible membrane that seamlessly covers the body surface and protects the underlying tissues and the whole organism from insults of physical (mechanical, thermal, radiation damage) and chemical nature; it contributes to thermoregulation and hydrosaline homeostasis, preventing dehydration; it forms a barrier towards the penetration of microorganisms and participates in the excretion of catabolites and calciferol synthesis. In addition, cutis accommodates numerous nerve endings, configuring itself as an efficient sensory organ. The thickness of cutis is greater in male rather than female individuals and varies from 0.5 mm thick around eyelids to 4 mm thick on the palms and the soles of the feet.

Cutis is composed, from the outermost to the innermost layer, of a cornified stratified squamous epithelium of ectodermal origin, the epidermis, which lays on a layer of dense irregular connective tissue of mesodermal origin, the dermis or corium. The two layers are tightly connected through the interdigitation of connective fingerlike projections (dermal papillae) intertwined with epithelial extensions (rete pegs), aimed at increasing the useful surface area for metabolic exchange. The dermo-epidermal junction, a complex example of a basement membrane in which both epithelial and dermal elements participate, represents the surface of physical and functional separation

between the epidermis and the dermis. The dermis is in turn connected to the underlying layers through the hypodermis or subcutaneous tissue, determining the degree of skin mobility.

1.1.1 *STRUCTURE OF CUTIS – EPIDERMIS*

The epidermis [from late Latin *epidermis -ĭdis*, from ancient Greek ἐπιδερμίς -ίδος, a compound of ἐπί «on top of» and δέρμα «skin»] is the outermost of the two layers composing cutis. From a histological point of view, it is an example of stratified squamous epithelium, cornified, primarily consisting of keratinocytes but also including other cell types which colonise the epidermis over the embryonic development: melanocytes, responsible for the production of melanin; Langerhans cells, tissue-resident macrophages involved in skin immune processes; Merkel cells, traditionally considered to be sensory receptors. The epidermis represents the epithelial layer of cutis, therefore avascular, in which cells are nourished by metabolites diffusing from the superficial dermis. The cells even in the deepest layers are nourished almost exclusively by oxygen diffused from the surrounding atmosphere rather than by dermal blood capillaries (Stücker et al., 2002).

The epidermis, with a thickness between 50 μm and 1.5 mm, is composed of 4 or 5 layers that, from the inside to the surface, reflect the life cycle of keratinocytes, through differentiation stages which correspond to the evolution from living cells to thin squames, with a progressively increasing degree of cornification and a continuous turnover of around 6 weeks (Iizuka, 1994).

Five layers, different in morphology and function, may be distinguished from the inside out (**Fig. 1**).

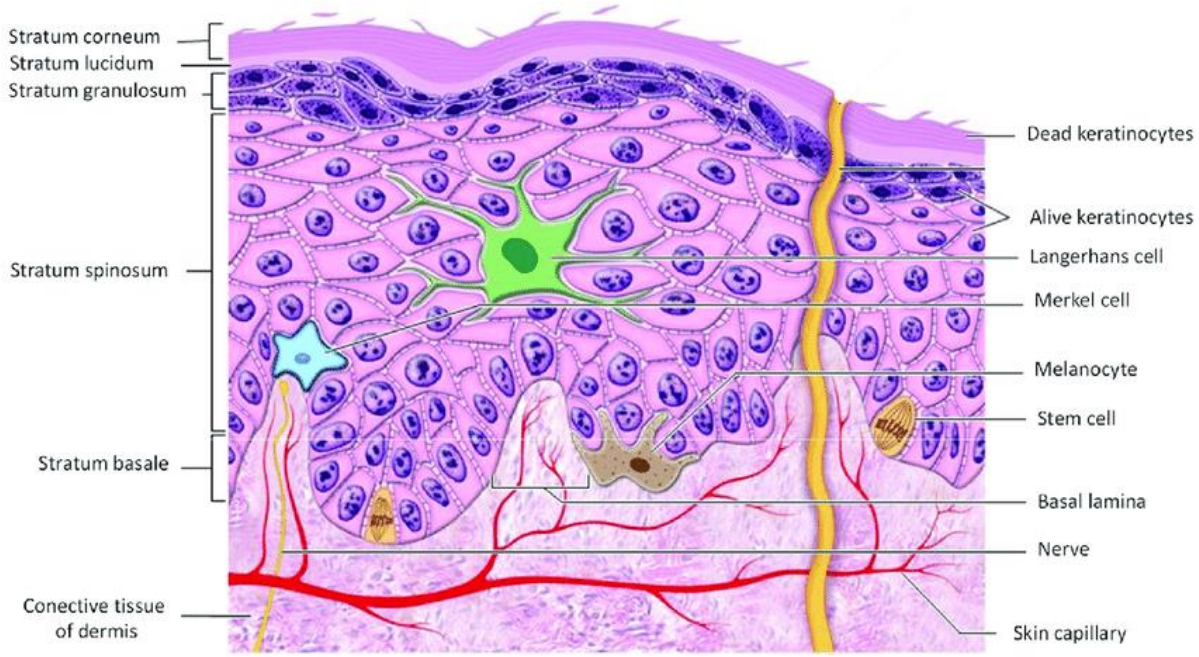

Figure 1 | *Cell types and organisation of the epidermal layers (Souto et al., 2022).*

❖ ***Stratum basale or germinativum*:** the basal layer is the deepest layer of the epidermis, composed of a continuous sheet of relatively undifferentiated prismatic cells, separated from the underlying dermal areolar connective tissue through the basement membrane. Although it is often described as composed of a single layer of cells, it may as well present two or three layers in correspondence with hairless skin and pathological conditions or hyperproliferative states (Rook, 2010). Basal cells are unipotent staminal cells that divide parallel to the surface by mitosis, originating a new staminal cell and a second cell that migrates towards the spinous layer above, to differentiate and replace the keratinocytes lost from more superficial layers. The cells of the basal layer are interconnected to each other through desmosomes and to the basement membrane through hemidesmosomes. The adhesion to the basal lamina is mediated by the integrin α6β4, whereas adhesions on the apical and lateral surfaces are mediated by the integrins α2β1 and α3β1 (Walko, Castañón, & Wiche, 2015). The cytoplasm includes melanin produced by the surrounding melanocytes and presents a cytoskeleton organised in

tonofilaments, oriented according to the major axis, consisting of keratin intermediate filaments with a thickness of 10 nm, which feature the keratin pair K5/K14.

❖ ***Stratum spinosum*:** the spinous layer is composed of 5-10 layers of polyhedral cells, flattened at more superficial levels. Whenever a staminal basal cell divides, a daughter cell migrates from the germinal layer to the spinous one, where the differentiation of keratinocytes begins. Nuclei are large and pale-staining; the cytoplasm begins to be acidophilic and cells are particularly active in the synthesis of fibrillar cytokeratins which constitute tonofilaments, a type of intermediate filaments. Tonofilaments, in turn, aggregate into tonofibrils that originate from and end in the *maculæ adhærentes*, desmosomes connecting adjacent cells and located on spiny protrusions which give cells the appearance of a horse chestnut fruit and the name to the layer. Tonofibrils, anchored to the cytoskeleton and extending crosswise from one extremity to the other reinforcing cell junctions, are peculiar structures of epithelia. It is believed that the protein filaggrin, synthesised as a large (>400 kDa) profilaggrin precursor and known to interact with keratin intermediate filaments, plays a pivotal role in aggregating tonofibrils (Sandilands, Sutherland, Irvine, & McLean, 2009). The migration of cells from the basal to the spinous layer implies the synthesis of a different keratin pair. Integrins, expressed on the entire cell membrane, belong to α2β1 and α3β1 subtypes. In addition, cells in the spinous layer synthesise proteins, such as involucrin, which accumulate on the cytoplasmic side of the plasma membrane, contributing to the formation of a cornified cellular envelope. Dark ellipsoidal membraned organelles called melanosomes, with dimensions of 0.3x0.7 μm, internally organised in dense concentric lamellae, are found in spinous cells. Melanosomes do not originate from keratinocytes themselves, to which are instead transferred at a later time, but are synthesised in melanocytes, dendritic cells interposed among the keratinocytes of the spinous layer. Besides melanosomes, also lamellar bodies, secretory organelles with a diameter of 0.2 μm containing a lipidic material responsible for the formation of an impermeable matrix after the release in the intercellular space, are found in spinous keratinocytes. Langerhans cells, which

represent the 3-8% of epidermal cells and play a pivotal role in eliciting the immune response towards pathogens and cancer cells, are present in the uppermost spinous layer.

❖ ***Stratum granulosum*:** the granular layer is located immediately above the spinous one and is composed of flattened keratinocytes engaged in the synthesis of high amounts of keratins and proteins constituting the keratohyalin. The granular layer is normally composed of 3-5 layers of cells, but their number may be increased in highly cornified regions such as palms and the soles of the feet. Nuclear structures are altered or absent, and the intense basophily, which allows the clear distinction of these cells, is due to the accumulation of keratohyalin in dense irregular granules without membrane, reflecting the process of cornification. Granules contain, among others, filaggrin and proteins rich in histidine and cysteine, the function of which is to aggregate tonofibrils and keratin filaments into thicker bundles. The synthesis rate of keratohyalin and cytokeratins is often influenced by environmental factors: skin friction causes an increment of the synthesis rate in the granular layer, causing a localised thickening of cutis and the formation of a protective callus. The granules may also contain loricrin, which together with the previously mentioned proteins contribute to the constitution of the cornified envelope. The granular layer represents the last vital layer. Keratinocytes flatten and become thinner, and the plasma membrane thickens, becoming less permeable. At the same time, granular cells lose nuclei and organelles becoming non-vital corneocytes (Ovaere, Lippens, Vandenabeele, & Declercq, 2009).

❖ ***Stratum lucidum*:** the translucent layer, thin and pale-staining, is easily visible by light microscopy only in areas of thick cutis, such as the palms of the hands and the soles of the feet, where it covers the granular layer. It is composed of 3-5 layers of clear, non-vital keratinocytes. The thickness of this layer is determined by the mitotic rate of the epidermal cells, while melanosomes influence its colour. Cells are flattened, without distinct borders, rich in glycogen, lipids, and eleidin, a sulphur-containing intermediate form of keratin, and are surrounded by an oily matrix resulting from the exocytosis of lamellar bodies accumulated during the migration through the spinous and granular

layers (Rook, 2010). The existence of the translucent layer is due to mechanical stress in those regions needing additional protection to grab objects, resist abrasions or shocks, and avoid wounding.

❖ ***Stratum corneum*:** the cornified layer is directly exposed to the external environment and is composed of 15-25 layers of cells, with a thickness between 10 and 40 µm, variable depending on the localisation. In the palms of the hands and the soles of the feet (sometimes in the knuckles of fingers, elbows, and knees) this layer derives from and is stabilised by the translucent layer, which allows cells to accumulate keratins and become cornified before migrating in a thicker and more cohesive layer. The cornified layer is composed of non-vital, extremely flattened, anucleated, completely cornified cellular elements, which gradually desquamate individually or in groups. They are arranged into two layers: the *stratum compactum*, deeper, in which corneodesmosomes operate in keeping together adjacent cells, and the *stratum disjunctum*, the uppermost and loosest layer in which junctional complexes are degraded by proteases, allowing superficial desquamation. The elements of the cornified layer are, occasionally, improperly called corneocytes. Extremely dehydrated, they are composed of 80% keratin filaments stabilised by disulphide bridges and cemented by filaggrin, immersed in a lipid matrix consisting of ceramides, cholesterol, and fatty acids. During the process of cornification, the plasma membrane thickens due to the development of a cornified envelope composed of involucrin, filaggrin, and loricrin, which covalently binds a layer of water-repellent ceramides, able to prevent evaporation. This complex surrounds cells in the cornified layer contributing to the barrier function of cutis (Ovaere et al., 2009). With their interweaved structure, together with the material present in the interlamellar spacing, corneocytes regulate the transepidermal passage of water and solutes. As previously mentioned, the intercellular space is occupied by a lipid extracellular matrix composed of fatty acids, cholesterol, sphingolipids, phospholipids, and glucosylceramides, secreted in the lamellar bodies of the spinous layer (Lampe et al., 1983). The cementing eleidin produced by deeper layers, sebum, and the aqueous component of sweat altogether form the

hydrolipidic film of skin, a slightly acidic protective emulsion with antibacterial functions. In this layer, several low molecular weight compounds, such as free amino acids deriving from the degradation of filaggrin and the hygroscopic salts of pyrrolidone carboxylic acid (PCA or pidolic acid), are also present and known as "natural moisturising factor" (NMF).

In the epidermis, various cell types can be distinguished.

❖ **Keratinocytes:** they represent the primary type of epidermal cells. Keratinocytes are cuboidal or prismatic elements, with their major axis perpendicular to the dermo-epidermal junction, displaying elongated nuclei and a highly basophilic cytoplasm, in which a variable amount of melanin may be found in the form of fine granulations gathered around the superficial nuclear apex. Along their life cycle, they undergo a series of modifications producing keratins, fibrous scleroproteins of increasing molecular weight, and are subject to an ordered sequence of transformations, from mitotically and metabolically active elements to inert cornified lamellae, originating diverse layers that result in the previously mentioned epidermal organisation.

Keratinocytes originate in the innermost germinal layer of the epidermis from unipotent stem cells and along their migration towards the surface undergo, starting from the spinous layer, the differentiation process of keratogenesis which leads them to death (in the granular layer) and the final transformation (in translucent and cornified layers) into corneocytes that will be shed off through desquamation. At a cellular level, the process of cornification is characterised by the succession of different stages.

- *Keratin synthesis*: keratins are structural proteins, insoluble in water and organic solvents, that protect the epithelial cells from damage and mechanical stress and represent the main substance composing the outermost layer of human cutis. Keratins forming the cornified layer, hairs, and nails belong to the family of a-keratins. The human genome possesses 54 functional genes coding for keratins, clustered on chromosomes 12 and 17, thus suggesting their evolutionary origin from a series of gene duplications (Moll, Divo, & Langbein, 2008). Keratin monomers build up in

bundles to form intermediate filaments, particularly abundant in keratinocytes of the cornified layer. Keratins and intermediate filaments are an integral part of the cytoskeleton, aimed at mechanically stabilising cells against physical stress through the interconnections between adjacent elements, mediated by desmosomes, and between cells and the basement membrane, mediated by hemidesmosomes.

- *Production of small proline-rich proteins (SPRRs)*: together with their transglutaminase activity, they contribute to the formation of the cornified envelope below the plasma membrane.
- *Terminal differentiation*: cell metabolism is gradually reduced, and cells are almost filled with keratins, incorporated in filaments longer and longer as cells become cornified.
- *Loss of nuclei and organelles in the final stage of cornification*: the nuclei and organelles disappear, metabolism stops, and cells undergo programmed death when fully cornified.

The differentiation of keratinocytes is partially promoted by a calcium gradient, gradually increasing from the basal layer to the granular layer, where it reaches a maximum, and gradually decreasing in the cornified layer. The concentration of calcium in the cornified layer is very low, due to the inability of relatively dehydrated cells to solvate ions. The calcium gradient orchestrates the differentiation of keratinocytes and is therefore considered a key driver of the generation of the epidermal layers (Proksch, Brandner, & Jensen, 2008). The increment of extracellular calcium levels induces an increment of intracellular free calcium (Hennings, Kruszewski, Yuspa, & Tucker, 1989), partly due to calcium released from intracellular stores (Pillai & Bikle, 1991) and partly due to calcium influx (Reiss, Lipsey, & Zhou, 1991) through calcium-activated chloride channels (Mauro, Pappone, & Isseroff, 1990) and voltage-independent cationic channels permeable to calcium (Mauro, Isseroff, Lasarow, & Pappone, 1993). In addition, it has been suggested that an extracellular calcium sensor (CaSR) might contribute to the increment of intracellular calcium levels (Tu, Oda, & Bikle, 1999).

The process of cornification involves the continuous replacement of the epidermal elements, shed through desquamation, by basal layer cells. When basal cells divide, they originate a cell that remains connected to the basal lamina and a second cell that migrates towards the surface being subjected to the transformations previously described. The balance among the processes of proliferation, differentiation, and desquamation makes it possible that the overall number of cells and epidermal thickness remain relatively constant so that in healthy skin the generation of new keratinocytes counterbalances the shedding by desquamation of corneocytes. Factors and mechanisms which regulate the timing of complete epidermal renovation, spanning from a few days in case of psoriasis up to 39-56 days in normal skin (Iizuka, 1994), are varied and complex. The migration from the basal to the granular layer takes around two weeks, while the time needed for the transition from the granular layer to the cornified one until the final desquamation is of about four weeks. Epidermal homeostasis is regulated by the interaction of numerous factors, both intrinsic and extrinsic, such as growth factors, cytokines, integrins, the balance between proteases and inhibiting factors, calcium levels, vitamin D, polyamines (Proksch et al., 2008), hormones (oestrogens, progesterone, adrenalin), prostaglandins, and retinoids.

1.1.2 *STRUCTURE OF CUTIS – DERMIS*

The dermis [from Ancient Greek δέρμα -ατος «skin»], or corium, is the layer of cutis situated below the epidermis. Of mesodermal origin, it is composed of a layer of dense irregular connective tissue, highly vascularised (unlike the epidermis), and innervated. It has an average thickness of 1-2 mm, variable depending on the body region: thicker at the level of the palms and the soles of the feet (3 mm), extremely thin in correspondence to the cutis of the eyelids, scrotum, and foreskin (0.5 mm). In depth, it is seamlessly continued in the loose connective tissue of the hypodermis. The dermis is connected to the epidermis through the dermo-epidermal junction, which, thanks to an elevated number of anchoring type VII collagen fibres, enables a tight cohesion between the two layers. Moreover, due to the presence of numerous collagen fibres, it gives

cutis its characteristics of stiffness and robustness, forming an elastic layer resistant to traction, but not to cutting.

Here are located skin appendages (sweat glands, hair follicles with hairs and related arrector pili, sebaceous glands), blood and lymph vessels, and nerve endings. From the histological point of view, the dermis is a connective tissue and as such hosts, mainly in the papillary layer, fibroblasts, macrophages, and mast cells as well as non-resident elements from the bloodstream such as leukocytes and plasma cells, especially during inflammatory processes. Mast cells are abundant and widely diffused throughout the dermis, more frequent around blood vessels of the subpapillary plexi.

The ground substance might be defined as an amorphous gel-like multiphasic colloidal system, composed of an aqueous dispersing phase, in which electrolytes are dissolved, and a dispersed phase, formed by enzymes, glycoproteins, and proteoglycans, sulphated or not, which give characteristics of viscosity and density. Hyaluronic acid is the most represented non-sulphated proteoglycan, while dermatan sulphate is the most abundant sulphated proteoglycan, usually associated with collagen fibres. Small quantities of chondroitin sulphate and heparan sulphate are also present. The sulphated components are responsible for tissue stiffness. Proteoglycans, thanks to their viscosity, contribute to supporting other dermal structures, the saline balance, and the regulation of the water content of the connective matrix; suffice it to say that a single molecule can bind 1000 times its volume in water.

The fibrous component is mainly represented by:

- *Collagen*: a fibrous glycoprotein synthesised by fibroblasts, the principal dermal cellular elements. Collagen fibres are organised in intimately intertwined bundles, highly resistant to tractions.
- *Elastin*: a fibrous glycoprotein synthesised by fibroblasts, showing, unlike collagen, remarkable elasticity. Elastin fibres are less abundant and thinner than collagen fibres and are not organised in bundles, but rather are branched and cross-linked. Elastin fibres are intertwined with collagen fibres and give elasticity to the entire cutis.

- *Striated muscle fibres*: found in the face, where facial mimic muscles insert on the dermis.
- *Smooth muscle cells*: found in the areola or belonging to the arrector pili in hair follicles.

This type of structural organisation gives the dermal connective tissue excellent properties of robustness, resistance, cushioning, and elasticity.

The dermis is composed of two layers, the one continuing into the other without a clear distinction.

❖ **Papillary dermis**: the layer directly beneath the epidermis and in contact with it. It is composed of loose areolar connective tissue, poor in elastic fibres and rich in blood capillaries and nerve endings, sometimes in the complex form of Meissner's corpuscles of fingertips. More cellular than the underlying reticular dermis, it forms conical or laminar extensions, the dermal papillae, interdigitated with the epidermis. The dermal papillae are generally not very pronounced, except for hairless regions, in which are numerous, large, and parallel to each other, following the pattern of superficial ridges.

❖ **Reticular dermis**: the innermost layer, extending from the papillary dermis to the hypodermis, composed of numerous robust intertwined bundles of collagen fibres parallel to the skin surface. Within the reticular region, there are abundant blood vessels and nerve endings. The orientation of bundles varies from region to region and determines lines of tension (Langer's lines), along which extensibility and resistance are at a minimum, relevant to surgical incisions and wound healing. The reticular layer is rich in elastic fibres, abundant near pilosebaceous follicles and gland adenomeres (periadnexal dermis). The deep connective bundles of the reticular layer form the large meshes of a net in which adipose lobules and gland glomeruli are located. In depth, the reticular layer is anchored, more or less tightly, to the superficial fascia through loose hypodermal connective tissue.

Different cell types are found in the dermis.

❖ **Fibroblasts**: the main dermal elements, derived from mesenchymal cells of the embryonic mesoderm, primarily committed to the synthesis and deposition of extracellular matrix components. Currently, it is known that staminal elements persist also in the adult as precursors of fibroblasts and other connective cell types (osteoblasts, adipocytes, and chondrocytes). Fibroblasts are located in the dermis and hypodermis along collagen fibre bundles and appear as spindle-like or branched elements with an elongated nucleus and two or more nucleoli. Those not actively engaged in the synthesis of fibres and amorphous matrix components are called fibrocytes. During wound healing, they become activated and proliferate to newly synthesise significant amounts of matrix components. In this state, they increase in volume and show a basophilic cytoplasm characterised by rough endoplasmic reticulum proliferation and a large number of secretory vesicles.

❖ **Macrophages**: deriving from circulating monocytes, they play a fundamental role in the defence against microorganisms and foreign bodies. Their duties include the secretion of cytokines, antigen presentation, and phagocytosis.

❖ **Adipocytes**: adipocytes are static connective cells of mesenchymal derivation, which represent the morpho-functional unit of the adipose tissue and may be divided into two types. Unilocular adipocytes contain a single lipid drop, composed of triglycerides, showing a "signet ring" morphology in processed tissue. Multilocular adipocytes are smaller and contain several lipid droplets, mitochondria, and dark granules. Adipocytes do not have phagocytic activity and their mitotic activity is extremely reduced.

Other cellular elements include plasma cells, which are an expression of defensive processes against microorganisms or foreign antigens; mast cells, morphologically similar to basophils, which release leukotrienes and are characterised by granules of heparin and histamine; other blood cells such as neutrophils, eosinophils, and lymphocytes, which take part in defensive, immune, and allergic processes.

1.2 CUTANEOUS WOUNDS AND WOUND HEALING

In pathology, wounds are acute injuries that damage the epidermis and may involve the puncture or laceration of skin (open wounds) or a contusion (closed wound). Vulnology is the branch of medicine that deals with the prevention, care, and treatment of wounds.

Open wounds are classified, according to the object that caused the injury, into incisions, lacerations (when margins are irregular and caused by a blunt trauma), abrasions or grazes (superficial wounds in which the epidermis is scraped off), avulsions (traumatic detachment of body structures or skin), puncture wounds, penetration wounds, and critical wounds (such as extensive burns). Closed wounds include haematomas (petechiae, purpura, and ecchymosis, if originating from internal blood vessel pathology; contusions or bruises, if originating from an external source of trauma) and crush injuries.

According to the level of bacterial contamination, wounds are classified as clean (if made under sterile conditions and likely to heal without complications), contaminated (usually resulting from accidental injuries and characterised by the presence of pathogenic organisms and foreign bodies), infected (if pathogens are multiplying with clinical signs of infection), colonised (chronically infected wounds difficult to heal).

1.2.1 *HEALING PROCESS*

Wound healing may be described as a sequence of discrete events, which encompass the whole process of post-traumatic tissue repair. In intact skin, the epidermis and dermis establish a protective barrier towards the external environment. However, when such a barrier falls short, a well-orchestrated cascade of biochemical and cellular events is initiated to repair the injury (Rieger, Zhao, Martin, Abe, & Lisse, 2015).

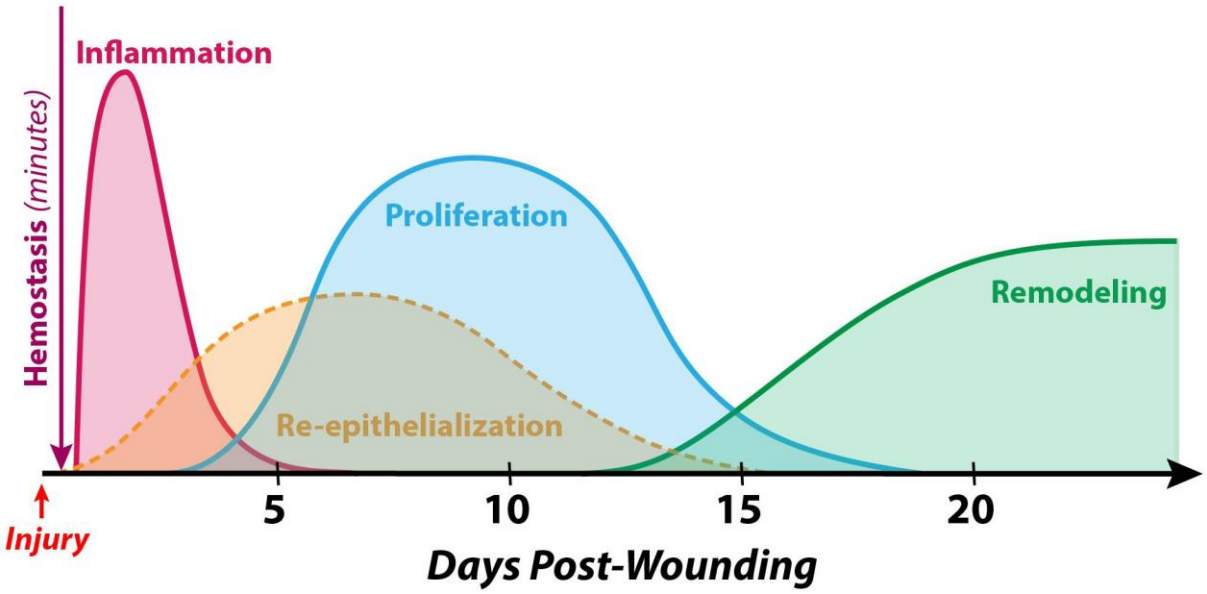

Figure 2 | ***Stages of wound healing*** *Normal wound healing takes place in four overlapping stages and their time boundaries are blurred depending on wound dimensions and healing conditions (desJardins-Park, Mascharak, Chinta, Wan, & Longaker, 2019).*

The healing process is divided into predictable, partially overlapping, phases (**Fig. 2**).

❖ **Haemostasis:** it is the local response to the haemorrhage caused by the rupture of blood vessels. Within a few minutes following the endothelial damage, components of the underlying extracellular matrix are exposed, and circulating thrombocytes begin to adhere taking an amorphous appearance and becoming activated with the release of pro-aggregative mediators. The tissue injury triggers the intrinsic and extrinsic pathways of coagulation, which result in the activation of fibrinogen and the formation of a fibrin clot that incorporates corpuscular elements of blood. The fibrin clot, which loosely occupies the injured site and may be displaced by small traumas, has the function of mechanically staunching the blood flow from ruptured vessels, slowing or preventing further bleeding (Versteeg, Heemskerk, Levi, & Reitsma, 2013). Moreover, it represents the main structural support of the wound until collagen deposition (Midwood, Williams, & Schwarzbauer, 2004).

According to some authors, instead of being a stage per se, haemostasis might be considered part of the inflammatory phase (Stadelmann, Digenis, & Tobin, 1998).

❖ **Inflammatory phase:** it is an innate immune response, non-specific but fundamental, which thanks to leukocyte phagocytic activity removes dead tissue, bacteria, and other pathogens from the injury. It normally resolves within one or two weeks, when infiltrated leukocytes regress to pre-inflammatory numbers and phenotypes (Nagaraja, Wallqvist, Reifman, & Mitrophanov, 2014). As soon as haemostasis begins, thrombocytes and leukocytes release soluble mediators, such as cytokines and chemokines which establish a chemotactic gradient to sustain the inflammatory process, in addition to molecules that initiate the proliferative phase. Among these mediators, the interleukins IL-1a, IL-1β, IL-6, IL-8, TNF-a (tumour necrosis factor a), PDGF (platelet-derived growth factor), and TGF-β (transforming growth factor β) can be counted. More specifically, PDGF plays an important role in triggering the chemotaxis of neutrophils, monocytes, and fibroblasts, while TGF-β stimulates the secretion of cytokines by macrophages and potentiates the chemotaxis of fibroblasts (Diegelmann & Evans, 2004). The inflammatory phase encompasses many important stages.

- *Coagulation*: thrombocytes, the most abundant elements immediately after the injury, are stimulated to begin the secretion in the bloodstream of cytokines, growth factors, and pro-inflammatory mediators such as serotonin, bradykinin, prostaglandins, prostacyclin, thromboxane, and histamine (Stadelmann et al., 1998), which induce vasodilation and increase vascular permeability.
- *Vasoconstriction and vasodilation*: following the rupture of blood vessels, damaged cells release thromboxane and prostaglandins which induce vasospasm to prevent the haemorrhage and localise corpuscular elements within the lesion site. Vasoconstriction lasts 5-10 minutes and is followed by vasodilation, resulting from the action of factors released by platelets and mast cells, in particular histamine, with a peak around 20 minutes following the injury. Histamine increases vascular permeability, inducing tissue oedema caused by the extravasation of proteins that raise interstitial osmolarity. In addition, the increased vascular permeability favours the

recruitment of circulating inflammatory cells, such as leukocytes, in the wound (Stadelmann et al., 1998).

- *Neutrophil recruitment*: within an hour from the lesion, polymorphonuclear leukocytes reach the injury, becoming the dominant cell type during the first two days, with a peak on the second day. Attracted by fibronectin, growth factors, and other substances such as kinins, neutrophils phagocytise debris and kill bacteria with free radicals generated by myeloperoxidase (Goldman, 2004) and by the "respiratory burst" (Greenhalgh, 1998). In addition, they debride the wound by secreting proteases which break down the damaged tissue. These include non-specific proteases, such as serin-proteases, or highly specialised proteases such as matrix metalloproteases (MMP-2 e MMP-9), which degrade collagen and its fragments (Xue & Jackson, 2015). Neutrophils have an average half-life of two days in the injury; once they have completed their tasks, they undergo apoptosis and are engulfed by macrophages (Martin & Leibovich, 2005).
- *Macrophage recruitment*: the role of macrophages is to engulf worn-out immune cells, bacteria, and tissue debris, degraded through the release of proteases (Deodhar & Rana, 1997). Macrophages are essential for wound healing and also play a role in regeneration (Newton, Watson, Wolowacz, & Wood, 2004). In a hypoxic environment, as wounds are, they release factors that stimulate angiogenesis (Greenhalgh, 1998), re-epithelisation, the formation of the granulation tissue, and the deposition of new extracellular matrix, advancing the healing process towards the next stages. Circulating monocytes, attracted by growth factors released by thrombocytes and other cells, enter the area crossing the wall of blood vessels and their number reaches a peak around 1-1.5 days (Santoro & Gaudino, 2005). Once in the wound, monocytes differentiate into macrophages, replacing polymorphonuclears as predominant cells within the first two days and further release growth factors, chemokines, and cytokines such as TGF-a, TGF-β, bFGF (basic fibroblast growth factor), PDGF, and VEGF (vascular endothelial growth factor), especially during the third

and fourth days to amplify and then resolve the inflammation, recruiting endothelial cells and fibroblasts implicated in the proliferative phase (Zhao, Liang, Clarke, Jackson, & Xue, 2016).

- *End of the inflammatory phase*: the secretion of pro-inflammatory factors declines; the ones present are degraded and the number of neutrophils and macrophages in the lesion site is reduced. These changes indicate that the inflammatory phase is going to finish, whereas proliferation is proceeding. When healing is not obtained by regeneration, the final event is the contraction of the scar, which might conduct to structural imperfections, deformity, and impaired flexibility (Hinz, 2006), and macrophages can persist until this stage. Some *in vitro* evidence obtained with the dermal equivalent model suggests that the presence of macrophages delays wound contraction, their disappearance being thus essential to allow the subsequent phases (Newton et al., 2004).

Since inflammation plays a pivotal role in contrasting infections, removing debris, and triggering the proliferative phase, it is a necessary step of wound healing and generally lasts until foreign bodies and tissue debris are present in the injury. If the host immune system is weakened and unable to remove debris, necrotic tissue, and microbic biofilm, such factors can contribute to the persistence of the inflammatory phase with consequent tissue damage, potentially leading to excessive scarring and chronicity (Midwood et al., 2004). For this reason, limiting inflammation is a common therapeutic aim.

❖ **Proliferative phase:** two or three days after the injury, fibroblasts begin to penetrate the lesion site determining the beginning of the proliferative phase, before the inflammatory phase is concluded. During the proliferative phase, cell activity is predominant upon the stimulation of cytokines such as EGF (epidermal growth factor), VEGF, and TGF-β (Werner & Grose, 2003). Like other phases of the healing process, the stages of the proliferative phase do not take place in serial succession but are partially overlapped.

- *Angiogenesis*: the process of angiogenesis, or neovascularisation, is concomitant with the proliferation of fibroblasts, at the moment in which

endothelial cells migrate to the injured site. The activities of fibroblasts and epithelial cells demand oxygen and nutrients, for this reason, angiogenesis is essential for concomitant cellular events. Angiogenesis takes place in overlapping stages in response to inflammation.

1. *Latency*: during haemostasis and inflammation, vasodilation and an increased vascular permeability enhance leukocyte migration, phagocytic activity, and wound debridement. The tissue oedema favours the subsequent angiogenesis, loosening the tangles of the extracellular collagen matrix.
2. *Endothelial activation*: when macrophages evolve from the pro-inflammatory phenotype to the reparative one, the secretion of chemotactic and growth factors to attract the endothelial cells nearby begins. Activated endothelial cells show peculiarly enlarged nucleoles and loosen intercellular junctions, normally extremely tight.
3. *Degradation of the endothelial basement membrane*: macrophages, mast cells, and endothelial cells as well release proteases (zinc-dependent metalloproteases, MMP-2 and MMP-9 among others) to break down the vascular basement membrane.
4. *Neovascularisation*: after the degradation of the basement membrane, staminal endothelial cells from undamaged capillaries develop pseudopodia and migrate through the matrix towards the wound, attracted by the fibronectin of the clot and by angiogenic factors released under hypoxia, building new vessels during the process (Greenhalgh, 1998). To migrate, endothelial cells need to secrete collagenase and plasminogen activator, to break down the clot and the extracellular matrix (Stadelmann et al., 1998). The sprouting of primitive capillaries is favoured by the hypoxic environment and acidosis, which characterise the wound, through the activation of the transcription factor HIF-1 (hypoxia-inducible factor 1) which transactivates angiogenic genes such as *VEGF* e *GLUT1*. When macrophages and other growth factor-releasing cells are no more in a hypoxic, lactic acid-rich environment, the production of angiogenic

factors is stopped (Greenhalgh, 1998). Once the tissue is adequately perfused, migration and proliferation of endothelial cells are reduced, and unnecessary vessels undergo apoptosis.

5. *Vascular maturation*: the vascular endothelium matures with the deposition of a new endothelial extracellular matrix, followed by the formation of a basement membrane and a layer of pericytes. The tissue in which angiogenesis takes place is typically erythematous due to the presence of newly formed capillaries.

- *Fibroplasia:* simultaneously with angiogenesis, fibroblasts begin to accumulate starting from 2-5 days after the injury, when the inflammatory phase is declining, thus forming the granulation tissue. Within the first week, fibroblasts become predominant and are primarily involved in the deposition of collagen matrix in the wound site (Stadelmann et al., 1998). It is believed that fibroblasts migrate from the undamaged neighbouring tissue; however, recent evidence suggests that some elements might derive from precursors or circulating adult staminal cells (Song et al., 2010). The process of fibroplasia can be exemplified in analogy with angiogenesis, considering fibroblasts instead of endothelial cells. In the stage of initial latency, the wound undergoes exudation of plasma, inflammatory decontamination, and debris removal. Oedema increases tissue accessibility, favouring the migration of fibroblasts. When inflammation progresses towards resolution, macrophages and mast cells release chemotactic and growth factors to activate fibroblasts in the neighbouring tissue, which lose connections with the surrounding cells and matrix. Then, phagocytes release proteases that degrade the matrix, setting activated fibroblasts free to migrate towards the injury and proliferate. Initially, fibroblasts take advantage of cross-linked fibrin fibres, synthesised at the end of the inflammatory phase, to migrate towards the lesion, and then they use the collagen deposited in the wound bed. Fibroplasia stops around the second and fourth week.
- *Formation of the granulation tissue*: a rudimental granulation tissue begins to form during the inflammatory phase, 2-5 days after the injury, and develops

until the wound bed is covered. It is composed of new blood vessels, inflammatory cells, endothelial cells, myofibroblasts, and fibroblasts which secrete components of a provisional extracellular matrix, including fibronectin, collagen, glycosaminoglycans, elastin, glycoprotein, and proteoglycans. The main components, fibronectin and hyaluronans, make the matrix hydrated and favour cell migration. This provisional matrix will be replaced by a matrix like that found in intact tissues. Growth factors (PDGF, TGF-β) and fibronectin stimulate proliferation, migration to the wound bed, and production of extracellular matrix by fibroblasts, which release also attracting factors for epithelial cells. The substantial difference between vascular neoformation and fibroblast proliferation is that while the first is mainly triggered by hypoxia, on the other hand, hypoxia can contribute also to proliferation and growth factor release but when excessive inhibits cell growth and the deposition of matrix components, leading to fibrosis and scarring.

- *Collagen deposition*: one of the principal tasks of fibroblasts is collagen deposition, which increases wound resistance. Until its deposition, it is the fibrin-fibronectin clot that keeps the wound closed; however, it does not give strength to the lesion (Greenhalgh, 1998). In addition, the collagen matrix laid down by fibroblasts is a site of adhesion, growth, and differentiation for cells involved in inflammation, angiogenesis, and reconstruction of the connective tissue (Ruszczak, 2003). Type III collagen and fibronectin, the principal tensile components until the later maturation stages in which they are substituted by the more robust type I collagen, begin to be significantly produced between ten hours and three days after the injury, depending on the wound size. Collagen deposition reaches its peak between one and three weeks. Although fibroblasts synthesise new collagen, collagenase and other factors are active in its degradation. Immediately after the injury, synthesis exceeds degradation and collagen levels in the wound increase; later, synthesis and degradation become equal, so that there is no net increment of collagen quantities (Greenhalgh, 1998). When such balance is obtained, the late phase of maturation

begins. Granulation gradually stops and the number of fibroblasts is reduced by apoptosis, turning the granulation tissue from a highly cellular environment into a substance mainly composed of collagen (Stadelmann et al., 1998).

- *Epithelisation*: the formation of the granulation tissue in an open wound enables the re-epithelisation phase, that is the migration of epithelial cells through the newly formed tissue to re-establish a barrier between the wound and the external environment. If the basement membrane is undamaged, epithelial cells are replaced within three days by division and migration from the basal layer, as it happens in intact cutis. Otherwise, re-epithelisation can only take place from wound margins and adnexa, which are layered with live keratinocytes. If the wound is deep, also adnexa may be damaged, and migration can only start from the margins. The migration of keratinocytes on the wound bed is stimulated by the loss of contact inhibition and mediators such as nitric oxide (Witte & Barbul, 2002), and begins starting a few hours after the injury. Epithelial cells need vital tissue through which migrate, so if the wound is deep, it must be previously filled with granulation tissue and the onset of migration might be delayed up to one day. During the re-epithelisation phase, cells surrounding the wound proliferate in the 2-3 days following the injury at a rate 17 times higher than normal tissues (Deodhar & Rana, 1997), to provide a wide number of elements ready to migrate. As long as the wound area is not completely covered, the only epithelial cells to proliferate are the ones at wound edges (Bartkova, Grøn, Dabelsteen, & Bartek, 2003). Before starting to migrate, keratinocytes detach from the basement membrane and change shape becoming elongated and flattened and originating cellular projections like lamellipodia and filopodia. In addition, keratinocytes must disrupt desmosomes and hemidesmosomes, which normally anchor cytoskeleton intermediate filaments to other cells and the extracellular matrix. Integrins, anchoring glycoproteins to the basement membrane, are relocated on actin filaments to allow the connection of pseudopodia to the matrix during migration (Santoro & Gaudino, 2005). As well as fibroblasts, also

keratinocytes exploit the fibrin synthesised during the inflammation as an attachment site (Deodhar & Rana, 1997). Epithelial cells migrate advancing as a layer. The first cells to anchor to the basement membrane will originate the basal layer, then they continue to migrate through the wound bed pulling the epithelial cells above (Bartkova et al., 2003). The more rapid the migration is, the less will be the scarring. Migrating keratinocytes can phagocytise debris, such as necrotic tissue and bacteria, which could obtrude their passage. To make their way into the tissue, keratinocytes must dissolve the clot and the damaged matrix, especially on the frontline, secreting tissue plasminogen activator. Migration is facilitated by a humid microenvironment since a dry one causes the formation of an extended and resistant clot (Deodhar & Rana, 1997). Keratinocytes continue to migrate through the wound until cells from both sides meet in the middle, then contact inhibition causes the arrest of migration, and cells secrete components of the new basement membrane, revert the changes needed for migration, reform desmosomes and hemidesmosomes and connect to the basement membrane (Santoro & Gaudino, 2005). Basal cells begin to divide and differentiate like in intact cutis and re-establish the layers of re-epithelised cutis.

- *Contraction*: it is a fundamental phase of healing by repair, but if prolonged can lead to loss of function (Hinz, 2006), thus there is much interest in elucidating the biology of wound contraction. Contraction starts approximately a week after the injury when fibroblasts differentiate into myofibroblasts (Eichler & Carlson, 2006). In full-thick wounds, contraction reaches a peak between five and fifteen days after the injury, can last several weeks and continues after the complete re-epithelisation of the wound (Stadelmann et al., 1998). A large wound may become 40-80% smaller after contraction. Usually, contraction does not take place symmetrically, but wounds show a principal contraction axis which enables cell organisation and alignment with collagen (Eichler & Carlson, 2006). At first, the process does not involve myofibroblasts, then, under the stimulus of mechanical tension and cytokine such as TGF-β, fibroblasts differentiate

into myofibroblasts, similar to smooth muscle cells (Mirastschijski, Haaksma, Tomasek, & Agren, 2004), which express the same isoform of a-actin found in smooth muscles (Hinz, 2006). Myofibroblasts are attracted by fibronectin and growth factors and migrate along fibrin within the provisional matrix to reach wound edges (Deodhar & Rana, 1997). At wound edges, they form connections with the matrix and with each other through desmosomes, while the actin of myofibroblasts is connected by means of the plasma membrane to extracellular matrix molecules such as fibronectin and collagen, a complex called fibronexus (Mirastschijski et al., 2004). These adhesions allow myofibroblasts to drag the matrix during contraction, reducing the wound size (Hinz, 2006), more rapidly than in the initial myofibroblast-independent part of the process (Mirastschijski et al., 2004). When myofibroblasts contract actin filaments and bring edges closer together, fibroblasts deposit collagen to strengthen the wound (Stadelmann et al., 1998). The degradation of the provisional matrix causes a reduction of hyaluronic acid in favour of chondroitin sulphate, which gradually arrests fibroblast migration and proliferation. These events mark the beginning of the maturation phase.

❖ **Maturation and remodelling**: during this phase, collagen is realigned along tension lines and unnecessary cells are removed through apoptosis. When the rates of collagen production and degradation are equal, the maturation phase begins (Greenhalgh, 1998). During maturation, type III collagen, prevalent in proliferation, is replaced by type I collagen and the fibres, initially non-organised, are re-arranged and cross-linked. The beginning of the maturation phase may vary, depending on the wound dimensions and whether the wound was closed or left open, from three days to three weeks. Maturation can last up to one year or even more. With the progression of this phase, the tensile strength of the wound increases. Collagen reaches 20% of its strength within three weeks, increasing to 80% within the twelfth week. The maximum strength of the scar is 80% of intact skin (Morton & Phillips, 2016). Since cellular activity in the wound is reduced, when the unnecessary vessels are removed through apoptosis the scar loses its rosy aspect (Greenhalgh, 1998).

Not only is the healing process complex but also delicate and susceptible to interruption or failure with the establishment of non-healing chronic wounds. The healing process comprises highly regulated cellular, humoral, and molecular events potentially flawlessly orchestrated to achieve perfect regeneration. However, in adults, wounds undergo a reparative process that does not lead to regeneration but scarring and sometimes chronification (Reinke & Sorg, 2012). Normally, the phases of healing follow a predictable sequence, if this does not happen healing may proceed improperly and generate a chronic wound (Midwood et al., 2004) or a pathological scar, like a keloid (O'Leary, Wood, & Guillou, 2002).

Multifactorial stimuli can generate and amplify a hostile microenvironment in which the delicate balance existing in acute injuries between pro-inflammatory cytokines, chemokines, proteases, and their inhibitors is perturbed so that chronic wounds show a no more definite and coordinated healing process and cannot reach a satisfying anatomic and functional outcome over a period quantified in three months (Nunan, Harding, & Martin, 2014). Being unable to progress through the stages of healing, wounds persist in a state of self-perpetuating inflammation and are untreatable despite adequate therapy. Multiple factors can delay wound healing, in particular tissue hypoxia, repeated traumas, and bacterial contamination, when combined with a defective cellular and systemic stress response of the host, perpetuate a deleterious cycle that impairs the progression to the proliferative phase of healing (Fonder et al., 2008). The intense mitogenic activity seen in acute wounds is absent in chronic ones (Stojadinovic, Carlson, Schultz, Davis, & Elster, 2008). Often, the removal of the primary noxa is effective in resolving many chronic wounds (Goldman, 2004). The excessive infiltration of neutrophils is thought to be a critical event in the self-perpetuating chronic inflammation of these wounds, is its biological marker (Diegelmann & Evans, 2004), and causes the overproduction of reactive oxygen species (ROS) which directly damage the matrix and cell membranes inducing early senescence. In addition, neutrophils release serin-proteases, such as elastase, and metalloproteases, such as neutrophil collagenase (MMP-8). The elastase degrades pivotal

mediators like PDGF and TGF-β so that even though the production of growth factors is often increased in chronic wounds, their bioavailability is reduced. Collagenase degrades and inactivates matrix components, and degradation products promote inflammation perpetuating the cycle (Demidova-Rice, Hamblin, & Herman, 2012). Both activated neutrophils and macrophages also produce pro-inflammatory cytokines such as IL-1β and TNF-a that not only increase the production of MMPs but also reduce their tissue inhibitors (TIMPs); such unbalance favours matrix degradation and impairs cell migration, fibroblast proliferation and collagen synthesis (Mast & Schultz, 1996).

1.2.2 *HYPOXIA-INDUCIBLE FACTORS (HIFS) AND WOUND HEALING*

Fluctuations in local oxygen tension induce the organism to implement an adaptation strategy through a series of orchestrated responses aimed at preserving cell integrity. At a molecular level, one of those responses is the activation of specific transcription factors known as hypoxia-inducible factors (HIFs) that respond to hypoxia, which is a marked reduction of oxygen availability in the cell environment (Wilkins, Abboud, Hancock, & Schofield, 2016). The HIF pathway is vital to mammal development, and gene deletion causes perinatal death. In addition, HIF plays a prominent role in human metabolism regulation (Formenti et al., 2010).

Most, if not all, oxygen-breathing species express the highly conserved transcriptional complex HIF-1, a heterodimer composed of an alpha subunit regulated by oxygen and induced under hypoxia, and a beta subunit, known as aryl hydrocarbon receptor nuclear translocator (ARNT), constitutively expressed (Wang, Jiang, Rue, & Semenza, 1995). HIF-1 belongs to a subfamily of basic helix-loop-helix (bHLH) receptors, characterised by a Per-Arnt-Sim (PAS) domain. The alpha and beta subunits are structurally similar, and both present the following domains (Yang et al., 2005):

- *N-terminus*: bHLH domain for the binding to DNA.
- *Core region*: Per-Arnt-Sim (PAS) domain to facilitate heterodimerisation.
- *C-terminus*: domain for the recruitment of transcriptional co-regulators.

The members of the human HIF transcription factor family are listed in **Table I**.

Table I | *Members of the HIF family*

Member	***Gene***	***Protein***
HIF-1α	*HIF1A*	*Hypoxia-inducible factor* 1, alpha subunit
HIF-1β	*ARNT*	*Aryl-hydrocarbon receptor nuclear translocator*
HIF-2α	*EPAS1*	*Endothelial PAS domain protein 1*
HIF-2β	*ARNT2*	*Aryl-hydrocarbon receptor nuclear translocator 2*
HIF-3α	*HIF3A*	*Hypoxia-inducible factor 3*, alpha subunit
HIF-3β	*ARNTL*	*Aryl-hydrocarbon receptor nuclear translocator 3*

The regulation of HIF-1α subunit activity (**Fig. 3**) involves post-translational modifications, in terms of hydroxylation of conserved proline residues (Pro402 and Pro564 in the human sequence, contained in the oxygen-dependent degradation [ODD] domain) by prolyl-hydroxylases (PHD), of which PHD2 is the principal physiological actor (Berra et al., 2003). PHD2 is a Fe(II)-/α-ketoglutarate-dependent dioxygenase that necessarily requires the presence of molecular oxygen as a co-substrate to be transferred to proline residues (Epstein et al., 2001). Due to its low oxygen affinity (K_m=250 μM, slightly greater than the atmospheric pO_2), PHD2 is often described as an "oxygen sensor" (Hirsilä, Koivunen, Günzler, Kivirikko, & Myllyharju, 2003). In normally oxygenated cells, the hydroxylated proline residue is recognised and received into the hydrophobic core of the oncosuppressor protein von Hippel-Lindau (VHL) (Hon et al., 2002) that interacts with elongin C, thus recruiting the E3 ubiquitin ligase complex, which tags HIF-1α with polyubiquitin for rapid 26S proteasome degradation (Maxwell et al., 1999).

This is what happens in normoxia; on the other hand, under hypoxia PHD2 is inhibited and so is HIF-1α degradation. Spared from proteolytic degradation, the protein can translocate into the nucleus where it dimerises with HIF-1β, but the initiation of transcription needs the further interaction of HIF-1 with co-activators and the DNA-polymerase II complex, which enable the binding to HIF-responsive elements (HRE) within the promoters of target genes characterised by the consensus sequence 5'-(A/G)CGTG-3' (Semenza, 2007).

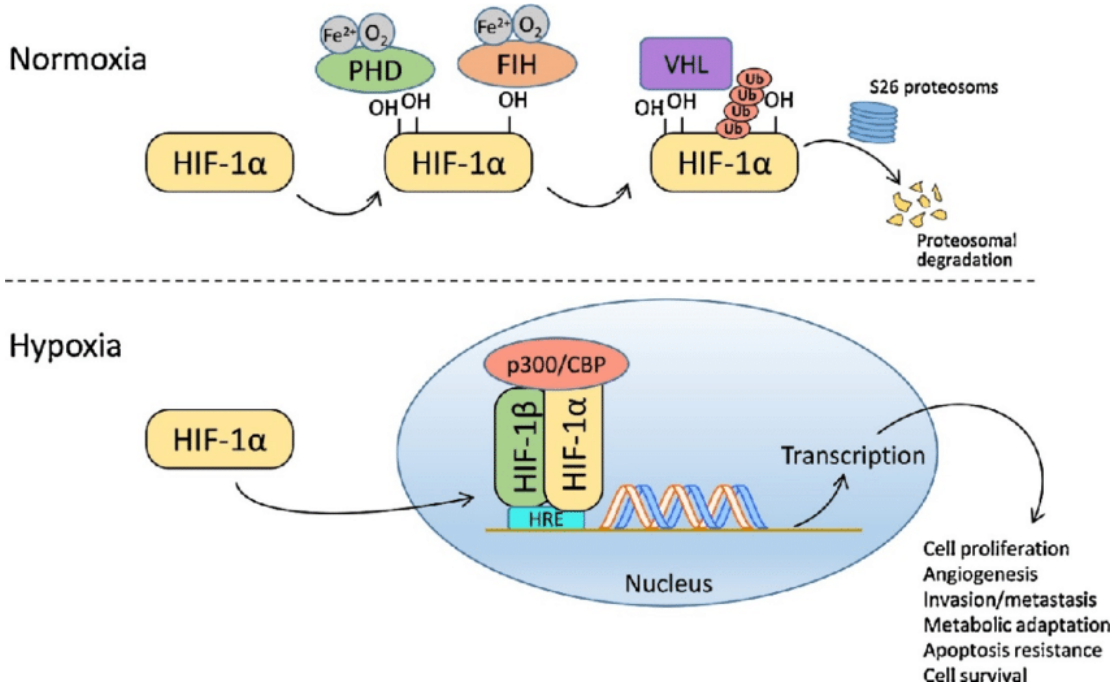

Figure 3 | ***HIF-1*** *Regulation of the transcription factor HIF-1a under normoxia and hypoxia (Ali, 2018).*

The hydroxylation of HIF-1a proline residues also regulates the ability of the transcription factor to associate with different co-activators under hypoxia (Sang, Fang, Srinivas, Leshchinsky, & Caro, 2002). Besides being hydroxylated by PHD, the activity of HIF-1a is also regulated by the oxygen-dependent hydroxylation of an asparagine residue (Asn803) by FIH-1 (factor inhibiting HIF-1), another a-ketoglutarate-dependent dioxygenase, which hinders the interaction with the transcriptional co-activator complex p300/CBP at the C-terminal transactivation domain (C-TAD) (Lisy & Peet, 2008). The affinity of FIH-1 for oxygen (K_m=90 μM, ~40% of atmospheric pO_2) is about a third of that of PHD2 (Koivunen, Hirsilä, Günzler, Kivirikko, & Myllyharju, 2004).

Like a few other transcription factors, HIF-1a presents two transactivation domains (TADs), one at the N-terminus (N-TAD, highly interspecifically conserved >90%) and one at the C-terminus (C-TAD, with a level of interspecific identity of about 100%), sharing less than 20% in similarity. Since FIH-1 exercise a repressive control only on C-TAD, based on the differential K_m between the two oxygen sensors PHD2 and FIH-1, a model has been proposed to explain the fine oxygen-dependent regulation of HIF-1a.

In more oxygenated areas, fully active PHD2 and FIH-1 lead to the complete degradation of HIF-1α, so that in these conditions only minimal basal levels of the inactive protein, characteristic of normoxia, can be found. The progressive reduction of the oxygen tension initially inhibits PHD2, causing increased stability of HIF-1α that exerts its transcriptional activity through the N-TAD, while the C-TAD is still repressed by FIH-1 activity. Few genes, the transcription of which is dependent on N-TAD only and are insensible to FIH-1 regulation (such as *GAPDH*), are already activated at intermediate levels of oxygen. Under drastic hypoxia when also FIH-1 activity is completely inhibited, the further decrease in oxygen tension leads to the full stabilisation of HIF-1α, which enables the interaction of the C-TAD with transcriptional co-activators and the induction of a family of genes sensible to N-TAD and/or C-TAD intervention, in particular those dependent on p300/CBP for their transcription (Dayan, Roux, Brahimi-Horn, Pouyssegur, & Mazure, 2006). The HIF-1 complex up-regulates many genes that promote cell survival under low oxygen tension, belonging more or less to two categories: some, such as erythropoietin (*EPO*), vascular endothelial growth factor (*VEGFA*), and inducible NO-synthase (*NOS2*), aim at re-establishing the local pO_2; others, involved in the acceleration of the glycolytic flux, enable the oxygen-independent ATP synthesis (Semenza, 2010).

As the individual steps of the wound healing cascade were elucidated, the involvement of oxygen at nearly every stage has become increasingly clear (Hong et al., 2014). Consequently, hypoxia is one of the chief microenvironmental factors in tissue injury and wound healing, and changes in oxygen tension activate precisely regulated pathways that modulate cell function. Indeed, the proliferation of human dermal fibroblasts is greatly enhanced under acute hypoxia, a condition in which they were found to secrete up to nine times more TGF-β (Hong et al., 2014). Nevertheless, while acute hypoxia seems to be beneficial in the early processes of wound healing, on the contrary, chronic extreme hypoxia might lead to cell death and tissue integrity disruption (Sen, 2009). HIF-1 is critically involved in virtually all processes of wound healing and remodelling, through the influence on angiogenesis, cell

migration, cell survival, growth factor release, and matrix synthesis (Semenza, 2014).

Inflammation and hypoxia signalling are mutually interdependent: a delay in wound healing and wound chronicity are directly linked to persistent inflammation, on the other hand, inflammatory states are frequently characterised by tissue hypoxia, or otherwise by the stabilisation of hypoxia-dependent transcription factors (Bartels, Grenz, & Eltzschig, 2013). However, though the exact role of HIF-1 signalling occurring during acute inflammation remains elusive, it surprisingly functions adaptively by increasing ischemia tolerance and limiting excessive inflammation. HIF-1 influences the cellular inflammatory response through a metabolic switch to glycolysis, which may be important for preventing the excessive generation of deleterious reactive oxygen species and impaired wound resolution (Papandreou, Cairns, Fontana, Lim, & Denko, 2006), and elicits the upregulation of many genes that enhance the wound repair process, such as adhesion proteins, soluble growth factors (TGF-β and VEGF), and matrix components. Consequently, the anti-inflammatory effects of hypoxia signalling have been linked to a transcriptional program under the control of HIF-1, which has been shown to dampen hypoxia-induced inflammation in a wide variety of inflammatory disease models, for example, through the enhanced production of anti-inflammatory signalling molecules (Eltzschig, Sitkovsky, & Robson, 2012; Rosenberger et al., 2009). In addition, Scholz et al. have provided compelling evidence that it is the hydroxylases, inhibited by hypoxic conditions, that might modulate inflammation via key post-translational modifications in the IL-1β pathway (Scholz et al., 2013). The activity of hydroxylases is required for IL-1β–induced NF-κB activation and, consequently, hypoxia and hydroxylase inhibitors may downregulate IL-1β–induced NF-κB signalling. Importantly, some of these effects seem to be independent of HIF-1a, thus indicating a more global role of PHDs outside of the HIF pathway (Bartels et al., 2013).

Following an injury, the closure of a skin wound is normally realised by repair, which implies healing by scarring and unfortunately represents the main form of wound healing in adult skin. However, during prenatal life and in some

classes of animals wound healing is achieved by regeneration, that is the specific substitution of the tissue. Recent evidence has attributed a pivotal role to HIF-1 also in the balance between repair and regeneration. Research on a super healing mouse strain, which displays spontaneous regeneration of skin wounds, showed a constitutionally increased activity of the hypoxia-inducible factor HIF-1a, but most interestingly demonstrated that the administration to normal mice of a synthetic inhibitor of prolyl-hydroxylases, hindering the aforementioned degradation of HIF-1a, also led to a regenerative phenotype, opening new perspectives for the exploitation of HIF-1 pathway modulation in wound healing and skin regeneration (Y. Zhang et al., 2015). In particular, it has been discovered that the pharmacological continuous up-regulation of HIF-1a can trigger the regeneration of lost or damaged tissue in mammals that generally display a reparative response; on the contrary, a continuous down-regulation causes healing by scarring in mammals that had previously shown a regenerative response to tissue loss. The regulation of HIF-1a may therefore influence the key processes of regeneration in mammals, eliciting their activation.

1.2.3 *PROPOLIS*

Propolis, or bee glue, is a complex resinous mixture composed of exudates gathered by western honeybees (*Apis mellifera* LINNAEUS, 1758) from buds, twigs, sprouts, vegetal apices, sap flows, or other botanical sources and elaborated with beeswax and salivary secretions (Silva-Carvalho, Baltazar, & Almeida-Aguiar, 2015). The etymology of the term propolis comes from the Ancient Greek προ- (*pro*-, "in front of/for") + πόλις (*pólis*, "city") and refers to the fundamental role of this product in the protection of the hive.

Western honeybees, kept to obtain bee products of commercial interest (honey, propolis, bee pollen, royal jelly, and bee venom), belong to the species *Apis mellifera* LINNAEUS, 1758, one of the two domesticated species in the genus *Apis* (the other one is *Apis cerana* FABRICIUS, 1793 or eastern honeybee). Like all honeybee species, they are eusocial hymenopteran insects, forming colonies of tens of thousands of mutually interdependent individuals, with a single fertile

female (the queen), a few fertile males (drones), and a host of normally non-fertile females (workers). Individuals hardly survive far from the colony, that is a "superorganism" in which each individual plays a specific task to guarantee the prosperity of the entire community. The division of tasks among worker bees is dependent on their age: from the first to the third day of life bees play the role of housekeepers, cleaning cells to accommodate new brood; from the 4th to the 10th day, they become nurses and attendant to the queen, providing elder bees with water, honey, and pollen, or the brood and the queen with royal jelly; from the 10th to the 16th day, wax glands come into operation and bees become architects; then, workers act as ventilators to preserve the hive microenvironment and dehydrate honey, until the 20th day when the defensive role takes over; finally, in the last stage of their life worker bees become foragers responsible for the collection of water and food outside of the hive. Honeybees involved in propolis production are forager bees. The search for botanical sources from which to gather raw materials is carried out during the hottest hours of the day when vegetal exudates are more pliable. The collection is carried out with mandibles. Then, with the aid of the front legs, bees shape little lumps of materials that are stored in the corbiculae (pollen baskets) on the hind legs. When the corbiculae are full, forager bees return to the hive, where specialised bees help unload the material, since forager bees would not be able to carry out this operation by themselves. The elaboration of propolis, which consists in mixing vegetal exudates with salivary secretions, enzymes, and waxes, starts immediately after the delivery of the material, is performed by young worker bees with active wax glands (from 10th to 16th day of life) and can take several hours.

From an ecological point of view, when foraging for resins honeybees are engaged in an energetically demanding activity, which does not give any clear reward to the individual. Nevertheless, it should be noticed that plants produce and secrete exudates characterised by antioxidant and antimicrobial properties to protect vegetal apices, buds, and young leaves in response to physical damage. It is likely that honeybees, which are eusocial hymenopterans, have evolutionarily developed the ability to gather

antimicrobial compounds from the surrounding environment and reuse them to reduce the deleterious effects of pathogens and parasites through the enhancement of social immunity at a colony level, rather than investing in individual immune defences only (Simone, Evans, & Spivak, 2009).

The purposes of propolis within the beehive are (Toreti, Sato, Pastore, & Park, 2013):

- Lining the internal surface of the hive with a thin layer able to provide thermal insulation, reduce water loss, and protect from the elements.
- Repairing and strengthening the comb.
- Sealing unwanted open spaces and gaps smaller than the bee space (approximately 6 mm).
- Inhibiting the germination of plants within the hive.
- Preventing putrefaction within the hive as in the case of cadavers of intruders which bees are unable to carry out.
- Sanitising the hive and preventing infections.

Propolis protects the colony from diseases thanks to its antiseptic and antimicrobial properties (Salatino, Teixeira, Negri, & Message, 2005). In experimental hives, it was demonstrated that propolis supplementation reduces the microbial burden and the activation of the immune system in bees, not directly but as a consequence of the low pathogen number, diminishing the energy demand with an increase in colony longevity and productivity (Simone et al., 2009). In addition, it contributes to the stability of the microbiome (Saelao, Borba, Ricigliano, Spivak, & Simone-Finstrom, 2020). The supplementation with 0.1% propolis as a food alternative to pollen has been shown to induce the overexpression of antimicrobial peptides, such as defensin-1, abaecin, and hymenoptaecin (Lourenço, Guidugli-Lazzarini, Freitas, Bitondi, & Simões, 2013) in honeybees infected with *Escherichia coli* compared to infected bees not receiving propolis or uninfected bees (Turcatto, Lourenço, & De Jong, 2018). The activity on pathogens has been further confirmed by the efficacy against the fungus *Ascosphaera apis* and the bacterium *Paenibacillus larvae*, responsible for infective diseases in the brood (Wilson, Brinkman, Spivak, Gardner, & Cohen, 2015).

Propolis deposition in beehives has been considered for years an inconvenience by beekeepers, who used to scrape it to keep the mechanical parts of the hive free from clutter. However, a trend reversal has made propolis a valuable product and the greater the size the greater the commercial value. Propolis is currently collected by scraping it from the inside of the hive or using specific propolis frames, taking advantage of the innate behaviour of bees to fill open spaces and gaps with propolis. In presence of propolis frames, the dimensions of the bee space are altered, stimulating bees to cover these artificial devices with propolis.

The colour of propolis varies from brown to black, but may also be red, green, or yellow and, like the typical aromatic smell, depends on the local flora of the area where the colony is settled. The consistency changes with temperature, under 15 °C propolis is hard and brittle, while at temperatures between 25 °C and 45 °C it becomes soft, ductile, and gluey. Above these temperatures, it becomes more and more viscous. If heated in a water bath for sufficient time, propolis eventually separates into two phases, a viscous phase which migrates downwards and a waxy aromatic liquid phase which rises to the surface.

Known since ancient times, propolis has always been part of traditional medicine. Ancient Egyptians used propolis in mummification (Martinotti & Ranzato, 2015), while Greek and Romans were aware of its medicinal properties and used it to alleviate physical ailments (Kuropatnicki, Szliszka, & Krol, 2013). Noteworthy are the mentions of propolis by Aristoteles in the *Historia Animalium*, in which the use against injuries and cutaneous suppurations is described, and by Pliny the Elder in the *Naturalis Historia* (Martinotti & Ranzato, 2015). It is also remarkable the use by Romans as an emergency remedy to treat battle wounds (Salatino et al., 2005). During the Middle Ages, propolis fell into disuse and only during the Renaissance the interest was renovated (Kuropatnicki et al., 2013). In the XVII century, propolis was included in various European pharmacopoeias for the preparations of medicinal ointments. It was not until the XIX century that attention was shifted to the chemical composition of propolis (Kuropatnicki et al., 2013) with a contextual interest in its use for

health purposes. In 1908, Helfenberg published a prodromal research article titled "The analysis of beeswax and propolis", dealing for the first time with the composition and chemical properties of bee products (A. Berretta et al., 2017). During the Second World War, propolis found wide applications to treat battle injuries (Anjum et al., 2019) and in 1969 the URSS approved its medical and veterinary use (Silva-Carvalho et al., 2015). After having remained for a long time a remedy used in traditional medicine, mainly in the Balkan regions, propolis has gained renovated pharmacological interest in the last 30 years and its use has widespread all over the world in complementary and alternative medicine. The knowledge of propolis chemical and biological properties has increased so much to give a new vision of this product: the complexity of propolis composition has always been known, but it was formerly believed that chemical components were more or less constant and that only a single type of propolis existed (V. Bankova, 2005b). Recent studies on various propolis samples from different parts of the world have demonstrated that several types and varieties do exist.

❖ **Chemical composition**: the chemical composition of propolis is influenced by various factors: the botanical sources from which resins are foraged, the geographical area (Bueno-Silva, Marsola, Ikegaki, Alencar, & Rosalen, 2017), and the foraging season (Regueira et al., 2017). As a result, an enormous variety of propolis can be recognised. Propolis is a complex mixture and chemical analysis is complicated by the fact that the proportion among different components is variable depending on the time and place of collection. For this reason, it is difficult to standardise propolis from a chemical point of view to commercialise it as a pharmaceutical substance (V. Bankova, de Castro, & Marcucci, 2000). Propolis in fact is assumed to be one of the most heterogeneous natural products, with more than 300 different molecules identified or characterised. It is grossly composed of resins and vegetal balsams (50-60%), waxes (30-40%), essential oil (5-10%), pollen and other substances including a diversity of minerals, vitamins, poly-/oligosaccharides, and phenolic compounds (3-5%) (Silva-Carvalho et al., 2015). The classes of organic compounds present in propolis include polyphenols (such as flavonoids,

phenolic acids, and their derivatives), terpenes and terpenoids, aromatic acids and esters, alcohols, aldehydes, steroids, amino acids, vitamins, fatty acids, and free hydrocarbons. In particular, resins and balsams are a mixture of terpenes, essential oils, and gums, whereas waxes are composed of organic acids and esters, long chain alcohols, and free hydrocarbons (Ahangari, Naseri, & Vatandoost, 2018). The polyphenolic fraction mainly refers to flavonoids and their derivatives, which contribute to the biological activity together with terpenes, responsible for the balsamic scent (S. Huang, Zhang, Wang, Li, & Hu, 2014). The principal fatty acids are represented by stearic acid, lignoceric acid, oleic acid, and palmitic acid, while organic acids include ferulic acid, myristic acid, benzoic acid, and cinnamic acid. Among cinnamic acid derivatives, caffeic acid, caffeic acid phenethyl ester (CAPE), and artepillin c are noteworthy (Endo et al., 2018). Together with minerals (such as zinc, iron, copper, phosphorus, magnesium, manganese, iodine, potassium, sodium and calcium), also toxic elements (arsenic, cadmium, mercury, and lead) can sometimes be found, especially in propolis samples collected in the surroundings of industrial or polluted areas (Cvek et al., 2008). The identified vitamins include vitamins of the B complex (thiamine, riboflavin, niacin, pantothenic acid, folic acid, and cobalamin), ascorbic acid, biotin, and tocopherol (Eroglu, Akkus, Yaman, Asci, & Silici, 2016).

The chemical components of propolis exclusively come from the vegetal exudates collected by honeybees and the material introduced during the elaboration within the hive (Marcucci, 1995). A debated issue concerns the addition of salivary secretions by bees. Irrelevant amounts of enzymes such as α-amylase, β-amylase, maltase, and some esterases are inevitably transferred to propolis during its elaboration. More contradictory is the possible addition of β-glucosidase, which could cause partial digestion of the plant material. However, experiments that separately analysed the composition of resins sampled from plants, pollen baskets of honeybees, and terminally elaborated propolis have demonstrated a substantial identity of the chemical profiles with the absence of significant changes in plant secondary metabolites (V. Bankova, Popova, & Trusheva, 2018). Moreover, it is quite unlikely that enzymes

might be active in propolis due to the low water activity and the high phenolic content, thus disproving the hypothesis of enzymatic digestion.

Propolis constituents are influenced by geographical provenance, the season of collection, climatic factors, and the botanical sources foraged by honeybees at the time of collection, meaning that propolis can be classified into several different varieties (V. Bankova et al., 2000). Numerous propolis samples from different geographical origins have been thoroughly characterised and tentatively classified based on their principal components and putative botanical sources. However, within the same propolis type the chemical composition of specific samples may be highly variable depending on plant ecology, season, climatic factors, and environmental conditions of the site of collection, thus making standardisation a great challenge (V. Bankova, 2005a; Sforcin & Bankova, 2011). In **Table II**, the most widespread and well-known propolis types, together with their chemical markers, are presented. Data about propolis collected in Africa, the Middle East, Australia, and to some extent North America are scarce and reveal multifarious chemistry. Hence, the classification of propolis types from these regions is difficult and still incomplete (Magnavacca et al., 2022). Although the chemical composition may vary, propolis from different origins usually demonstrate a considerable and comparable biological activity (Kujumgiev et al., 1999).

Table II | *Classification of the principal propolis types (Magnavacca, Sangiovanni, Racagni, & Dell'Agli, 2022)*

Propolis type	Propolis subtype	Geographical origin	Botanical origin	Components – Phytochemical markers	References
Poplar type propolis			*Populus* spp.	Flavonoids, phenolic acids, and their esters - Pinocembrin, chrysin, galangin, pinobanksin, pinobanksin 3-acetate	(Ahn et al., 2007; Greenaway, Scaysbrook, & Whatley, 1990; Marcucci, 1995)
Aspen type propolis			*Populus tremula* L.	*p*-coumaric acid, ferulic acid, benzoic acid, benzyl *p*-coumarate, benzyl ferulate, glycerol esters of substituted cinnamic acids (phenolic glycerides).	(Vassya Bankova, Popova, Bogdanov, & Sabatini, 2002; Isidorov, Szczepaniak, & Bakier, 2014; Popravko, Sokolov, & Torgov, 1982)
Mediterranean type propolis			*Cupressus sempervirens* L.	Diterpenes - Isocupressic acid, pimaric acid, agathadiol, isoagatholal, totarol. N.B. Usually does not contain flavonoids and phenolic acids	(M. Popova et al., 2012; M. P. Popova, Graikou, Chinou, & Bankova, 2010)
Pacific type propolis (Pacific islands: Taiwan, Okinawa, Indonesia)			*Macaranga tanarius* (L.) Müll.Arg.	Prenylated flavanones (propolins)	(W. J. Huang et al., 2007; S. Kumazawa et al., 2008; B. Trusheva et al., 2011)
Mangifera indica type propolis			*Mangifera indica* L.	Phenolic lipids (cardanols, cardols, anacardic acid derivatives)	(Knodler et al., 2008; B. Trusheva et al., 2011)
Mixed propolis types			2 or 3 plant sources ex. aspen-poplar, *Cupressus*-poplar, Pacific-*Mangifera indica* propolis		(Vassya Bankova et al., 2002; B. Trusheva et al., 2011)
Birch type propolis		Russia	*Betula pendula* Roth	Flavones and flavonols	(M Popova et al., 2013)

Table II | *Continued*

Caribbean type propolis		Cuba, Venezuela	*Clusia spp*	Polyprenylated benzophenones (7-epi-nemorosone)	(Camargo et al., 2013; Diaz-Carballo et al., 2012; Diaz-Carballo et al., 2010)
Canarian type propolis		Canary Islands	*Unknown*	Furofurano lignanes	(Kujumgiev et al., 1999)
Brazilian type propolis					
	3 (Poplar type propolis)	Paraná State	*Populus spp.*	Mainly flavonoids (chrysin, pinocembrin, pinobanksin, apigenin and galangin)	(Y. Park, Ikegaki, & Alencar, 2000; Y. K. Park, Alencar Sm Fau - Aguiar, & Aguiar, 2002)
	6 (Brown type propolis)	Bahia State	*Hyptis divaricata* Pohl ex Benth.	Prenylated benzophenone	(Castro et al., 2009; Y. Park et al., 2000; Y. K. Park et al., 2002)
	12 (Green type propolis)	São Paulo State	*Baccharis dracunculifolia* DC.	Prenylated cinnamic acids and flavonoids Phenolic actives, prenylated phenolic acids, flavonoids (artepillin C, drupanin, p-coumaric acid, dihydrocinnamic acid)	(V. Bankova et al., 1999; Shigenori Kumazawa et al., 2003; Y. Park et al., 2000; Y. K. Park et al., 2002; Paulino et al., 2008)
	13 (Red type propolis)	Alagoas State	*Dalbergia ecastaphyllum* (L.) Taub.	Mainly isoflavonoids (formononetin, vestitol, neovestitol and daidzein) and chalcones Isoflavans, pterocarpans (vestitol, medicarpin, neovestitol, 7-O-methylvestitol, formononetin)	(Alencar et al., 2007; Bueno-Silva et al., 2016; Lopez, Schmidt, Eberlin, & Sawaya, 2014; Lotti et al., 2010; Oldoni et al., 2011; Piccinelli et al., 2011; Silva et al., 2008; Boryana Trusheva et al., 2006)

❖ **Brazilian propolis**: propolis varieties from Brazil have been initially classified into 12 groups based on geographical origin, physical-chemical properties, and botanical sources. Five groups have been identified out of samples from southern Brazil, six groups out of samples from north-eastern regions, while the last one refers to green propolis, characteristic of southwestern and central-western Brazil and known for its colour varying from yellow-green to dark green due to the presence of chlorophyll in the exudates foraged (Y. Park et al., 2000). In 2007 this classification has been further expanded with the discovery of a thirteenth variety native to the states of Sergipe, Alagoas, Paraíba, Pernambuco, and Bahia known as red propolis (Daugsch, Moraes, Fort, & Park, 2008). The most widespread and sold variety of Brazilian propolis is the green one. Brown, yellow, and red varieties are also relevant, and their secondary metabolites have been widely characterised. Out of thirteen groups, it was possible to identify with confidence the botanical source for only four of them. The buds of *Populus nigra* L. are the main source of type-3 propolis, *Hyptis divaricata* Pohl ex Benth. is the source of type-6 propolis, while that of type-12 propolis is represented by the buds and non-expanded leaves of *Baccharis dracunculifolia* DC. (Y. K. Park et al., 2002). Finally, the main botanical source of red propolis is *Dalbergia ecastaphyllum* (L.) Taub., a leguminous plant known for the presence of red pigments composed of cationic C_{30} isoflavans (Piccinelli et al., 2011).

➢ <u>*Green propolis*</u>: the production of green propolis is typical of the states of São Paulo, Minas Gerais, and Paraná and, as previously mentioned, the main botanical source is *Baccharis dracunculifolia* DC., belonging to the family Asteraceae. Also known as "alecrim-do-campo (rosemary-of-field)", it is a perennial branched shrub that can reach a height of 3 meters, native to Brazil, Bolivia, Argentina, and Uruguay, and diffused in the Atlantic Forest ("Mata Atlântica"), a region stretching on the Atlantic coastline of Brazil from the Rio Grande do Norte to the Rio Grande do Sul. Leaves are lanceolate and alternate. The plant is dioic and flowers twice a year, from December to May (Bastos, Santana, Calaça-Costa, & Thiago, 2011). Flowers are small, pale yellow in males and white in females, clustered in

axillar inflorescences with a peculiar scent. Notably, female flowers lack nectar. Pollination is entomophilous, while the mature achenes are dispersed by wind. The plant does not show agamospermy, which means that seeds are not produced in absence of fecundation (Espírito-Santo et al., 2003). *Baccharis dracunculifolia* DC. shows complex interactions with insects, in particular, it has been noticed that male plants are principally infested by parasitic insects responsible for the formation of galls, whereas female plants preferentially attract *Apis mellifera* that show a preference for buds and non-expanded leaves. Increasing the percentage of female plants in the field seems to increase the production of green propolis (Rodrigues, De Souza, Arruda, Pereira, & Bastos, 2020). In any case, honeybees collect exudates on both male and female plants and independently from the phenological stage (Bastos et al., 2011). The extracts of *Baccharis dracunculifolia* DC. have shown antimicrobial and anti-inflammatory activities, also found in green propolis, traditionally exploited for the treatment of gastric and cutaneous ulcers (da Silva Filho et al., 2008). The parts used are flowers, leaves, and twigs. The essential oil is traditionally used as an immunostimulant, antimicrobial, and anti-inflammatory agent (Brandenburg et al., 2020). Green propolis presents a high variability in its chemical composition, in fact, all polyphenolic compounds, with the exception of artepillin C which remains the main component, undergo fluctuations during the collection season (Nunes & Guerreiro, 2012). The most abundant components are members of the phenylpropanoid class such as cinnamic acid, coumaric acid, caffeic and caffeoylquinic acids (Salatino et al., 2005). Noteworthy is the presence of prenylated phenylpropanoids, in particular 4-hydroxycinnamic acid prenylated derivatives (Banskota, Tezuka, Midorikawa, Matsushige, & Kadota, 2000), which can be distinguished between cyclised chromenes, such as 2,2-dimethyl-8-prenylchromene, and compounds which do not cyclise such as artepillin C and drupanin (Szliszka et al., 2013). Artepillin C (3,5-diprenyl-4-hydroxycinnamic acid) stands out due to its abundance and important biological activities (Shahinozzaman, Basak, Emran, Rozario,

& Obanda, 2020). For this reason, the quantity of artepillin c is considered an important indicator and chemical marker for the quality control of Brazilian green propolis (Matsuda & de Almeida-Muradian, 2008). Flavonoids are minor components, among which flavonols (kaempferide, kaempferol, galangin, quercetin, rutin), flavanonols (dihydrokaempferol/aromadendrine, dihydrokaempferide, pinobanksin), flavanones (isosakuranetin, pinocembrin), and flavones (apigenin, chrysin, tectochrysin) have been identified (Maróstica Junior et al., 2008). The presence of kaempferide is interesting due to its potent antioxidant properties (Simões et al., 2004). Common is the presence of mono- and sesquiterpenes (such as farnesol, nerolidol, β-caryophyllene, spathulenol, δ-cadinene, longipinene, selina-3,7(11)diene), which confer the characteristic scent and contribute to the antimicrobial activity (V. Bankova, Popova, & Trusheva, 2014; Koo et al., 2003). Among diterpenes, labdane derivatives such as isocupressic acid and agathic acid are the principal.

- <u>*Red Propolis*</u>: its main botanical source is *Dalbergia ecastaphyllum* (L.) Taub., a leguminous plant known for the presence of red pigments composed of cationic C_{30} isoflavans, which belongs to the family Fabaceae (Piccinelli et al., 2011). It is a perennial sarmentose shrub, often arboreal, with branches up to 10 m long and a maximum height of 7 m, mainly distributed in the tropical regions of South and Central America, Madagascar, and Southern Asia. In particular, *Dalbergia ecastaphyllum* (L.) Taub. is frequently found along shorelines and rivers in north-eastern Brazil, in the states of Alagoas, Paraiba, Sergipe, and Bahia, where it is known as "rabo de bugio" (Daugsch et al., 2008). The plant presents alternate compound leaves with oval or long petiolate leaflets. Flowers, which bloom in August and September, are white with oval or reniform bracts and are clustered in axillar inflorescences, while fruits are coppery pods containing one seed each. This plant is the principal source of red propolis (Daugsch et al., 2008) elaborated by *Apis mellifera* with the reddish resinous exudates found on the trunk surface or in cavities made by insects in the branches. Roots and

barks are traditionally used for the treatment of uterine infections and against anaemia (Moise & Bobiş, 2020). The evidence reporting the chemical characterisation of red propolis shows a certain variability in terms of qualitative and quantitative composition, depending on the samples analysed. Flavonoids, and in particular the subclass of isoflavonoids, are undoubtedly the major components (Jacob, Parolia, Pau, & Davamani Amalraj, 2015), of which antimicrobial (Cushnie & Lamb, 2005), antifungal, anticancer (Militão et al., 2006), and antioxidant activities have been widely demonstrated. Many of the compounds found in red propolis have been also identified in the plant *Dalbergia ecastaphyllum* (L.) Taub., thus confirming the botanical source (Piccinelli et al., 2011). The principal molecules identified in red propolis belong to the classes of flavonols (quercetin, rutin), flavanonols (pinobanksin), flavones (luteolin), flavanones (liquiritigenin, pinocembrin-3-acetate), isoflavones (daidzein), the neoflavone dalbergin, and the chalcone isoliquiritigenin (Daugsch et al., 2008). Other compounds identified are elemicin, isoelemicin, homopterocarpan (A. Berretta et al., 2017), caffeic acid, ferulic acid, 2,4-hydroxycinnamic acid, 4-hydroxycinnamic acid, genistein, kaempferol, catechin and epicatechin, naringenin (de Mendonça et al., 2015), vestitol and neovestitol (Nani et al., 2018). Formononetin, biochanin A, pinocembrin, and medicarpin are characteristic compounds used to identify red propolis samples (A. Berretta et al., 2017). Among volatile compounds, terpineol, camphor, ferruginol, lanosterol, lupeol, a-bisabolol, and valencene can be counted. These compounds together with phenolics are responsible for the characteristic scent of red propolis (Moise & Bobiş, 2020). Phenolic acids are represented by hydroxycinnamic acids such as caffeic acid, ferulic acid, *p*-coumaric acid, and umbellic acid (2,4-dihydroxycinnamic acid) (F. R. Corrêa, Schanuel, Moura-Nunes, Monte-Alto-Costa, & Daleprane, 2017). Among pentacyclic triterpenes, there are lupeol, lupeol acetate, and lupenone (de Carvalho et al., 2020). The pigments responsible for the red colour are the retusapurpurins A and B (Piccinelli et al., 2011).

❖ **Biological activities**: due to the discovery of a broad spectrum of biological activities associated with the utilisation of this natural product, which include anti-inflammatory, immunostimulant, antimicrobial and antiviral properties, the interest in propolis has increased over the last few years unfolding new research and therapeutic horizons. The biologically active components of propolis can be extracted with the aid of a variety of different solvents, which include alcohols (mainly ethanol), glycols (such as propylene glycol), and oils. For analytical purposes, organic solvents such as methanol, chloroform, dichloromethane, and hexane may be used. Sometimes propolis is extracted with water, but, since it is a lipophilic material, water solubility is very limited. Most commonly, hydroethanolic mixtures are used to extract both polar and non-polar compounds. Due to the complexity of the product, the choice of the solvent significantly influences the chemical composition of the extracts, and such an extreme variability should be considered in the evaluation of the biological activities since it is correlated to variability in the effects encountered (A. A. Berretta, Silveira, Cóndor Capcha, & De Jong, 2020).

- *Antimicrobial activity*: propolis possesses a wide spectrum of antibacterial activity (Mirzoeva, Grishanin, & Calder, 1997) that has been tested on over 600 aerobic and anaerobic strains. The antimicrobial activity is explicated in two modes: direct action on the microorganisms and the additive stimulation of the host immune system, attributed to cinnamic acid derivatives, artepillin C (Kimoto et al., 1998), and flavonoids such as quercetin and naringenin (Pobiega, Gniewosz, & Kraśniewska, 2017). Specifically, propolis alters the permeability of the bacterial cell membrane, disrupting membrane potential and hindering ATP synthesis, and inhibits motility. The activity is explicated preferentially against gram-positive bacteria, due to the differences in the bacterial wall (Przybyłek & Karpiński, 2019) and the ability of gram-negative bacteria to produce enzymes which inactivate propolis components (Kurek-Górecka et al., 2021). The activity of propolis has been demonstrated against *Staphylococcus* spp., *Streptococcus* spp., *Escherichia coli*, *Klebsiella pneumoniae*, *Proteus vulgaris*, *Pseudomonas aeruginosa*, and *Helicobacter pylori* (Martinotti &

Ranzato, 2015). Red propolis extracts possess marked antimicrobial efficacy against *Enterococcus* spp., *Staphylococcus aureus*, and *Klebsiella* spp. with MIC values of around 50 µg/mL. Green propolis extracts seem to possess lower antimicrobial activity, with MIC values ranging from 250 to 500 µg/mL. The antifungal activity of propolis is documented in literature as well (Zulhendri et al., 2021). According to some studies, a higher flavonoid content directly correlates with antimycotic activity (Freires et al., 2016). It was seen that propolis damages the cell membrane, altering permeability and hindering the morphogenesis and the energetic homeostasis of fungi (J. L. Corrêa et al., 2020; Peng et al., 2012). Among other components, cinnamic acid derivatives stand out for their antifungal activity (Papp et al., 2021). Volatile compounds, such as nerolidol, show analogous properties (Fonseca Bezerra et al., 2020). The antifungal activity has been demonstrated on different fungi and moulds including *Candida* spp., *Trichosporon* spp., *Aspergillus* spp., and *Penicillium* spp. (Pobiega et al., 2017; Zulhendri et al., 2021).

- *Antioxidant, anti-inflammatory, and immunomodulatory activities*: propolis is renowned for its potent antioxidant capacity (Wagh, 2013), attributed to the presence of flavonoids, phenolic acids such as cinnamic acid and its derivatives (Oryan, Alemzadeh, & Moshiri, 2018), but also of the vitamins C and E (Zaccaria et al., 2017). Brazilian propolis varieties have demonstrated potent anti-inflammatory and immunomodulatory activities on a wide range of immune cells, and several studies have enabled the comprehension of the principal mechanisms of action, highly heterogeneous, and able to potentiate or suppress the immune response. This double action, apparently antithetical, is related to chemical variability and mainly attributed to phenolic components, in particular flavonoids. Many bioactive compounds isolated from Brazilian propolis varieties, such as apigenin, artepillin C, vestitol, and neovestitol among others, have been proven to play a significant immunomodulatory role through the inhibition of IκBa, ERK1/2, JNK, and p38 MAPK phosphorylation, NF-κB activation, inflammatory cytokine (TNF-a) and chemokine (CXCL1 and CXCL2)

release, neutrophil adhesion and transmigration (ICAM-1, VCAM-1 and E-selectin expression) (Franchin et al., 2018). Several flavonoids are active in inhibiting COX-2 and the production of prostaglandin E2 (Hämäläinen et al., 2011), as well as in downregulating lipo- and cyclooxygenases. Propolis can regulate the synthesis and release of the principal pro-inflammatory cytokines, including IL-8, IL-6, IL-1β (Bachiega, Orsatti, Pagliarone, & Sforcin, 2012), IL-12 (Bueno-Silva et al., 2017), and TNF-a (de Almeida et al., 2013) while increasing the expression of anti-inflammatory cytokines such as IL-4 and IL-10. The ability to inhibit the secretion of IL-1β is mediated by the action on the inflammasomes, intracellular multiproteic complexes assembled in response to pathogens or tissue damage (Hori, Zamboni, Carrão, Goldman, & Berretta, 2013). Many of the major anti-inflammatory mechanisms of action are related to the modulation of NF-κB and AP-1 signalling (Washio, Kobayashi, Saito, Amagasa, & Kitamura, 2015). The anti-inflammatory activity is exerted by a synergy among various propolis components, even though a prominent role has been attributed to caffeic acid phenethyl ester (CAPE) (Borrelli et al., 2002). However, it is absent in green propolis, which instead shows interesting properties due to the presence of artepillin C (Banskota et al., 2000). Artepillin C explicates anti-inflammatory effects thanks to the inhibition of nitric oxide and prostaglandin E2, through the modulation of NF-κB (Paulino et al., 2008). Green Brazilian propolis, after 4 days of treatment, can inhibit a wide range of inflammatory events, such as the recruitment, adhesion, and migration of neutrophils (Lima et al., 2014). The same effect is explicated during the acute inflammatory phase by red propolis, attributed to the presence of vestitol and neovestitol (Franchin et al., 2016). In particular, leukocyte recruitment is associated with NO release (Bueno-Silva et al., 2017) and it seems that red propolis can induce the upregulation of calmodulin 1 (Calm1 or CaM) in macrophages, reducing the expression of inducible NO synthase (iNOS) and impairing the subsequent production of NO (Weber et al., 2006). On the other hand, propolis also has the ability to activate

macrophages and increase their microbicidal activity, enhance NK cell activity and stimulate antibody production (Sforcin, 2007).

- *Effect on wound healing*: as previously mentioned, propolis has demonstrated antimicrobial (Grange & Davey, 1990), antiviral (Magnavacca et al., 2022), antioxidant, anti-inflammatory, immunostimulant (Sforcin, 2007) properties, and overall, it may be inferred that all these activities synergically cooperate to favour wound healing and repair. Interestingly, the reparative activity of propolis is not limited to skin, in fact, artepillin c has been seen to exert beneficial effects in gastric ulcers, accelerating the healing of the damaged tissue (Costa et al., 2020; de Barros, Sousa, Bastos, & de Andrade, 2007). Propolis and other bee products have traditionally been used for the topical treatment of burns and minor injuries (Siheri, Alenezi, Tusiimire, & Watson, 2017). It inhibits the formation of the bacterial biofilm, which is in many cases a cause of chronification, reduces the time needed to achieve healing, limits the risk of superinfections, exerts analgesic effects (Stojko, Wolny, & Włodarczyk, 2021), reduces the formation of scars, and favours the proliferation of keratinocytes and fibroblasts (Oryan et al., 2018). Noteworthy, previous studies have suggested that propolis, depending on its concentration, origin and cell type, could have either a stimulatory or an inhibitory effect on migration and proliferation (Jacob et al., 2015). A lower efficacy of red propolis seems probably due to the high content in isoflavonoids, which in fact possess anticancer activities through the suppression of cell growth and proliferation. Propolis creates a microenvironment favourable for repair and its usefulness has been demonstrated also in case of a pathological delay in wound healing, such as in geriatric, immunosuppressed (Siheri et al., 2017) and diabetic (Chylińska-Wrzos, Lis-Sochocka, & Jodłowska-Jędrych, 2017) patients. Innovative medicinal products containing Brazilian green and red propolis are being developed to be used in wound management, increasing the efficacy of healing and improving the quality of life (de Almeida et al., 2013). Batista et al. evaluated Brazilian red and green propolis ointment for wound treatment in rats, and complete

epithelialisation was observed in animals treated with the ointment of green propolis. Nevertheless, there was no apparent correlation between the total flavonoid content and the activity of propolis (L. L. Batista et al., 2012). It has been demonstrated that the administration of a collagen film containing red propolis can improve cutaneous repair by modulating collagen deposition (Albuquerque-Júnior et al., 2009), a process significantly improved by the activation of the TGF-β1/Smad2,3 signalling (Hozzein et al., 2015). Another study demonstrated that red propolis may favour the substitution of type III collagen with type I collagen and improve epithelisation inducing keratinocyte proliferation, increasing levels of myofibroblasts in 14-21 days and reducing the severity of the inflammatory state (de Almeida et al., 2013). Due to the ability to stimulate the expression of TGF-β, which participates in the early phases of wound repair such as haemostasis and inflammation, propolis stimulates significant increases in ECM components during the initial stages and affects collagen type I deposition in the earlier steps of the repair process, playing an important role in the contraction of wound edges and the maturation of granulation tissue. Probably, the attenuation of inflammatory cell recruitment might accelerate the proliferative phase of the repair process promoting the rapid transformation of type III collagen into type I collagen, thus indicating that propolis could have a favourable influence on the biochemical environment supporting re-epithelisation (Moura et al., 2011).

- *Effects on HIF-1 signalling pathway*: as previously mentioned, the activation of HIF-1 translates into an improvement of cell migration, survival, proliferation, the release of growth factors, and synthesis of matrix during wound healing, favouring a regenerative outcome (Hong et al., 2014). Limited evidence has been reported regarding the action of CAPE as a FIH1 inhibitor able to stabilise HIF-1a; however, this compound has not been significantly detected in Brazilian green and red propolis. A single study, limited to Brazilian green propolis, has highlighted a possible involvement in the modulation of the activity of the transcription factor HIF-1. The existing data have been obtained in a model of human embryonic kidney (HEK)

cells transfected with a reporter plasmid. Five compounds (baccharin, betuletol, kaempferide, isosakuranetin, and drupanin) were found able to act at this level. Drupanin, baccharin, and kaempferide seem to inhibit the activation of HIF-1a and downstream target genes such as *GLUT1* and *VEGFA*. On the other hand, the flavonoids isosakuranetin and betuletol induced HIF-1 transcriptional activity in both hypoxic and normoxic conditions (Hattori et al., 2011).

2 AIM

Cutis represents a physical barrier, which limits water loss and protects the organism from external aggressions and pathogens. In particular, the epidermis, which is a squamous stratified epithelium composed of diverse cell types, including keratinocytes, melanocytes, and Langerhans cells, fulfils this function through the continuous renewal and thanks to keratinisation, pigmentation, and the production of the cutaneous hydrolipidic film (Proksch et al., 2008). Keratinocytes, highly specialised cells which represent the principal elements of the epidermis, not only maintain but, following an injury, also restore the integrity of cutis in cooperation with fibroblasts.

Wound healing is a complex and dynamic multiphasic process of skin repair, encompassed within the four cascading and often overlapping stages of haemostasis, inflammation, proliferation, and remodelling. It implicates the participation of several actors, including keratinocytes, endothelial cells, fibroblasts, and immune cells, and requires the spatiotemporal orchestration of cellular elements and mediators in the damaged area. At the beginning of the inflammatory phase, a provisional matrix assists the migration of immune cells towards the injury, where they release pro-inflammatory cytokines (such as IL-6, IL-1, and TNF-α) which stimulate the subsequent tissue deposition and epithelisation by fibroblasts and keratinocytes, respectively. When the microenvironment is favourable, under the stimulus of growth factors, cytokines, and chemokines, keratinocytes undergo the reorganisation of the cytoskeleton and the expression of surface receptors, pivotal to re-epithelisation, that enable their migration (Pastar et al., 2014). The ultimate purpose of these activities is to regain tissue integrity and restore local homeostasis.

If multifactorial deleterious stimuli disrupt the delicate balance between pro-inflammatory cytokines, chemokines, proteases and their inhibitors, the reparative process is arrested in an inflammatory state which precludes the progression towards the proliferative stage (Nunan et al., 2014). Besides inflammation also hypoxia plays a prominent role in wound healing so that together they can be considered two sides of the same coin. Indeed, recent

evidence has correlated the hypoxic conditions and oxygen-dependent prolyl-hydroxylase activity to key post-translational modifications which may modulate the IL-1β pathway (Scholz et al., 2013). Oxygen availability, essential for the processes of cell proliferation, angiogenesis, and protein synthesis, is a necessary factor to sustain all the healing stages and stands out as one of the major determinants of wound healing. It is well known that local hypoxia, caused by vasculopathy or perilesional fibrosis, alters the healing process favouring inflammatory phaenomena (Toledo-Pereyra, Lopez-Neblina, & Toledo, 2004). At the same time, however, hypoxia is an important stimulus and prognostic determinant of wound healing and represents a common physiological and pathophysiological trigger to enhance the expression of survival genes through the activation of the oxygen-sensible transcription factors of the HIF complex, transcending their role as master regulators of cellular responses under hypoxia (Hong et al., 2014). Whereas persistent hypoxia leads to a delay in wound closure, an early condition of relatively mild hypoxia has conversely been demonstrated to promote wound healing.

Most commonly, the ultimate outcome of mammalian skin wound healing in adults is repair, a form of incomplete regeneration characterised by fibrosis and the formation of a scar proportional to the duration and severity of inflammation. However, recent evidence suggests that the pharmacological stabilisation of the transcription factor HIF-1a, through the inhibition of PHDs, has a role in evoking a regenerative phenotype in mammals, implying the specific substitution of the tissue (Y. Zhang et al., 2015). The non-hypoxic induction of HIF-1 transcriptional activity may then have an influence on cell survival, wound closure, and tissue regeneration, suggesting that targeting this pathway during wound healing can improve the overall process (Botusan et al., 2008; Kalucka et al., 2013; X. Zhang et al., 2013; Y. Zhang et al., 2015). Positive regulators of HIF-1, such as PHD inhibitors which prevent HIF-1a from proteasomal degradation, are currently undergoing clinical trials for the treatment of several human ischemic conditions (Bonham et al., 2018; Duscher et al., 2015).

Although many studies have been conducted to evaluate the healing potential of various therapeutic agents, there still is a scarcity of scientific

reports on substances that could facilitate the process of wound healing at a cellular and molecular level. The use of natural products and medicinal plants in the treatment of skin ailments used to be a customary practice until, in the last decades, it was gradually replaced by the introduction of synthetic drugs, which yet do not lack shortcomings, limitations, and side effects. Natural products can display multifaceted mechanisms of action in the context of wound healing, addressing different aspects of the healing process to achieve better clinical outcomes with minimal complications. In particular, the ideal candidate should be able to counteract the deleterious drawbacks of a prolonged and extensive inflammatory state, while at the same time exploiting the non-hypoxic activation of the HIF-1 pathway to trigger the cellular regenerative programme and enhance repair and possibly regeneration of cutaneous injuries.

Propolis is a natural product traditionally used for wound healing due to its renowned antimicrobial (Grange & Davey, 1990), antioxidant (Daleprane & Abdalla, 2013), and anti-inflammatory properties (Sforcin, 2007). An ointment of green Brazilian propolis has been shown to induce complete re-epithelisation in rats; however, no apparent correlation was found between the flavonoid content and the biological activity (L. L. Batista et al., 2012), demanding the elucidation of the molecular mechanisms involved and the role of the compounds found in Brazilian propolis, to unravel which molecules might be essential to the healing process. Propolis potentially integrates the ability to modulate HIF-1a stabilisation. The activity of caffeic acid phenethyl ester (CAPE), a characteristic compound commonly found in European propolis, on HIF-1 activation through prolyl-hydroxylase inhibition has been previously demonstrated (Choi et al., 2010); however, CAPE is virtually absent in Brazilian propolis. Nevertheless, Brazilian propolis has been shown to produce similar effects in a single work considering the activity of green propolis in HEK cells transfected with a reporter plasmid (Hattori et al., 2011). The choice of the model was probably dictated by the easy transfectability of HEK cells but does not reflect the complexity of the wound healing context. For this reason, it would be of great interest to investigate the same activity at the skin level,

expanding the characterisation to red propolis, which has been mainly studied for its anti-bacterial activity (Rufatto et al., 2018), and discriminating which are the molecules responsible for the effect. Until now, no bioguided fractionation of propolis components to assess the activity in the context of wound healing has been conducted and therefore the implications of the molecular effects on HIF-1 still need to be elucidated.

The aim of this project is a comprehensive *in vitro* evaluation of the biological activities, still largely unknown, of green and red Brazilian propolis varieties on cellular models of human keratinocytes and dermal fibroblasts, to elucidate their role in wound healing by specifically investigating their effects on HIF-1 pathway. Following a thorough review of the available, actually limited, scientific literature to outline the research context and formulate the research question, a two-pronged research approach was designed, directed on the one hand to the deep analytical characterisation of green and red Brazilian propolis samples and on the other to the elucidation of their spectrum of molecular activities on skin cells, with particular attention to the context of wound healing. In particular, the purpose of the investigation of anti-inflammatory, HIF-1-modulating activities, and their interrelationships is to showcase the potential of Brazilian propolis as an all-round healing agent able to elicit a regenerative cell behaviour triggered by a hypoxia-mimicking survival response. A bioguided fractionation was planned to further clarify the role of Brazilian propolis components and define the active compounds, possibly relating their structure to the observed activity.

In conclusion, the application of green and red Brazilian propolis in the context of wound healing remains speculative but highly promising. The utilisation for research purposes of thoroughly characterised propolis samples, and the comparative study of propolis belonging to different types and coming from different geographic areas appears to be one of the most interesting methodologies in recent research in this field. Brazilian propolis are well tolerated with a very rare incidence of allergy and are excellent candidates for wound management that hold all the trumps to be exploited as healing therapeutic agents. In fact, they might elicit several biological effects to

accelerate and improve the repair and regeneration process, thus offering promising perspectives for their clinical topical administration in the future.

The results of this study will contribute to elucidating the compounds and the molecular mechanisms behind the encouraging activity of Brazilian propolis in wound healing and will provide preliminary safety and efficacy data, shedding light on the possible exploitation of these natural products in skin regeneration and stimulating further pre-clinical and clinical research.

3 MATERIALS AND METHODS

3.1 BRAZILIAN PROPOLIS SAMPLES

- *Green Brazilian Propolis:* green propolis hydroethanolic tincture was purchased from "Apiário Silvestre" (Piracaia, Sâo Paulo State, South-Eastern Brazil). The sample was packaged in a 30 mL amber glass dropper bottle. The content is a dark green hydroalcoholic solution, with a flowery pungent odour, certified to contain at least 11% of green propolis.
- *Red Brazilian Propolis:* red propolis hydroethanolic tincture was purchased from "Apiário Cajueiro" (located between the cities of Una and Ilhéus, Bahia State, North-Eastern Brazil). The sample was packaged in a 30 mL amber glass dropper bottle. The content is a carmine red, aromatic hydroalcoholic solution.

Both propolis tinctures were kept overnight at -20 °C to favour the precipitation of inert waxes, which were then filtered out by vacuum filtration. The filtrate was evaporated to dryness using a rotary evaporator (Laborota 4000 efficient, Heidolph Instruments GmbH & Co., Schwabach, Germany) and the dry residue was redissolved at a concentration of 50 mg/mL in a mixture of 75:25 EtOH:H_2O, aliquoted, and stored at -20 °C for subsequent experiments.

3.2 DENSITY AND DRY RESIDUE

The density and dry residue of both propolis tinctures were calculated.

- *Density*: 500 µL of tincture were carefully withdrawn and weighed with an analytical balance. The procedure was repeated at least five times. Density was expressed as g per mL.
- *Dry residue*: the dry residue, as defined by Ph. Eur. 10.8 20816 (01/2008), was determined by evaporating to dryness a weighed amount of propolis tincture with a rotary evaporator (T = 40 °C, 280 rpm) (Laborota 4000 efficient, Heidolph Instruments GmbH & Co., Schwabach, Germany). The obtained dry residue was weighed, and the results were calculated as mass percentage.

3.3 TOTAL PHENOLIC CONTENT (TPC)

The total phenolic content was determined according to the Folin-Ciocâlteu method. Briefly, propolis samples were preliminarily diluted in deionised water (1 mg/mL) and 20 µL, corresponding to 20 µg of extract, were further diluted to a final volume of 800 µL. Then, 50 µL of 2 N Folin–Ciocâlteu reagent (Merck Life Science, Milan, Italy) and 150 µL of 20%$_{w/v}$ Na_2CO_3 were added. After 30 min of incubation at 37 °C, the absorbance of the samples was measured with a JASCO V630 UV-Vis cuvette spectrophotometer (JASCO International Co. Ltd., Tokyo, Japan) at 765 nm. The total phenolic content was quantified using a calibration curve of gallic acid (0-15 µg/mL). The assay was repeated at least in triplicate and results were expressed as mean mg of gallic acid equivalents per g of dry extract ± SD and related to the original hydroethanolic tincture.

3.4 OXYGEN RADICAL ABSORBANCE CAPACITY (ORAC) ASSAY

The oxygen radical absorbance capacity assay was carried out according to Dávalos et al. (Dávalos, Gómez-Cordovés, & Bartolomé, 2004), with minor modifications. Briefly, propolis samples were preliminarily diluted in deionised water (5 µg/mL) and 20 µL, corresponding to 0.1 µg of extract, were aliquoted into a black 96-well plate (Greiner Bio-One Italia S.r.l, Cassina de' Pecchi, Italy). Then, 120 µL of fluorescein solution (final concentration 70 nM) in phosphate buffer (75 mM, pH 7.4) were added to each well. Alkyl peroxyl radicals were generated by the addition of 60 µL of 40 mM AAPH solution [2-2'-azobis(2-aminidinopropane) dihydrochloride] (Merck Life Science, Milan, Italy). The plate was immediately put in a multilabel plate reader (VICTOR X3, PerkinElmer Italia S.p.a., Milan, Italy) thermostated at 37 °C and fluorescence (Ex. = 485 nm / Em. = 535 nm) was recorded, after shaking, every 2 min for 31 repeats. Trolox (0–120 µM) was used as a reference radical scavenger. The area under the curve (AUC) was calculated for each sample and compared with the standard Trolox curve. The assay was repeated at least in triplicate and results were expressed as mean µmol of Trolox equivalents per g of dry extract ± SD and related to the original hydroethanolic tincture.

3.5 HPLC-UV-DAD ANALYSIS

Analyses were conducted on ethanolic samples, further diluted 1:20 in ethanol and centrifuged (16000 x g, 5 min), using a Varian 940-LC analytical/semi-preparative instrument (Agilent, Cernusco sul Naviglio, Italy) equipped with binary pumps, autosampler, and UV-DAD detector operating at λ = 200–400 nm and set at the acquisition wavelength of λ = 325 nm. The chromatographical separation was obtained using a Kinetex biphenyl column (10 cm × 4.6 mm, 2.6 µm) (Phenomenex, Castel Maggiore, Italy).

Mobile phase: aqueous formic acid 0.05% (mobile phase A) and acetonitrile formic acid 0.05% (mobile phase B). Gradient: 10% B for 2 min, then 10-60% in 58 min. Flow rate: 1.6 mL/min.

3.6 GC-EI-MS ANALYSIS

- *Sample preparation*: samples for GC analysis were derivatised by silylation to mask the -OH in hydroxyl and carboxyl groups and enable volatilisation at relatively lower temperatures. Few milligrams of propolis extract, evaporated to dryness, were treated with 70 µL of the silylating agent BSTFA [N,O-bis(trimethylsilyl)trifluoroacetamide] (Merck Life Science, Milan, Italy) in 30 µL of pyridine and 100 µL of ethyl acetate. The reaction was conducted for 3 h at 70 °C, and then 1.0 µL was injected into the gas chromatograph.
- *GC-EI-MS operating parameters*: GC-MS analysis was conducted on a Bruker SCION SQ gas chromatograph (Bruker Daltonics, Macerata, Italy), equipped with a Zebron ZB-5HT Inferno column (30 m; ID 0.25 mm, df 0.25 µm) (Phenomenex, Castel Maggiore, Italy) coupled with EI source and single quadrupole (SQ) analyser.

  GC oven temperature program: 60 °C (3 min), 8.0 °C/min to 120 °C (1 min hold), 4.0 °C/min to 280 °C (1.5 min hold), 10.0 °C/min to 380°C (2 min hold) for a total runtime of 60 min. Inlet temperature: 250 °C. Flow rate: 1.00 mL/min. Carrier gas: helium 5.5. Ionisation energy: 70 eV. Split/splitless ratio 1:30 after 45 s.

Peaks were assigned by matching experimental mass spectra with those present in NIST mass spectral library (version 2.0, 2011). The relative abundance of compounds was obtained through peak area normalisation.

3.7 HPLC-ESI-HRMS ANALYSIS

Analyses were conducted on ethanolic samples, further diluted 1:20 in ethanol and centrifuged (16000 x g, 5 min), using a SYNAPT G2-Si mass spectrometer (Waters, Sesto San Giovanni, Italia) equipped with an autosampler, UPLC-PDA detector operating in the range λ = 190-400 nm, ESI source and TOF analyser. The chromatographical separation was obtained using an ACQUITY UPLC HSS T3 column (75 mm × 2.1 mm, 1.8 µm) (Waters, Sesto San Giovanni, Italia). Injection volume: 10.0 µL.

Mobile phase: acetonitrile (mobile phase A) and water (mobile phase B). Gradient: 10% A for 2 min, then 10-60% in 48 min, then 60-90% in 10 min. Desolvation is obtained with nitrogen heated at 180 °C, capillary voltage 2 kV. Data were acquired in negative mode.

3.8 CELL CULTURES

- *Human keratinocytes*: HaCaT (CVCL-0038, Cell Line Service GmbH, Germany), a stable cell line of human keratinocytes, spontaneously transformed *in vitro*, obtained from a 62-year-old Caucasic male donor (Boukamp et al., 1988) were grown as adherent monostrate in DMEM medium (Merck Life Science, Milan, Italy), supplemented with penicillin (100 units/mL) and streptomycin (100 µg/mL) (Pen Strep Gibco, Thermo Fisher Scientific, Rodano, Italy), 2 mM L-glutamine (Gibco, Thermo Fisher Scientific, Rodano, Italy), and 10% heat-inactivated foetal bovine serum (Euroclone S.p.A, Pero, Italy), at 37 °C in humidified atmosphere with 5% CO_2.
- *Human dermal fibroblasts*: HDF (ECACC, Porton Down, UK), a stable cell line of normal adult dermal fibroblasts were grown as adherent monostrate in DMEM medium (Merck Life Science, Milan, Italy), supplemented with penicillin (100 units/mL) and streptomycin (100 µg/mL) (Pen Strep Gibco, Thermo Fisher Scientific, Rodano, Italy), 2 mM L-glutamine (Gibco, Thermo

Fisher Scientific, Rodano, Italy), and 10% heat-inactivated foetal bovine serum (Euroclone S.p.A, Pero, Italy), at 37 °C in humidified atmosphere with 5% CO_2.

Every 4 days, at 80-90% of confluence, cells were detached from 75 cm^2 culture flasks (Euroclone S.p.A, Pero, Italy) using 0.25% trypsin-EDTA solution (Gibco, Thermo Fisher Scientific, Rodano, Italy), counted, and replaced in a new flask at a density of $1.5 \cdot 10^6$ cells per flask to allow the cell line expansion. For the experimental procedures, cells were seeded in flat-bottom culture plates or dishes (Falcon, Corning Life Sciences B.V., Amsterdam, The Netherlands) at a standard density of $1.5\text{-}3 \cdot 10^4$ cells/cm^2 and cultured for 72 h before the treatment.

3.9 CELL TREATMENTS

After 72 h of growth, HaCaT and HDF cells were treated with different concentrations of green and red propolis extracts using a serum-free medium. Depending on the biological parameter to be evaluated, cells were co-stimulated according to the following experimental paradigms:

- TNF-α 10 ng/mL, 6 h: assessment of NF-κB-driven transcription and IL-8 release;
- IL-1β 10 ng/mL, 6 h: assessment of NF-κB-driven transcription;
- TNF-α 10 ng/mL + IFN-γ 5 ng/mL, 24 h: assessment of IL-6 release.

3.10 CYTOTOXICITY ASSAYS

The integrity of cell morphology before and after the treatments was assessed by light microscope inspection. The viability of HaCaT and HDF cells in presence of propolis samples was investigated by MTT [3-(4,5-Dimethyl-2-thiazolyl)-2,5-diphenyl-2H-tetrazolium bromide] (Denizot & Lang, 1986), LDH (lactate dehydrogenase) release (Smith, Wunder, Norris, & Shellman, 2011), and NRU (neutral red uptake) (Repetto, del Peso, & Zurita, 2008) assays.

- *MTT*: following the treatment, the medium was removed and replaced with 0.25 mg/mL MTT [3-(4,5-Dimethyl-2-thiazolyl)-2,5-diphenyl-2H-tetrazolium bromide] (Merck Life Science, Milan, Italy) solution in PBS, then cells were

incubated for 30 min at 37 °C. At the end of incubation, the MTT solution was discarded, formazan crystals were dissolved with a 90:10 iPrOH:DMSO solution and the absorbance was measured at 570 nm using a multilabel plate reader (EnVision 2101, PerkinElmer Italia S.p.a., Milan, Italy).

- *LDH*: following the treatment, the amount of LDH released in the medium compared to total intracellular LDH was measured with LDH Cytotoxicity Detection Kit (Takara Bio Europe, Saint Germain-en-Laye, France), following the manufacturer's instructions. After 30 min of incubation at room temperature, absorbance was read at 490 nm using a multilabel plate reader (VICTOR X3, Perkin Elmer S.p.a., Milan, Italy). The results, expressed in terms of cell viability, have been calculated according to the equation modified by Smith et al. (Smith et al., 2011).
- *NRU*: following the treatment, the medium was removed and replaced with 40 µg/mL neutral red (3-amino-7-dimethylamino-2-methyl-phenazine hydrochloride) (Merck Life Science, Milan, Italy) solution in PBS, and then cells were incubated for 2 h at 37 °C. At the end of the incubation the medium was discarded, cells were thoroughly washed with PBS, and a destaining solution (EtOH 50%$_{v/v}$ + 1%$_{v/v}$ glacial acetic acid) was added to each well. The plate was kept on a plate shaker for 10 min, then the absorbance was measured at 535 nm with a multilabel plate reader (EnVision 2101, PerkinElmer Italia S.p.a., Milan, Italy).

3.11 REPORTER PLASMID ASSAYS

Two reporter plasmids were used to transiently transfect HaCaT and HDF cells:

- NF-κB-Luc, a luciferase reporter construct containing three κB responsive elements from the E-selectin gene, was a gift of Dr N. Marx (Department of Internal Medicine-Cardiology, University of Ulm, Ulm, Germany).
- HRE-Luc, a luciferase reporter construct containing three hypoxia-responsive elements (24-mers) from the Pgk-1 gene (Emerling, Weinberg, Liu, Mak, & Chandel, 2008), was a gift from Navdeep

Chandel (Addgene plasmid # 26731; http://n2t.net/addgene:26731; RRID:Addgene_26731).

- *Plasmid amplification*: plasmid amplification was obtained in transformed *Escherichia coli*, strain DH5a. Bacteria from frozen glycerinates were grown in LB broth supplemented with 100 µg/mL ampicillin (Merck Life Science, Milan, Italy), keeping flasks overnight in an orbital shaker at 37 °C. The following day, bacteria were pelleted by centrifugation (5000 rpm, 10 min, 4 °C) and the plasmid was extracted using a commercial kit according to the manufacturer's instructions (NucleoBond® Xtra Maxi; MACHEREY-NAGEL GmbH & Co. KG, Düren, Germany). The purified plasmid was resuspended in nuclease-free water and quantified with a NanoDrop ND-1000 spectrophotometer (Thermo Fisher Scientific, Rodano, Italy).
- *Transient transfection*: after preliminary titration of reporter plasmid signal to noise response, the amounts of 250 ng/well for 24-well plates and 42 ng/well for 96-well plates were chosen. Cells were transiently transfected with Lipofectamine 3000 transfection reagent (Thermo Fisher Scientific, Rodano, Italy). After incubation overnight, cells were treated and the luciferase produced was assessed using the Britelite Plus reporter gene assay system (PerkinElmer Italia S.p.a., Milan, Italy), according to the manufacturer's instruction. The luminescence generated by the reaction between luciferase and luciferin was measured with a multilabel plate reader (VICTOR X3, PerkinElmer Italia S.p.a., Milan, Italy). The assay was repeated at least in triplicate and results were expressed as mean ± SEM.

3.12 MEASUREMENT OF IL-8, IL-6, AND VEGF RELEASE

The release of IL-8, IL-6, and VEGF was evaluated by enzyme-linked immunosorbent assay (ELISA) on culture media. Human IL-8 (ABTS), IL-6 (TMB), and VEGF (ABTS) ELISA development kits were purchased from PeproTech (PeproTech, London, UK). In brief, 96-well EIA/RIA plates (Corning Life Sciences B.V., Amsterdam, The Netherlands) were coated overnight at room temperature with a capture antibody contained in the kit. The amounts of IL-8, IL-6, and VEGF in the samples were detected by measuring the absorbance

resulting from the colourimetric reaction between an HRP-conjugate and 2,2'-azino-bis(3-ethylbenzothiazoline-6-sulfonic acid) (ABTS) or 3,3',5,5'-tetramethylbenzidine (TMB) substrate (Merck Life Science, Milan, Italy). Absorbance was measured at 405 nm (ABTS) or 450 nm (TMB) using a multilabel plate reader (VICTOR X3; PerkinElmer, Milan, Italy). IL-8, IL-6, and VEGF levels were extrapolated from a standard curve of the mediator of interest. The assay was repeated at least in triplicate and results were expressed as mean ± SEM.

3.13 REACTIVE OXYGEN SPECIES (ROS) ASSAY

The intracellular ROS levels were measured in HaCaT cells with the general oxidative stress indicator CM-H2DCFDA (Thermo Fisher Scientific, Rodano, Italy). After the treatment, cells were washed with warm PBS and incubated at 37 °C for 30 min with the fluorescent probe (25 µM) diluted in HBSS without phenol red (Merck Life Science, Milan, Italy). Then, cells were washed twice with PBS and stimulated for 1 h with 1 mM H_2O_2 in a serum-free medium. At the end of the incubation, cells were washed with PBS and fluorescence intensity (Ex. = 485 nm / Em. = 535 nm) was measured with a multilabel plate reader (VICTOR X3, PerkinElmer Italia S.p.a., Milan, Italy). Trolox (500 µM) was used as a reference compound. The assay was repeated at least in triplicate and results were expressed as mean ± SEM.

3.14 IMMUNOCYTOCHEMISTRY

For immunocytochemistry experiments, cells were seeded on Nunc Lab-Tek II chamber slides (Thermo Fisher Scientific, Rodano, Italy). At the end of the treatment, cells were washed with PBS and fixed with buffered 4% formaldehyde solution for 15 min. Cells were washed 3 times with PBS and incubated for 1 h in a blocking solution consisting of 5% normal goat serum (Cell Signaling Technology B.V., Leiden, The Netherlands) + 0.3% Triton X-100 (Merck Life Science, Milan, Italy) in PBS. Then, the blocking solution was removed, and cells were incubated overnight at 4 °C with the primary antibody (HIF-1a D1S7W XP Rabbit mAb #36169, Cell Signaling Technology B.V., Leiden, The Netherlands) diluted 1:800 in 1% BSA (Merck Life Science, Milan, Italy) + 0.3% Triton X-100 (Merck Life Science, Milan, Italy) in PBS. The day after, cells were

washed 3 times with PBS and incubated for 1.5 h with the secondary antibody (Anti-rabbit IgG (H+L) F(ab')$_2$ Fragment Alexa Fluor 647 conjugate #4414, Cell Signaling Technology B.V., Leiden, The Netherlands) diluted 1:1500 and ActinRed 555 (Thermo Fisher Scientific, Rodano, Italy). Finally, cells were washed 3 times with PBS, mounted with coverslips using a drop of ProLong Gold antifade reagent with DAPI (Cell Signaling Technology B.V., Leiden, The Netherlands), and imaged with a confocal laser scanning microscope (LSM 900, Carl Zeiss S.p.a., Milan, Italy).

3.15 WESTERN BLOTTING

At the end of the treatment, cells were washed with PBS and total protein lysates were obtained by addition of RIPA buffer (50 mM Tris-HCl pH 8.0, 150 mM NaCl, 1% IGEPAL CA-630, 0.5% sodium deoxycholate, and 0.1% SDS) supplemented with a protease inhibitor cocktail (Merck Life Science, Milan, Italy). Protein concentration in each lysate was determined with the bicinchoninic acid (BCA) protein assay method (Quantum Protein, Euroclone S.p.A., Pero, Italy). An amount of cell lysate containing 35 µg or 40 µg of proteins, for HaCaT and HDF cells respectively, was mixed with 4x Laemmli sample buffer, boiled at 95 °C for 5 min, centrifuged at 16000 × g for 1 min, and loaded on 7.5% SDS-polyacrylamide gel. After running the gel, proteins were transferred to a nitrocellulose membrane using the iBlot™ Gel Transfer Device (Thermo Fisher Scientific, Rodano, Italy). Then the membrane was stained with Ponceau S solution for transfer quality assessment, cut into strips with a razor blade, and blocked for 1 h with 5% BSA (Merck Life Science, Milan, Italy) in TBST. Strips were incubated overnight at 4 °C with the primary antibodies anti-HIF-1a (HIF-1a D1S7W XP Rabbit mAb #36169, Cell Signaling Technology B.V., Leiden, The Netherlands) diluted 1:1000 and anti-β-actin (Monoclonal Anti-β-Actin Clone AC-15 produced in mouse, Merck Life Science, Milan, Italy) diluted 1:2500. After washing 3 times with TBST, membranes were incubated with anti-rabbit and anti-mouse secondary antibodies (Anti-rabbit IgG, HRP-linked Antibody #7074 and Anti-mouse IgG, HRP-linked Antibody #7076, Cell Signaling Technology B.V., Leiden, The Netherlands), respectively, for 1.5 h at room

temperature. Immunocomplexes were visualised by enhanced chemiluminescence (ECL) (Westar Antares, Cyanagen S.r.l., Bologna, Italy) and imaged with a ChemiDoc MP imaging system (Bio-Rad Laboratories S.r.l., Segrate, Italy). Protein levels were quantified with Image Studio Lite (ver. 5.2, LI-COR Biosciences GmbH, Bad Homburg vor der Höhe, Germany).

3.16 GENE EXPRESSION ANALYSIS

- *RNA extraction*: at the end of the treatment, the medium was removed, and cells were washed with PBS and lysed with QIAzol Lysis Reagent (QIAGEN S.r.l., Milan, Italy) according to the manufacturer's instructions. The lysates were homogenised and stored at -80 °C until the following RNA purification steps. Total RNA was isolated from cell lysates with miRNeasy Mini Kit (QIAGEN S.r.l., Milan, Italy), according to the manufacturer's protocol. A set of RNase-free DNase (QIAGEN S.r.l., Milan, Italy) was used to provide efficient on-column digestion of genomic DNA. Total RNA was eluted with nuclease-free water and the concentration and quality were assessed spectrophotometrically using a NanoDrop ND-1000 spectrophotometer (Thermo Fisher Scientific, Rodano, Italy). Sample purity was estimated by measuring A260/280 and A260/230 ratios to check for possible contaminants co-purified during the RNA isolation.
- *qPCR*: real-time quantitative PCR was performed using the iScript One-Step RT-PCR kit for probes (Bio-Rad Laboratories S.r.l., Segrate, Italy) according to the manufacturer's instructions, on a CFX38 Real-Time PCR Detection System (Bio-Rad Laboratories S.r.l., Segrate, Italy). Primer and probes were obtained from Eurofins Genomics Italy (Vimodrone, Italy):

Gene		5'→3' sequence
hVEGFA	Forward	CGAGGCAGCTTGAGTTAA
	Reverse	CTGTATCAGTCTTTCCTGGTG
	Probe	CTCGGCTTGTCACATCTGCAAGT
hIL6	Forward	GGGAACGAAAGAGAAGCTC
	Reverse	AGGCAACTGGACCGAA
	Probe	CGCTTGTGGAGAAGGAGTTCAT
h36B4	Forward	CCACGCTGCTGAACATGC
	Reverse	TCGAACACCTGCTGGATGAC
	Probe	AACATCTCCCCCTTCTCCTTTGGGCT

The threshold cycle value for each gene was automatically provided by the software CFX Manager (Bio-Rad Laboratories S.r.l., Segrate, Italy), depending on the amplification curves, and quantification was performed with the standard curve method. Expression data were normalised to the housekeeping gene *36B4* (ribosomal protein lateral stalk subunit P0).

3.17 HUMAN SKIN EQUIVALENT

- *HaCaT/HDF Co-cultures*: to obtain a human skin equivalent, $2 \cdot 10^5$ HDF cells were resuspended in 50 µl of FBS (Euroclone S.p.A, Pero, Italy) supplemented with penicillin (100 units/mL) and streptomycin (100 µg/mL) (Pen Strep Gibco, Thermo Fisher Scientific, Rodano, Italy) and then mixed on ice with 300 µl of type I bovine collagen (Gibco, Thermo Fisher Scientific, Rodano, Italy), 50 µl of 10x DMEM (Merck Life Science, Milan, Italy), 10 µl of 1N NaOH, and 90 µl of sterile water. The mixture was added to a 1.13 cm^2 Nunc polycarbonate cell culture insert (Thermo Fisher Scientific, Rodano, Italy) and incubated for 1 h at 37 °C to enable collagen gelation. Once the matrix was completely formed, $3 \cdot 10^5$ HaCaT cells in 500 µL of medium were seeded on top of collagen in the upper compartment, while 1000 µL of medium were added in the inferior compartment. After 24 h, keratinocytes were exposed to air and skin equivalents were cultured for 14 days, changing the medium in the inferior compartment every other day with a medium supplemented with 50 µg/mL ascorbic acid and 2 ng/mL TGF-a (Stark, Szabowski, Fusenig, & Maas-Szabowski, 2004).
- *Histology*: at the end of the experiment, skin equivalents were processed for histological analysis. In brief, co-cultures were fixed in 10% neutral buffered formalin, dehydrated in a series of alcohol, clarified in xylene, infiltrated, and embedded in paraffin. Paraffin blocks were cut into 5 µm sections using a microtome, and thin sections were floated on a warm water bath and placed on glass slides. Some slides were stained with haematoxylin and eosin (Bio-Optica Milano S.p.a., Milan, Italy) for morphology assessments in imaged with a Zeiss Axioskop 2 Plus light microscope (Carl Zeiss S.p.a., Milan, Italy). Other slides were further processed for fluorescent

immunohistochemistry. After being rehydrated, slides were subjected to heat-induced antigen retrieval in pH 6.0 10 mM citrate buffer, washed 3 times with TBST, blocked with 5% BSA + 0.3% Triton X-100 (Merck Life Science, Milan, Italy) in TBS, and then incubated overnight at 4 °C with the primary antibodies anti-K1 (Cytokeratin 1 Antibody LHK1 [NB100-2756], Novus Biologicals, Centennial, USA) diluted 1:500, anti-K10 (Cytokeratin 10 Antibody 3C2F5 [NBP2-61736], Novus Biologicals, Centennial, USA) diluted 1:500, and anti-INV (Involucrin Antibody SY5 [NBP2-34264], Novus Biologicals, Centennial, USA) diluted 1:1000. The day after, slides were washed 3 times with TBST and incubated for 1.5 h with the secondary antibody (Goat anti-mouse IgG H&L Alexa Fluor 488 ab150113, Abcam, Cambridge, UK) diluted 1:1500. Finally, slides were washed 3 times with TBST, mounted with coverslips using a drop of ProLong Gold antifade reagent with DAPI (Cell Signaling Technology B.V., Leiden, The Netherlands), and imaged with a confocal laser scanning microscope (LSM 900, Carl Zeiss S.p.a., Milan, Italy).

3.18 BIOGUIDED FRACTIONATION

- *Partition between immiscible solvents*: green and red Brazilian propolis were fractionated according to the protocol published by Santos et al. (Santos et al., 2002). In brief, an amount of propolis dry extract was dissolved in 80% EtOH and partitioned with CH_2Cl_2 (3 x 50 mL). The organic phase was sequentially partitioned with 5% aqueous $NaHCO_3$ (3 x 30 mL) to obtain organic acids, 5% aqueous Na_2CO_3 (3 x 30 mL) to obtain strong phenols, and 10% aqueous NaOH (3 x 30 mL) to obtain weak phenols, according to the sequence shown in **Fig. 43** in the Results section**.** Solvents were removed using a rotary evaporator (Laborota 4000 efficient, Heidolph Instruments GmbH & Co., Schwabach, Germany), whereas aqueous phases were freeze-dried (Modulyo 4K, Edwards Vacuum, Cinisello Balsamo, Italy). Dry residues were redissolved at a concentration of 25 or 50 mg/mL in a mixture of 80:20 EtOH:H_2O, aliquoted, and stored at -20 °C for subsequent experiments.

- *Column chromatography*: fractions obtained from partition between immiscible solvents and found to be active in screening biological assays were submitted to gravity-flow liquid chromatography on a Sephadex LH-20 column. In brief, a glass C 10/20 column (height 200 mm, column ID 10 mm; Amersham Pharmacia Biotech Italia, Cologno Monzese, Italy) was packed with Sephadex LH-20 (Cytiva Europe GmbH, Freiburg im Breisgau, Germany), pre-swollen overnight in MeOH. After loading samples, the elution was performed with MeOH. Subfractions were collected using a RediFrac fraction collector (Amersham Pharmacia Biotech Italia, Cologno Monzese, Italy), concentrated under a gentle nitrogen stream, and checked for diversity through thin layer chromatography (TLC). TLC analysis was performed on silica gel 60 G plates (Merck Life Science, Milan, Italy). Elution was conducted halfway up with EtOAc:AcOH:HCOOH:H_2O (100:11:11:26), and then the plate was dried and eluted again with DCM:EtOAc:HCOOH (85:15:0.5) up to the top. After spraying with 1% methanolic 2-aminoethyl diphenylborinate (Merck Life Science, Milan, Italy) followed by 5% methanolic PEG 4000 (Merck Life Science, Milan, Italy), plates were visualised under UV light (366 nm) and imaged. Subfractions showing high similarities were brought together, evaporated to dryness, redissolved at a concentration of 25 mg/mL in a mixture of 80:20 EtOH:H_2O, aliquoted, and stored at -20 °C for subsequent experiments.

3.19 STATISTICAL ANALYSIS

All the experiments were performed at least in triplicate. The results of TPC and ORAC assays are expressed as mean ± SD unpaired two-sample t-test. All other results are expressed as mean ± SEM and the statistical significance of differences between means has been calculated through unpaired one-way ANOVA followed by Dunnett's post-hoc test for multiple comparisons. Statistical analyses and IC_{50} calculations have been conducted using GraphPad Prism 8.0.1 (GraphPad Software Inc., San Diego, USA); *p* values less than 0.05 were considered statistically significant.

4 RESULTS

4.1 CHEMICAL CHARACTERISATION OF GREEN AND RED BRAZILIAN PROPOLIS

4.1.1 *DENSITY AND DRY RESIDUE OF THE EXTRACTS*

Brazilian green and red propolis extracts were purchased in the form of commercial hydroethanolic tinctures obtained by maceration, that were evaporated to dryness for further chemical analysis and use in biological assays. Following solvent evaporation, propolis dry extracts show different appearances: green propolis tincture takes on a soft, gluey, consistency and is characterised by a dark olive-green colour; on the other hand, red propolis tincture originates a brilliant cinnabar red powdery residue. **Table III** shows the density and dry residue values of Brazilian propolis tinctures.

Table III | *Density and dry residue (expressed as mass percentage) of Brazilian green and red propolis hydroethanolic tinctures*

	Density (g/mL)	***Dry residue (‰$_{w/w}$)***
Green propolis	0.825	18.99
Red propolis	0.871	12.14

Although the two hydroethanolic tinctures present analogous values of density, the dry residue of green propolis is greater than that of red propolis. In order to avoid any influence due to the original solvent or tincture concentration, only dry extract residues were used in subsequent experiments, redissolved at the same concentration in the appropriate solvent requested for the assays.

4.1.2 *TOTAL PHENOLIC CONTENT*

The total phenolic content (TPC) of Brazilian green and red propolis dry extracts was determined using the Folin-Ciocâlteu reagent and the gallic acid equivalent (GAE) method. **Table IV** shows the TPC values of propolis dry extracts and their relation with the original hydroethanolic tinctures.

Table IV | *Total phenolic content of Brazilian green and red propolis extracts. The results are expressed as mg of gallic acid per g of extract or tincture ± SD*

	TPC (mg GAE / g dry extract)	***TPC (mg GAE / g hydroethanolic tincture)***
Green propolis	100.67 ± 7.94	11.63 ± 0.92
Red propolis	200.59 ± 12.80	17.84 ± 1.14

A statistically significant difference in TPC between the two propolis samples was observed (unpaired two-sample t-test: dry extracts, p = 0.0003; hydroethanolic tinctures, p = 0.0018), with red propolis showing a content of total polyphenols approximately twice that of green propolis.

4.1.3 *OXYGEN RADICAL ANTIOXIDANT CAPACITY*

The oxygen radical antioxidant capacity (ORAC) of Brazilian green and red propolis dry extract was assessed and **Table V** shows the results for propolis dry extracts and their relation with the original hydroethanolic tinctures.

Table V | *ORAC values of Brazilian green and red propolis extracts. The results are expressed as µmol of Trolox per g of extract or tincture ± SD*

	ORAC value (µmol Trolox equivalents / g dry extract)	***ORAC value (µmol Trolox equivalents / g hydroethanolic tincture)***
Green propolis	44511 ± 3659	5144 ± 423
Red propolis	98009 ± 19	8719 ± 2

The two propolis samples demonstrate a statistically significant difference in the antioxidant capacity (unpaired two-sample t-test: dry extracts, p = 0.0023; hydroethanolic tinctures, p = 0.0069). Considering the potential involvement of phenolic compounds in determining the antioxidant capacity, red propolis shows an antioxidant capacity which is approximately twice, consistently with the results of the TPC.

4.1.4 *INHIBITION OF ROS GENERATION*

To assess whether the strong antioxidant capacity observed in the ORAC assay (**Table V**) was paralleled in a cellular model, the ability of green and red Brazilian propolis to inhibit ROS generation in HaCaT keratinocytes was investigated (**Fig. 4**). Cells were pre-treated for 24 h with non-cytotoxic concentrations of extracts (see paragraph 4.2.1 below) and then exposed to a pro-oxidant stimulus (H_2O_2 1 mM, 1 h). As expected, both green and red propolis showed statistically significant and pronounced inhibition of reactive oxygen species production.

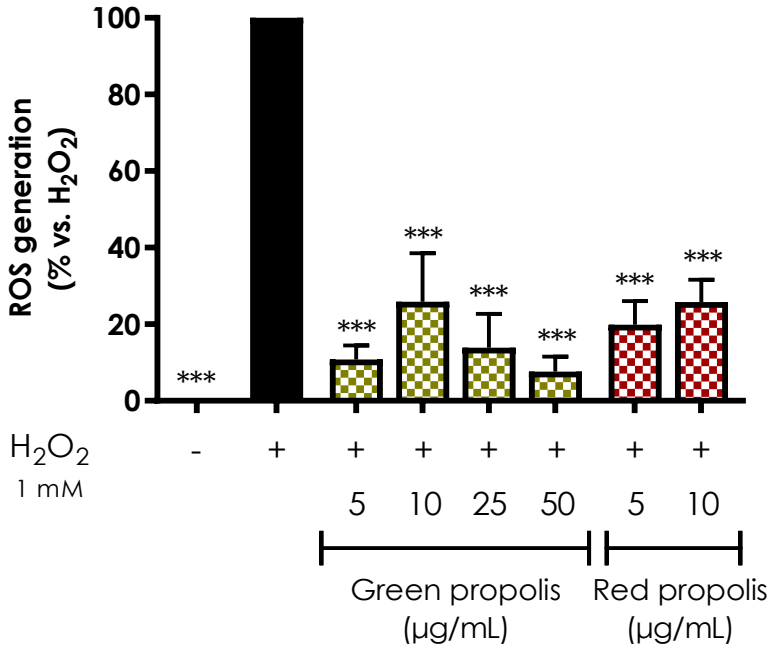

Figure 4 *| Antioxidant activity of green and red Brazilian propolis in HaCaT cells. Cells were pre-treated for 24 h with increasing non-cytotoxic propolis concentrations, then intracellular ROS production was induced by 1 mM H_2O_2 for 1 h. Data are reported as percentages with respect to the stimulus, which was arbitrarily assigned the value of 100%. *** $p < 0.001$ versus TNF-α.*

4.1.5 *HPLC-UV-DAD ANALYSIS*

Propolis chemotype and chemical characterisation were assessed in collaboration with Prof. Giangiacomo Beretta and Unitech COSPECT.

The HPLC-UV-DAD chromatograms of Brazilian green and red propolis samples (**Fig. 5 A** and **5 B**, respectively) at λ = 325 nm are shown in **Fig. 5**.

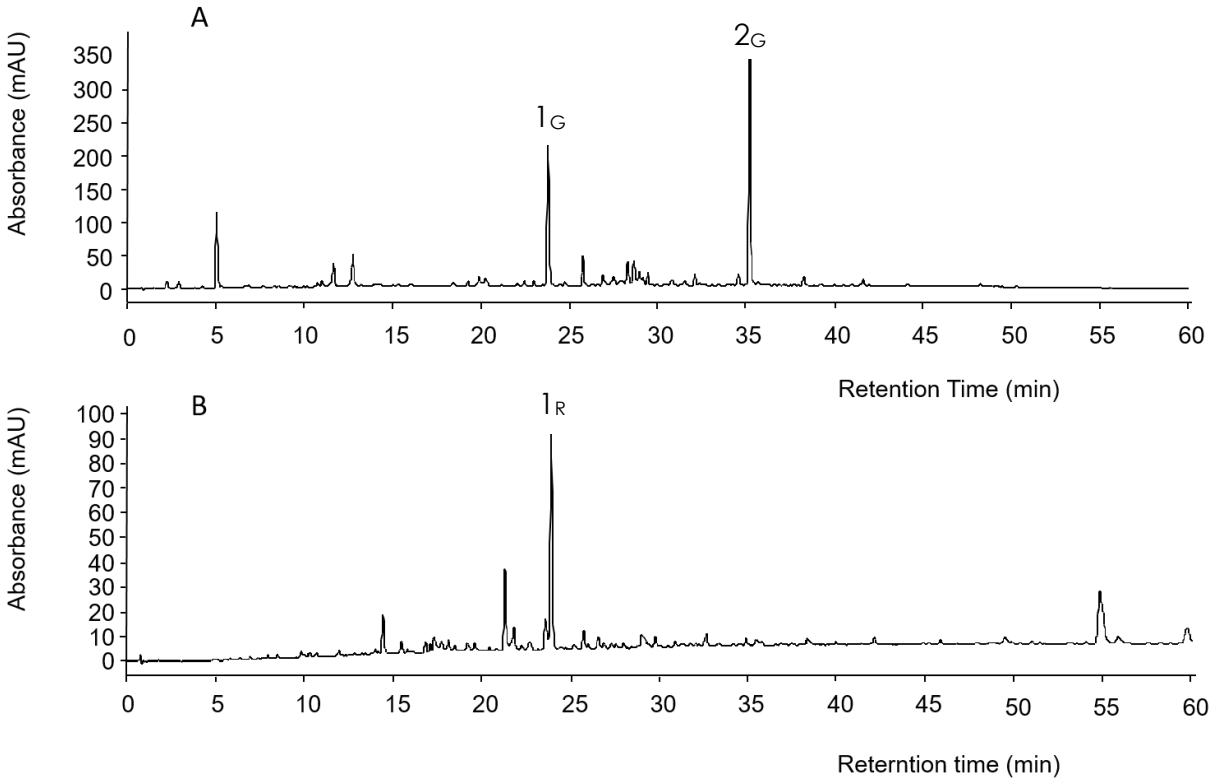

Figure 5 *| HPLC-UV-DAD (λ = 325 nm) chromatograms of green propolis (**A**) and red propolis (**B**). Numbers indicate the principal peaks that were assigned a hypothetical structure*

Upon preliminary examination of the chromatographic profiles, there are obvious differences in peak intensity and retention time between the two samples. Despite the presence of several peaks in both the chromatograms, attention has been initially focused on the compounds responsible for the main peaks detected. The assignment of spectral peaks (**Table VI**) was conducted based on the correspondence between the spectroscopic and chromatographic parameters with those present in the literature (V. Bankova et al., 2019).

In the case of green propolis, from the comparison between λ_{max} seen in UV spectra and the evidence present in literature (V. Bankova et al., 2019), the two main peaks have been attributed to the chemical structure of drupanin (RT = 23.76 min, λ_{max} = 231 nm, 315 nm, peak **1G**) and artepillin C (RT = 35.16 min, λ_{max} = 234 nm, 314 nm, peak **2G**), shown in **Fig. 6**. In addition, the accuracy of the structural assignment is supported by the similarities between UV-DAD absorption profiles shown in **Fig. 7**, which confirm that the two compounds belong to the same structural class (*p*-coumaric acid prenylated derivatives).

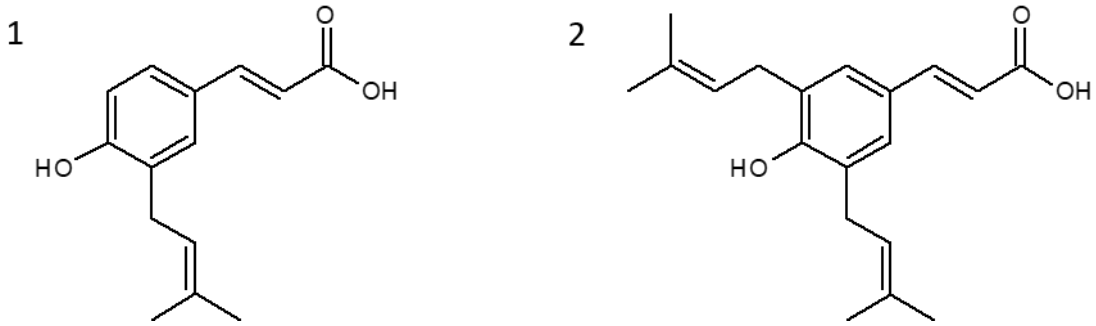

Figure 6 | *Chemical structure of drupanin (**1**) and artepillin C (**2**)*

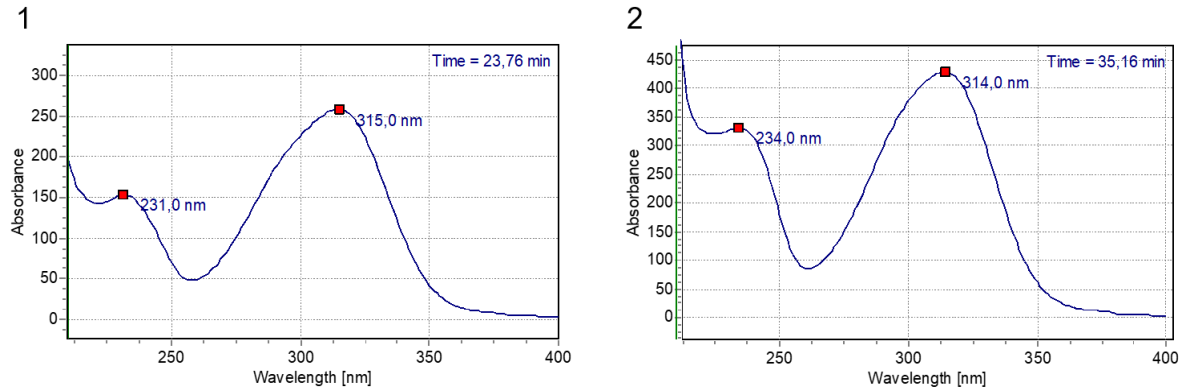

Figure 7 | *UV-Vis spectra of peak 1G (RT = 23.76 min) (**1**) and peak 2G (RT = 35.16 min) (**2**) of green propolis.*

Since chromatographical separation is conducted in reversed phase, it is expected that more lipophilic compounds will elute with greater RT. Drupanin possesses only one prenyl group in its structure, while artepillin C possesses two prenyl groups. Therefore, artepillin C will show more affinity for the stationary

phase needing more time to elute. The observed RT values are in line with the structural hypotheses proposed.

On the contrary, in the case of red propolis, it was more difficult to hypothesise a structure for the main peak seen in **Fig. 5 B** since in the literature there are no data consistent with the UV spectrum of the peak acquired at λ = 325 nm and shown in **Fig. 8.**

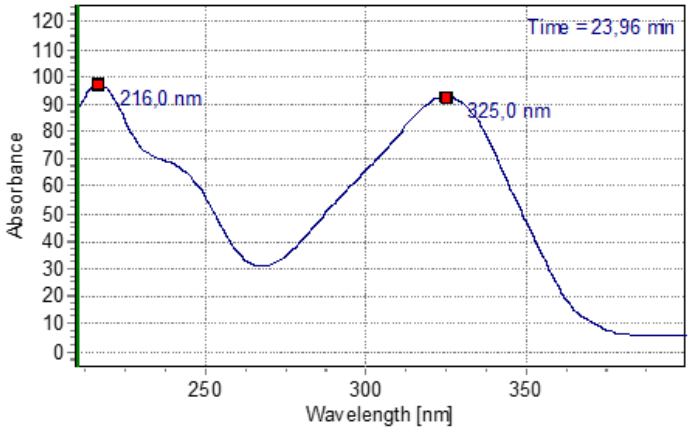

Figure 8 | *UV-Vis spectrum of the peak 1_R (RT = 23.96 min) of red propolis.*

Table VI | *Main substances found in Brazilian propolis extracts and structural hypotheses made based on literature data.*

Peak n°	***RT (min)***	***Compound***	***λ_{max} (nm)***
1_G	23.76	Drupanin	231, 315
2_G	35.16	Artepillin C	234, 314
1_R	23.96	Unknown	216, 325

Nevertheless, by carefully analysing the bidimensional UV-DAD map, it was possible to highlight two chromatographic peaks generated by substances possessing a λ_{max} of about 280 nm, with absorption profiles consistent with compounds previously reported in red propolis, vestitol and neovestitol (V. Bankova et al., 2019). **Figure 9** shows the HPLC-UV-DAD chromatographic profile of red propolis extract acquired at λ = 280 nm, while in **Table VII** are reported the chromatographic and spectroscopic data of the structures hypothesised for peaks **2_R** and **3_R**.

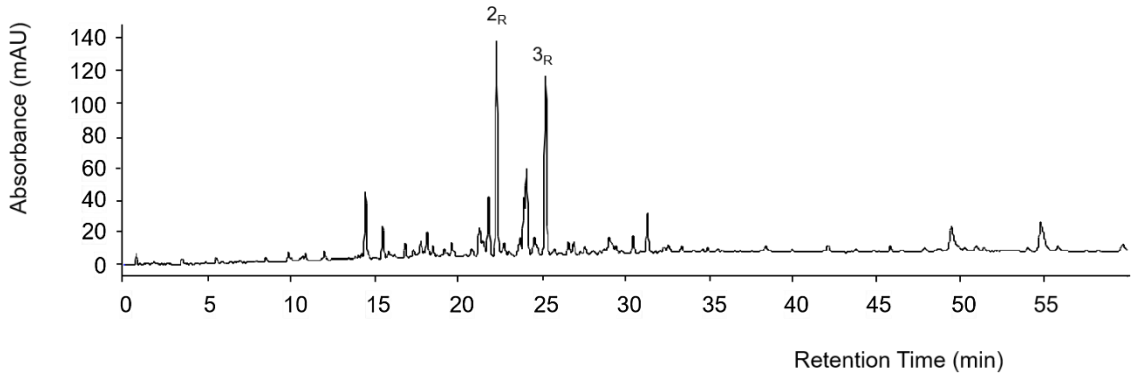

Figure 9 *| HPLC-UV-DAD (λ = 280 nm) chromatograms of red propolis. Numbers indicate the principal peaks that were assigned a hypothetical structure.*

Table VII *| Main substances found in red propolis extract, hypothesised on the basis of literature data.*

Peak n°	***RT (min)***	***Compound***	***λ_{max} (nm)***
2R	22.29	Vestitol/neovestitol	281
3R	25.21	Vestitol/neovestitol	283

Fig. 10 shows that the two molecules share the same core structure of 5-deoxyisoflavans.

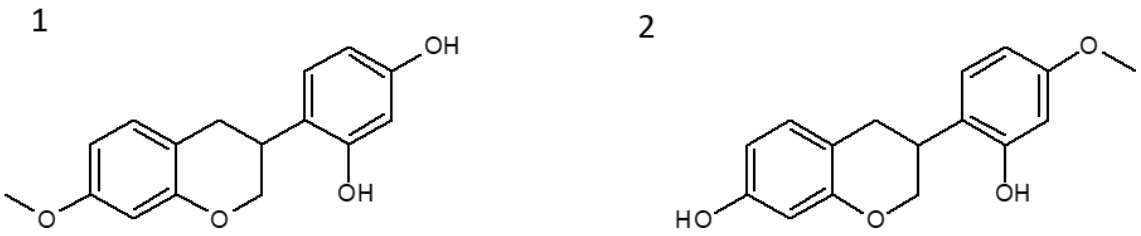

Figure 10 *| Chemical structure of neovestitol (**1**) and vestitol (**2**).*

The similarities between UV-DAD absorption profiles shown in **Fig. 11** confirm that the molecules belong to the same structural class.

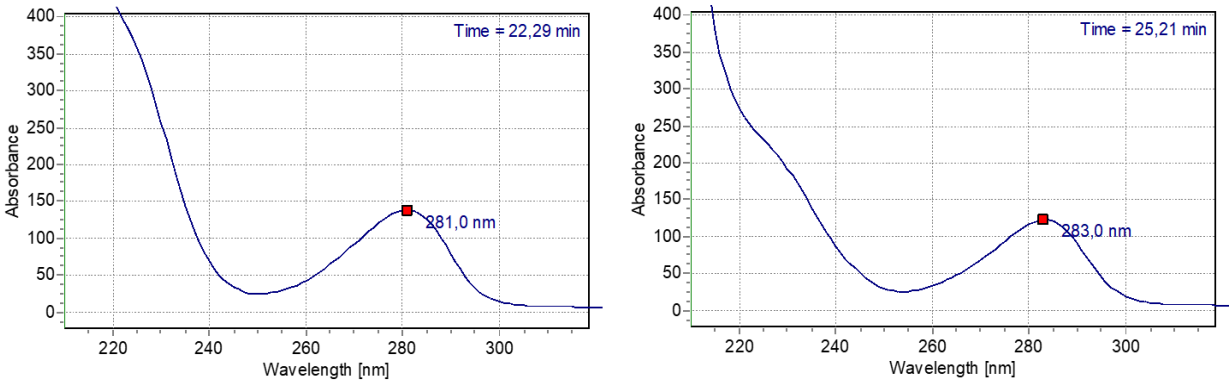

Figure 11 | *UV-Vis spectra of peak 1 (RT = 22.29 min) and peak 2 (RT = 25.21 min) of red propolis.*

Neovestitol and vestitol are structural isomers, which differ in the position of a methoxy group, and in absence of reference standards, it is difficult to interpret their retention times and unequivocally assign the peaks.

The need to obtain more information on green and red propolis composition asked for a complementary analytical technique, such as gas chromatography coupled with mass spectrometry.

4.1.6 *GC-EI-MS*

The GC-EI-MS chromatograms of previously silylated green and red Brazilian propolis samples (**Fig. 12 A** and **12 B**, respectively) are shown in **Fig. 12**. Even in this case, it is evident that the two propolis samples possess completely different composition profiles.

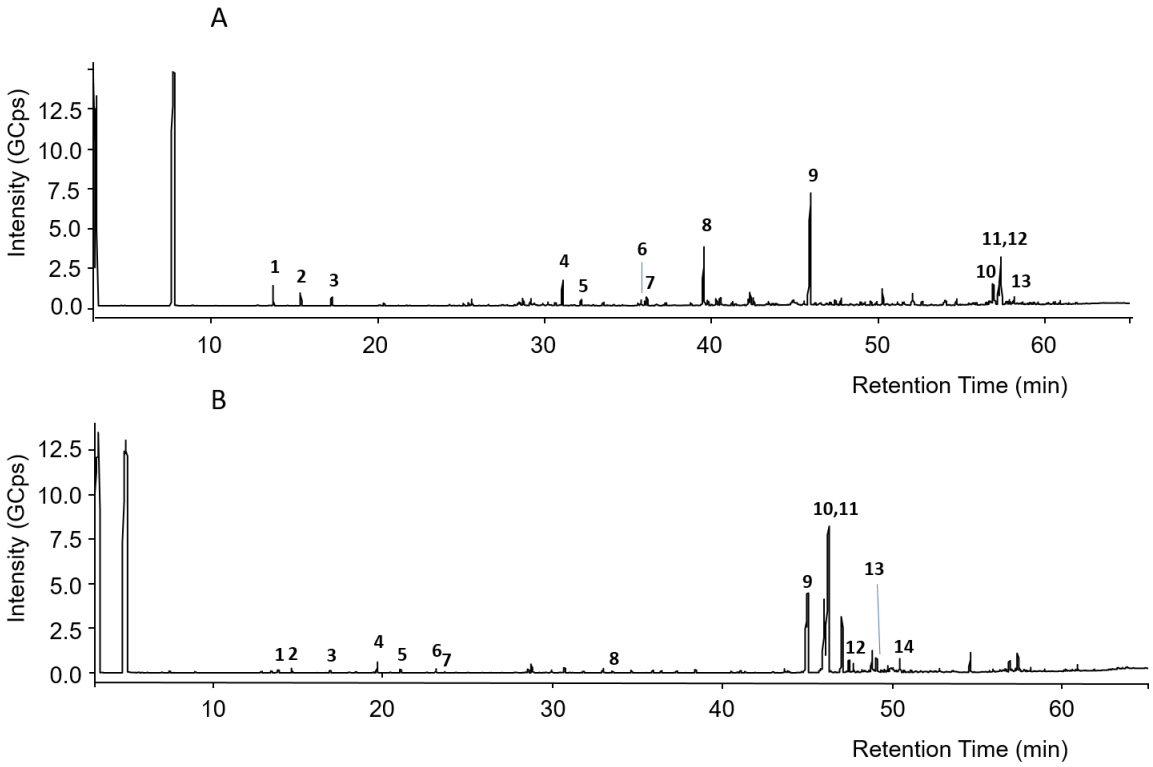

Figure 12 *| GC-MS chromatograms of silylated green propolis (A) and red propolis (B). Numbers indicate the principal peaks that were assigned a structure through a comparison of mass spectra with those found in the literature. Numbers refer to compounds listed in* ***Table VIII*** *and* ***Table IX****.*

The assignment of peaks, listed in **Tables VIII** and **IX**, has been conducted by comparison of recorded mass spectra with those in the NIST 2011 mass spectral library or reported in the literature (V. Bankova et al., 2019; Freires et al., 2016; Rohloff, 2015).

Table VIII *| Compounds identified by GC-EI-MS in green propolis. TMS: trimethylsilyl group*

Peak n°	***RT (min)***	***Compound***	***Relative %***
1	13.763	Glycerol 3TMS	0.9
2	15.411	Di-hydrocinnamic acid, ethyl ester	0.6
3	17.261	Di-hydrocinnamic acid TMS	0.4
4	31.095	*p*-coumaric acid 2TMS	1.3
5	32.202	Palmitic acid, ethyl ester	0.3
6	35.791	Caffeic acid 3TMS	0.3
7	36.137	Oleic acid, ethyl ester	0.5
8	39.541	Drupanin 2TMS	3.6
9	45.923	Artepillin C 2TMS	8.5
10	56.864	β-amyrin TMS	1.8
11	57.204	α-amyrin TMS	1.0
12	57.310	Cycloartenol acetate	3.4
13	58.115	Lupeol acetate	0.4

In green propolis, the relative intensity of peaks demonstrates that the principal compounds, identified as TMS derivatives; are artepillin C (*m/z* = 444.3 $[M+H]^+$, peak 9), drupanin (*m/z* = 376.2 $[M+H]^+$, peak 8), *p*-coumaric acid (*m/z* = 308.1 $[M+H]^+$, peak 4), as well as some sesquiterpenes such as cycloartenol acetate (*m/z* = 468.5 $[M+H]^+$, peak 12) and β-amyrin (*m/z* = 498.5 $[M+H]^+$, peak 10), the structure of which are shown **Fig. 13**.

The evidence that drupanin and artepillin C are the most abundant compounds in the GC profile of green propolis corroborates the structural hypotheses formulated based on HPLC-UV-DAD analysis.

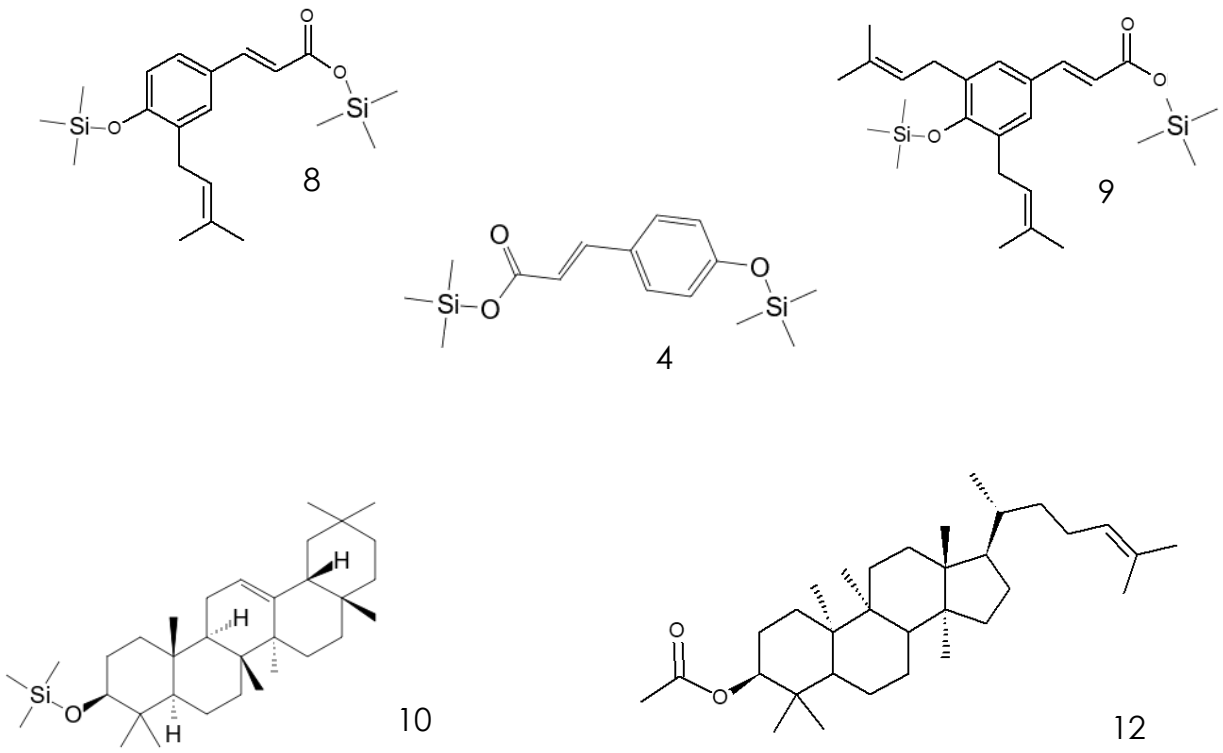

Figure 13 *| Structures of the main compounds identified in green propolis through GC-EI-MS.*

Table IX *| Compounds identified by GC-EI-MS in red propolis. TMS: trimethylsilyl group*

Peak n°	***RT (min)***	***Compound***	***Relative %***
1	13.794	Estragole	0.13
2	14.591	Succinic acid 2TMS	0.24
3	16.861	Methyleugenol	0.11
4	19.627	Malic acid 3TMS	0.57
5	21.015	Elemicin	0.17
6	23.099	Eugenol TMS	0.21
7	23.612	Asarone	0.07
8	33.498	Palmitic acid TMS	0.09
9	44.993	Medicarpin TMS	9.73
10	45.963	Neovestitol 2TMS	7.52
11	46.205	Vestitol 2TMS	14.60
12	47.429	Liquiritigenin 2TMS	0.8
13	49.05	Formononetin TMS	1.12
14	50.422	Isoliquiritigenin 3TMS	0.94

In red propolis, the relative intensity of peaks demonstrates that the principal compounds, identified as TMS derivatives, are vestitol (*m/z* = 416.2 $[M+H]^+$, peak 11), neovestitol (*m/z* = 416.2 $[M+H]^+$, peak 10), and medicarpin (*m/z* = 342.2 $[M+H]^+$, peak 9), while liquiritigenin (*m/z* = 400.2 $[M+H]^+$, peak 12) and formononetin (*m/z* = 340.2 $[M+H]^+$, peak 13) are marginally present. Based on these results, it was hypothesised that the two most intense peaks seen in HPLC-UV-DAD might actually be related to the two main compounds observed in GC-EI-MS analysis, neovestitol and vestitol, the structures of which, together with those of other identified compounds, are reported in **Fig. 14**.

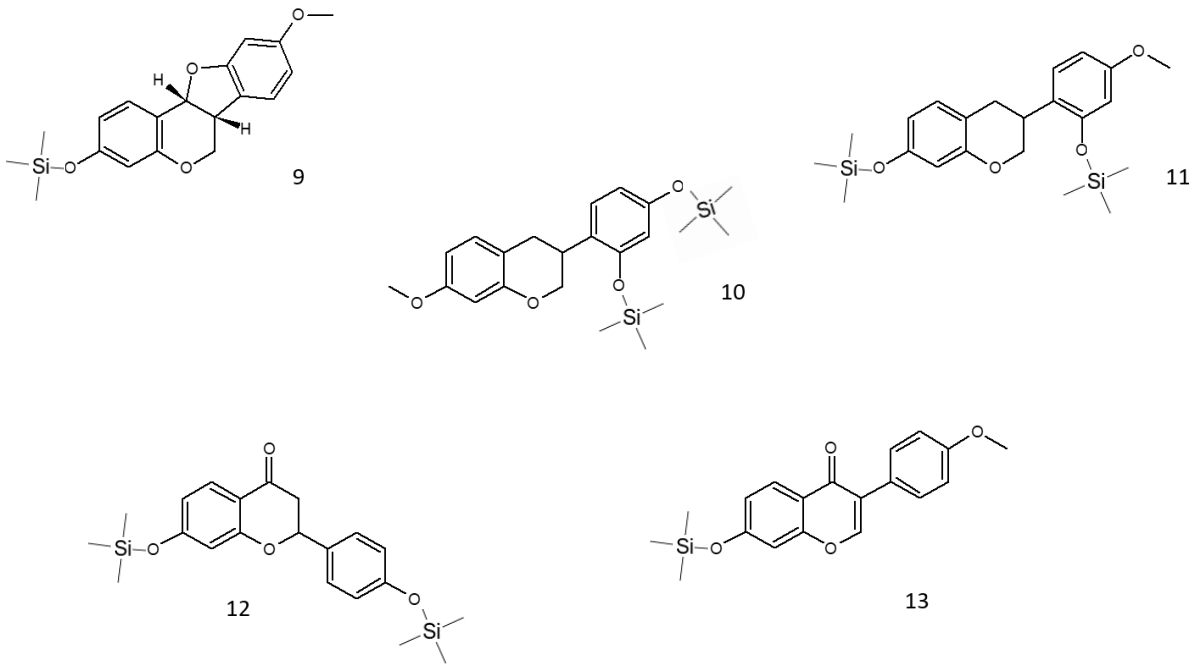

Figure 14 | *Structures of the main compounds identified in red propolis through GC-EI-MS.*

4.1.7 *HPLC-ESI-HRMS*

In **Fig. 15** and **16** the chromatograms obtained for green and red propolis, respectively, in HPLC-UV/PDA-ESI-HRMS analysis, are compared. The identified compounds are listed in **Tables X** and **XI**.

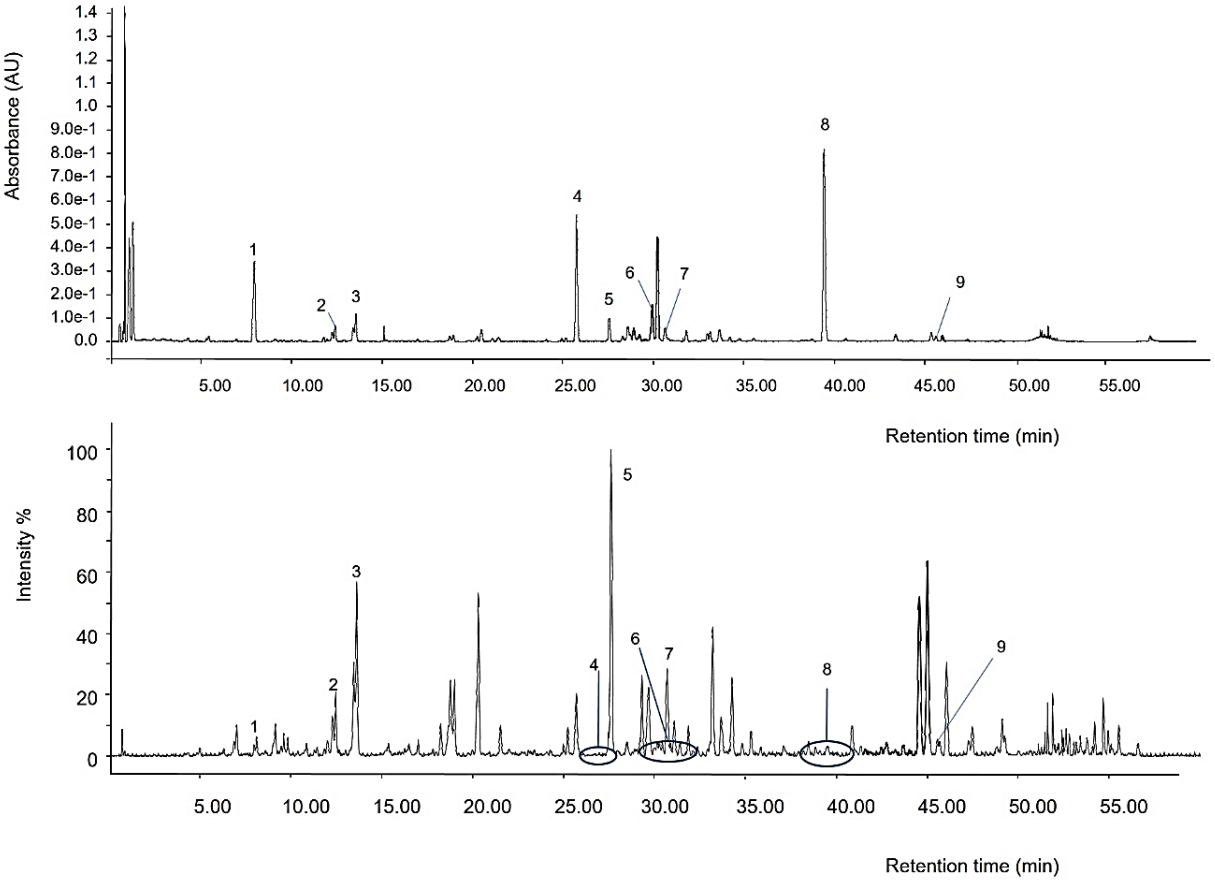

Figure 15 | *Comparison of HPLC-UV/PDA and MS/TOF chromatograms of green propolis. Numbers indicate the principal peaks that were assigned a structure based on the spectroscopic and spectrophotometric parameters observed. Numbers refer to compounds listed in* ***Table X****.*

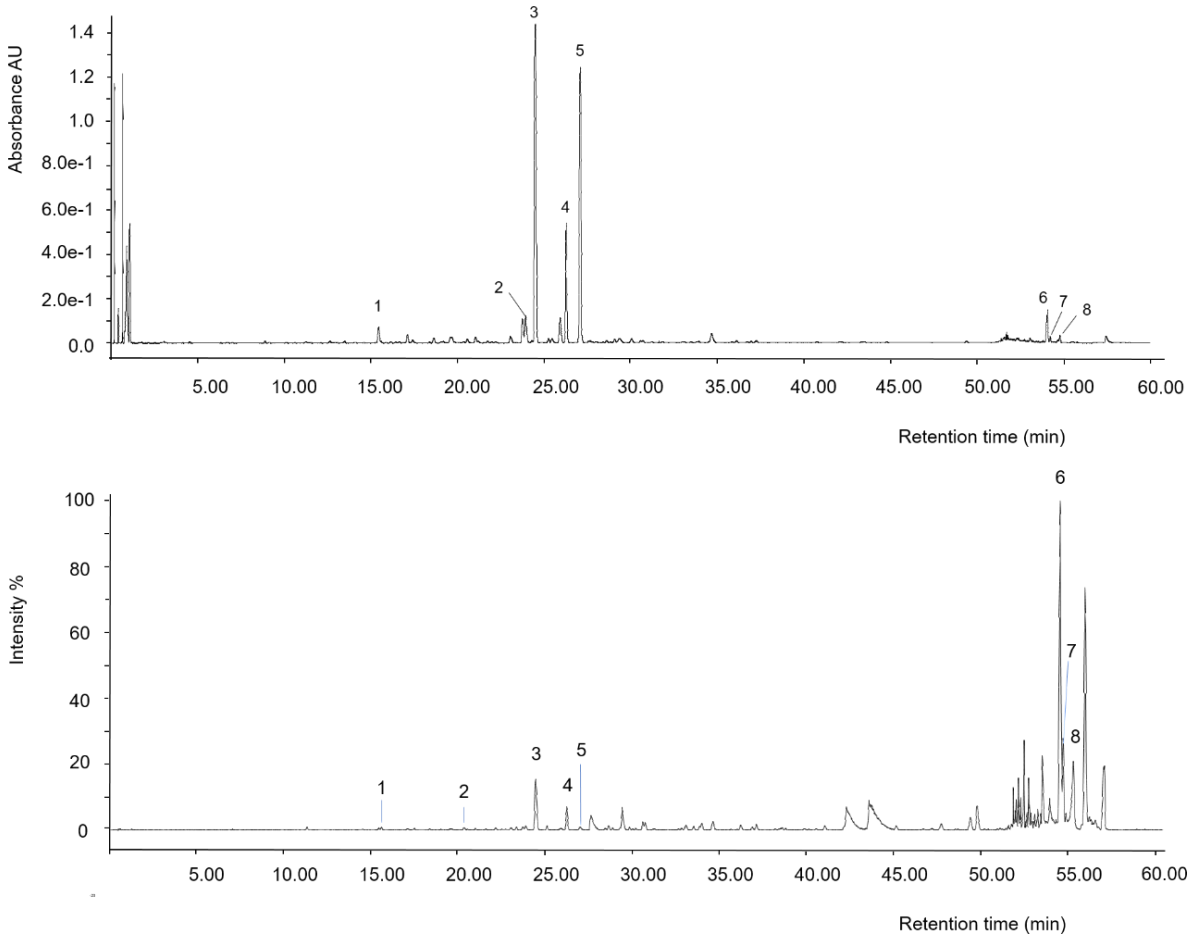

Figure 16 | *Comparison of HPLC-UV/PDA and MS/TOF chromatograms of red propolis. Numbers indicate the principal peaks that were assigned a structure on the basis of the spectroscopic and spectrophotometric parameters observed. Numbers refer to compounds listed in* ***Table XI****.*

Table X *| Compounds identified in green propolis through HPLC-ESI-HRMS analysis.*
§compounds identified also in GC-MS analysis.

Peak n°	RT (min, UV/PDA)	RT (min, MS-TOF)	m/z exp. ESI (-)	m/z calc (-)	Compound	λ_{max}	Formula
1	7.93	7.959	163.0399	163.0401	*p*-coumaric acid§	228, 310	$C_9H_8O_3$
2	12.40	12.457	515.1195	515.1195	Di-O-caffeoylquinic	244, 327	$C_{25}H_{24}O_{12}$
3	13.54	13.605	515.1190	515.1195	Di-O-caffeoylquinic	244, 326	$C_{25}H_{24}O_{12}$
4	25.73	25.724	231.1029	231.1027	Drupanin§	236, 315	$C_{14}H_{16}O_3$
5	27.54	27.607	315.1601	-	Not identified	240, 314	$C_{19}H_{23}O_4$
6	29.93	30.019	389.1965	299.0561	Kaempferide	266, 369	$C_{16}H_{12}O_6$
7	30.62	30.684	329.0660	329.0667	Dimethylquercetin	370	$C_{17}H_{14}O_7$
8	39.42	39.548	299.1633	299.1653	Artepillin C§	238, 314	$C_{19}H_{24}O_3$
9	45.60	45.591	363.1591	363.1602	Baccharin	283	$C_{23}H_{24}O_4$

The principal compounds identified in green propolis are *p*-coumaric acid (*m/z* 163 $[M-H]^-$, peak 1), drupanin (*m/z* 231 $[M-H]^-$, peak 4), artepillin C (*m/z* 299 $[M-H]^-$, peak 8). The structures of identified molecules are reported in **Fig. 17.**

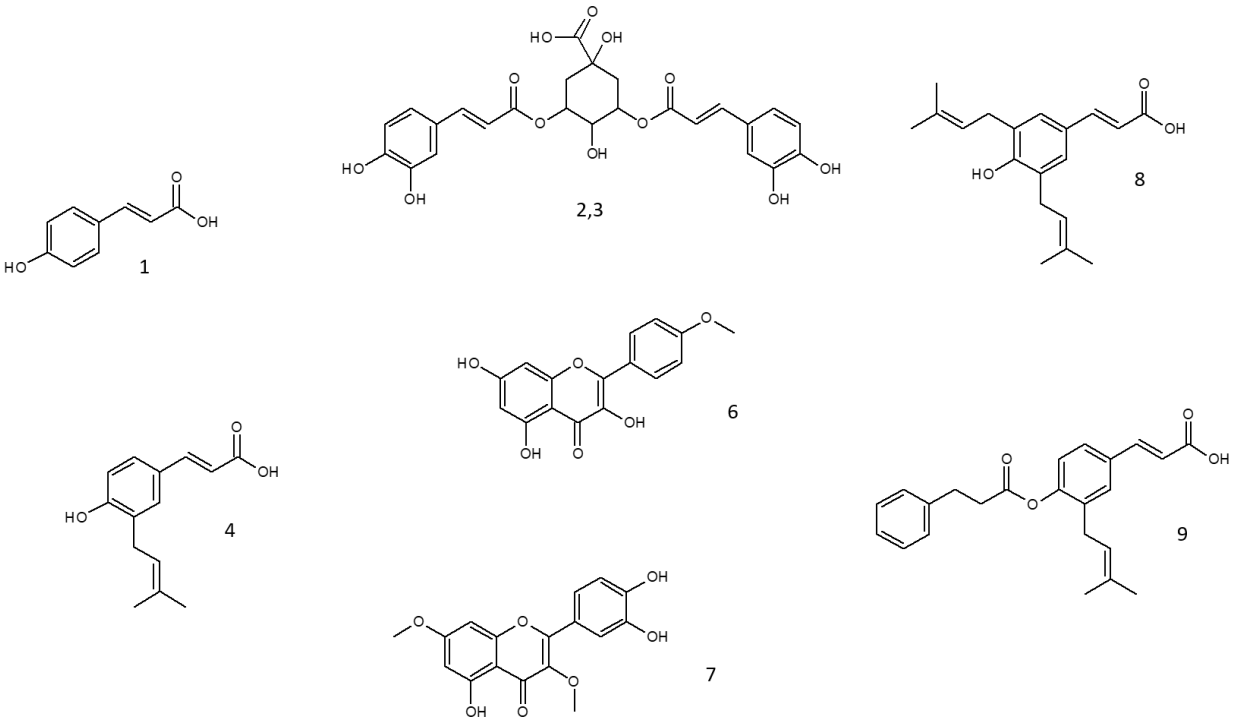

Figure 17 | *Structures of the main compounds identified in green propolis through HPLC-ESI-MS.*

***Table XI** | Compounds identified in red propolis through HPLC-ESI-HRMS analysis.*
§compounds identified also in GC-MS analysis.

Peak n°	RT (min, UV/PDA)	RT (min, MS-TOF)	m/z exp. ESI (-)	m/z calc (-)	Compound	λ_{max}	Formula
1	15.30	15.349	255.0657	255.2460	Liquiritigenin§ / isoliquiritigenin§	236, 276	$C_{15}H_{12}O_4$
2	23.66	23.701	267.0658	267.2567	Formononetin§ / isoformononetin§	249	$C_{16}H_{11}O_4$
3	24.23	24.284	271.0974	271.2884	Vestitol/neovesitol§	202, 280	$C_{16}H_{16}O_4$
4	25.99	26.031	271.0972	271.2884	Vestitol/neovesitol§	202, 280	$C_{16}H_{16}O_4$
5	26.76	26.801	269.0813	269.2726	•Medicarpin§ •4,4'-dihydroxi-2-methoxychalcone •(7 S)-dalbergiphenol	205, 287	$C_{16}H_{14}O_4$ $C_{16}H_{14}O_4$ $C_{16}H_{14}O_4$ $C_{16}H_{14}O_4$
6	54.06	54.148	601.3535	601.7926	Guttiferone	252, 354	$C_{38}H_{50}O_6$
7	54.21	54.303	601.3531	601.7926	Guttiferone	254, 345	$C_{38}H_{50}O_6$
8	54.79	54.88	501.3003	501.6768	Nemorosone	305	$C_{33}H_{42}O_4$

The principal compounds identified in red propolis are vestitol and neovestitol (*m/z* 271, peaks 3,4), medicarpin/4'-dihydroxy-2-methoxychalcone/(7 S)-dalbergiphenol (all with *m/z* 269 and the same molecular formula, peak 5), guttiferone (*m/z* 601, peaks 6,7). The structures of identified molecules are reported in **Fig. 18**.

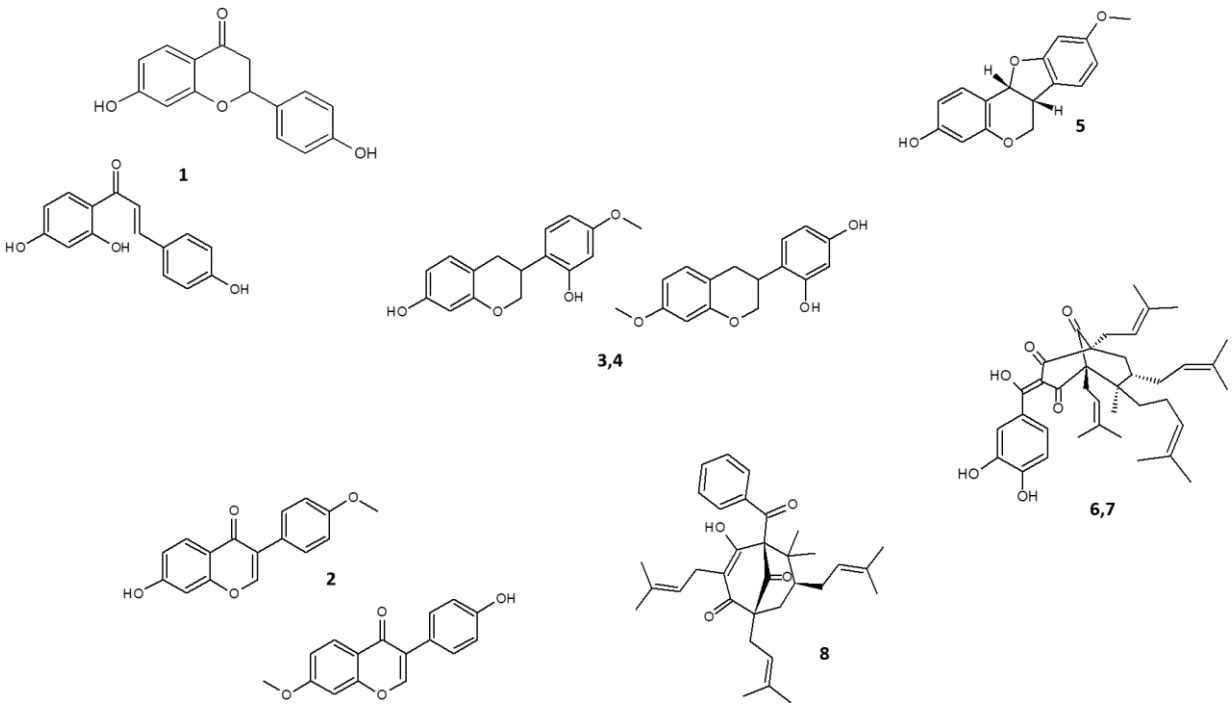

Figure 18 | *Structures of the main compounds identified in red propolis through HPLC-ESI-MS.*

The assignment of the main peaks to the respective compounds was made possible by the comparison of spectroscopic and spectrophotometric parameters with those reported in the literature [Green propolis: (V. Bankova et al., 2019; Pellati, Orlandini, Pinetti, & Benvenuti, 2011); Red propolis: (V. Bankova et al., 2019; da Cruz Almeida et al., 2017; de Mendonça et al., 2015)]. Since the signal was acquired in negative ion mode, MS peak assignment was conducted taking into consideration *m*/z values corresponding to $[M-H]^-$. Further confirmation was obtained through the elemental analysis of *m*/z fragments of interest. The results of this analysis are reported in **Appendix B**.

In some cases, besides the deprotonated pseudomolecular peaks, it was possible to appreciate peaks with *m*/z value corresponding to $[2M-H]^-$, indicating molecule dimerisation within the ion source.

In **Fig. 19** the case of neovestitol/vestitol is reported as an example.

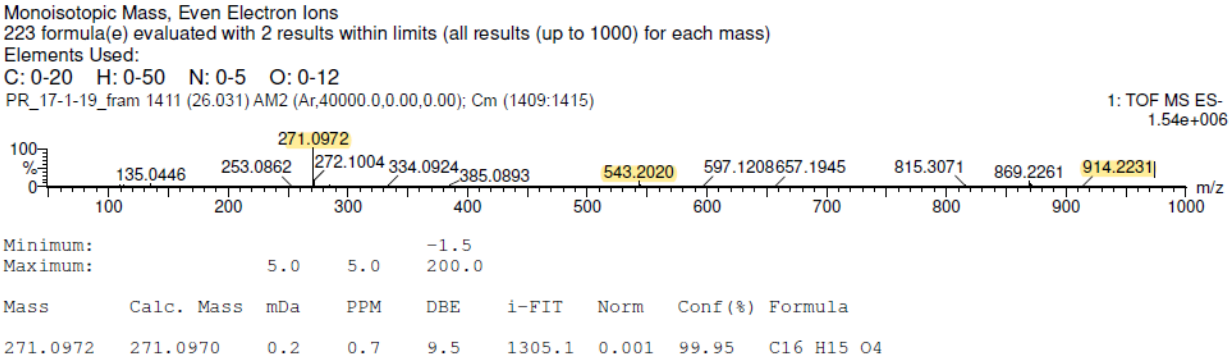

Minimum:				-1.5				
Maximum:		5.0	5.0	200.0				
Mass	Calc. Mass	mDa	PPM	DBE	i-FIT	Norm	Conf(%)	Formula
271.0972	271.0970	0.2	0.7	9.5	1305.1	0.001	99.95	C16 H15 O4

Figure 19 *| TOF mass spectrum of neovestitol/vestitol. The molecular peak has m/z s 271.0972 $[M-H]^-$, the dimer peak has m/z 543.2020 $[M-H]^-$*

4.2 BIOLOGICAL ACTIVITY OF GREEN AND RED BRAZILIAN PROPOLIS

4.2.1 *CYTOTOXICITY ASSAYS*

Before proceeding with the evaluation of the biological activities in keratinocytes and fibroblasts, cytotoxicity was evaluated to assess the influence on cell viability and determine the maximum concentrations to be used in cell treatments.

At 6 h, green Brazilian propolis extract did not affect viability, neither in HaCaT (**Fig. 20**) nor HDF (**Fig. 21**) cells. On the other hand, red propolis extract induced a slight reduction of viability in HaCaT cells, measured by MTT assay at the concentrations of 25 and 50 µg/mL. Given a certain variability and to dispel possible doubts, cytotoxicity at the highest concentrations was assessed also by LDH assay, demonstrating the substantial absence of significant cytotoxic effects. As a consequence, in 6 h treatments both propolis have been used up to the concentration of 50 µg/mL.

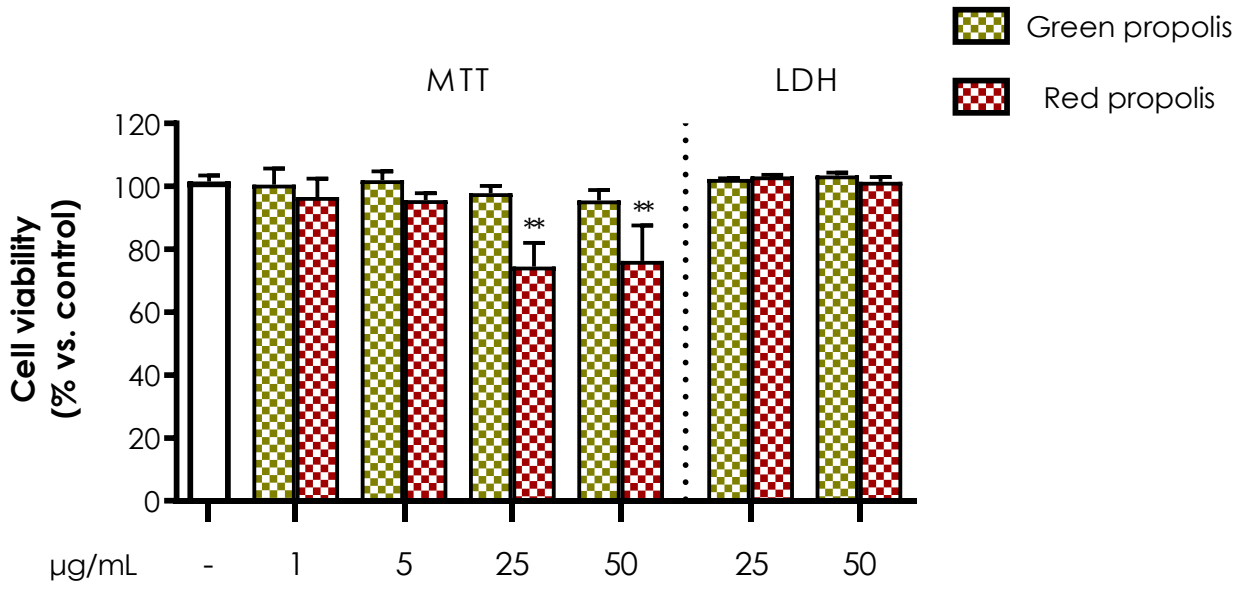

Figure 20 *| Assessment of green and red Brazilian propolis effect on HaCaT cell viability through MTT and LDH assays. HaCaT cells were treated for 6 h in presence of increasing propolis concentrations. Data are reported as percentages with respect to the control, which was arbitrarily assigned the value of 100%. ** $p < 0.01$ versus control.*

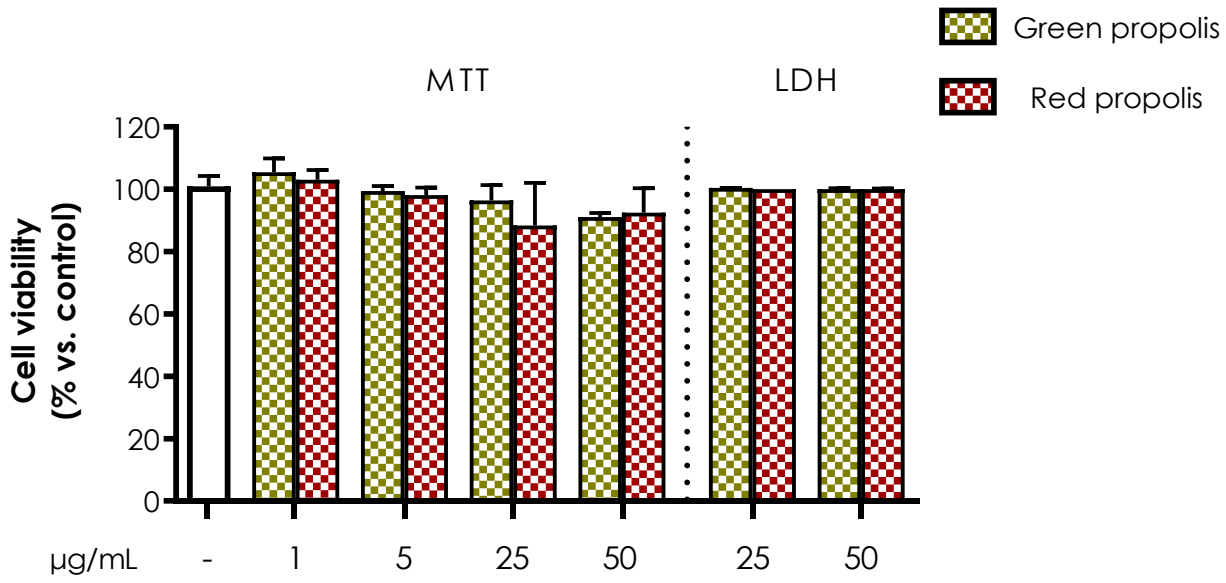

Figure 21 | *Assessment of green and red Brazilian propolis effect on HDF cell viability through MTT and LDH assays. HDF cells were treated for 6 h in presence of increasing propolis concentrations. Data are reported as percentage with respect to the control, which was arbitrarily assigned the value of 100%.*

At 24 h, once again green propolis extract did not affect viability, neither in HaCaT (**Fig. 22 A**) nor HDF (**Fig. 22 B**) cells. Instead, red propolis extract showed significant cytotoxic effects in HaCaT cells at the concentrations that had yielded dubious results at 6 h. As a consequence, in 24 h treatments in HaCaT cells red propolis has been used up to the concentration of 10 µg/mL.

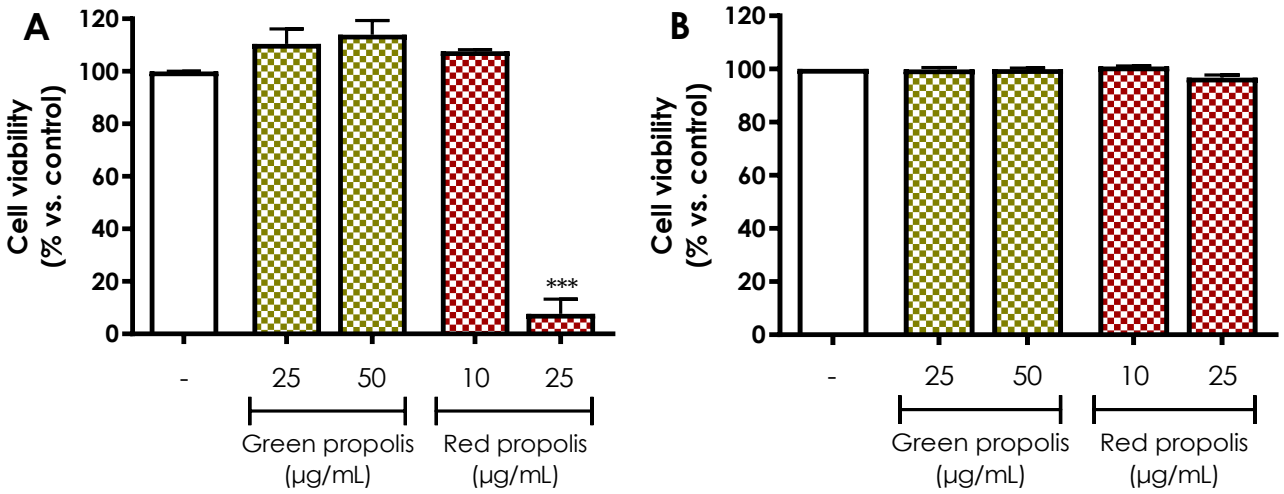

Figure 22 *| Assessment of green and red Brazilian propolis effect on HaCaT (**A**) and HDF (**B**) cell viability through LDH assay. Cells were treated for 24 h in presence of increasing propolis concentrations. Data are reported as percentage with respect to the control, which was arbitrarily assigned the value of 100%. *** p < 0.001 versus control.*

4.2.2 *EFFECT ON NF-κB-DRIVEN TRANSCRIPTION*

To assess the ability of green and red Brazilian propolis to inhibit NF-κB-driven transcription in keratinocytes and fibroblasts, cells were transiently transfected with an NF-κB-Luc reporter plasmid, subjected to a pro-inflammatory stimulus (TNF-α 10 ng/mL, 6 h), and concomitantly treated with increasing concentrations of propolis (1-50 µg/mL).

In HaCaT cells (**Fig. 23**), green propolis was able to partially inhibit NF-κB-driven transcription, in a statistically significant manner, only at the concentrations of 25 and 50 µg/mL, with an IC_{50} of 40.29 µg/mL. The effect of red propolis is greater and markedly concentration-dependent, with an IC_{50} of 8.51 µg/mL. At 25 and 50 µg/mL, NF-κB-driven transcription was brought back to basal levels.

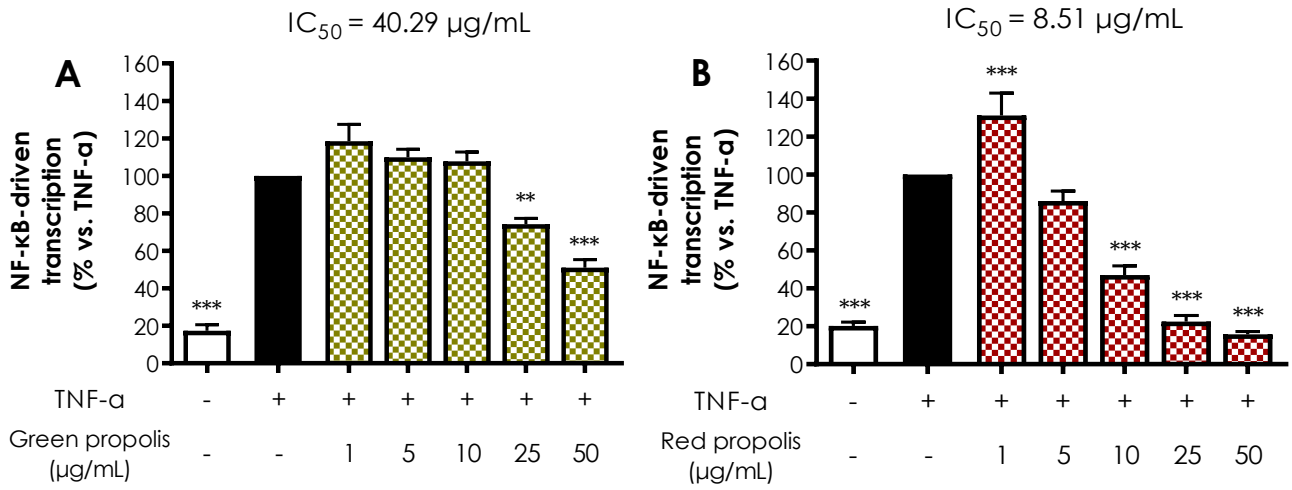

Figure 23 *| Assessment of green (**A**) and red (**B**) Brazilian propolis effect on NF-κB-driven transcription in HaCaT cells. Cells were stimulated with 10 ng/mL of TNF-α and treated for 6 h with increasing propolis concentrations. Data are reported as percentage with respect to the stimulus, which was arbitrarily assigned the value of 100%. ** p < 0.01, *** p < 0.001 versus TNF-α.*

In HDF cells (**Fig. 24**), in the case of green propolis, a concentration-dependent response was not observed, even though at the highest concentrations a slight inhibition of NF-κB-driven transcription could be seen. On the contrary, despite the entity of the effect being lower compared to

HaCaT cells, red propolis was once again able to bring NF-κB-driven transcription back to basal levels in a concentration-dependent manner, with an IC_{50} of 23.83 µg/mL.

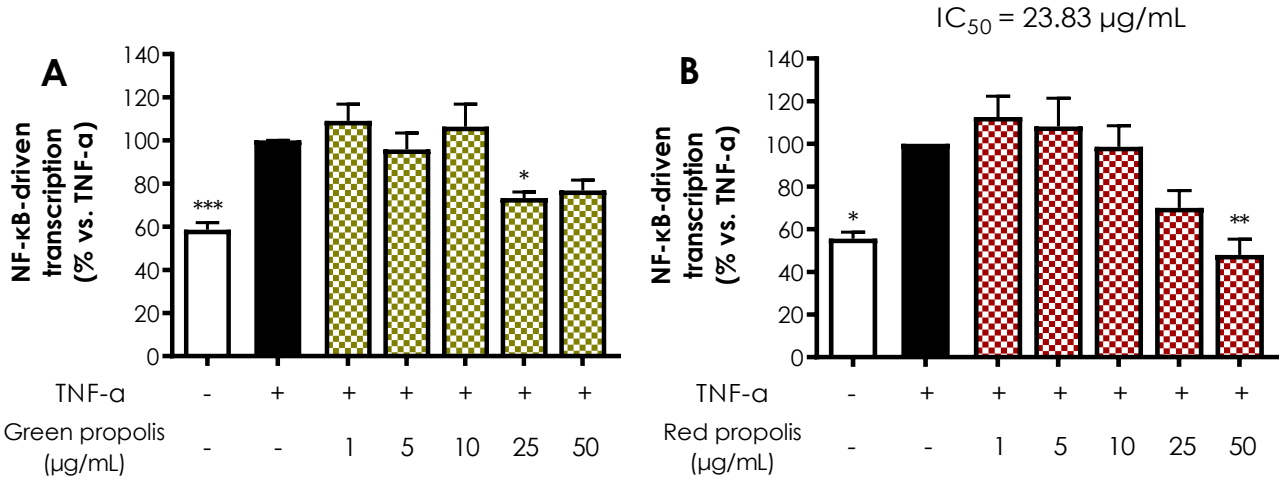

Figure 24 *| Assessment of green (**A**) and red (**B**) Brazilian propolis effect on NF-κB-driven transcription in HDF cells. Cells were stimulated with 10 ng/mL of TNF-α and treated for 6 h with increasing propolis concentrations. Data are reported as percentage with respect to the stimulus, which was arbitrarily assigned the value of 100%. * p < 0.05, ** p < 0.01, *** p < 0.001 versus TNF-α.*

The effect on NF-κB-driven transcription has been further evaluated using IL-1β (10 ng/mL, 6 h) as a pro-inflammatory stimulus, only in HaCaT cells since in HDF cells NF-κB activation was found not to be elicited by this cytokine. The rationale behind this experiment lies in evidence that prolyl-hydroxylases (PHDs), involved in the regulation of HIF-1 pathway activation, might also modulate inflammation via key post-translational modifications in the IL-1β pathway, being required for IL-1β-induced NF-κB activation (Scholz et al., 2013). Thus, substances able to inhibit PHDs, and potentially enhance HIF-1 signalling, would likewise be able to limit IL-1β-induced NF-κB-driven transcription exerting anti-inflammatory effects. For this reason, dimethyloxalylglycine (DMOG), a synthetic PHD inhibitor which substitutes for 2-oxoglutarate hindering the enzymatic activity (Yuan et al., 2014), has been used as a reference compound.

Green propolis determined a slight inhibition of IL-1β-induced NF-κB-driven transcription at the highest concentration tested of 50 µg/mL (**Fig. 25 A**), reaching a level comparable to DMOG. The effect of red propolis was greater, with an IC_{50} of about 10 µg/mL (**Fig. 25 B**). At the concentrations of 25 and 50 µg/mL, it brought NF-κB-driven transcription back to basal levels and proved to be by far superior compared to DMOG, demonstrating the existence of an alternative additive mechanism on the IL-1β pathway other than the putative inhibition of PHD activity.

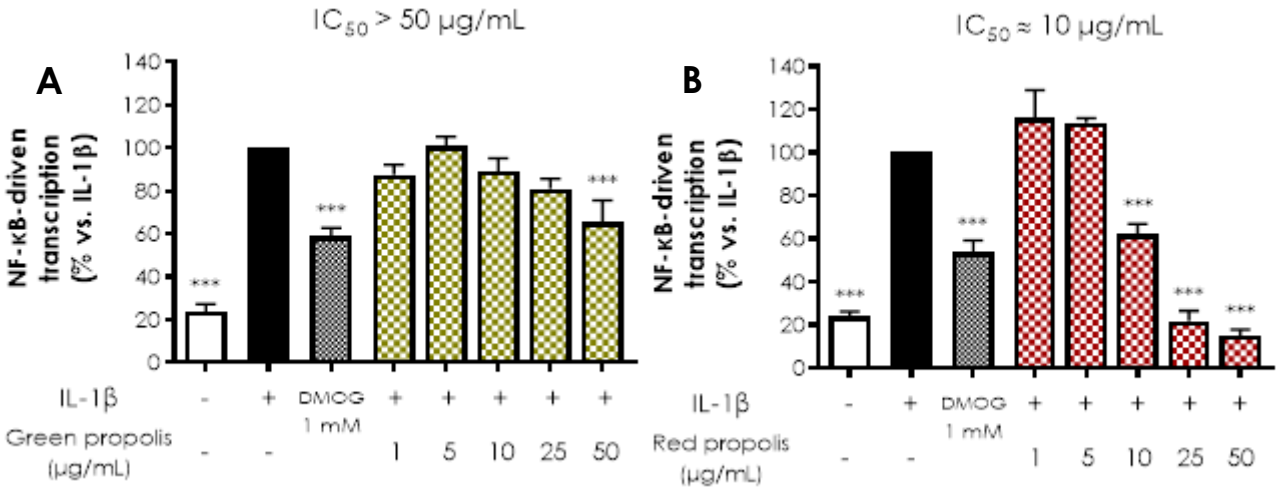

Figure 25 *| Assessment of green (**A**) and red (**B**) Brazilian propolis effect on NF-κB-driven transcription in HaCaT cells. Cells were stimulated with 10 ng/mL of IL-1β and treated for 6 h with increasing propolis concentrations. Data are reported as percentage with respect to the stimulus, which was arbitrarily assigned the value of 100%. *** p < 0.001 versus IL-1β.*

4.2.3 *EFFECT ON IL-8 SECRETION*

To assess the ability of green and red Brazilian propolis to inhibit IL-8 release in keratinocytes and fibroblasts, cells were subjected to a pro-inflammatory stimulus (TNF-α 10 ng/mL, 6 h) and concomitantly treated with increasing concentrations of propolis (1-50 µg/mL).

In HaCaT cells (**Fig. 26**), green propolis did not prove appreciably active in inhibiting TNF-α-induced IL-8 release. Red propolis, instead, showed statistically significant activity at concentrations higher than 10 µg/mL, with an IC_{50} of 11.89 µg/mL.

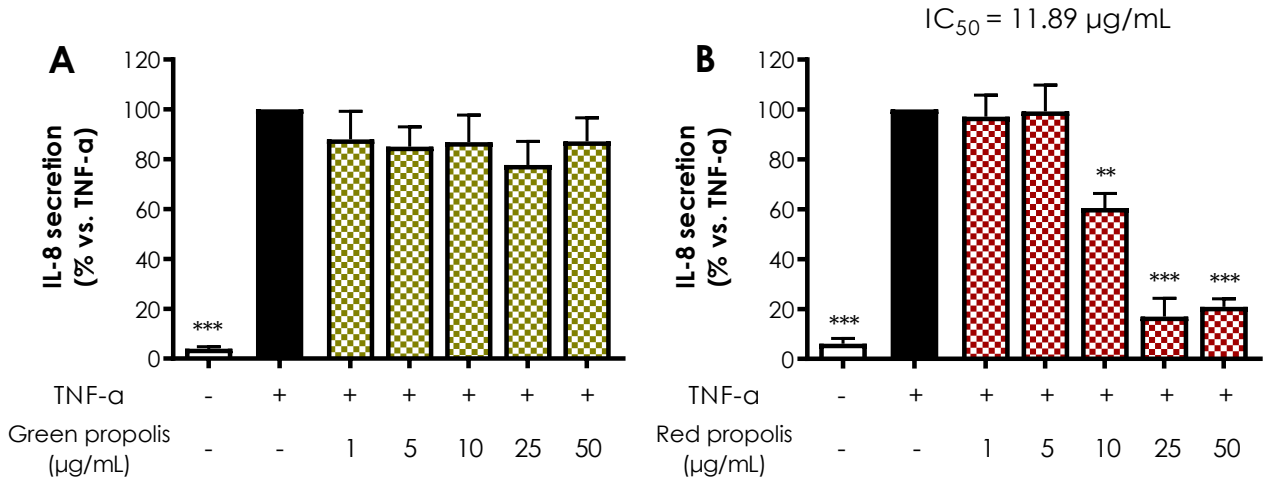

Figure 26 *| Assessment of green (**A**) and red (**B**) Brazilian propolis effect on IL-8 release in HaCaT cells. Cells were stimulated with 10 ng/mL of TNF-α and treated for 6 h with increasing propolis concentrations. Data are reported as percentage with respect to the stimulus, which was arbitrarily assigned the value of 100%. ** p < 0.01, *** p < 0.001 versus TNF-α.*

In HDF cells (**Fig. 27**), green propolis demonstrated a limited inhibitory activity on TNF-α-induced IL-8 release, with a slight and non-statistically significant reduction at 25 μg/mL. In the same experimental conditions, red propolis showed significant concentration-dependent inhibition of IL-8 release starting at 1 μg/mL, with an IC_{50} of 5.89 μg/mL.

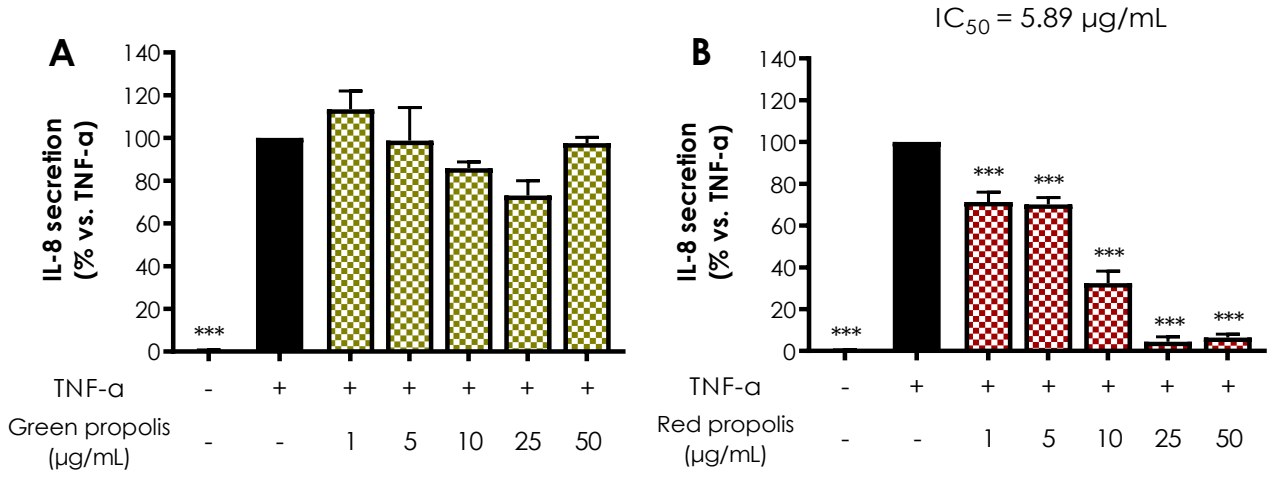

Figure 27 *| Assessment of green (**A**) and red (**B**) Brazilian propolis effect on IL-8 release in HDF cells. Cells were stimulated with 10 ng/mL of TNF-α and treated for 6 h with increasing propolis concentrations. Data are reported as percentage with respect to the stimulus, which was arbitrarily assigned the value of 100%. *** p < 0.001 versus TNF-α.*

4.2.4 *EFFECT ON IL-6 EXPRESSION AND SECRETION*

As mentioned in the introduction, IL-6 is a cytokine with pleiotropic functions in cutaneous wound healing, which alternatively act as a pro- or anti-inflammatory, pro- or anti-fibrotic agent. It generally unfolds its action in the initial phases, during the early inflammatory response, being favourable for a successful outcome. The switch from a pro-inflammatory to a reparative microenvironment must be tightly regulated and IL-6 is a key modulator of the inflammatory and reparative process, involved in the differentiation, activation, and proliferation of leukocytes, endothelial cells, keratinocytes, and fibroblasts (Johnson, Stevenson, Prêle, Fear, & Wood, 2020). Moreover, it is also crucial for the formation of new vessels and collagen deposition. Knockout mice for IL-6 present a delay in wound healing (Lin, Kondo, Ishida, Takayasu, & Mukaida, 2003).

In both HaCaT (**Fig. 28 A**) and HDF (**Fig. 28 B**) cells, green propolis and, in particular, red propolis were able to significantly induce the overexpression of *IL6* gene. Interestingly, the effect induced by red propolis was significantly higher than that of green propolis.

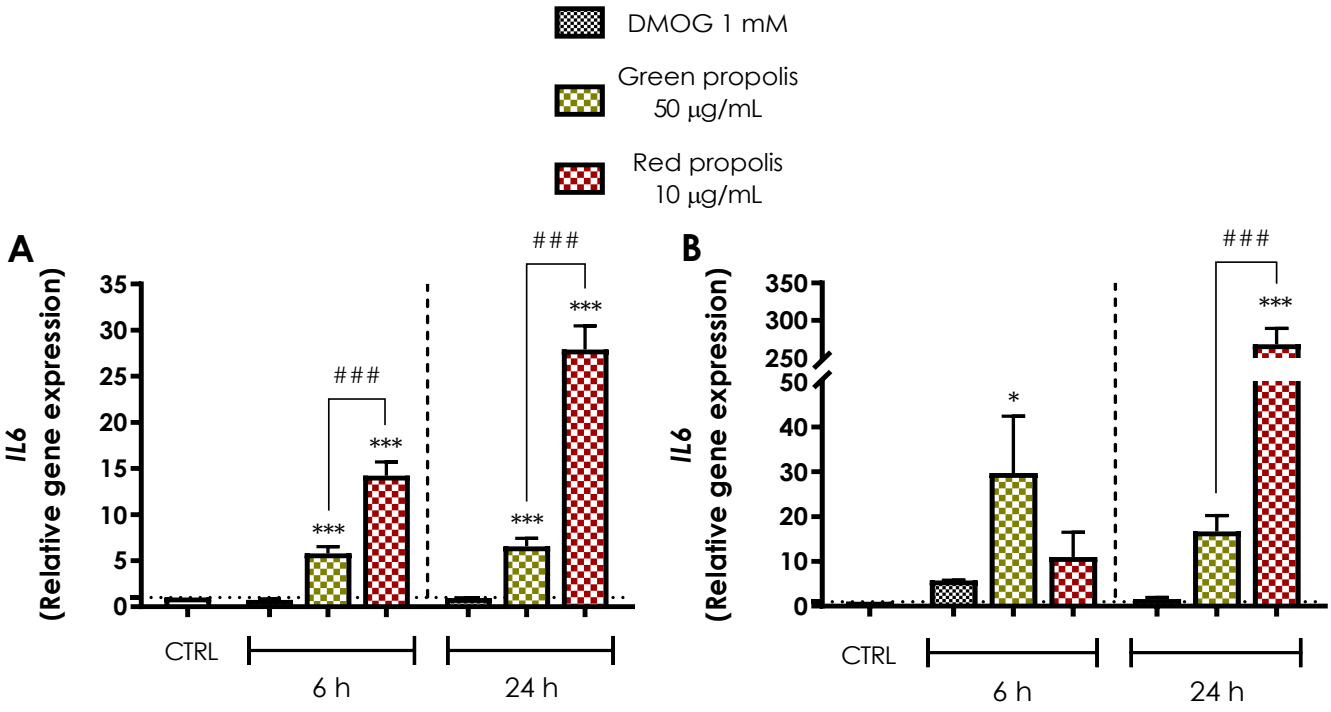

Figure 28 | *Gene expression analysis of* IL6 in *HaCaT (**A**) and HDF (**B**) cells treated for 6 or 24 h with green and red Brazilian propolis. * p < 0.05, ** p < 0.01, *** p < 0.001 versus control; ###p < 0.001 green propolis vs. red propolis.*

The amount of IL-6 released in the culture medium was measured by ELISA assay, to determine whether secretion paralleled the overexpression detected by qPCR. However, in the experimental conditions used no secretion of IL-6 could be detected. Consequently, the experiment was repeated in presence of a pro-inflammatory stimulus (TNF-α 10 ng/mL + IFN-γ 5 ng/mL), known to facilitate IL-6 secretion, to evaluate a possible modulation of the secreted levels of the cytokine.

In HaCaT cells (**Fig. 29**), the highest concentrations tested, which were the same used in the previous experiments, caused a significant increase of IL-6 release above the stimulated levels.

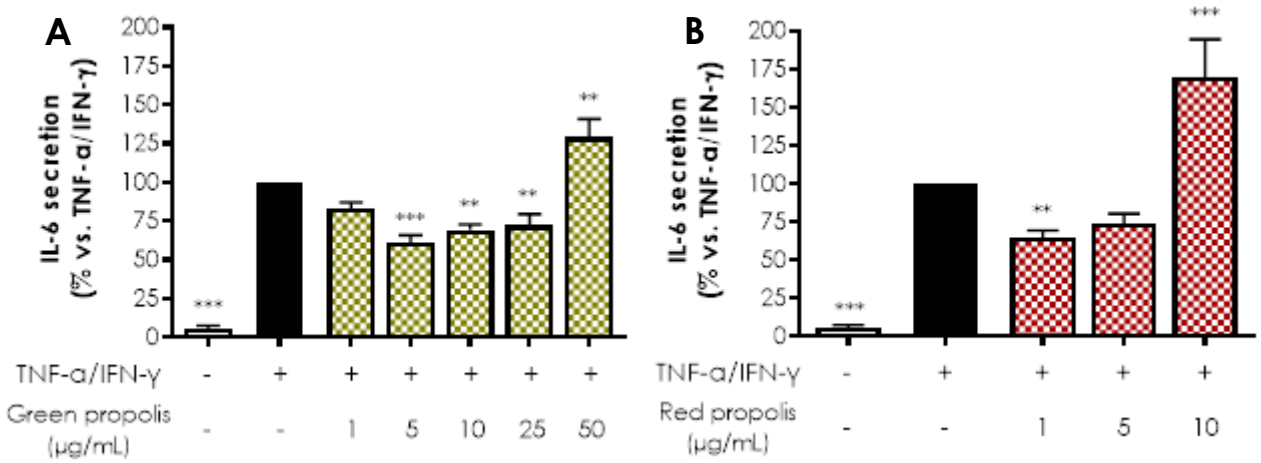

Figure 29 *| Assessment of green(**A**) and red (**B**) Brazilian propolis effect on IL-6 release in HaCaT cells. Cells were stimulated with 10 ng/mL of TNF-α and 5 ng/mL of IFN-γ and treated for 24 h with increasing propolis concentrations. Data are reported as percentage with respect to the stimulus, which was arbitrarily assigned the value of 100%. ** p < 0.01, *** p < 0.001 versus TNF-α/IFN-γ.*

In HDF cells (**Fig. 30**), the direction of the effect was similar to HaCaT cells but of modest entity.

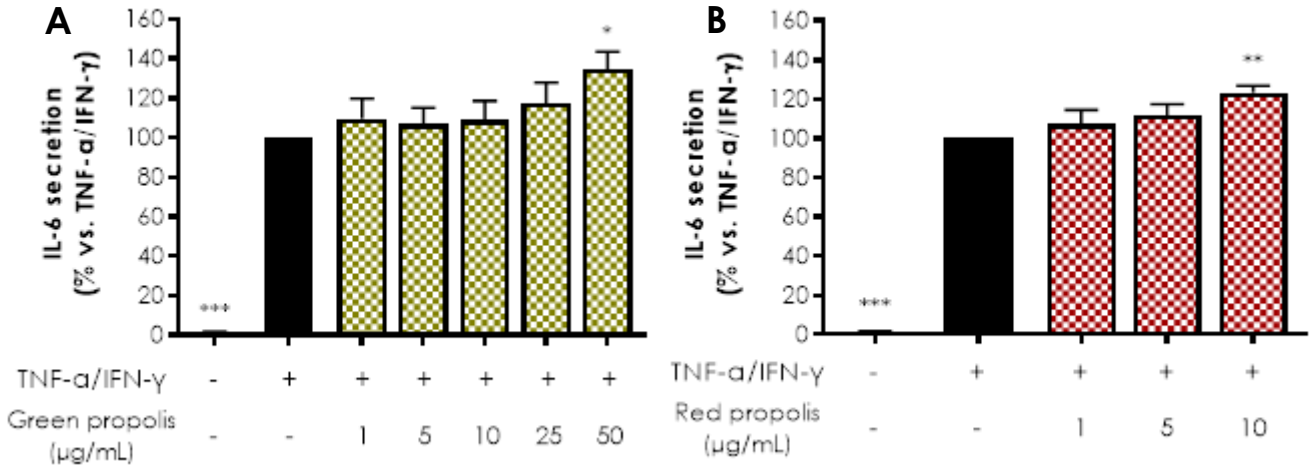

Figure 30 *| Assessment of green(**A**) and red (**B**) Brazilian propolis effect on VEGF release in HDF cells. Cells were stimulated with 10 ng/mL of TNF-α and 5 ng/mL of IFN-γ and treated for 24 h with increasing propolis concentrations. Data are reported as percentage with respect to the stimulus, which was arbitrarily assigned the value of 100%. * p < 0.05, ** p < 0.01, *** p < 0.001 versus TNF-α/IFN-γ.*

4.2.5 *EFFECT ON HIF-1α STABILISATION – IMMUNOCYTOCHEMISTRY*

As fully described in the introduction, the transcription factor HIF-1 is widely involved in the expression of several genes fundamental for cell survival, successful wound healing, and possibly tissue regeneration. Therefore, to evaluate the role of green and red Brazilian propolis in the activation of HIF-1 in keratinocytes and fibroblasts, the focus was placed on the stabilisation of the subunit HIF-1a, investigated through fluorescent immunocytochemistry in confocal microscopy. HaCaT and HDF cells were treated in a time-course for 1-3-6-24 h with green or red propolis extracts at the highest common non-toxic concentrations of 50 and 10 µg/mL, respectively, to allow for direct comparability. DMOG was used as a reference inductor of HIF-1a stabilisation. Controls, as expected, show the absence of HIF-1a, that in normal conditions undergoes rapid degradation with a half-life of less than 10 minutes (Berra, Roux, Richard, & Pouysségur, 2001). On the other hand, when cells are treated with DMOG the activity of PHDs is impaired, thus leading to the accumulation of HIF-1a in the cytoplasm and promoting its prompt translocation to the nucleus, where it can be detected by immunofluorescence. At 1 and 3 h, no sign of translocation could be detected, whereas the most interesting results have been obtained at 6 and 24 h.

In HaCaT cells at 6 h (**Fig. 31**) and 24 h (**Fig. 32**), both green and red propolis determined a significant nuclear accumulation of HIF-1a, indicating the ability to induce HIF-1 transcriptional activity.

In HDF cells at 6 h (**Fig. 33**), only the reference inductor DMOG caused an appreciable nuclear translocation of HIF-1a, while propolis seemed to be inactive. However, at 24 h (**Fig. 34**) red propolis proved capable of inducing a significant stabilisation and nuclear translocation of the transcription factor subunit, whereas green propolis remained inactive in this cell line.

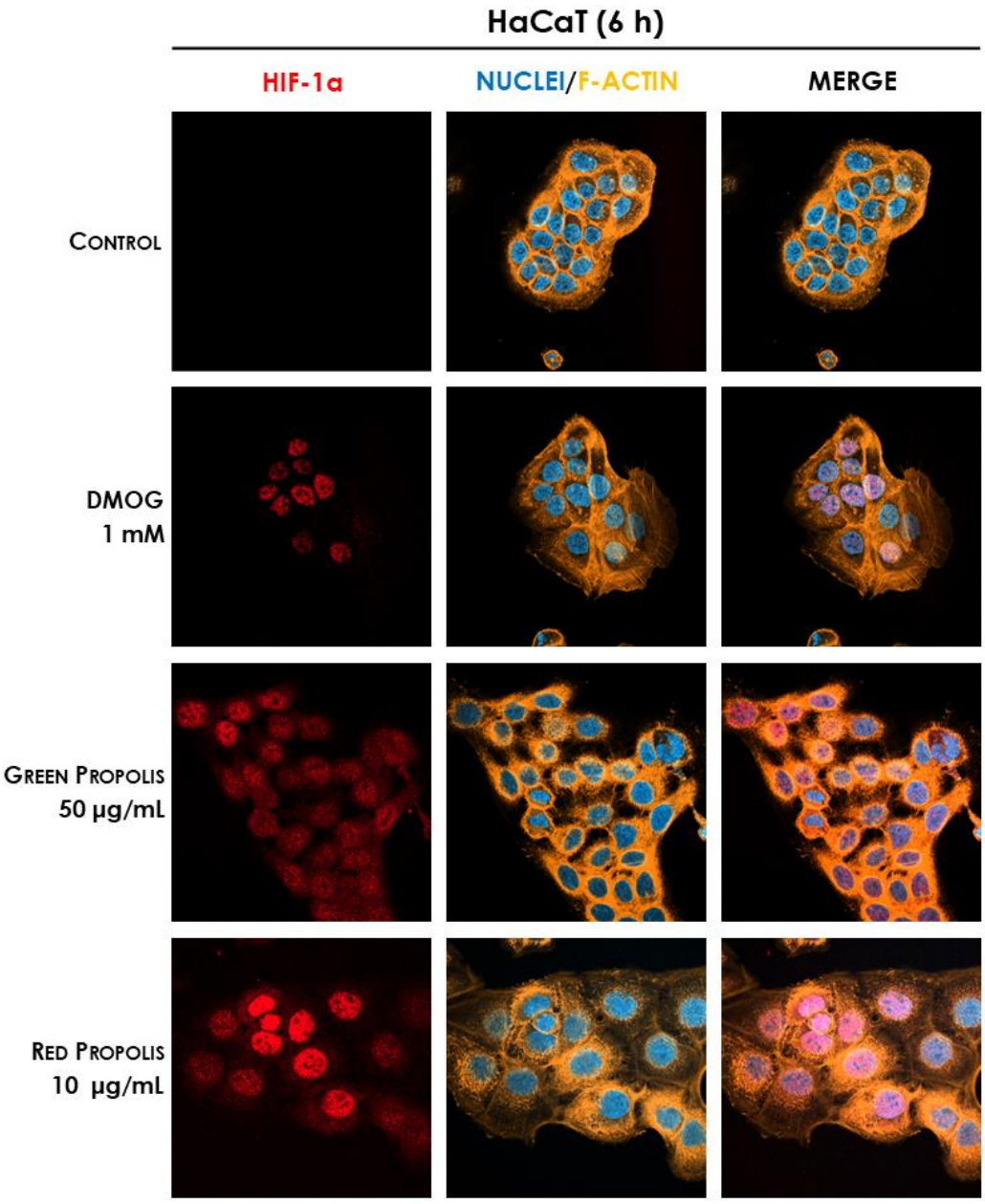

Figure 31 *| Representative confocal micrographs of the fluorescent immunostaining of HIF-1a (red) to assess the effect of Brazilian propolis on HIF-1a stabilisation and nuclear translocation in HaCaT cells after 6 h of treatment. Nuclei were stained with DAPI (blue), whereas F-actin with TRITC-phalloidin (orange).*

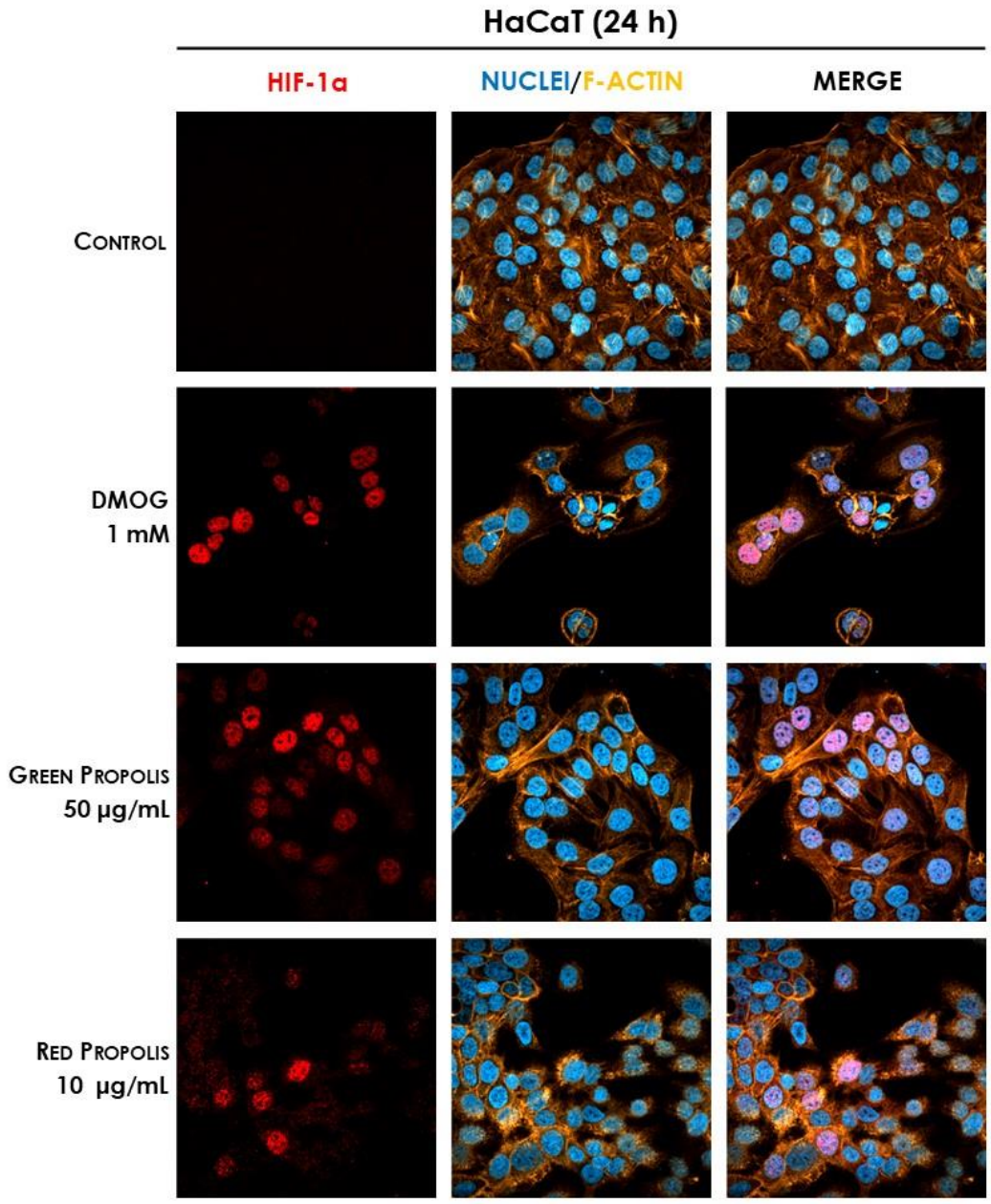

Figure 32 | *Representative confocal micrographs of the fluorescent immunostaining of HIF-1a (red) to assess the effect of Brazilian propolis on HIF-1a stabilisation and nuclear translocation in HaCaT cells after 24 h of treatment. Nuclei were stained with DAPI (blue), whereas F-actin with TRITC-phalloidin (orange).*

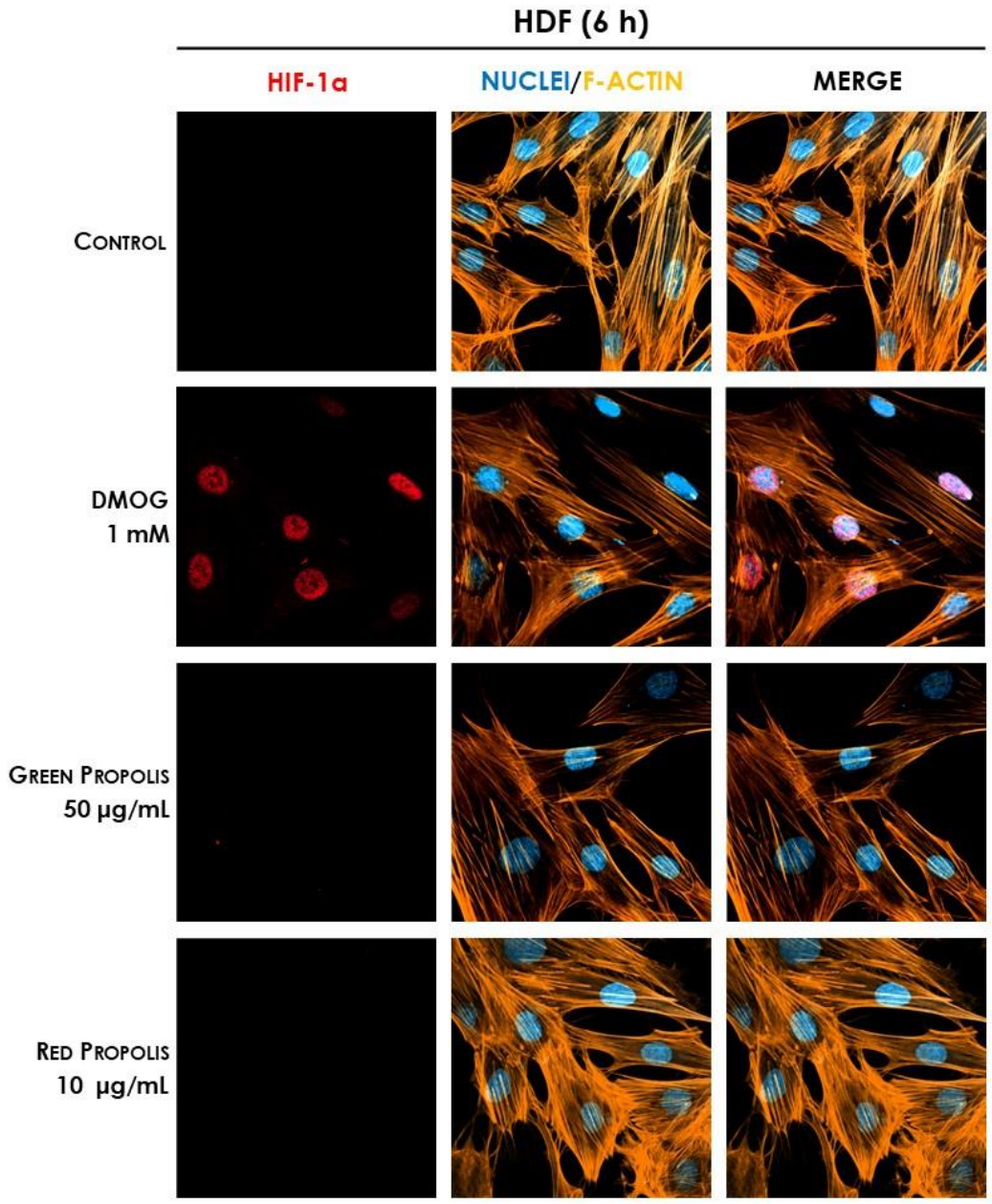

Figure 33 | *Representative confocal micrographs of the fluorescent immunostaining of HIF-1a (red) to assess the effect of Brazilian propolis on HIF-1a stabilisation and nuclear translocation in HDF cells after 6 h of treatment. Nuclei were stained with DAPI (blue), whereas F-actin with TRITC-phalloidin (orange).*

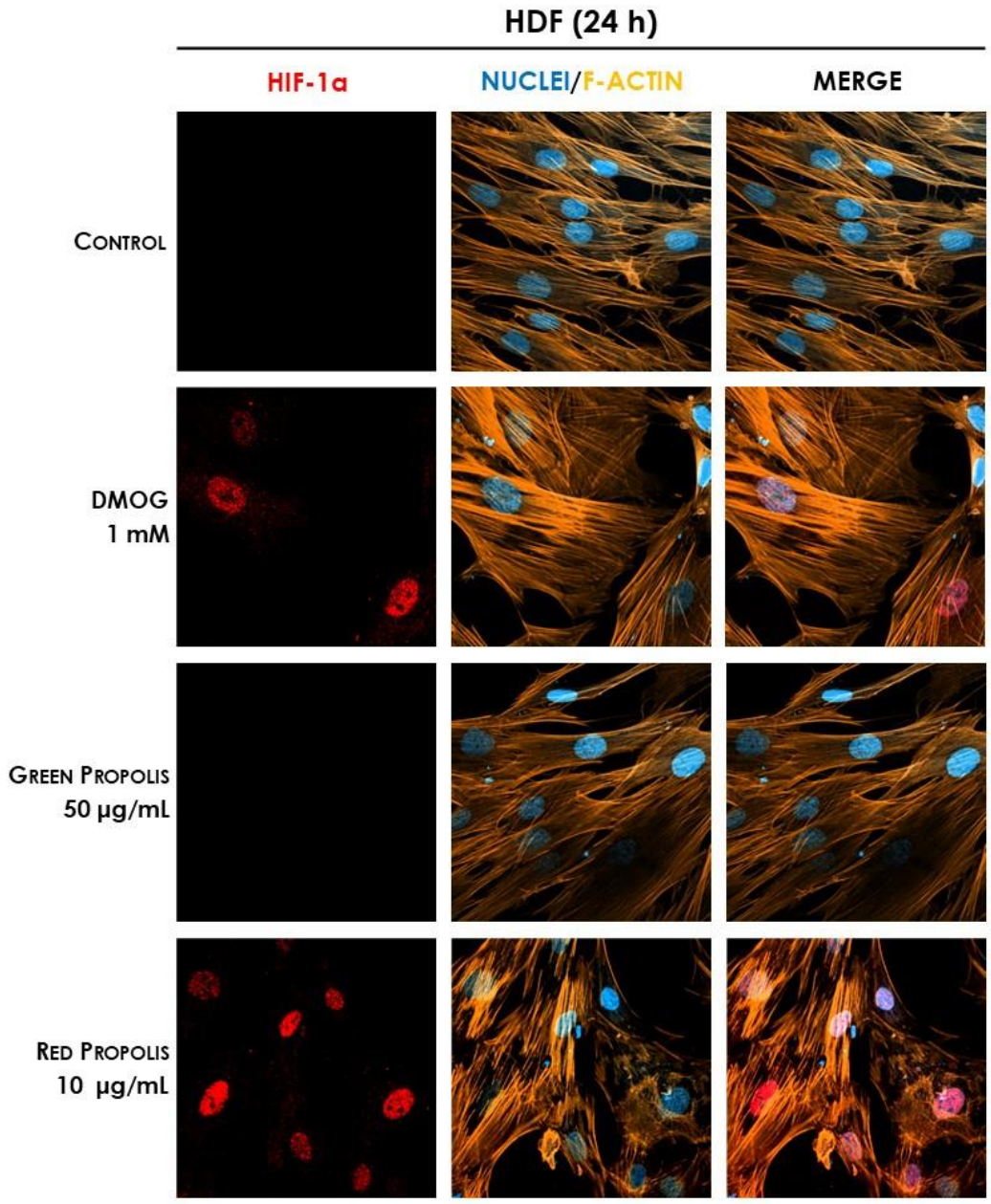

Figure 34 *| Representative confocal micrographs of the fluorescent immunostaining of HIF-1a (red) to assess the effect of Brazilian propolis on HIF-1a stabilisation and nuclear translocation in HDF cells after 24 h of treatment. Nuclei were stained with DAPI (blue), whereas F-actin with TRITC-phalloidin (orange).*

4.2.6 *EFFECT ON HIF-1α STABILISATION – WESTERN BLOT*

To confirm the evidence obtained in immunofluorescence images and quantify the entity of the effect, western blotting was performed on HaCaT and HDF cells treated according to an analogous experimental paradigm.

In HaCaT cells (**Fig. 35**) both green and red propolis proved able to induce the accumulation of HIF-1α in whole-cell lysates; however, only green propolis determined a statistically significant effect.

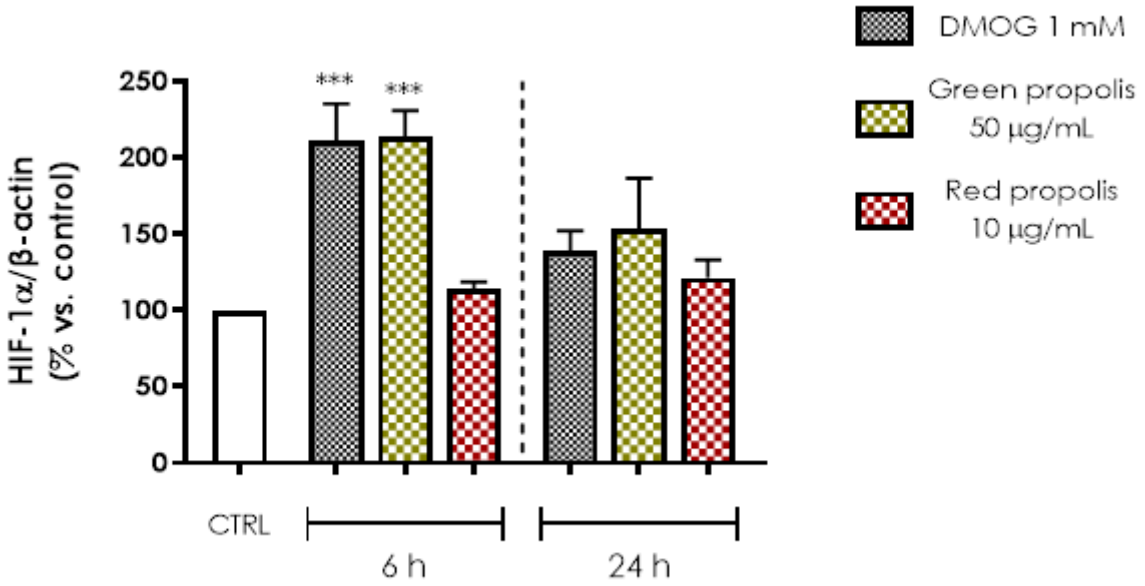

Figure 35 *| Western blot analysis aimed at assessing the effect of Brazilian propolis on HIF-1α stabilisation and intracellular accumulation in HaCaT whole-cell lysates after 6 or 24 h of treatment. *** p < 0.001 versus control.*

In HDF cells (**Fig. 36**) only red propolis proved able to induce the accumulation of HIF-1α in whole-cell lysates and the effect was elicited only after 24 h of treatment, thus reasserting the evidence previously obtained with immunofluorescence. Noteworthy, the effect of the PHD inhibitor DMOG was particularly significant at 6 h, while strongly decreased at 24 h. On the contrary, the effect of Brazilian propolis manifests itself at 24 h when that of DMOG is waning, thus suggesting a putative mechanism of induction other than PHD inhibition.

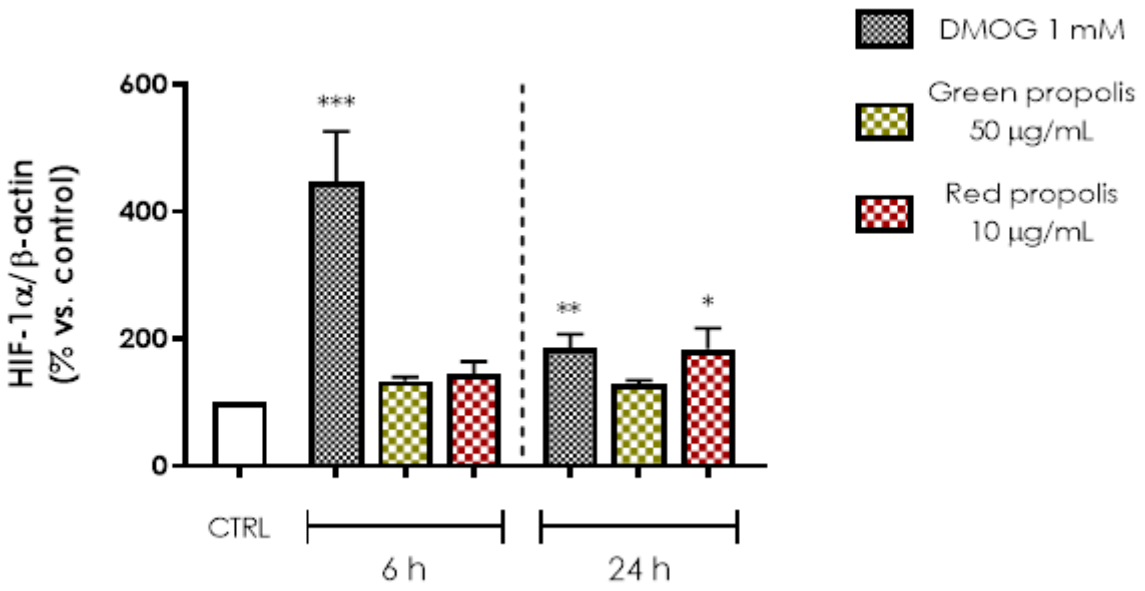

Figure 36 | *Western blot analysis aimed at assessing the effect of Brazilian propolis on HIF-1a stabilisation and intracellular accumulation in HDF whole-cell lysates after 6 or 24 h of treatment. * $p < 0.05$, ** $p < 0.01$, *** $p < 0.001$ versus control.*

4.2.7 *EFFECT ON VEGF EXPRESSION AND SECRETION*

To obtain further confirmation of the actual induction of HIF-1 transcriptional activity, the expression of *VEGFA*, one of the main target genes downstream of HIF-1 activation (Forsythe et al., 1996), was investigated by qPCR. HaCaT and HDF cells were treated according to the same paradigm used for immunofluorescence and western blotting.

In HaCaT cells (**Fig. 37 A**), green propolis was responsible for a significant overexpression of *VEGFA*, increasing with treatment time. This result is in line with the western blot, which demonstrated the preferential accumulation of HIF-1a upon green propolis treatment. On the other hand, in HDF cells (**Fig. 37 B**) a significant overexpression of *VEGFA* was induced by red propolis at 24 h, paralleling previous results obtained with complementary techniques. Once again, it was demonstrated that, like in western blot, the effect of Brazilian propolis manifests itself at longer time points compared to DMOG, claiming for different mechanisms of HIF-1 activation.

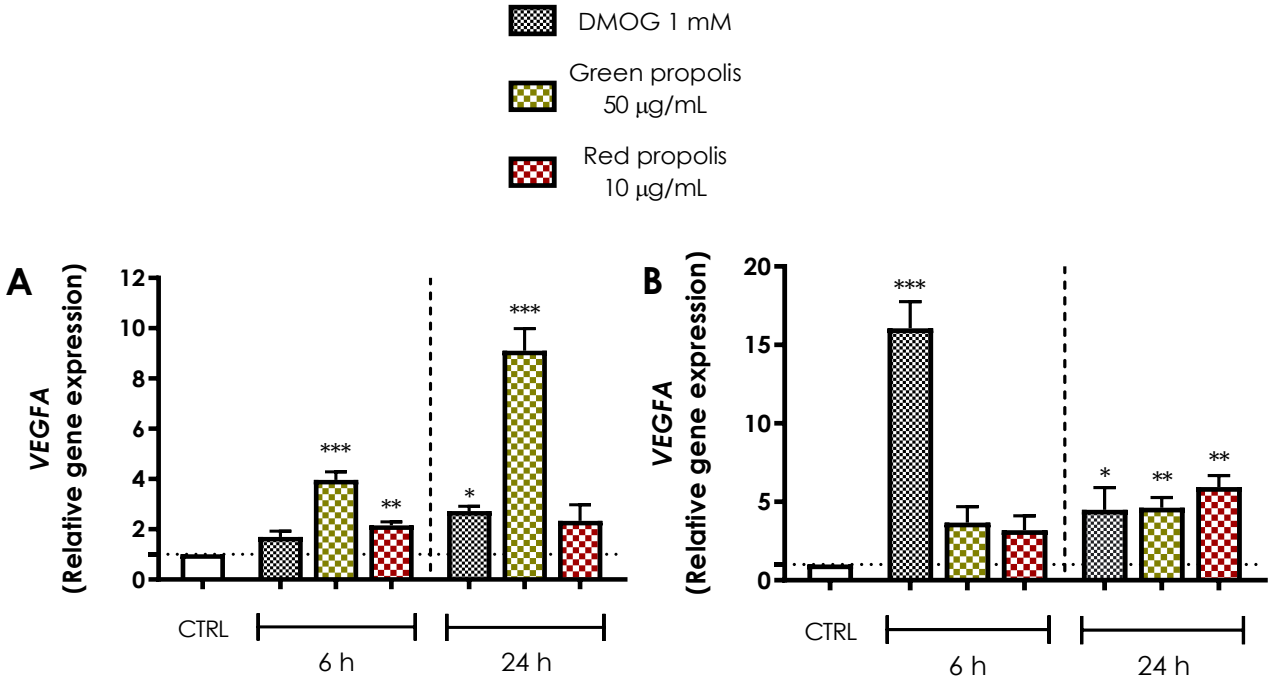

Figure 37 | *Gene expression analysis of* VEGFA in *HaCaT (**A**) and HDF (**B**) cells treated for 6 or 24 h with green and red Brazilian propolis. * $p < 0.05$, ** $p < 0.01$, *** $p < 0.001$ versus control.*

The amount of VEGF released in the culture medium was measured at 24 h by ELISA assay, to determine whether secretion paralleled the overexpression detected by qPCR. In HaCaT cells (**Fig. 38**), only the highest concentration tested, which was the same used in the previous experiments, caused a significant increase in VEGF release. In HDF, unexpectedly, no secretion could be detected.

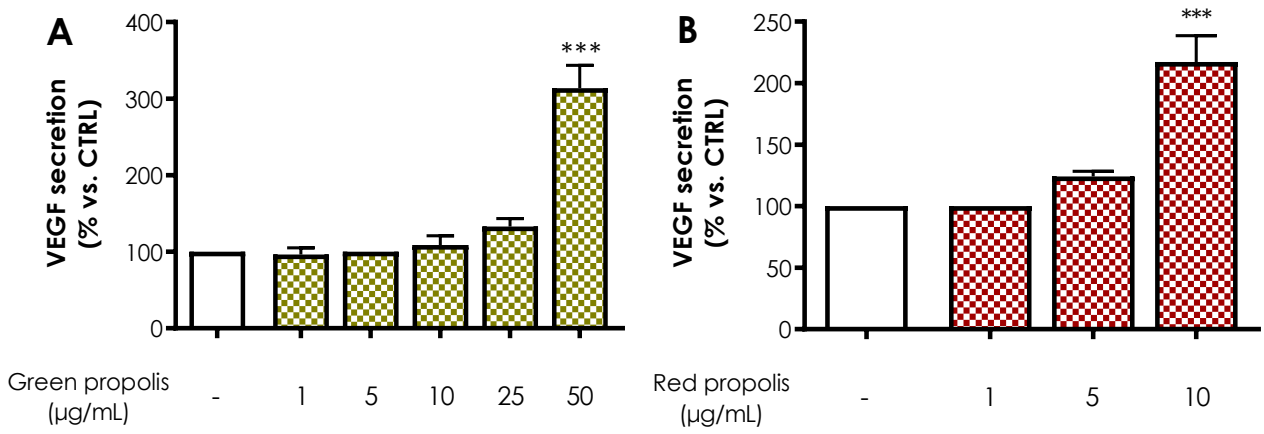

Figure 38 *| Assessment of green(**A**) and red (**B**) Brazilian propolis effect on VEGF release in HaCaT cells. Cells were treated for 24 h with increasing propolis concentrations. Data are reported as percentage with respect to the control, which was arbitrarily assigned the value of 100%. *** p < 0.001 versus control.*

4.2.8 *HUMAN SKIN EQUIVALENT CONSTRUCTION AND CHARACTERISATION*

The possibility to have reliable and reproducible *in vitro* skin models would be of pivotal importance to facilitate the research into the mechanisms of wound healing and the evaluation of natural substances with reparative and regenerative properties. The development of human skin equivalents (HSEs) has progressed in parallel to tissue engineering and regenerative medicine (Z. Zhang & Michniak-Kohn, 2012), in particular in recent years, in which efforts have been made to optimise these models and perfection culture conditions to better imitate the *in vivo* organisation of skin (Niehues et al., 2018). Currently, many kinds of HSE are commercially available or may be constructed from scratch and are considered a valid alternative to laboratory animal models, used in experimental research to study cutaneous processes such as wound

healing (Reijnders et al., 2015). HSEs are generally based on co-cultures of fibroblasts incorporated in type I collagen hydrogel, which acts as a scaffold for the whole structure and simulates dermis, and keratinocytes, seeded on top of the collagen matrix, that differentiate to originate epidermis. Cells normally used are human dermal fibroblasts and primary keratinocytes from tissue explant, difficult to obtain and culture, not to mention the source of variability that they introduce, but the use of other cell lines such as HaCaT has been evaluated (Klicks, Molitor, Ertongur-Fauth, Rudolf, & Hafner, 2017). Nevertheless, HaCaT cells are widely considered unsuitable for this aim since many studies report evidence of their inability to completely differentiate and form the ordered layers of the mature epidermis (Boelsma, Verhoeven, & Ponec, 1999; Rikken, Niehues, & van den Bogaard, 2020; Schoop, Mirancea, & Fusenig, 1999).

An attempt was made to obtain a functional human skin equivalent with stable cell lines, co-culturing HDF fibroblasts interspersed in a bovine type I collagen matrix, surmounted by a layer of HaCaT cells cultured at the air-liquid interface for 2 weeks. To enhance the formation and differentiation of a multilayer epithelium by HaCaT cells in the organotypic co-culture, the medium was supplemented with 2 ng/mL TGF-a (Stark et al., 2004), to compensate for HaCaT deficiencies in IL-1 production and KGF and GM-CSF receptor expression.

The morphological examination of co-cultures demonstrated the physiological contraction of the collagen matrix, usually reported during HSE maturation. The haematoxylin and eosin staining (**Fig. 39**) showed the stratification of epidermal layers, occasionally reported for HaCaT cells in literature studies, with the presence of flattened, desquamating corneocytes on the surface. However, the number of keratinocyte layers appears lower than what can be observed *in vivo*.

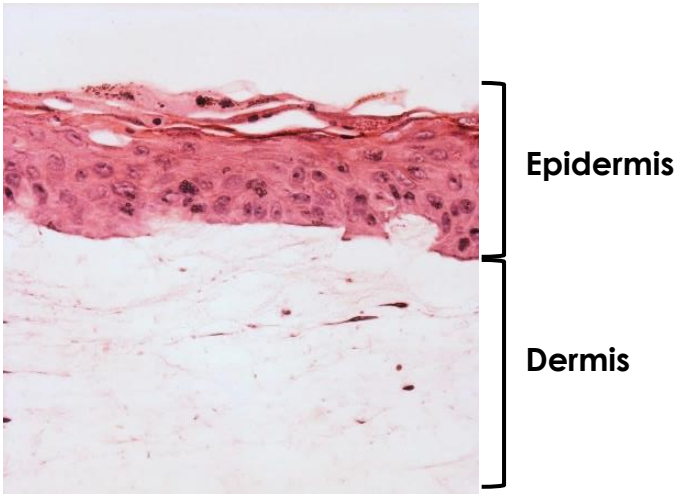

Figure 39 | *Architecture of organotypic HaCaT/HDF co-cultures. Cells were co-cultured for 2 weeks, keeping the HaCaT layer at the air-liquid interface. After tissue processing and paraffin embedding, thin sections were stained with haematoxylin and eosin. Magnification 200x.*

For the first time, it was possible to demonstrate in a HaCaT/HDF co-culture the localisation of keratin 1 (K1) in basal keratinocytes, keratin 10 (K10) in suprabasal layers, and involucrin (INV) in most superficial and desquamating layer (**Fig. 40**), thus resembling the physiological organisation of normal skin (**Fig. 41**).

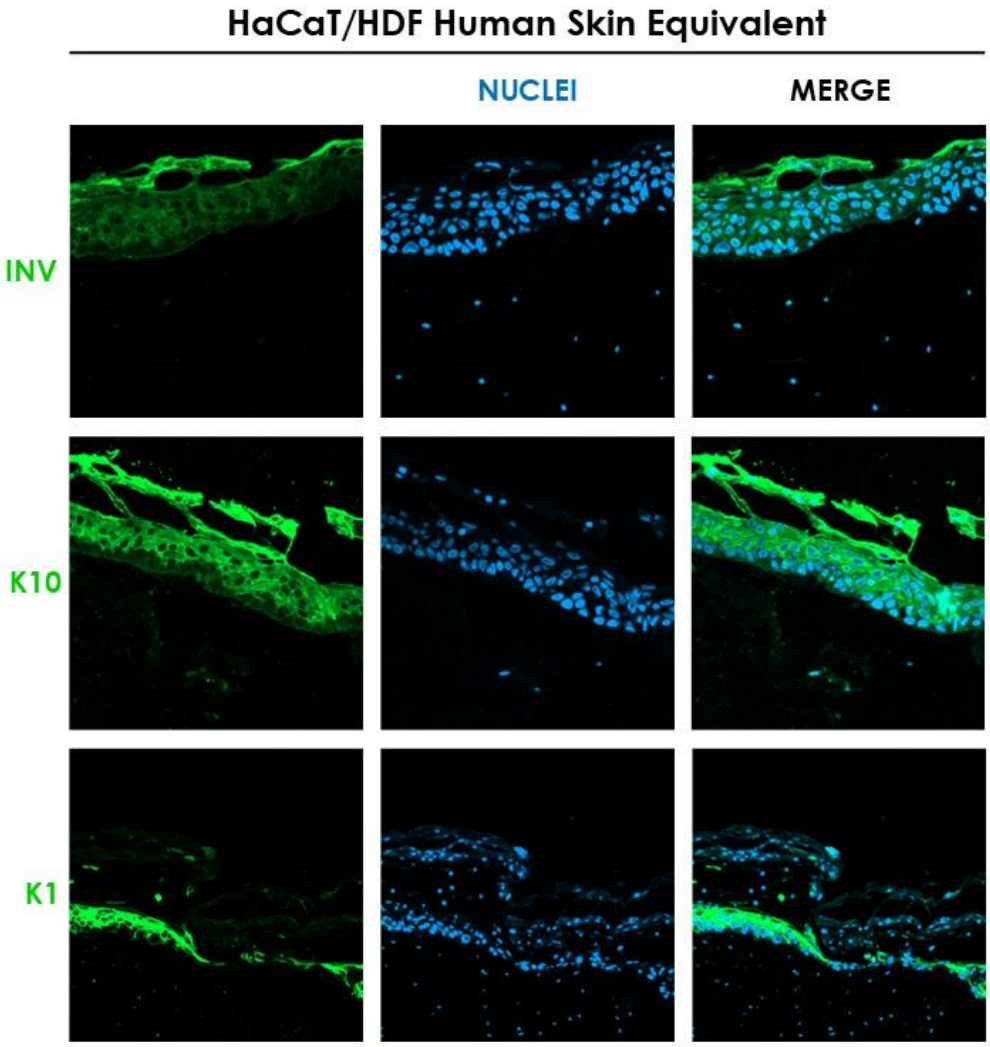

Figure 40 *| Architecture of organotypic HaCaT/HDF co-cultures. Cells were co-cultured for 2 weeks, keeping the HaCaT layer at the air-liquid interface. After tissue processing and paraffin embedding, thin sections were subjected to fluorescent IHC for the detection and localisation of keratin 1 (K1), keratin 10 (K10), and involucrin (INV) (green). Nuclei were stained with DAPI (blue). Magnification 100x.*

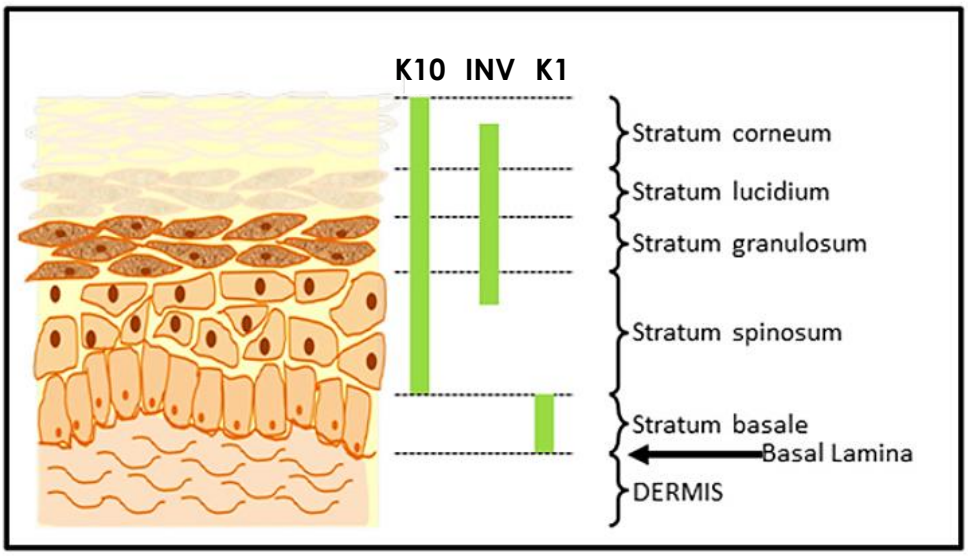

Figure 41 | *Physiological localisation of keratin 1 (K1), keratin 10 (K10), and involucrin (INV) in the normal epidermis (Strudwick, Lang, Smith, & Cowin, 2015).*

To assess the functional response of HaCaT/HDF co-cultures, the amount of VEGF released in the culture medium, following the treatment with Brazilian propolis, was measured in time-course by ELISA assay. As previously mentioned, green and red propolis at the concentrations of 50 and 10 µg/mL, respectively, proved able to induce a significant overexpression of the *VEGFA* gene in HaCaT and HDF cells (**Fig. 37**), and a significant release of VEGF in HaCaT cells (**Fig. 38**). This effect was confirmed also in co-cultures, showing a VEGF secretion peak at 24 h and paralleling the results obtained in cell lines taken individually.

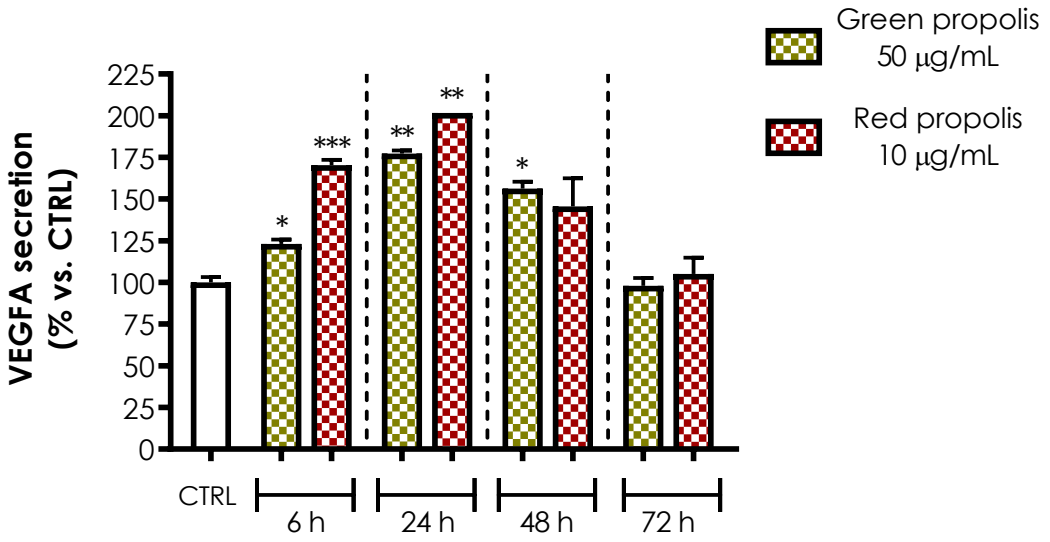

Figure 42 *| Assessment of green(**A**) and red (**B**) Brazilian propolis effect on VEGF release in HaCaT/HDF co-cultures. Cells were treated in time-course for 6-24-48-72 h. Data are reported as percentage with respect to the control, which was arbitrarily assigned the value of 100%. * p < 0.05, ** p < 0.01, *** p < 0.001 versus control.*

4.3 GREEN AND RED BRAZILIAN PROPOLIS BIOGUIDED FRACTIONATION

4.3.1 *FRACTIONATION*

As mentioned in the introduction, propolis is assumed to be one of the most heterogeneous natural products, with more than 300 different molecules identified or characterised. To better clarify the role of green and red Brazilian propolis components in HIF-1a stabilisation and subsequent induction of the transcriptional activity of genes involved in cell survival, successful wound healing, and possibly regeneration, propolis samples were fractionated by partitioning between immiscible solvents according to the protocol published by Santos et al. (Santos et al., 2002). This protocol, which exploits the pH-dependent differential partitioning behaviour of molecules between aqueous and organic phases, allowed the obtainment of organic acids, strong phenolic substances, weak phenolic substances and related aqueous fractions.

The fractionation scheme and names assigned to green and red propolis fractions are reported in **Fig. 43**.

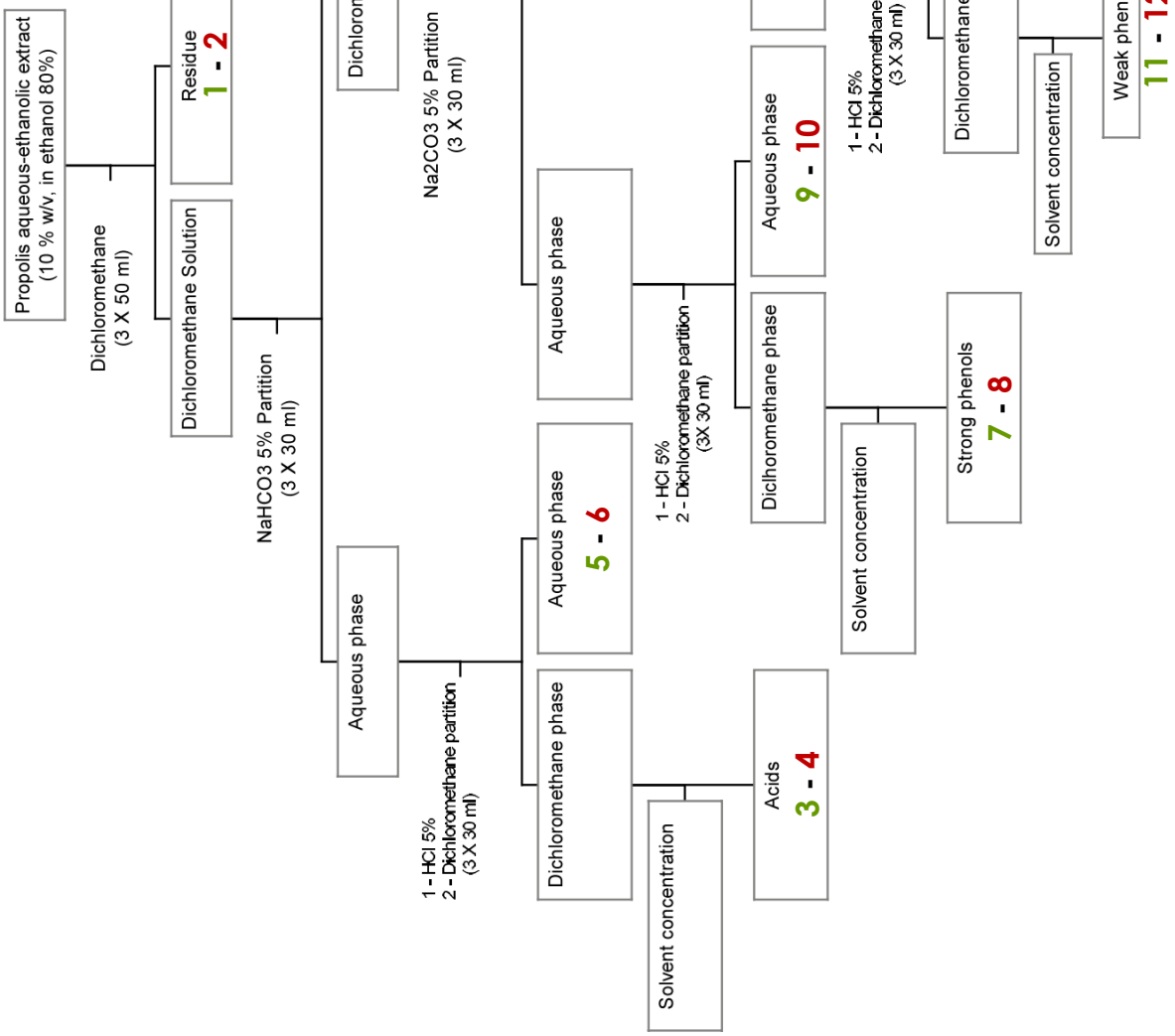

Figure 43 | *Fractionation scheme of green and red Brazilian propolis samples (Santos et al., 2002).*

4.3.2 *CYTOTOXICITY ASSAYS*

Before proceeding with the investigation of the biological activities in keratinocytes and fibroblasts, cytotoxicity was extensively evaluated to assess the influence of fractions on cell viability and to determine whether the fractionation process had separated or concentrated cytotoxic substances.

The cytotoxicity profile of green propolis fractions after 24 h of treatment in HaCaT and HDF cells is reported in **Fig. 44** (**A** and **B**, respectively). The cytotoxicity profile of red propolis fractions after 24 h of treatment in HaCaT and HDF cells is reported in **Fig. 45** (**A** and **B**, respectively). Treatment concentrations were progressively reduced until the obtainment of a non-cytotoxicity threshold, primarily defined by the absence of LDH release. The results of the NRU assay may indicate initial toxicity also in absence of LDH release; however, while in HaCaT cells NRU assay was demonstrated to be highly predictable providing results in line with the LDH assay, predictability was scarce in HDF cells due to low sensitivity of the assay in this cell line.

Also considering the results of these assays, a common screening concentration of 5 µg/mL, far below the cytotoxicity thresholds detected, was chosen to allow direct comparability of the biological activity results.

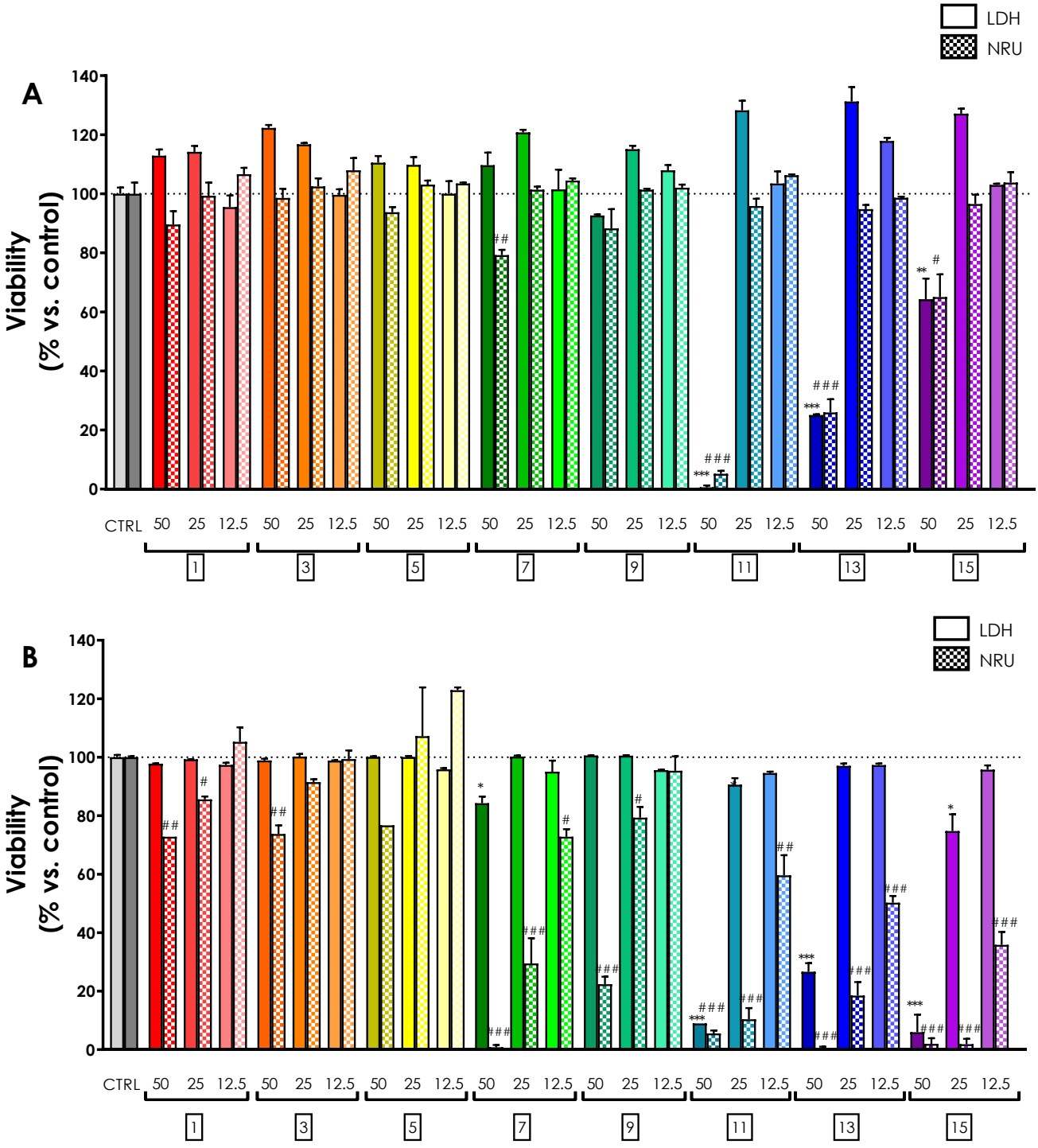

Figure 44 *| Assessment of green Brazilian propolis fraction effect on HaCaT (**A**) and HDF (**B**) cell viability through LDH and NRU assays. Cells were treated for 24 h in presence of increasing fraction concentrations. Data are reported as percentage with respect to the control, which was arbitrarily assigned the value of 100%. * $p < 0.05$, ** $p < 0.01$, *** $p < 0.001$ versus CTRL LDH; # $p < 0.05$, ## $p < 0.01$, ### $p < 0.001$ versus CTRL NRU.*

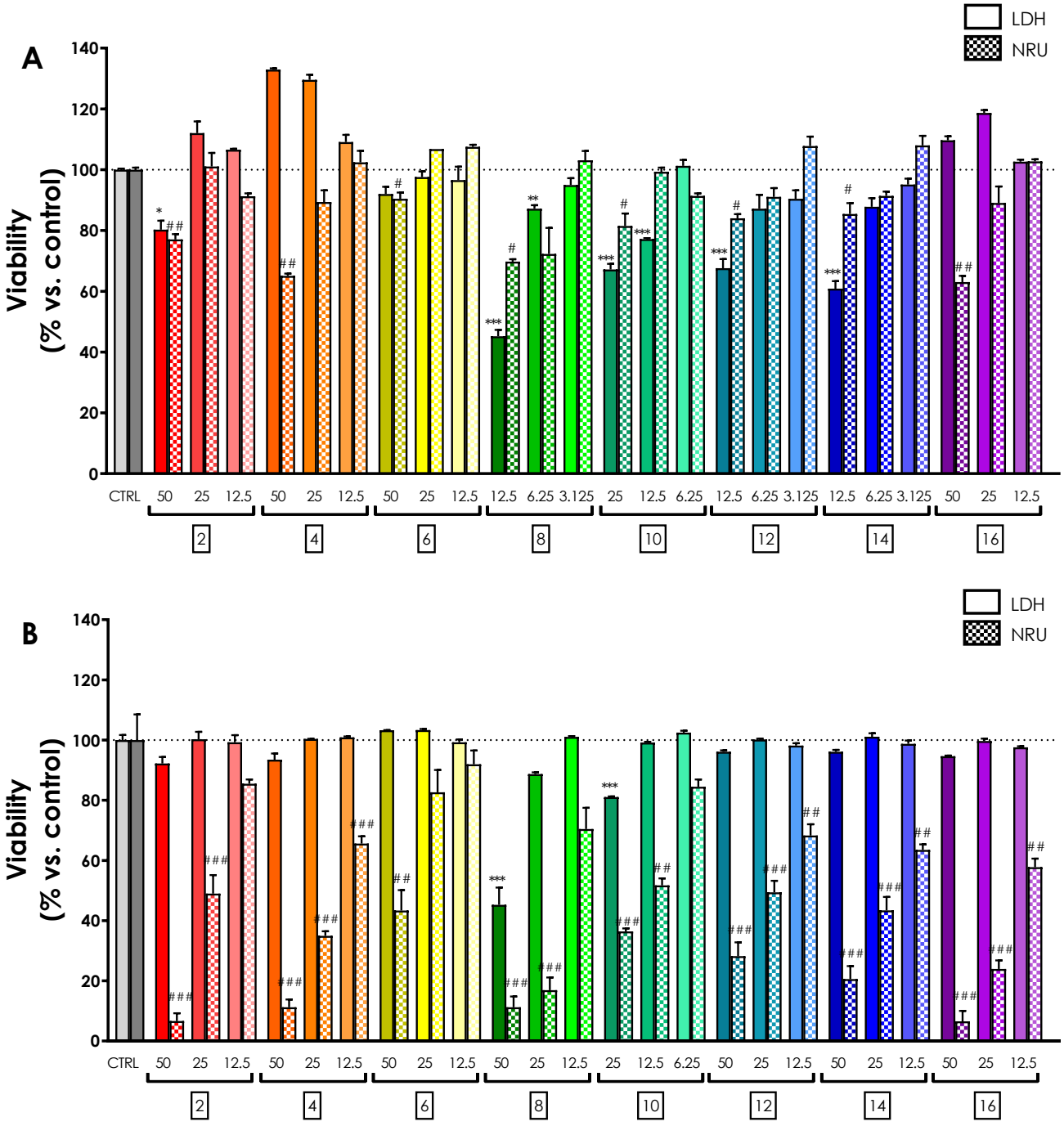

Figure 45 | *Assessment of red Brazilian propolis fraction effect on HaCaT (**A**) and HDF (**B**) cell viability through LDH and NRU assays. Cells were treated for 24 h in presence of increasing fraction concentrations. Data are reported as percentage with respect to the control, which was arbitrarily assigned the value of 100%. * $p < 0.05$, *** $p < 0.001$ versus CTRL LDH; # $p < 0.05$, ## $p < 0.01$, ### $p < 0.001$ versus CTRL NRU.*

4.3.3 *EFFECT ON HIF-1 – PART I*

To assess which of green and red Brazilian propolis fractions possessed the ability to induce the stabilisation of HIF-1a and the subsequent HIF-driven transcription, HaCaT and HDF cells were transiently transfected with an HRE-Luc reporter plasmid and concomitantly treated for 24 h with a screening concentration (5 µg/mL) of each fraction. The most promising fractions have also been investigated through fluorescent immunocytochemistry in confocal microscopy to assess the actual stabilisation and nuclear translocation of the subunit HIF-1a.

In HaCaT cells, among green propolis fractions, fractions 7, 1, and 3 determined a statistically significant induction of HIF-driven transcription (**Fig. 46**). Fluorescent immunocytochemistry confirmed the stabilisation and nuclear translocation of HIF-1a by these fractions in HaCaT cells (**Fig. 47**).

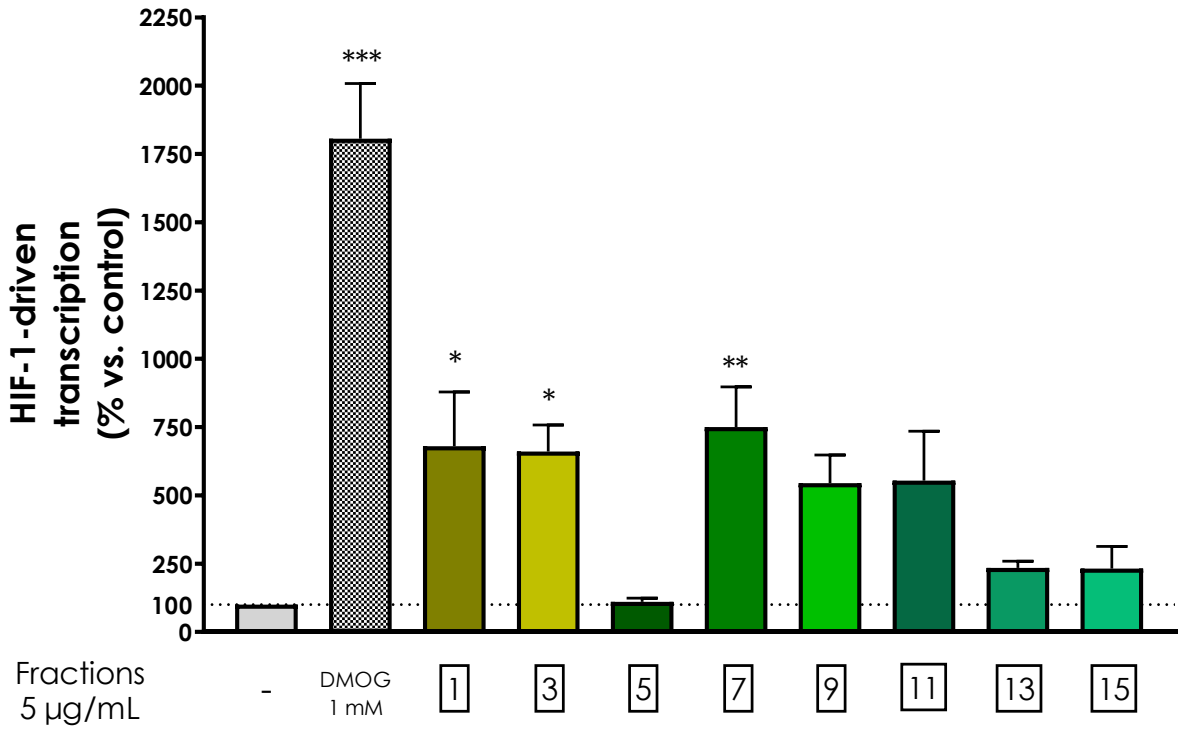

Figure 46 | *Assessment of green Brazilian propolis fraction effect on HIF-driven transcription in HaCaT cells. Cells were treated for 24 h with 5 µg/ mL of each fraction. Data are reported as percentage with respect to the control, which was arbitrarily assigned the value of 100%. * p < 0.05, ** p < 0.01, *** p < 0.001 versus control.*

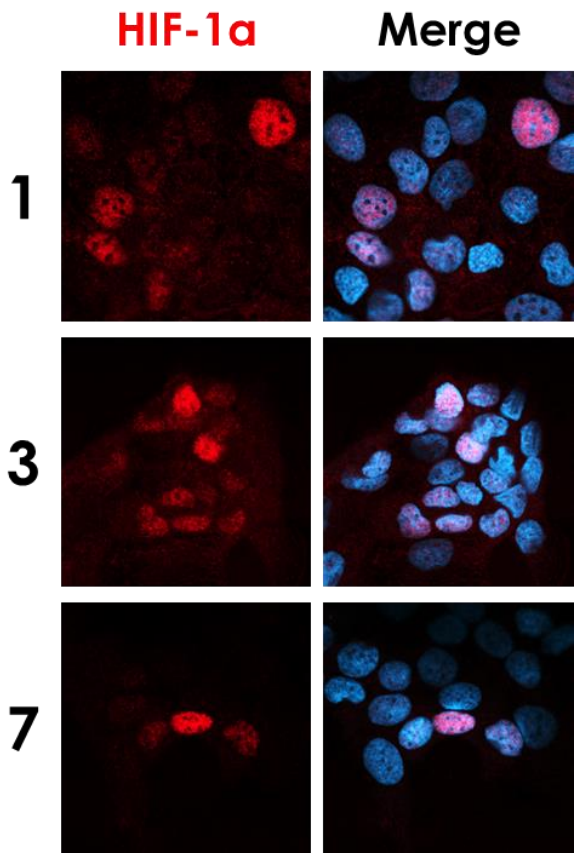

Figure 47 | *Representative confocal micrographs of the fluorescent immunostaining of HIF-1a (red) to confirm the effect of significantly active green propolis fractions on HIF-1a stabilisation and nuclear translocation in HaCaT cells after 24 h of treatment. Nuclei were stained with DAPI (blue).*

Among red propolis fractions, fractions 10, 4, 6, and 2 determined a statistically significant induction of HIF-driven transcription (**Fig. 48**). Fluorescent immunocytochemistry confirmed the stabilisation and nuclear translocation of HIF-1a by these fractions in HaCaT cells (**Fig. 49**).

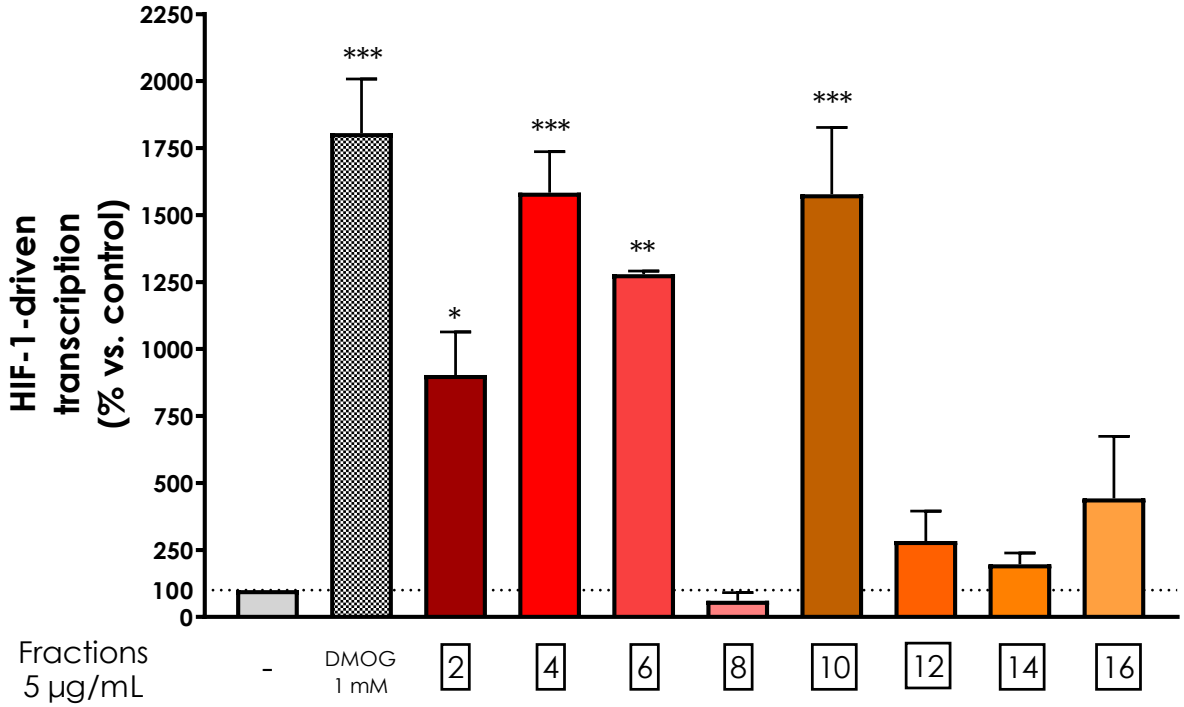

Figure 48 | *Assessment of red Brazilian propolis fraction effect on HIF-driven transcription in HaCaT cells. Cells were treated for 24 h with 5 µg/ mL of each fraction. Data are reported as percentage with respect to the control, which was arbitrarily assigned the value of 100%. * p < 0.05, ** p < 0.01, *** p < 0.001 versus control.*

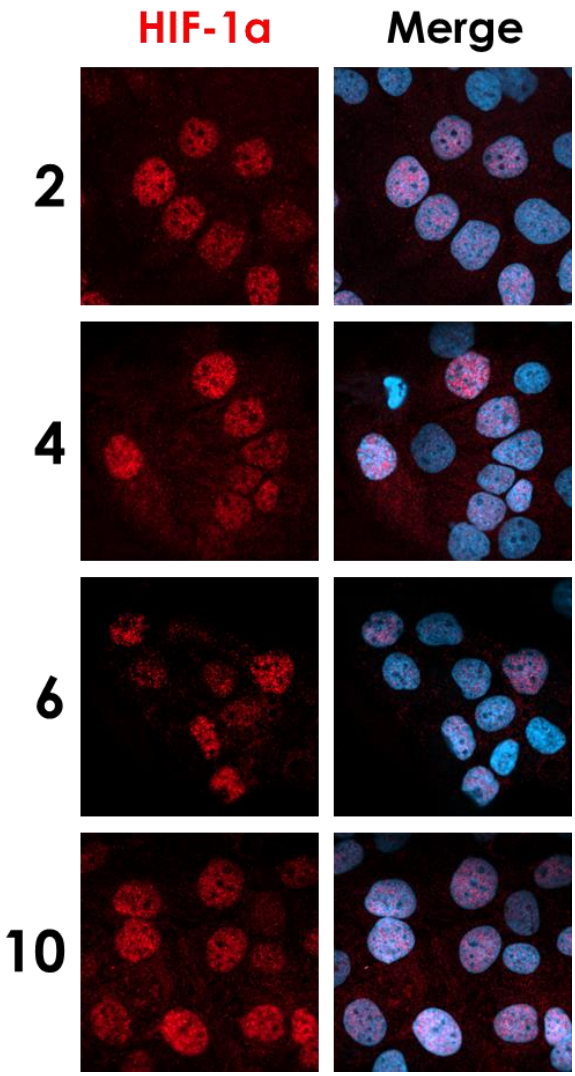

Figure 49 | *Representative confocal micrographs of the fluorescent immunostaining of HIF-1a (red) to confirm the effect of significantly active red propolis fractions on HIF-1a stabilisation and nuclear translocation in HaCaT cells after 24 h of treatment. Nuclei were stained with DAPI (blue).*

In HDF cells, as expected, none of green propolis fractions was able to induce HIF-driven transcription (**Fig. 50**). These results confirm the absence of activity for green propolis on this parameter in HDF cells, previously demonstrated through immunocytochemistry (**Fig. 33** and **34**) and western blotting (**Fig. 36**).

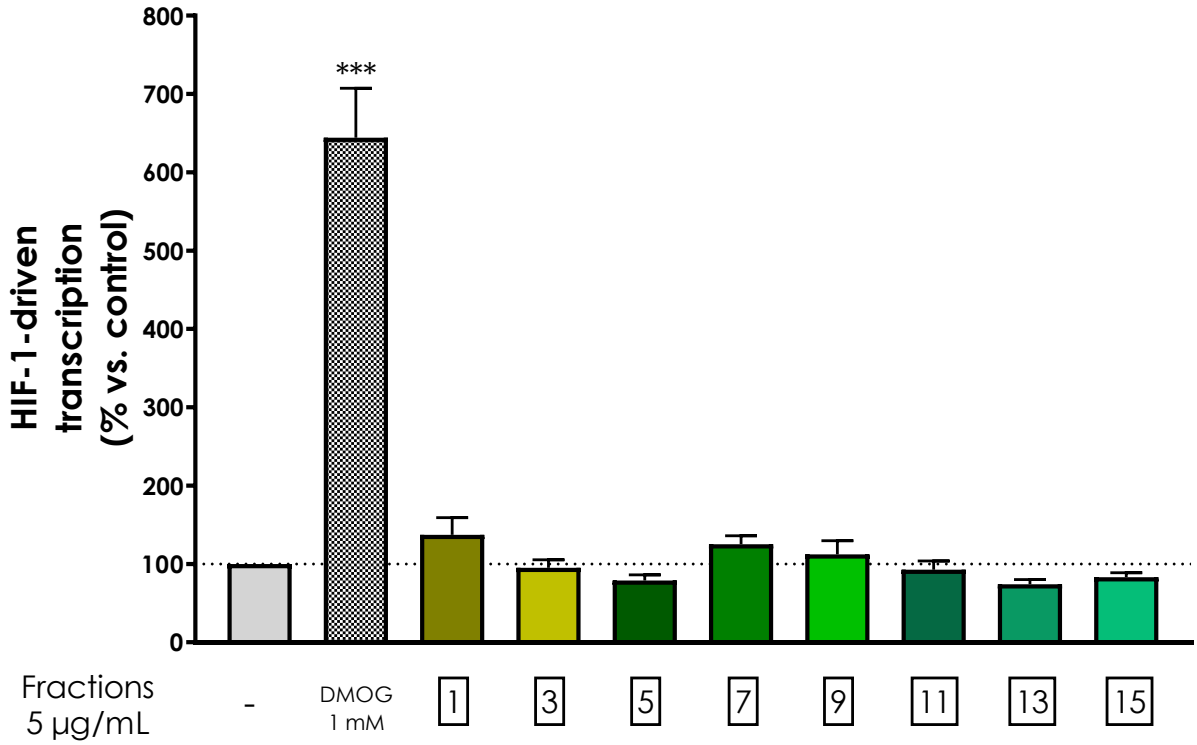

Figure 50 | *Assessment of green Brazilian propolis fraction effect on HIF-driven transcription in HDF cells. Cells were treated for 24 h with 5 µg/ mL of each fraction. Data are reported as percentage with respect to the control, which was arbitrarily assigned the value of 100%.*

Among red propolis fractions, only fraction 2 determined a statistically significant induction of HIF-driven transcription (**Fig. 51**). Fluorescent immunocytochemistry confirmed the stabilisation and nuclear translocation of HIF-1a by this fraction in HDF cells (**Fig. 52**).

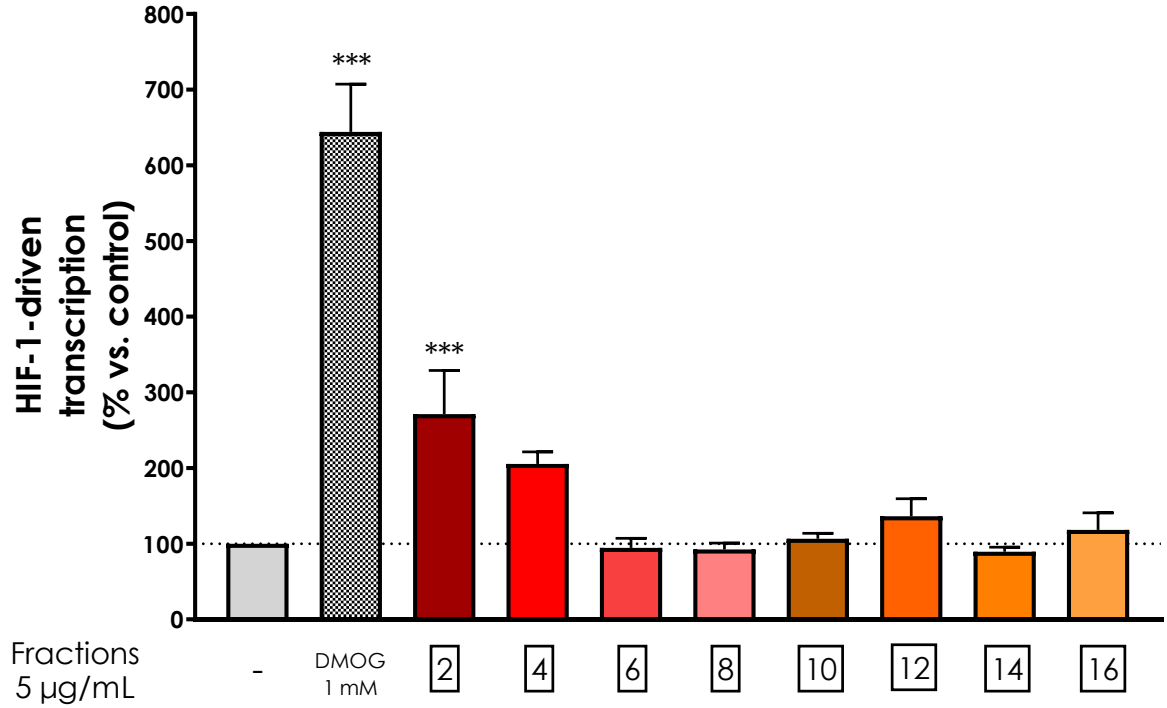

Figure 51 | *Assessment of red Brazilian propolis fraction effect on HIF-driven transcription in HDF cells. Cells were treated for 24 h with 5 µg/ mL of each fraction. Data are reported as percentage with respect to the control, which was arbitrarily assigned the value of 100%. *** $p < 0.001$ versus control.*

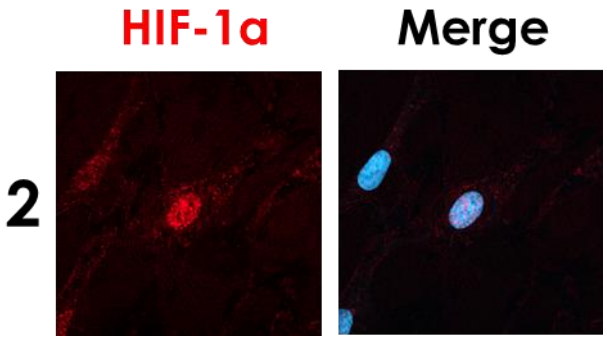

Figure 52 | *Representative confocal micrographs of the fluorescent immunostaining of HIF-1a (red) to confirm the effect of significantly active red propolis fractions on HIF-1a stabilisation and nuclear translocation in HDF cells after 24 h of treatment. Nuclei were stained with DAPI (blue).*

4.3.4 *SUBFRACTIONATION*

To get closer to the identification of the molecular entities present in green and red Brazilian propolis fractions and actively involved in the induction of HIF-1 transcriptional activity, the most promising fractions identified in previous experiments were further subfractioned by gel permeation chromatography on a Sephadex LH-20 column. Subfractions were then analysed by thin layer chromatography to check for similarities and related subfractions were gathered according to the schemes reported in **Fig. 53**.

A

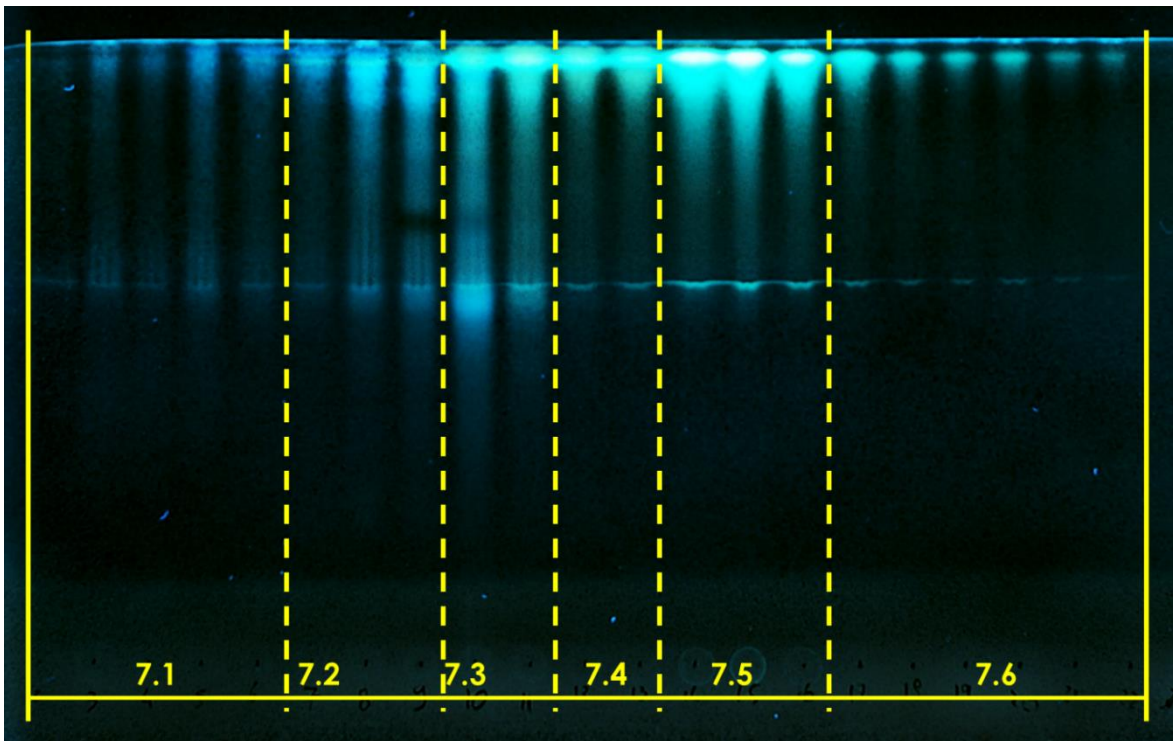

B

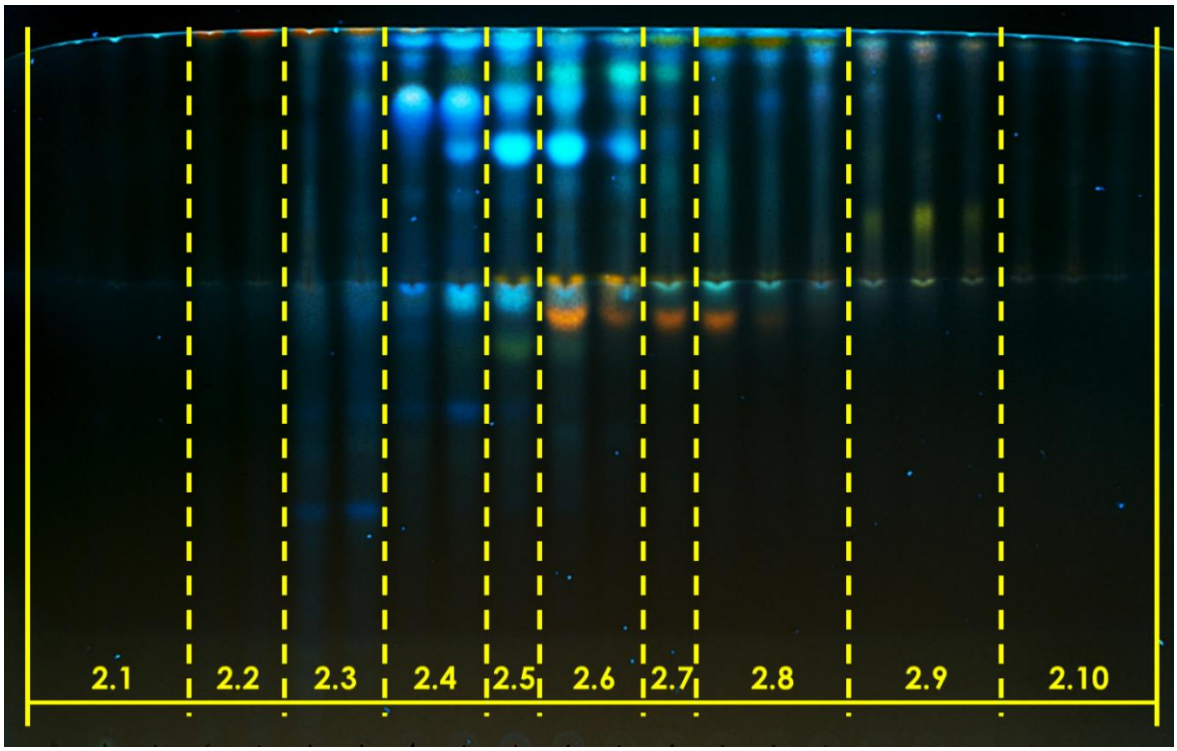

C

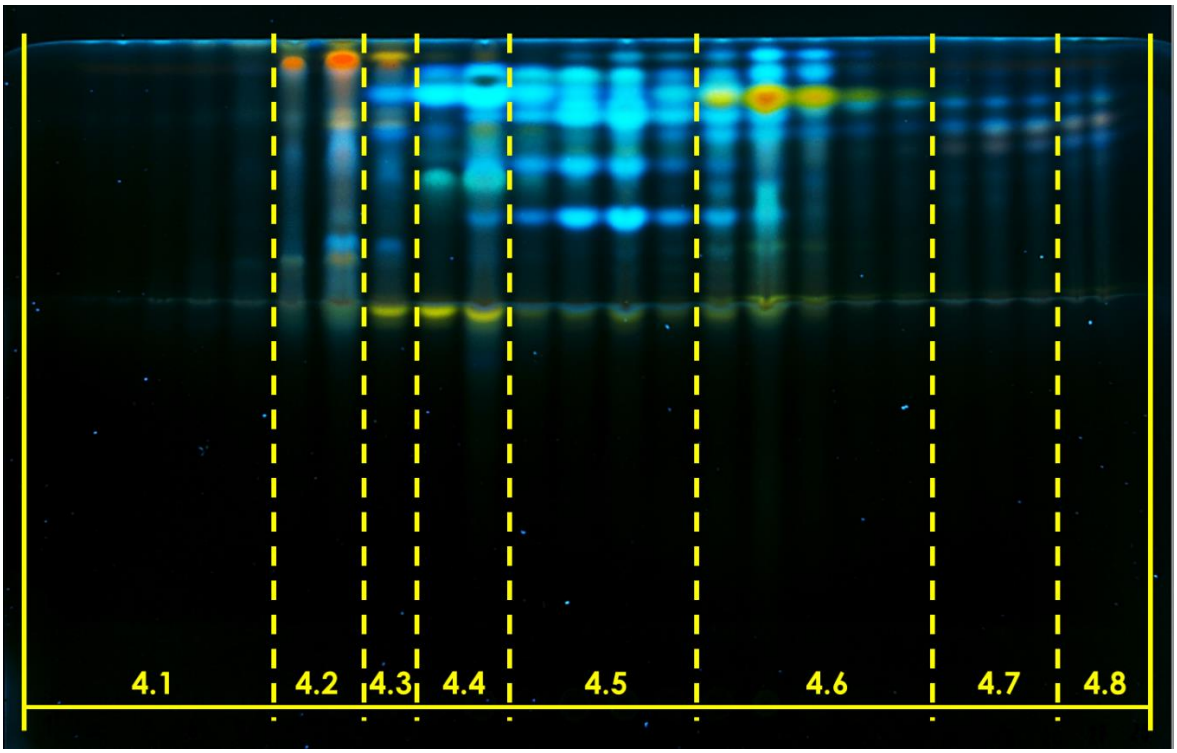

D

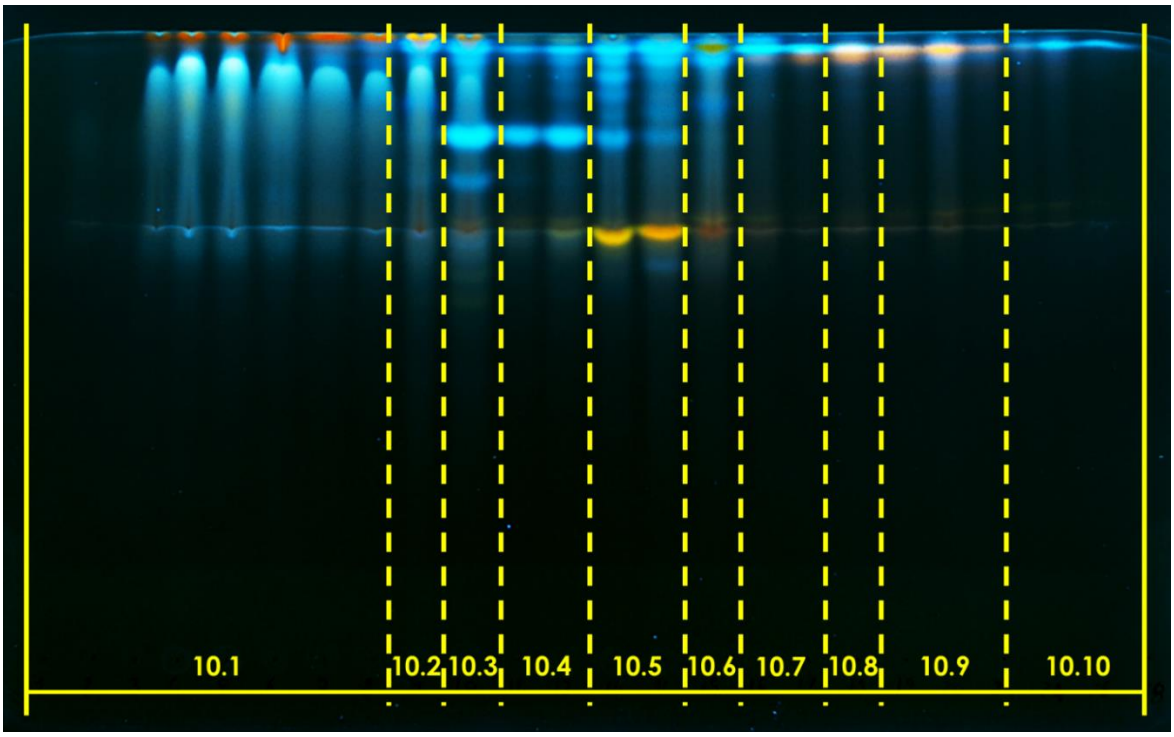

Figure 53 *| TLC assessment of the similarities among subfractions of fractions 7 (**A**), 2 (**B**), 4 (**C**), and 10 (**D**). Samples were loaded on silica gel plates, twice eluted with EtOAc:AcOH:HCOOH:H_2O 100:11:11:26 and DCM:EtOAc:HCOOH 85:15:0.5, and revealed under 366 nm UV light after spraying with NP/PEG reagent. Subfractions showing high similarities were brought together and renamed according to the scheme depicted.*

4.3.5 *EFFECT ON HIF-1 – PART II*

To assess which of green and red Brazilian propolis subfractions possessed the ability to induce the stabilisation of HIF-1a and the subsequent HIF-driven transcription, HaCaT and HDF cells were transiently transfected with an HRE-Luc reporter plasmid and concomitantly treated for 24 h with a screening concentration (5 µg/mL) of each fraction.

In HaCaT cells, among the subfractions of green propolis fraction 7, only 7.3 determined a statistically significant induction of HIF-driven transcription (**Fig. 54**).

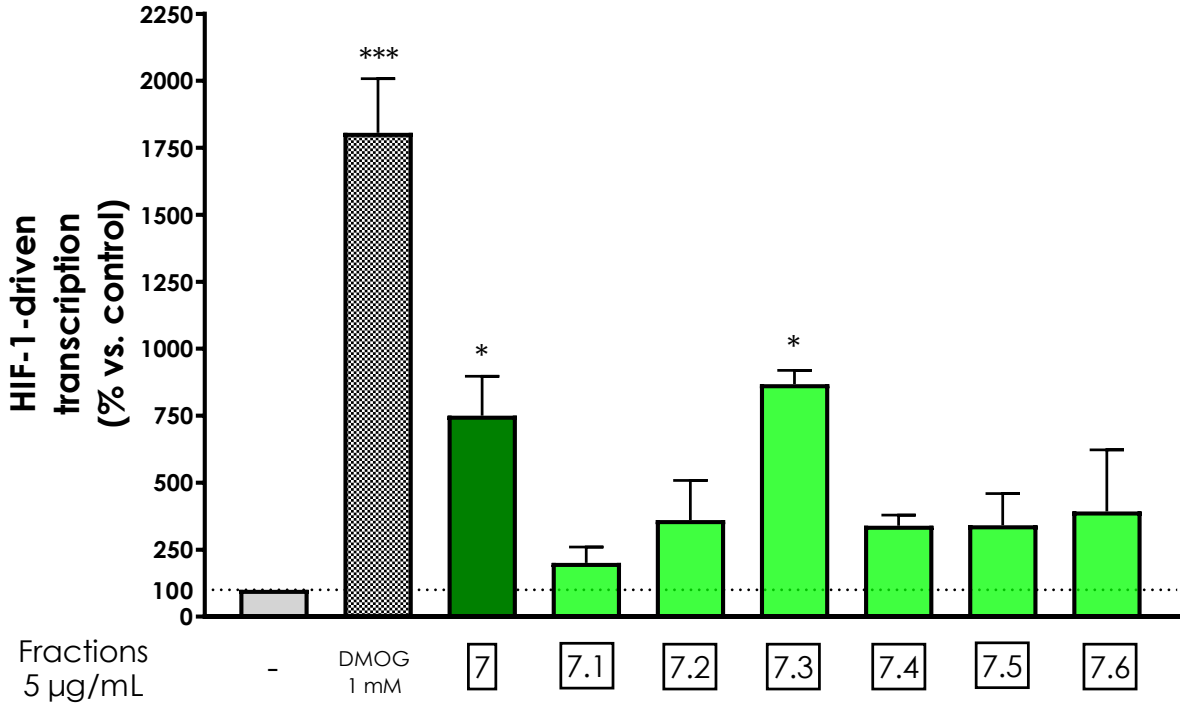

Figure 54 | *Assessment of green Brazilian propolis fraction 7 and related subfraction effect on HIF-driven transcription in HaCaT cells. Cells were treated for 24 h with 5 µg/ mL of each subfraction. Data are reported as percentage with respect to the control, which was arbitrarily assigned the value of 100%. * p < 0.05 versus control.*

Among the subfractions of red propolis fraction 4, a statistically significant induction of HIF-driven transcription was induced by 4.1 and subfractions around 4.5 (**Fig. 55**). These results indicate the possible presence of two active molecules, one present in subfraction 4.1 and one present in subfractions from 4.3 to 4.6 with a peak in 4.5.

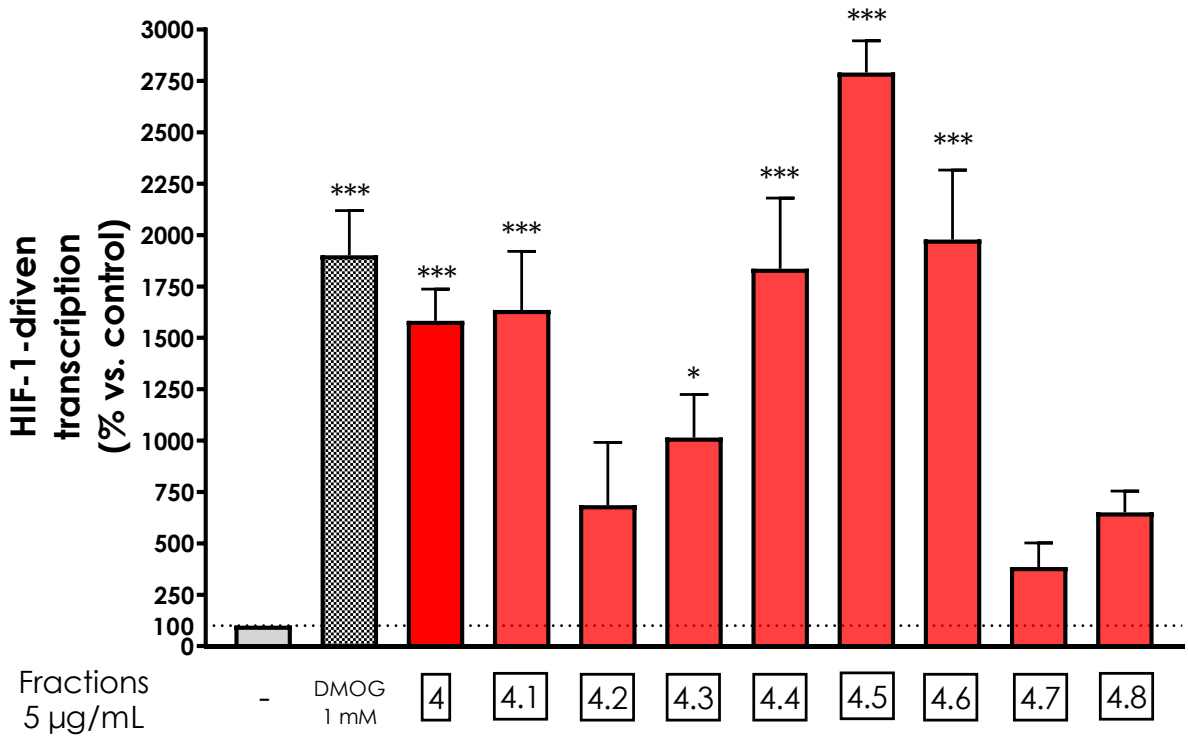

Figure 55 | *Assessment of red Brazilian propolis fraction 4 and related subfraction effect on HIF-driven transcription in HaCaT cells. Cells were treated for 24 h with 5 µg/ mL of each subfraction. Data are reported as percentage with respect to the control, which was arbitrarily assigned the value of 100%. * $p < 0.05$, *** $p < 0.001$ versus control.*

Among the subfractions of red propolis fraction 10, a statistically significant induction of HIF-driven transcription was induced by subfractions around 10.2 and 10.5 (**Fig. 56**). Also in this case, these results indicate the possible presence of two active molecules.

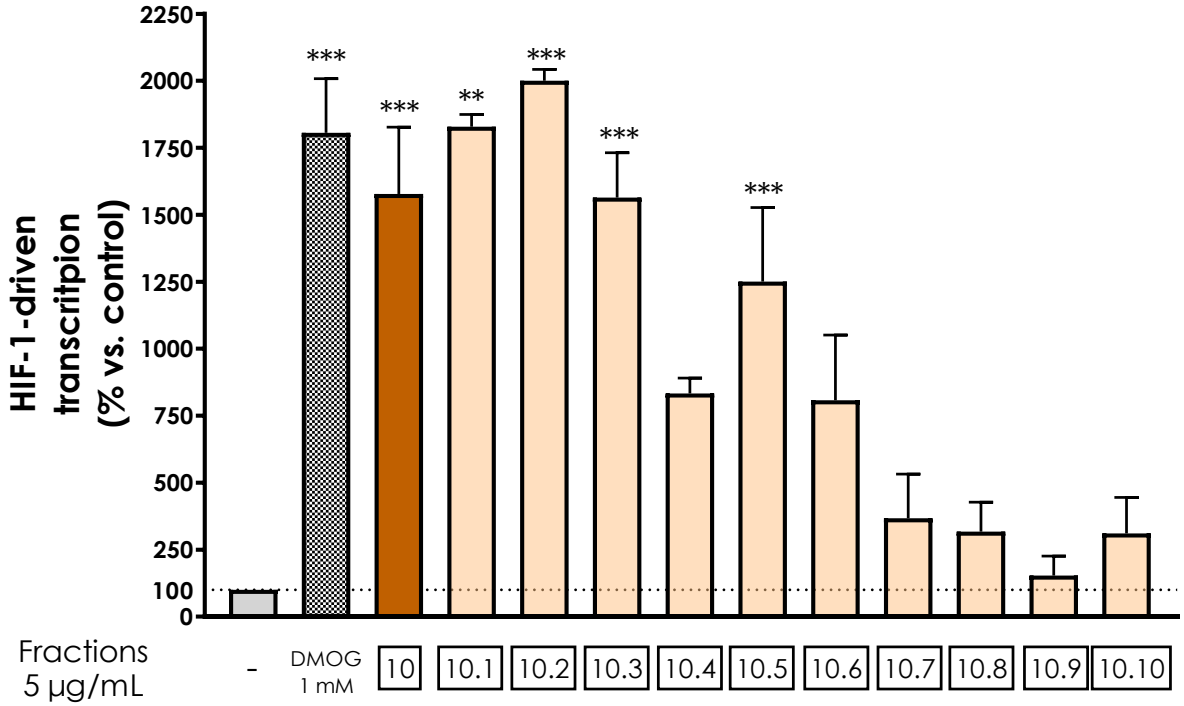

Figure 56 | *Assessment of red Brazilian propolis fraction 10 and related subfraction effect on HIF-driven transcription in HaCaT cells. Cells were treated for 24 h with 5 µg/ mL of each subfraction. Data are reported as percentage with respect to the control, which was arbitrarily assigned the value of 100%. ** p < 0.01, *** p < 0.001 versus control.*

In HDF cells, among the subfractions of red propolis fraction 2, only 2.8 determined a statistically significant induction of HIF-driven transcription (**Fig. 57**).

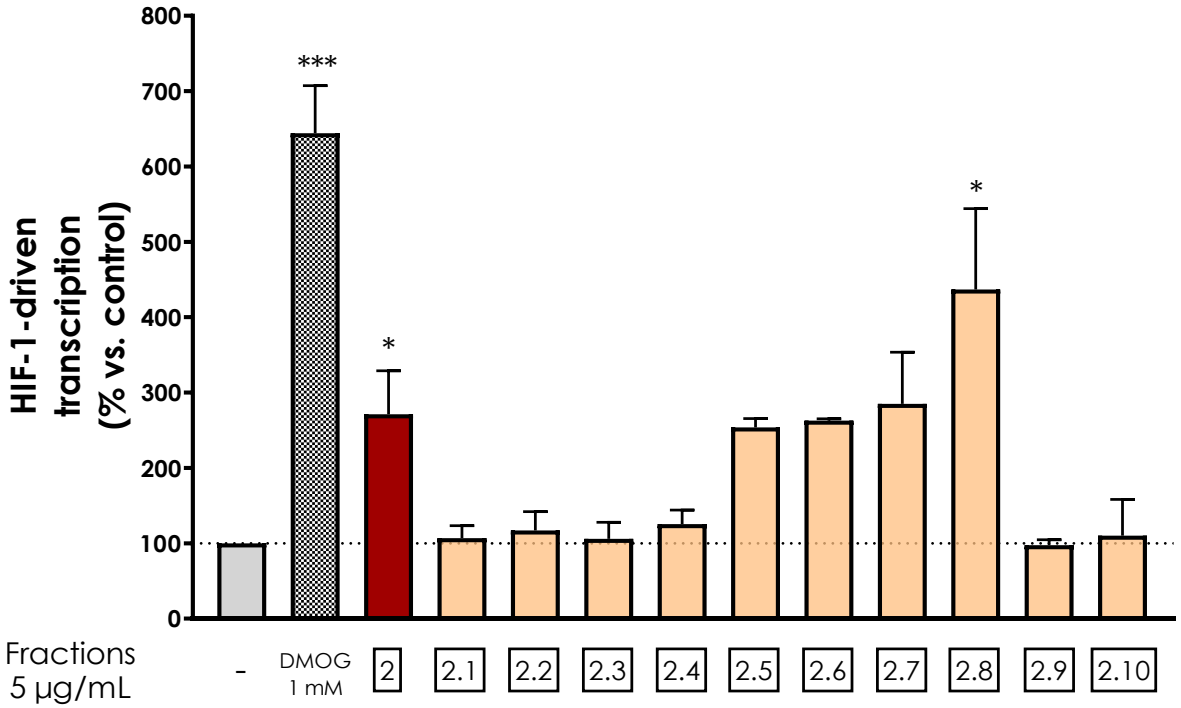

Figure 57 | *Assessment of red Brazilian propolis fraction 2 and related subfraction effect on HIF-driven transcription in HDF cells. Cells were treated for 24 h with 5 µg/ mL of each subfraction. Data are reported as percentage with respect to the control, which was arbitrarily assigned the value of 100%. * p < 0.05 versus control.*

Among the subfractions of red propolis fraction 4, 4.6 determined a statistically significant induction of HIF-driven transcription (**Fig. 58**), paralleling the results obtained in HaCaT cells and suggesting the presence of a molecule active in both cell lines.

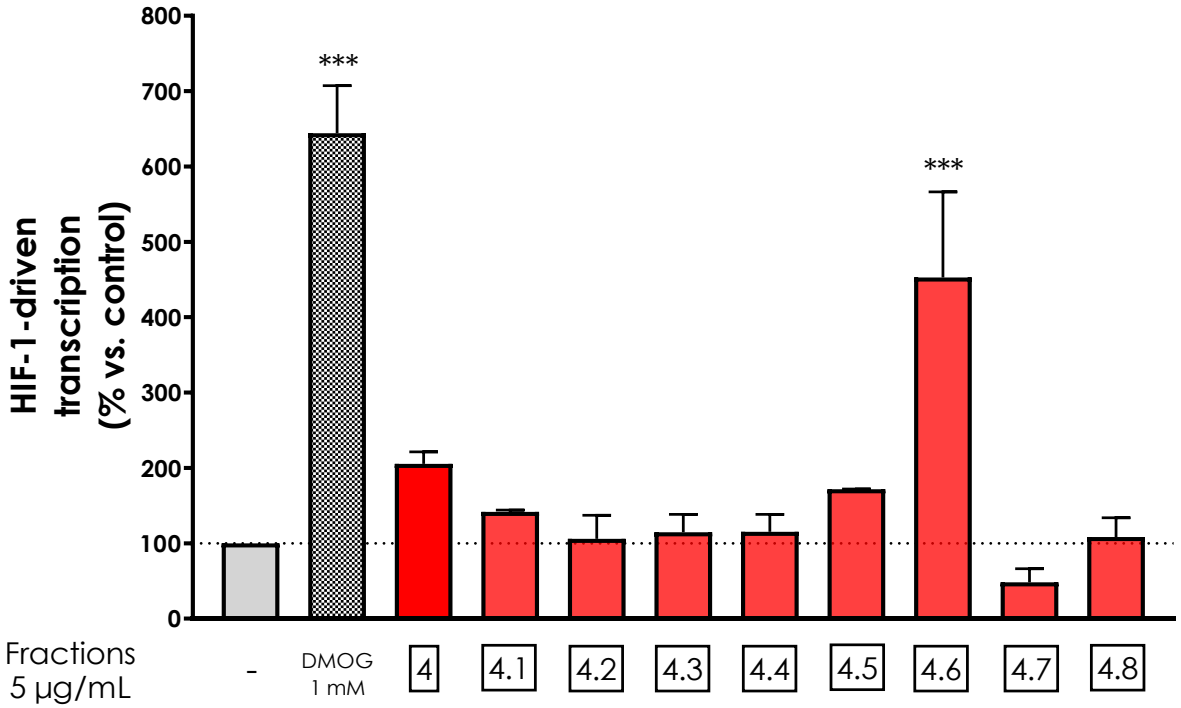

Figure 58 | *Assessment of red Brazilian propolis fraction 4 and related subfraction effect on HIF-driven transcription in HDF cells. Cells were treated for 24 h with 5 µg/ mL of each subfraction. Data are reported as percentage with respect to the control, which was arbitrarily assigned the value of 100%. *** p < 0.001 versus control.*

To conclude the bioguided fractionation, the HPLC-ESI-MS/MS qualification of the molecules present in bioactive subfractions has been set up. The analysis was preliminary conducted on subfraction 4.5, which had determined a particularly significant activity in HaCaT cells (**Fig. 55**), and adjacent subfractions. By carefully observing the pattern of bioactivity across subfractions, it is in fact possible to infer that the compounds of interest had been eluted in contiguous subfractions. For this reason, the identification of chromatographical peaks characterised by intensity paralleling the distribution of the biological activity could provide strong indication of the molecules active on HIF-1 pathway activation. A peak with RT = 34.26 min showed a strict correlation between intensity (**Fig. 59**) and the pattern of biological activity and was putatively assigned to medicarpin on the basis of the *m/z* of parent and fragment ions.

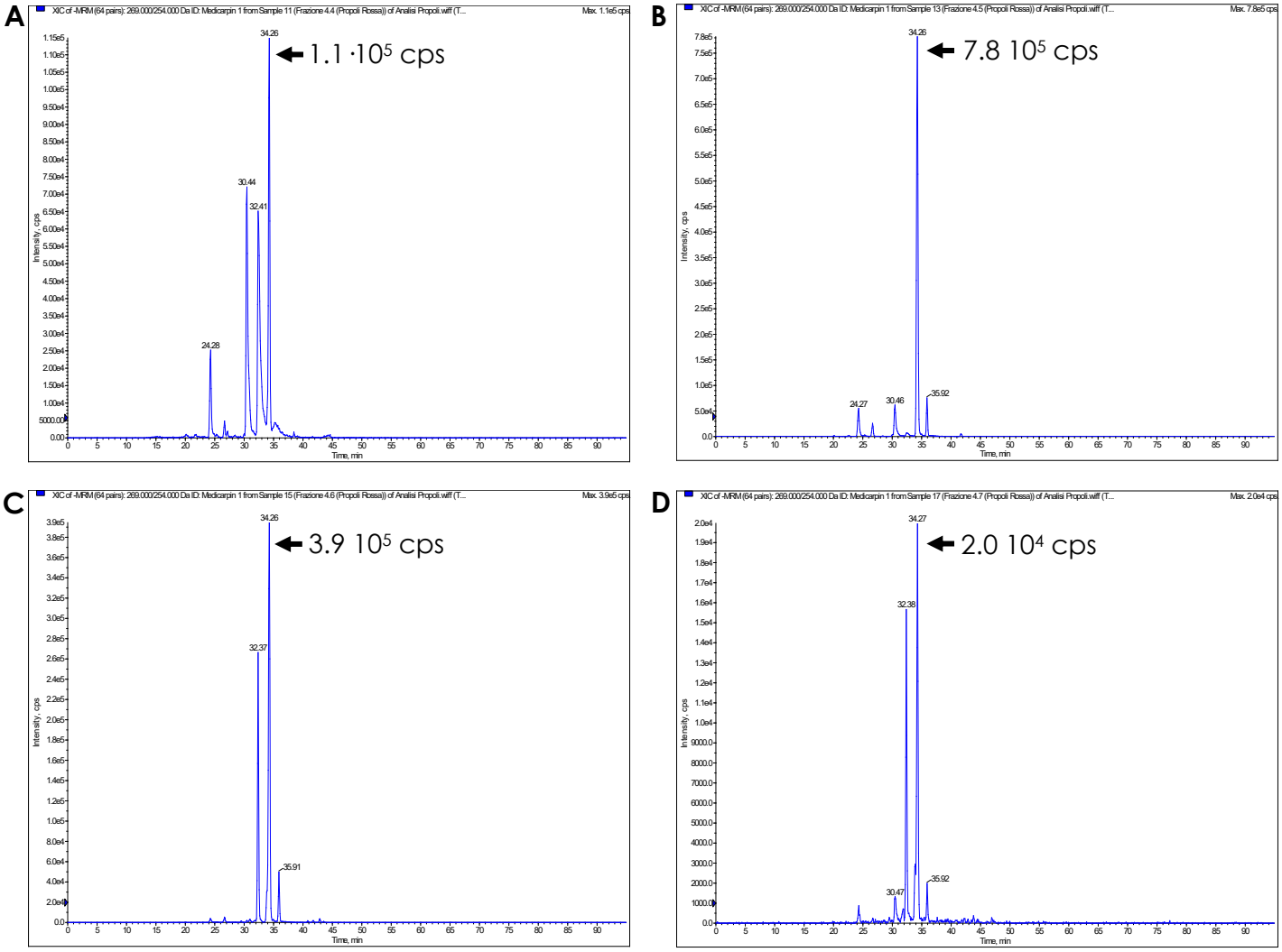

Figure 59 | *Extracted-ion chromatograms of MRM 269.00 → 254.00 (ESI-) of subfractions 4.4 (**A**), 4.5 (**B**), 4.6 (**C**), and 4.7 (**D**). The peak at RT = 34.26 was putatively assigned to medicarpin.*

Although no literature data report the activity of medicarpin on HIF-1, this molecule is interestingly able to activate the PI3K/Akt pathway (Chern et al., 2021), which has a prominent role in the regulation of HIF-1 activation and signalling (Z. Zhang, Yao, Yang, Wang, & Du, 2018).

5 DISCUSSION

Cutis, a fundamental part of the integumentary system with the function of covering the entire organism, is composed of a stratified cornified epithelium, the epidermis, sustained by a layer of dense connective tissue, the dermis. The epidermal barrier protects underlying tissues from external insults and plays numerous functions of physiological relevance. From a histological point of view, various cell types that contribute to the formation and function of the epidermis can be identified, among which keratinocytes, organised in layers that, from inside up to the surface, reflect their evolution from living cells to corneocytes interweaved in a lipid matrix, are the main exponents.

Cutis can be subjected to various types of external injuries, which undermine its integrity and the capacity to act as a protective barrier. When such a barrier falls short, a well-orchestrated cascade of biochemical and cellular events is initiated to repair the injury, and the success of wound healing depends on cells, molecular mediators, and structural elements involved. Wound healing can be described as a sequence of discrete events, which temporally encompass the entire process of post-traumatic tissue repair, consisting of widely overlapping stages: haemostasis and inflammatory phase, proliferative phase, and remodelling. Besides being complex, the healing process is likely to be interrupted and fail. When a hostile microenvironment prevails and the delicate balance between pro-inflammatory mediators, chemokines and proteases, characteristic of acute injuries, is disrupted, wounds demonstrate the inability to progress in a coordinated manner through the stages of healing. The process stops in a self-perpetuating inflammatory state, and wounds remain untreatable despite adequate therapy.

Propolis is a multifaceted bee product that has been traditionally used to facilitate wound healing and its therapeutic properties, known since ancient times, are currently experiencing a renewed and deserved interest in pharmacological research. "Propolis" is an umbrella term used to define a complex product, which is only outwardly uniform in features, macroscopic appearance, and composition, but implies a dramatical diversity in molecular components due to the geographical area, the botanical species present

around the apiary, and the climatic conditions at the collection time (V. Bankova, 2005a). Moreover, also methods of extraction from the raw material influence the final composition, leading to highly diverse propolis extracts (Cottica et al., 2011). Despite the extreme chemical variability, which inevitably poses serious issues about product standardisation, different propolis types demonstrate general pharmacological properties in terms of antioxidant, antimicrobial, anti-inflammatory, and immunomodulatory activities, which constitute the primary motivation for its therapeutic exploitation. In addition, resins and exudates collected by honeybees contain a plethora of plant-specific secondary metabolites characteristic of the local flora and responsible for additional biological activities. Beyond the multifariousness of propolis composition, a common thread unites samples with similar biological activities: the presence of high concentrations of flavonoids or phenolic acids. To overcome propolis inherent diversity and facilitate research in this field, many efforts have been made to classify and characterise propolis varieties according to their geographical origin and physical-chemical properties. Two of the varieties that are arousing more interest are green and red Brazilian propolis, native to diametrically opposed regions of Brazil and foraged from different botanical sources, *Baccharis dracunculifolia* DC. and *Dalbergia ecastaphyllum* (L.) Taub., respectively. The most innovative field of application of these propolis varieties is probably the treatment of cutaneous diseases. Recent *in vivo* evidence in rodent models has in fact highlighted the protective effects against UV-induced skin oxidative stress (C. M. Batista et al., 2018; Fonseca et al., 2011; Saito, Tsuruma, Ichihara, Shimazawa, & Hara, 2015) and the adjuvant activity in wound healing (F. R. Corrêa et al., 2017; de Moura et al., 2011; Jacob et al., 2015).

The present research project aimed at the comprehensive *in vitro* investigation of the molecular mechanisms, which could modulate the injury microenvironment favouring cutaneous wound healing, elicited by green and red Brazilian propolis in models of human keratinocytes and fibroblasts. Considering propolis variability, the varieties being studied were a fortiori chosen because of their certain origin from known botanical sources. In

addition, green Brazilian propolis is one of the most studied and commercialised varieties, although the evidence in the field of cutaneous wound healing is still scarce. As an example, it has been reported that green Brazilian propolis ointment can induce the complete re-epithelisation of the wound bed in rats (L. L. Batista et al., 2012). Nevertheless, the underlying molecular mechanisms have not been elucidated and the authors could not find any apparent correlation with the flavonoid content, suggesting the involvement of still unravelled actors. Even in the case of the well-established anti-inflammatory activity, the research on the pharmacological mechanisms through which the effect is explicated at a cellular level suffers from serious limitations, especially with regard to green and red Brazilian propolis varieties.

The investigations, object of the present work, have been conducted on multiple fronts, to elucidate potential differences and strengths of the two extracts under study. A thorough chemical characterisation, conducted with different and complementary chromatographical techniques, allowed the identification and relative quantification of numerous compounds present in green and red Brazilian propolis. The results of the analyses indicated artepillin C (8.5%, relative abundance) and drupanin (3.6%, relative abundance) as the main components of green propolis, whereas vestitol (14.6%, relative abundance), medicarpin (9.73%, relative abundance), and neovestitol (7.52%, relative abundance) were the most abundant in red propolis, thus confirming the evidence already reported in the literature (Alencar et al., 2007; Nunes & Guerreiro, 2012). This characterisation confirmed the higher flavonoid content of red propolis, while in green propolis the amount of flavonoid appears limited in favour of higher amounts of prenylated derivatives of phenolic acids. A considerable total phenolic content was demonstrated in both samples through the Folin-Ciocâlteu assay, significantly higher in red propolis consistently with the work of Machado et al. who demonstrated that, among other varieties of Brazilian propolis, red propolis presented the highest phenolic content (Machado et al., 2016). Red propolis also showed a greater antioxidant capacity in the ORAC assay, paralleled by the biological results obtained in keratinocytes with the assessment of ROS generation. There is in

fact a close correlation between the antioxidant capacity and the molecular structure of phenolic compounds (Cuvelier, Richard, & Berset, 1992), the efficacy of which is related to the presence of aromatic hydroxy groups that can donate hydrogen to free radicals, forming in turn stable phenolic radicals and preventing cell dysfunction and cytotoxicity. The biological activities have been investigated in two *in vitro* models of stable human cell lines representative of the principal actors involved in the process of wound healing, HaCaT keratinocytes and HDF dermal fibroblasts. Preliminary studies, assessing mitochondrial function and intracellular lactate dehydrogenase release, have been conducted to determine the cytotoxicity of the extracts and define treatment concentrations for subsequent experiments. Green propolis did not induce cytotoxic effects up to 50 µg/mL and 24 h of treatment. On the other hand, red propolis showed in HaCaT cells prodromal toxicity signs at the highest concentration at 6 h, which became fully manifested at 24 h, limiting at 10 µg/mL the maximum usable concentration at longer time points. On the basis of literature data, cytotoxic effects have been attributed to the elevated isoflavone content (da Silva et al., 2015). Nevertheless, a putative protein synthesis inhibitory mechanism has been excluded based on the results of the O-propargyl-puromycin assay.

The anti-inflammatory properties of green and red Brazilian propolis, although being quite well-established in literature (Dos Santos et al., 2022), have never been explored neither in keratinocytes nor in dermal fibroblasts. Consequently, the ability to inhibit NF-κB-driven transcription, representative of one of the principal pathways involved in skin inflammatory processes, has been extensively evaluated in HaCaT and HDF cells. In HaCaT cells, both extracts, and red propolis in a much more significant manner, were active in inhibiting the activation of NF-κB under TNF-α pro-inflammatory stimulation. In HDF cells, the effect was less pronounced and manifested with a certain significance only for red propolis at the highest concentration tested. The ability to inhibit NF-κB-driven transcription under another pro-inflammatory stimulus, IL-1β, has been further examined; however, only in HaCaT cells since this cytokine could not elicit NF-κB activation in HDF cells. It is known that prolyl-hydroxylases

(PHDs) involved in the regulation of HIF-1a stability are also required to modulate IL-1β-induced NF-κB activation via key post-translational modifications in the IL-1β pathway (Scholz et al., 2013). Green propolis determined, at the highest concentration tested, a slight significant inhibition of IL-1β-induced NF-κB-driven transcription, similar to the effect obtained with dimethyloxalylglycine (DMOG), a synthetic inhibitor of PHDs used as a reference compound, and thus suggesting a putative mechanism involving PHDs. Red propolis, instead, showed a greater activity abolishing, at the highest concentration tested, NF-κB-driven transcription and proving much more effective than DMOG. These results claim for the existence of additive or synergic alternative anti-inflammatory mechanisms on the IL-1β pathway, other than the inhibition of PHD activity.

The NF-κB pathway is implicated in the downstream modulation of the expression of several inflammatory chemokines and cytokines, including IL-8 and IL-6 (Pahlavani et al., 2020). These mediators are expressed in cutis during the inflammatory phase of wound healing, but an excessive or prolonged secretion is correlated with the chronification of cutaneous injuries (Iocono et al., 2000). Red propolis exerted a significant inhibitory effect on IL-8 release in both HaCaT and, to a greater extent, HDF cells under TNF-a pro-inflammatory stimulation, thus confirming the anti-inflammatory properties previously inferred. On the other hand, limited or no effect was seen in the case of green propolis. The greater efficacy of red propolis emerging from these results is probably associated with the higher phenolic content and especially with the presence of flavonoids (Moise & Bobiş, 2020). Both propolis, in absence of any other stimulation, resulted able to increase the expression of *IL6* gene, which was further investigated by evaluating cytokine secretion levels. In basal conditions, it was not possible to detect any cytokine release. However, when HaCaT and HDF cells were treated under the pro-inflammatory stimulus of TNF-a and IFN-γ, known to facilitate IL-6 release, both extracts and in particular red propolis induced, at the highest concentrations tested, a significant increase in IL-6 secretion, above the cytokine-stimulated levels. It is noteworthy the evidence that, while the overexpression of *IL6* gene seen in basal conditions was not

paralleled in absence of stimulation, cytokine secretion was actually enhanced in an inflammatory model mimicking the injury microenvironment. This is particularly interesting considering the favourable involvement in the initial phases of cutaneous repair of IL-6, which exerts a proliferative effect on keratinocytes, is a chemoattractant for neutrophils, and may have a role in collagen deposition and angiogenesis (Johnson et al., 2020). It has in fact been demonstrated that *IL6* knockout mice present a significant delay in wound healing (Lin et al., 2003).

The putative molecules possibly able to explicate the abovementioned anti-inflammatory activities may be recognised for red propolis in vestitol, able to inhibit the release of chemokines and the migration of neutrophils in the inflammatory site, and neovestitol, which modulates the NO pathway to inhibit leukocyte recruitment (Franchin et al., 2016). However, apart from this evidence, activities on the transcription factor NF-κB analogous to those demonstrated in this work have never been reported nor related to any specific component. For green propolis, the ability to modulate the NF-κB pathway, and consequently inhibit the production of prostaglandin E_2 and nitric oxide, has been previously demonstrated for the main component artepillin C (Paulino et al., 2008). All these molecules have been identified in propolis samples considered in this study and, on the basis of their relative abundance, were found to be the principal characterising compounds and, therefore, the main candidates for the attribution of the anti-inflammatory activities observed.

Once the anti-inflammatory activities had been elucidated, the focus was shifted to other possible molecular mechanisms that might be targeted by green and red Brazilian propolis to facilitate the cutaneous healing process, and in particular on the role of the interaction with the HIF-1 transcriptional complex. HIF-1 is a heterodimer composed of an oxygen-regulated alpha subunit, the stability of which is enhanced by hypoxia, and a constitutively expressed beta subunit (Wang et al., 1995), able to induce the expression of genes that promote cell survival, re-establish tissue oxygenation (e.g. *VEGFA*), and sustain glycolytic metabolism to produce ATP under oxygen shortage (Semenza, 2010). In fact, among a myriad of factors that can delay wound

healing, tissue hypoxia combined with a defective cell response can perpetuate a deleterious cycle that impedes the transition towards the proliferative phase. HIF-1 is normally activated by hypoxic stimuli that can be present in acute and chronic injuries and contributes to the induction of a transcriptional programme aimed at the re-establishment of cutaneous integrity. Several mediators are under the control of HIF-1 and while its deficiency is related to alterations in the proliferative phase, collagen deposition, and the establishment of chronic injuries, on the contrary, its unregulated activation may lead to fibroproliferative diseases (Hong et al., 2014), thus highlighting the importance of fine-tuning. The ultimate outcome of cutaneous wound healing is most commonly repair, a form of incomplete regeneration that ends in the formation of a scar proportional to the duration and severity of inflammation. Nevertheless, it has been recently demonstrated that the hypoxia-independent induction of HIF-1 activity, obtained with the pharmacological inhibition of PHDs, evokes a regenerative phenotype in mammals (Y. Zhang et al., 2015) and may therefore influence cell survival, wound closure, and tissue regeneration, suggesting that targeting this pathway can improve the wound healing process (Botusan et al., 2008; Kalucka et al., 2013; X. Zhang et al., 2013; Y. Zhang et al., 2015). In addition, PHD inhibitors such as the iron chelating agents deferoxamine and deferiprone, are successfully used for the treatment of difficult-to-heal diabetic and pressure ulcers (Bonham et al., 2018; Duscher et al., 2015).

Initial screening immunocytochemistry experiments have demonstrated that both propolis are able to induce the stabilisation and nuclear translocation of HIF-1a in HaCaT cells, while only red propolis seems to be active at 24 h in HDF cells. Further confirmations have been obtained by western blotting, which allowed the quantification of the effect. The results showed greater activity of green propolis in HaCaT cells and reconfirmed that in HDF cells only red propolis is active at longer time points. Noteworthy, in HDF cells the effect on HIF-1a stabilisation appeared temporally disjoint from that of DMOG, thus suggesting different underlying molecular mechanisms. Gene expression analysis of *VEGFA*, one of the principal target genes downstream of HIF-1 involved in

angiogenesis, cell proliferation, and migration (Forsythe et al., 1996), has demonstrated a significant overexpression, especially in the case of green propolis in HaCaT cells, in line with the results obtained in immunocytochemistry and western blotting. Once again, in HDF cells only red propolis was active and the effect manifested itself at significantly longer timepoints than DMOG. *VEGFA* modulation was further investigated evaluating protein secretion levels. Similarly to what had been observed in the previous experiment, both green and red propolis, at the highest concentrations tested, induced in HaCaT cells a significant release of VEGF at 24 h. On the contrary, unexpectedly, no secretion could be detected in HDF cells.

The significance of the previous findings and their translatability *in vivo* would benefit from the use of three-dimensional organotypic co-cultures, capable of taking into account the interplay between fibroblasts and keratinocytes. For this reason, a model of *in vitro* reconstructed skin was developed, implementing a co-culture of the two cell lines considered in the present work, HaCaT keratinocytes and HDF fibroblasts. HDF cells were interspersed in a bovine type I collagen matrix and covered with a layer of HaCaT cells, cultured at the air-liquid interface for 2 weeks. Preliminary data provided unexpected results since a number of literature studies stated the difficulty if not the impossibility to obtain the differentiation of HaCaT cells into mature epidermal layers (Boelsma et al., 1999). Nevertheless, the analysis of haematoxylin and eosin micrographs obtained by light microscopy demonstrated the morphological stratification of keratinocytes, and it was possible to notice their flattening and the loss of nuclei towards the surface. In addition, confocal fluorescence micrographs displayed the physiological localisation of keratin 1 in basal cells, keratin 10 in suprabasal layers, and involucrin in desquamating corneocytes. These considerations confirm the obtainment of a stratification analogous to that observed *in vivo*; however, the number of keratinocyte layers is inferior and there is the possibility that the reconstructed epidermis might be parakeratotic. The functional response of the *in vitro* skin equivalent was preliminarily assessed by measuring the release of VEGF in co-cultures treated with green and red Brazilian propolis.

Consistently with the results obtained in cell monolayers, propolis proved able to induce VEGF secretion, showing a peak at 24 h of treatment. Based on this data, the newly implemented reconstructed skin model surely deserves future development to obtain an *in vitro* wound healing model suitable for the evaluation of natural products potentially able to enhance repair and regeneration.

In a successive phase of the work, to overcome the confounding factors resulting from propolis inherent variability, a bioguided fractionation has been conducted with the aim of elucidating the actual role of green and red Brazilian propolis components in the elicitation of HIF-1 induction, an innovative and neglected molecular mechanism potentially exploitable to obtain successful wound healing and cutaneous regeneration. Propolis samples were initially partitioned between immiscible solvents, yielding eight fractions for each variety. The cytotoxicity profile of propolis fractions has been initially determined by assessing neutral red uptake and intracellular lactate dehydrogenase release, showing the fractionation of toxic effects, consistently in HaCaT and HDF cells. A common concentration of 5 µg/mL, far below the cytotoxicity threshold for all fractions, was chosen to screen the ability to induce HIF-1-driven transcription in a reporter plasmid assay that allowed the identification of the most active fractions. The stabilisation and nuclear translocation of the subunit HIF-1a were further confirmed through fluorescent immunocytochemistry in confocal microscopy. As expected, in accordance with previous experimental results, all green propolis fractions turned out to be inactive in HDF cells.

Active fractions were further subfractioned by Sephadex LH-20 column chromatography, to possibly obtain and identify the compounds responsible for the molecular mechanism of interest. Then, subfractions were analysed by thin layer chromatography, and similar samples were gathered before proceeding with the screening of the biological activity. The pattern of activity across subfractions, with a bell-shaped trend, revealed that the responsible molecules had probably eluted in contiguous subfractions. Taking advantage of this phenomenon, the most active subfractions and the adjacent ones were

subjected to HPLC-ESI-MS analysis to verify if the fluctuation in activity was paralleled by fluctuations in one of the analytes. Preliminary results obtained in red propolis subfractions suggested medicarpin as one of the molecules putatively responsible for the induction of HIF-1 activity. Nevertheless, the characterisation of active green and red propolis subfractions still needs to be completed, and hypothetically bioactive molecules will have to be confirmed through the assessment of the activity of pure compounds.

In conclusion, cutaneous injuries represent extremely frequent and widespread conditions, which can result debilitating if not managed properly. Cutaneous wound healing appears to be a complex process, to the point that certain aspects are still to be elucidated and current pharmacological treatments are often non-specific and ineffective. It is influenced by several local and systemic factors: cellular elements, growth factors, and cytokines must be tightly orchestrated to lead to a favourable outcome, avoiding the establishment of pathological states. For this reason, the research and development of innovative products that could enhance the reparative, and possibly regenerative, processes are of pivotal importance.

As previously stated, propolis is a complex natural product with a broad spectrum of activities in a number of processes relevant to wound healing, which go far beyond the simple sum of its isolated components. The results of this research project have demonstrated the high chemical diversity existing between propolis with different origins and botanical sources. Green and red Brazilian propolis showed different cytotoxicity profiles, anti-inflammatory, and HIF-1 modulating activities, as well as differential biological activities in HaCaT keratinocytes and HDF fibroblasts, attributable to the qualitative and quantitative differences in chemical composition. Nevertheless, propolis stands out as a "super-blend" of biologically active compounds, evolutionarily sorted by honeybees to satisfy their eusocial need to safeguard the health of the superorganism, which pharmacological research can and should exploit to its advantage. Propolis antioxidant (Daleprane & Abdalla, 2013), antimicrobial (Grange & Davey, 1990), and anti-inflammatory (Sforcin, 2007) activities potentially integrate at different levels in the healing process. In addition,

propolis exerts complex immunomodulatory activities, ranging from immunosuppressive effects, related to its anti-inflammatory properties, on different T lymphocytes subsets, to the paradoxical activation of macrophagic and NK cell functions, demonstrating the ability to prevent infections and enhance resolution while dampening the inflammatory state (Magnavacca et al., 2022).

This study has investigated for the first time and elucidated, at least in part, the molecular mechanisms of action responsible for green and red Brazilian propolis anti-inflammatory activity in human keratinocytes and fibroblasts. In particular, red Brazilian propolis resulted able to significantly inhibit in a concentration-dependent manner the pathway of NF-κB and the secretion of IL-8, while inducing at the same time the expression of the multifunctional cytokine IL-6, which was, however, released only under noxious stimulation, outlining a potential anti-inflammatory and resolving activity. For the first time, the ability of Brazilian propolis to modulate the HIF-1 pathway has been demonstrated in human keratinocytes and fibroblasts, thus suggesting a favourable effect on wound healing and cutaneous regeneration. In addition, a bioguided fractionation strategy has paved the way to the identification of bioactive propolis components, suggesting medicarpin as one of the molecules putatively responsible for the activity of red propolis on HIF-1 pathway. Nevertheless, a more complete characterisation of green and red propolis active subfractions is needed to draw definitive conclusions.

Altogether, these findings reveal Brazilian propolis as an interesting natural product that showcases a wide range of activities to be exploited, particularly taking advantage of the combined ability to limit inflammatory states and favour a cellular programme of survival and regeneration, an innovative aspect scarcely investigated in the scientific literature, to achieve better clinical outcomes, thus offering promising perspectives for its clinical topical application in the near future.

6 APPENDIX A

6.1 UV-VIS ABSORPTION SPECTRA OF COMPOUNDS IDENTIFIED IN GREEN BRAZILIAN PROPOLIS THROUGH HPLC-ESI-HRMS ANALYSIS

- *p*-coumaric acid (RT = 7.93 min, λ_{max} = 228, 310 nm)

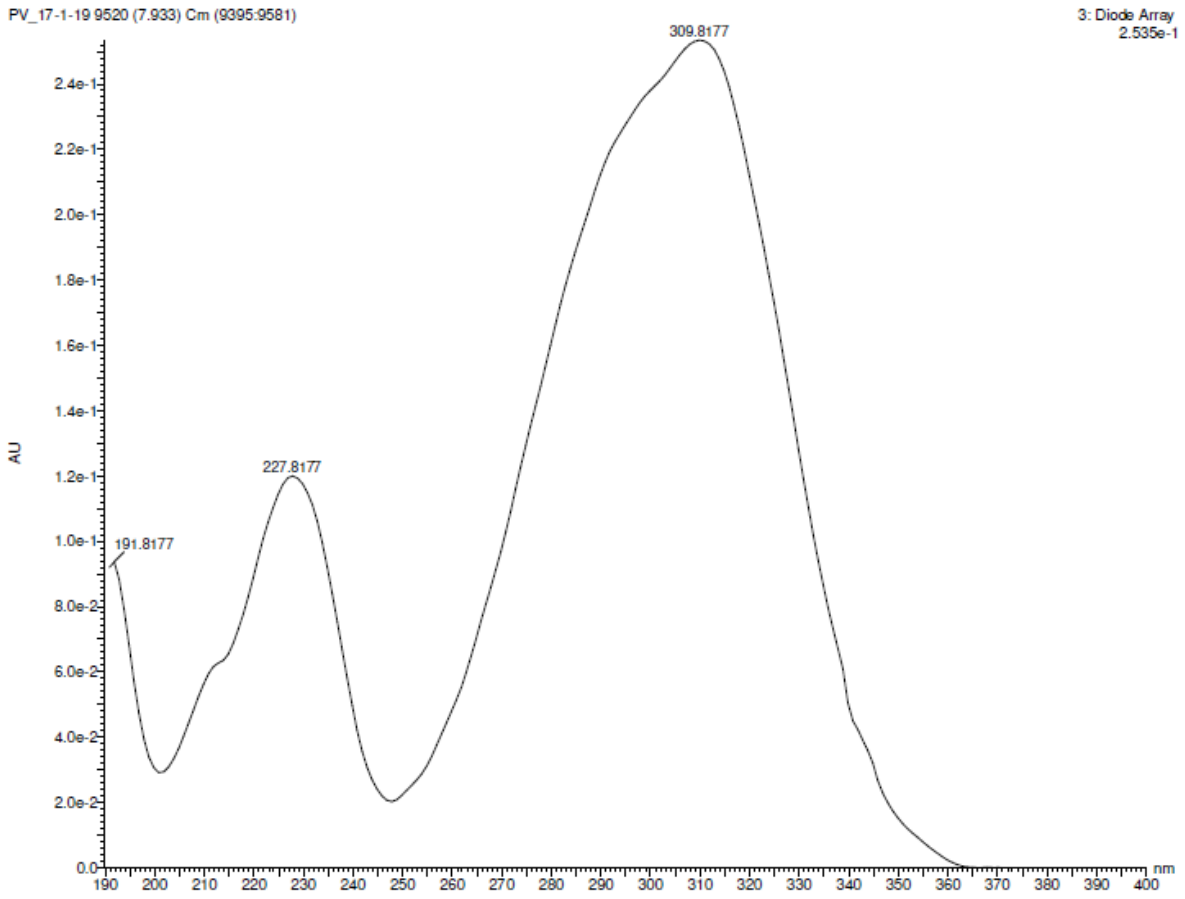

- Di-O-caffeoylquinic acid (RT = 12.40 min, λ_{max} = 244, 327 nm)

- Di-O-caffeoylquinic acid (RT = 13.605 min, λ_{max} = 244, 326 nm)

- Drupanin (RT = 25.724 min, λ_{max} = 236, 315 nm)

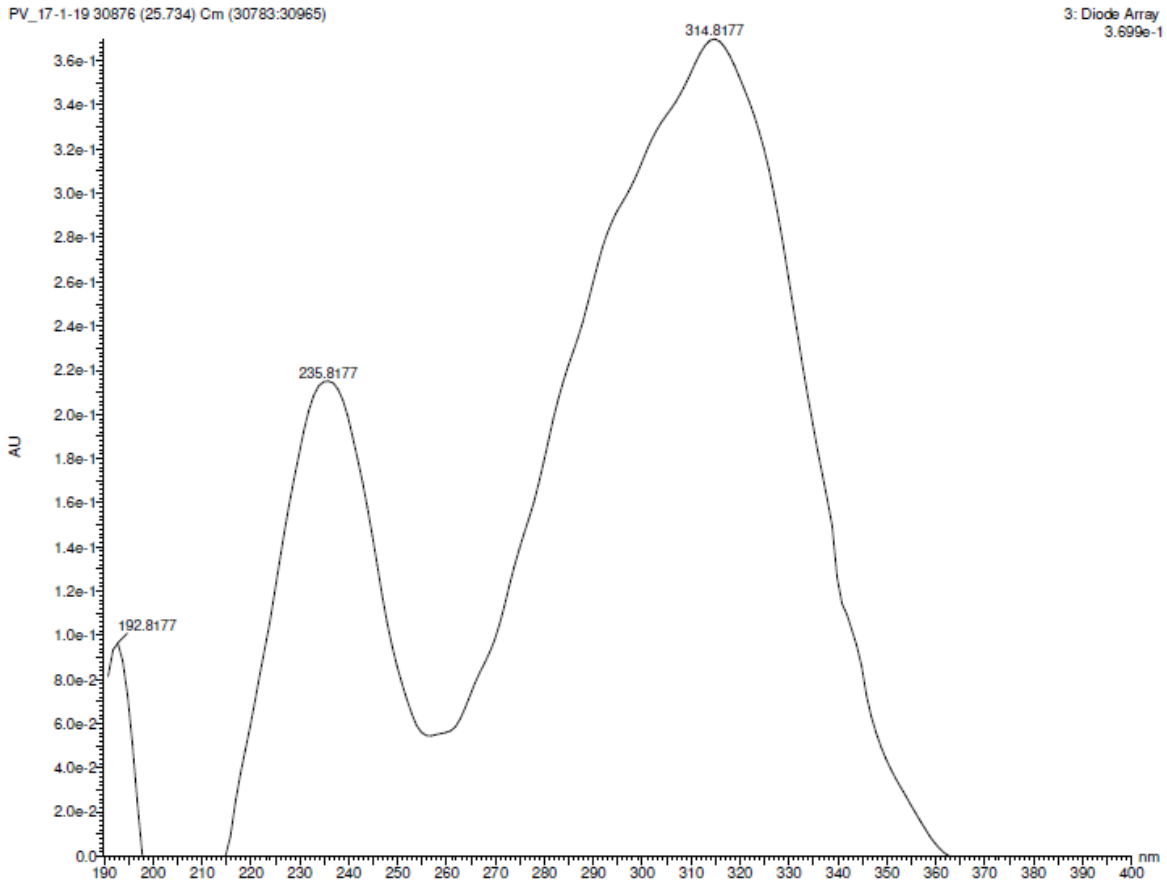

- Kaempferide (RT = 29.93 min, λ_{max} = 266, 369 nm)

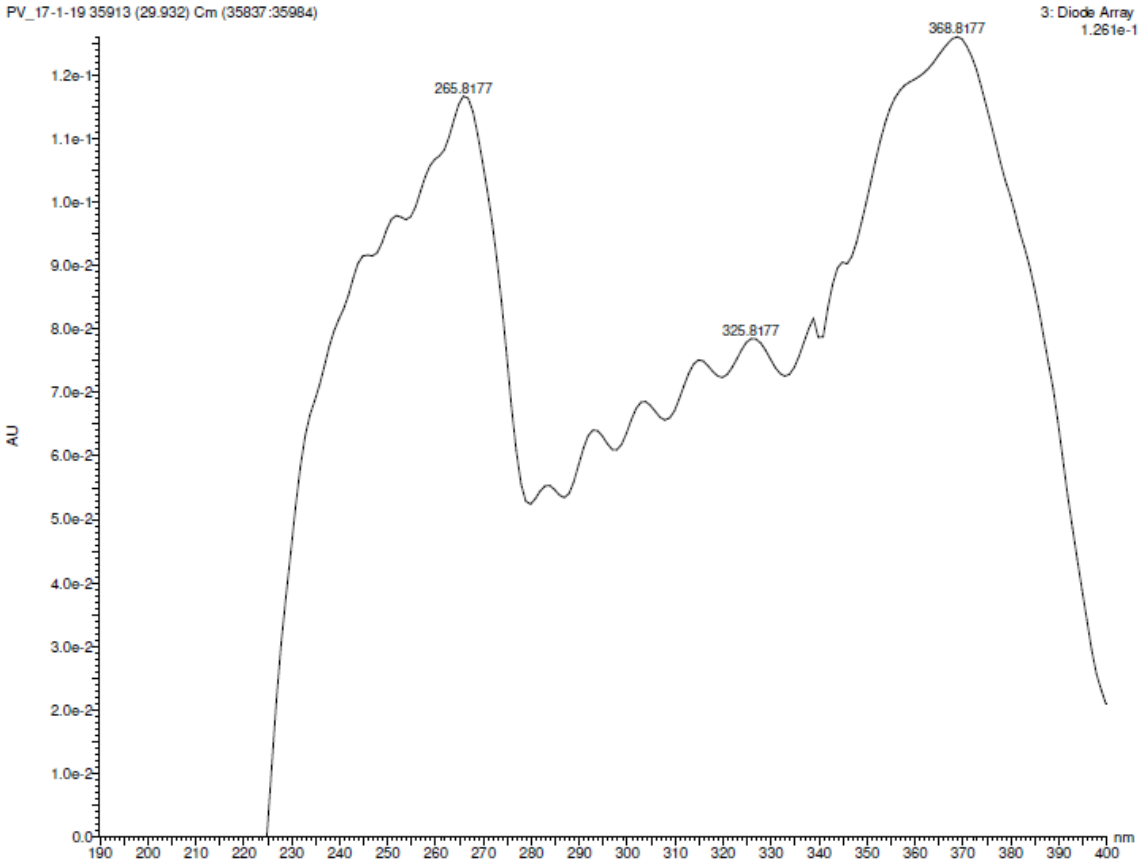
PV_17-1-19 35913 (29.932) Cm (35837:35984)
3: Diode Array
1.261e-1
368.8177
265.8177
325.8177
AU
1.2e-1
1.1e-1
1.0e-1
9.0e-2
8.0e-2
7.0e-2
6.0e-2
5.0e-2
4.0e-2
3.0e-2
2.0e-2
1.0e-2
0.0
190 200 210 220 230 240 250 260 270 280 290 300 310 320 330 340 350 360 370 380 390 400
nm

- Dimethylquercetin (RT = 30.62 min, λ_{max} = 370 nm)

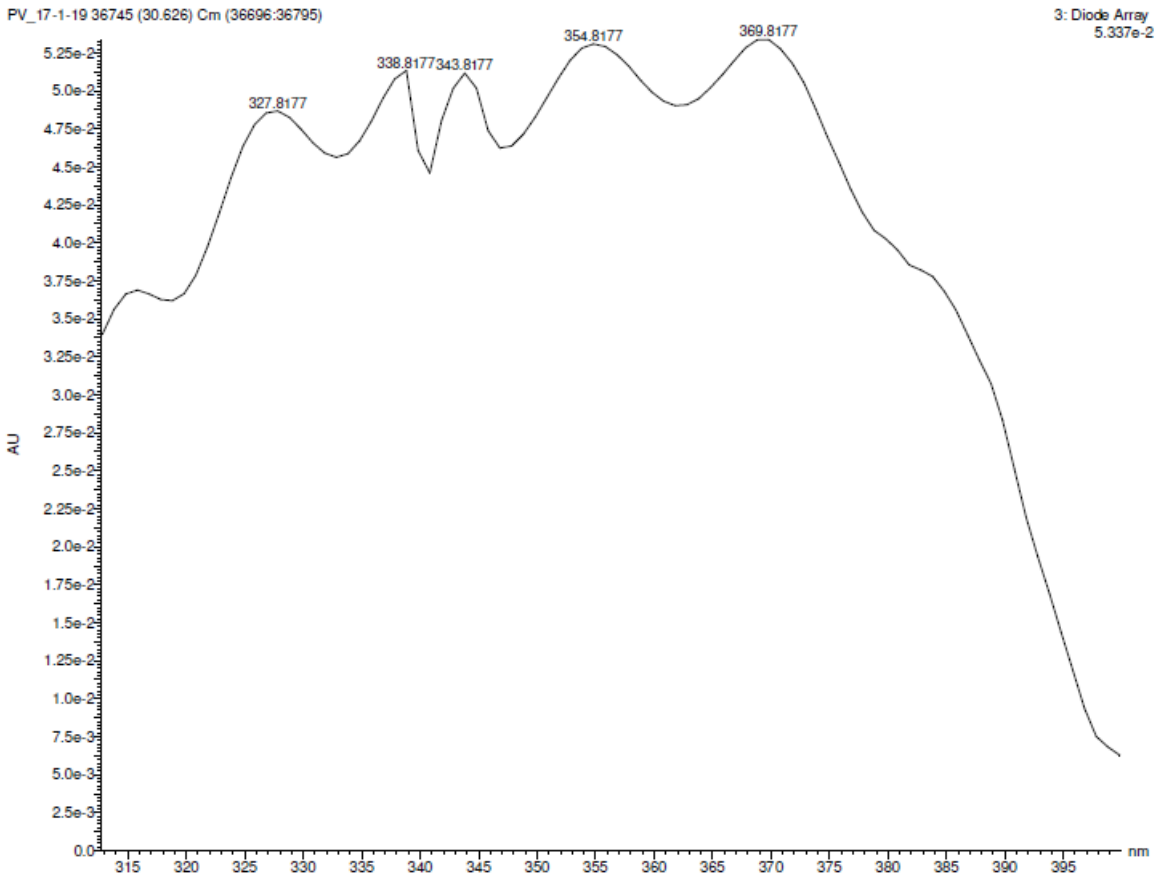

- Artepillin C (RT = 39.42 min, λ_{max} = 238, 314 nm)

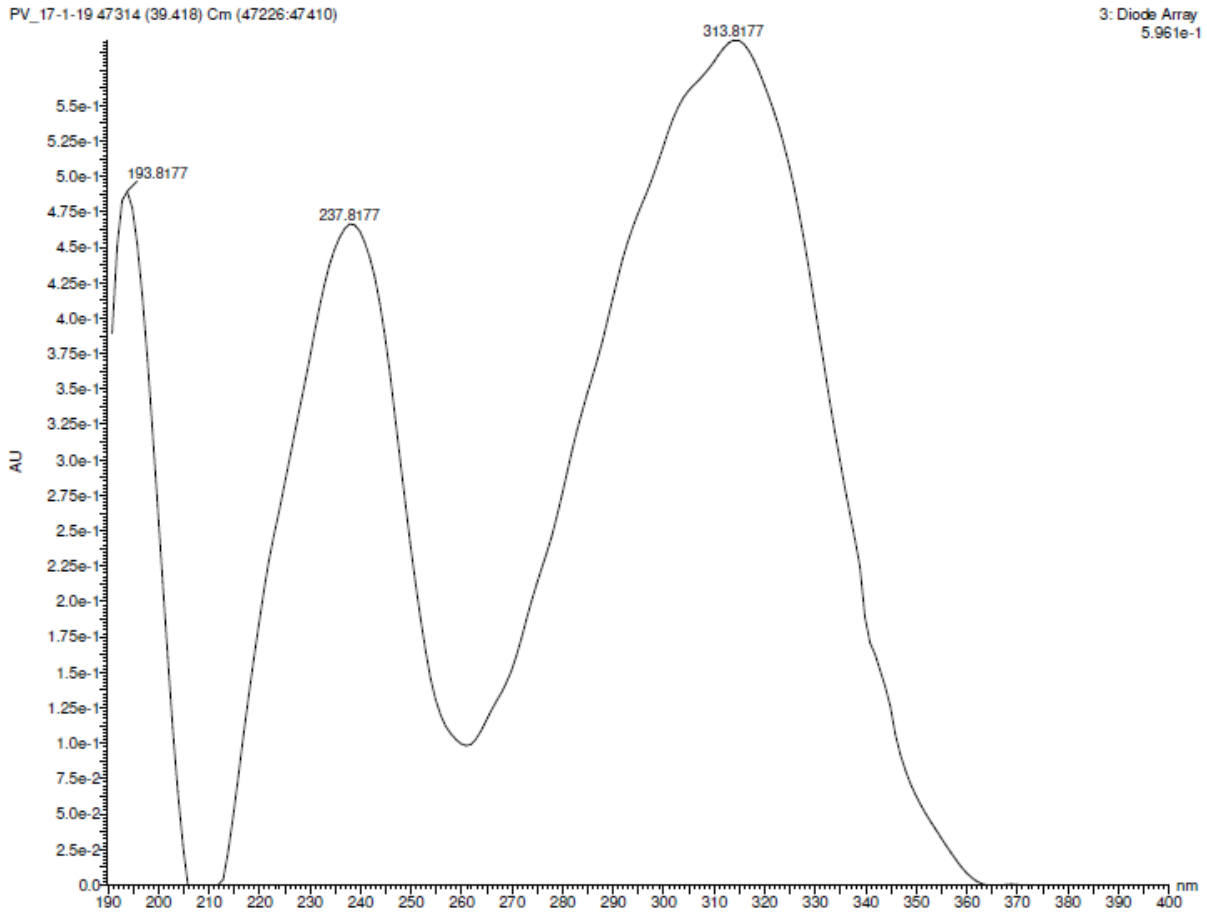

- Baccharin (RT = 45.60 min, λ_{max} = 283 nm)

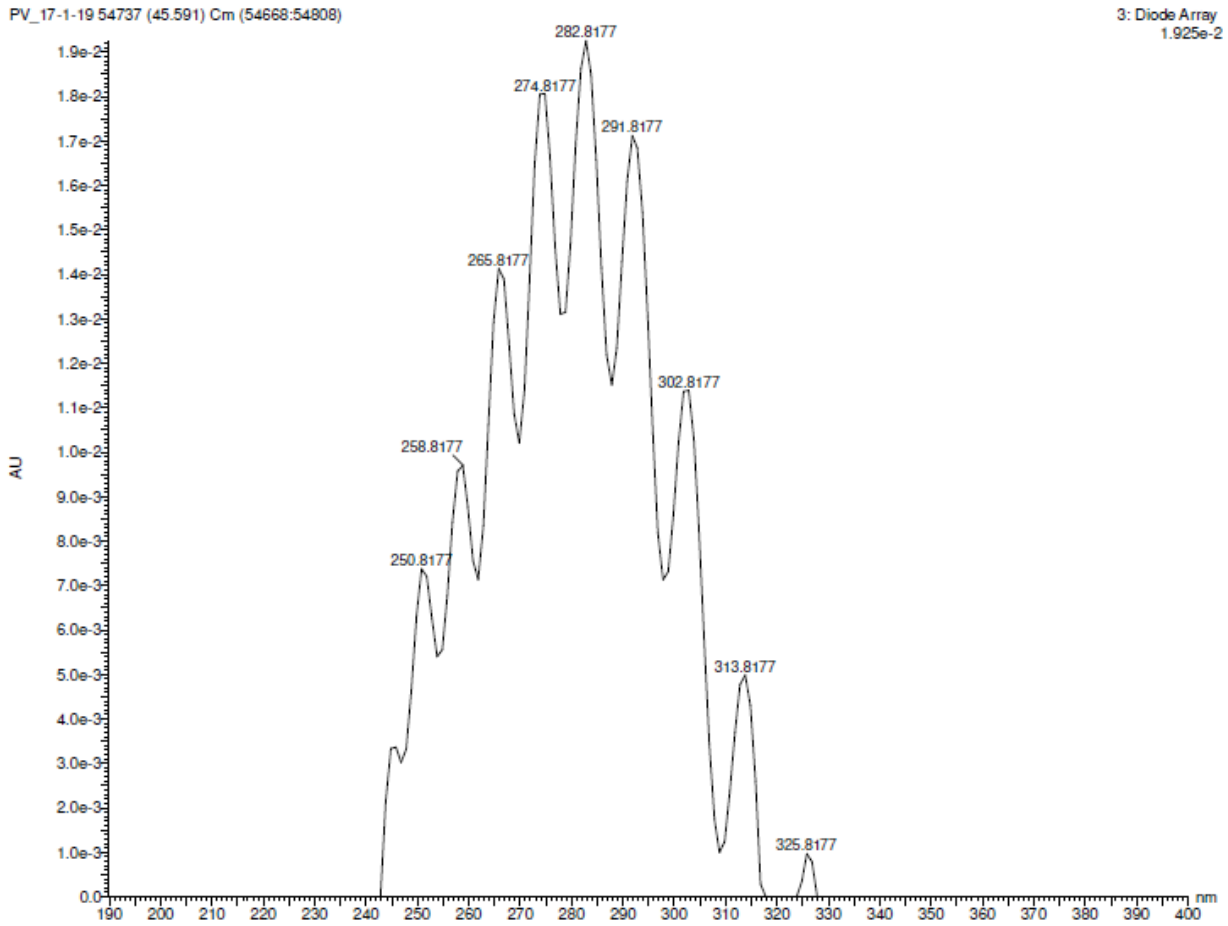

6.2 UV-VIS ABSORPTION SPECTRA OF COMPOUNDS IDENTIFIED IN RED BRAZILIAN PROPOLIS THROUGH HPLC-ESI-HRMS ANALYSIS

- Liquiritigenin/isoliquiritigenin (RT = 15.30 min, λ_{max} = 236, 276 nm)

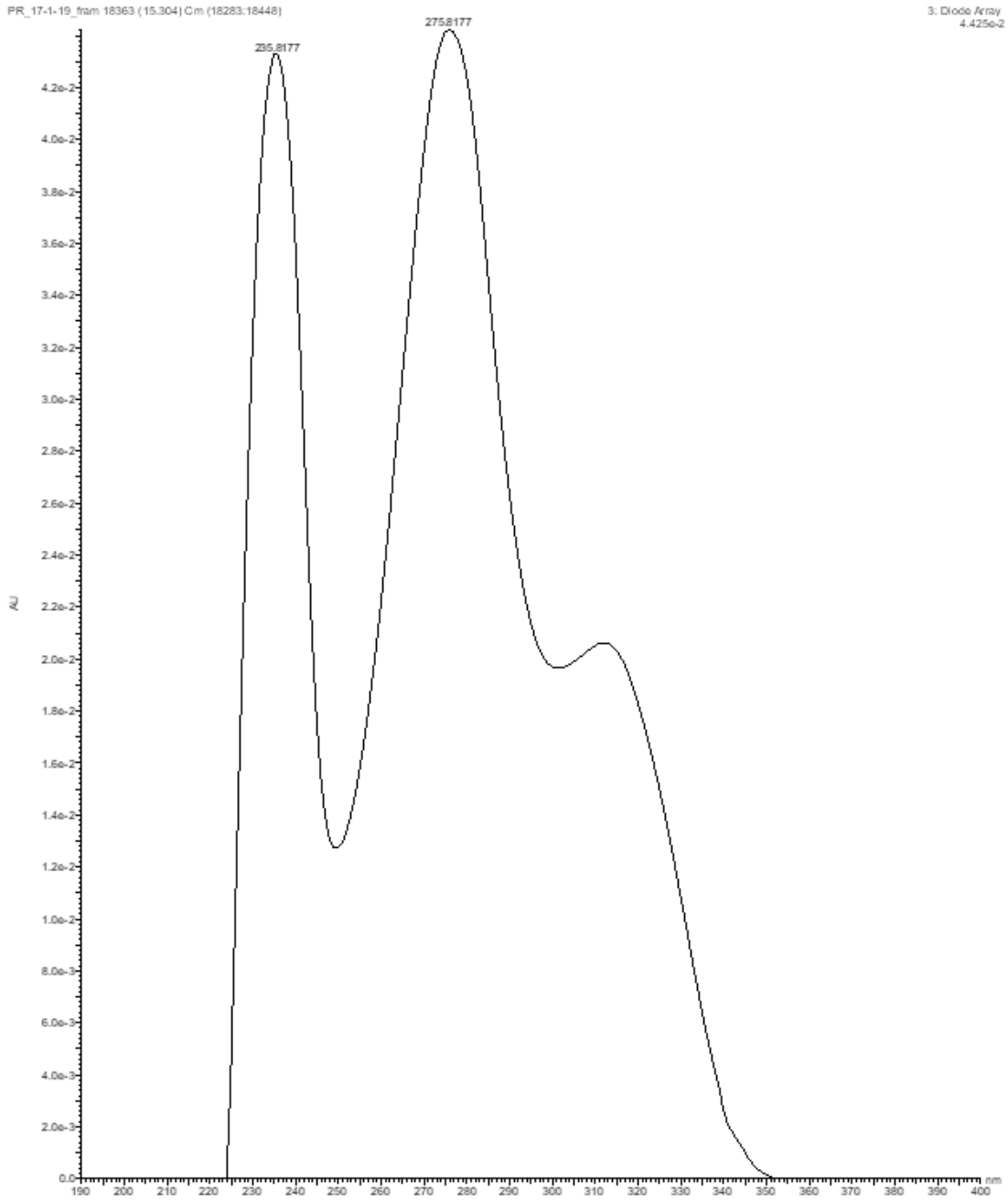

- Formononetin/isoformononetin (RT = 23.66 min, λ_{max} = 249 nm)

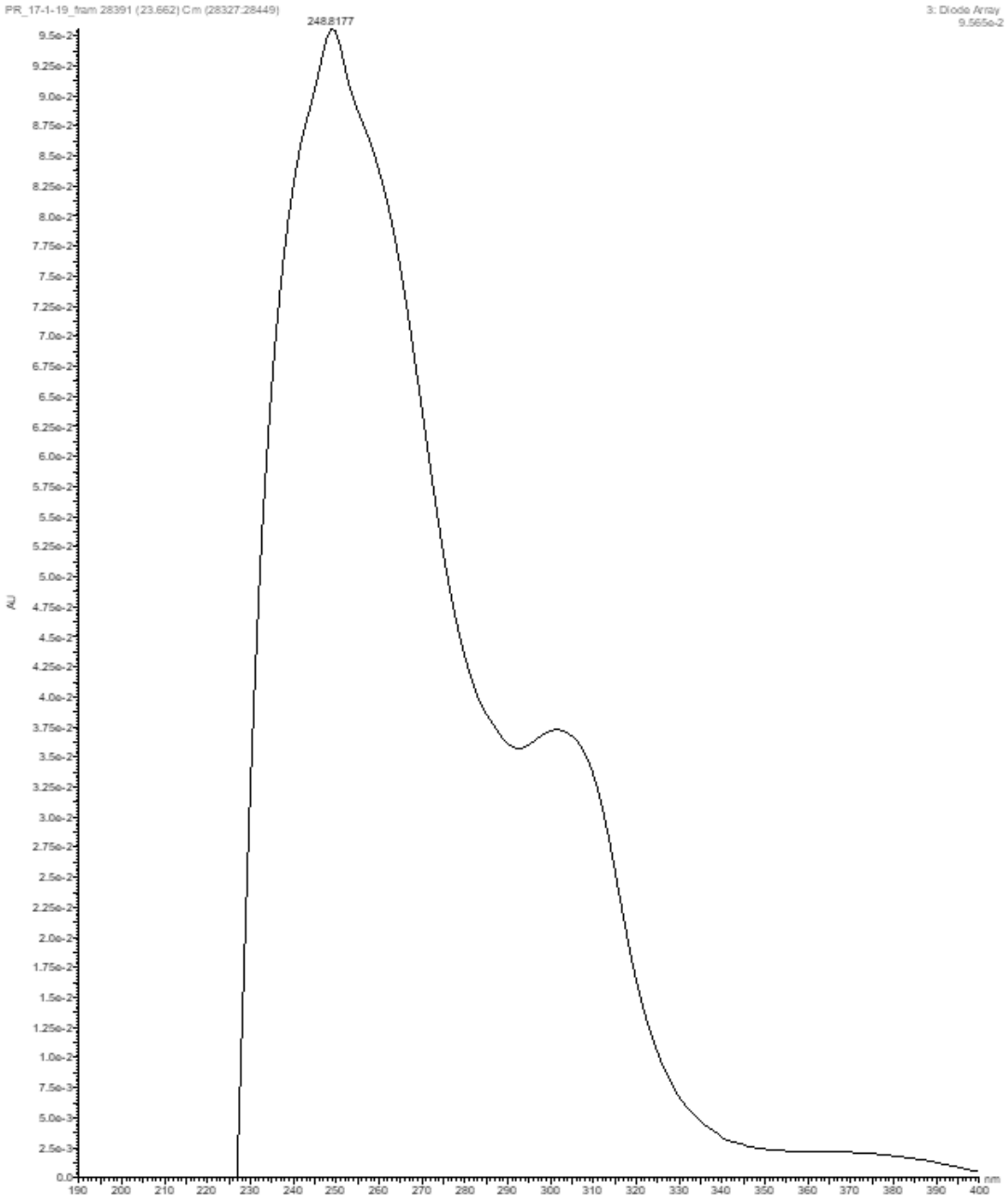

- Vestitol/neovestitol (RT = 24.23 min, λ_{max} = 202, 280 nm)

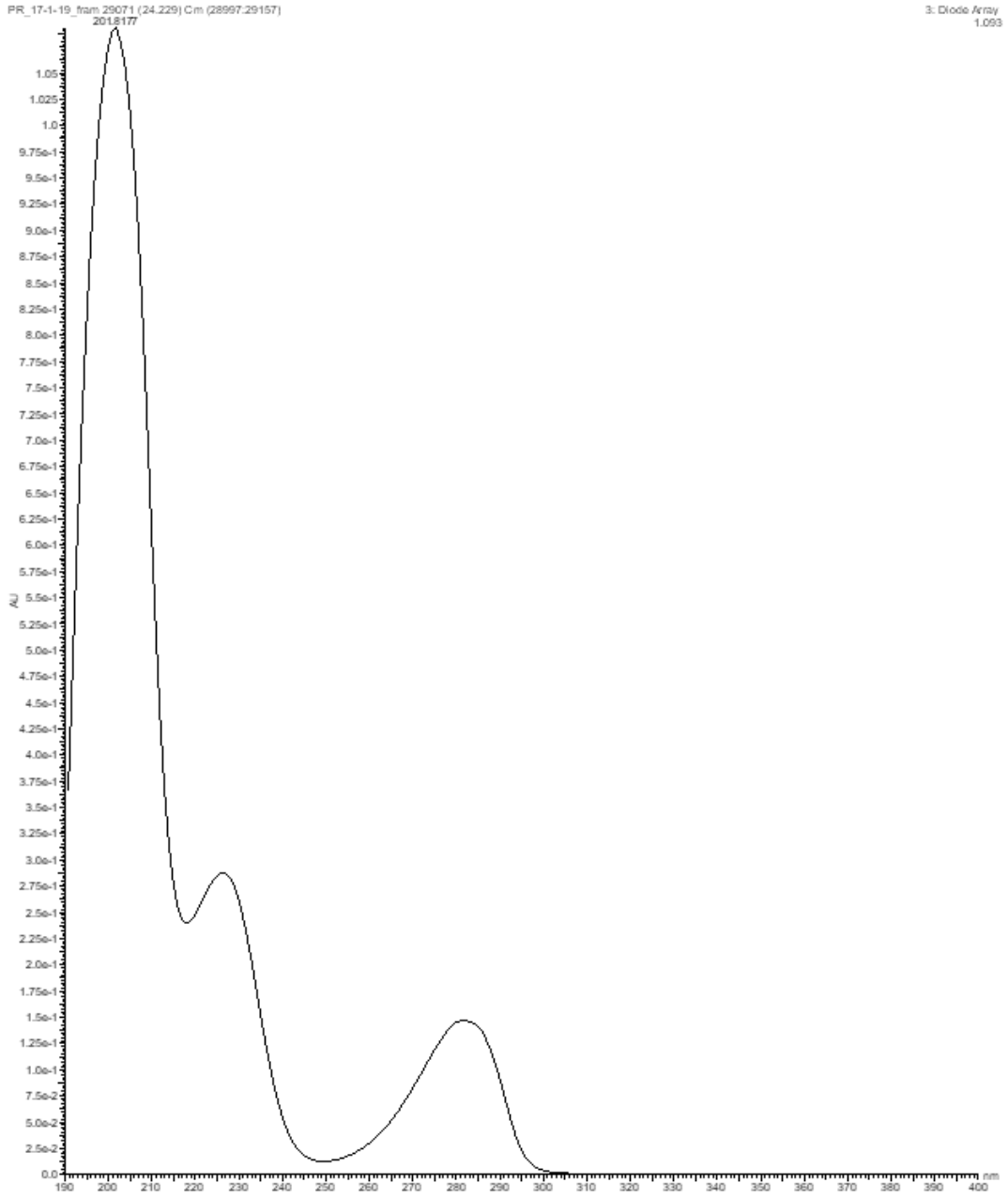

- Vestitol/neovestitol (RT = 25.99 min, λ_{max} = 202, 280 nm)

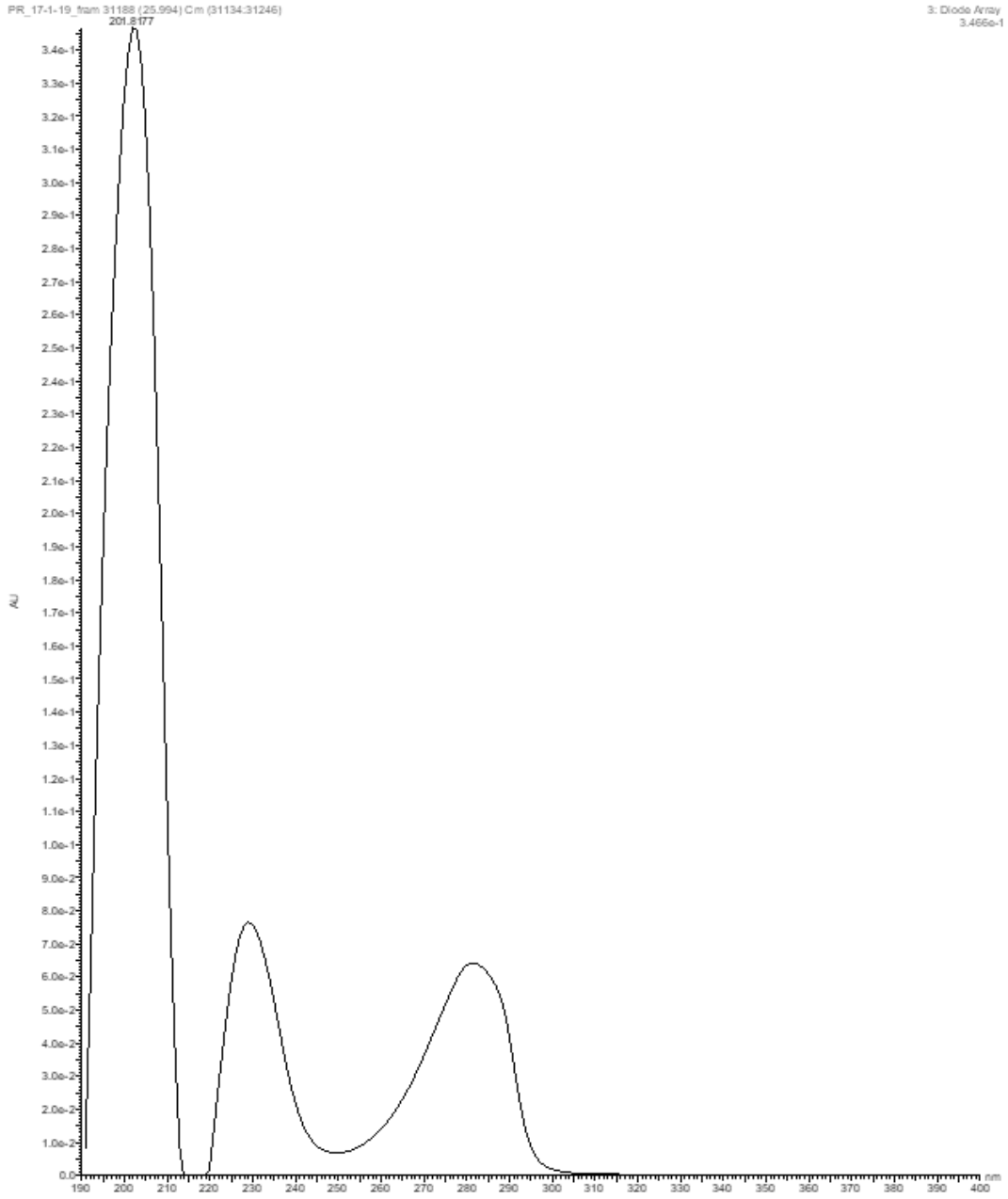

- Medicarpin (RT = 26.76 min, λ_{max} = 205, 287 nm)

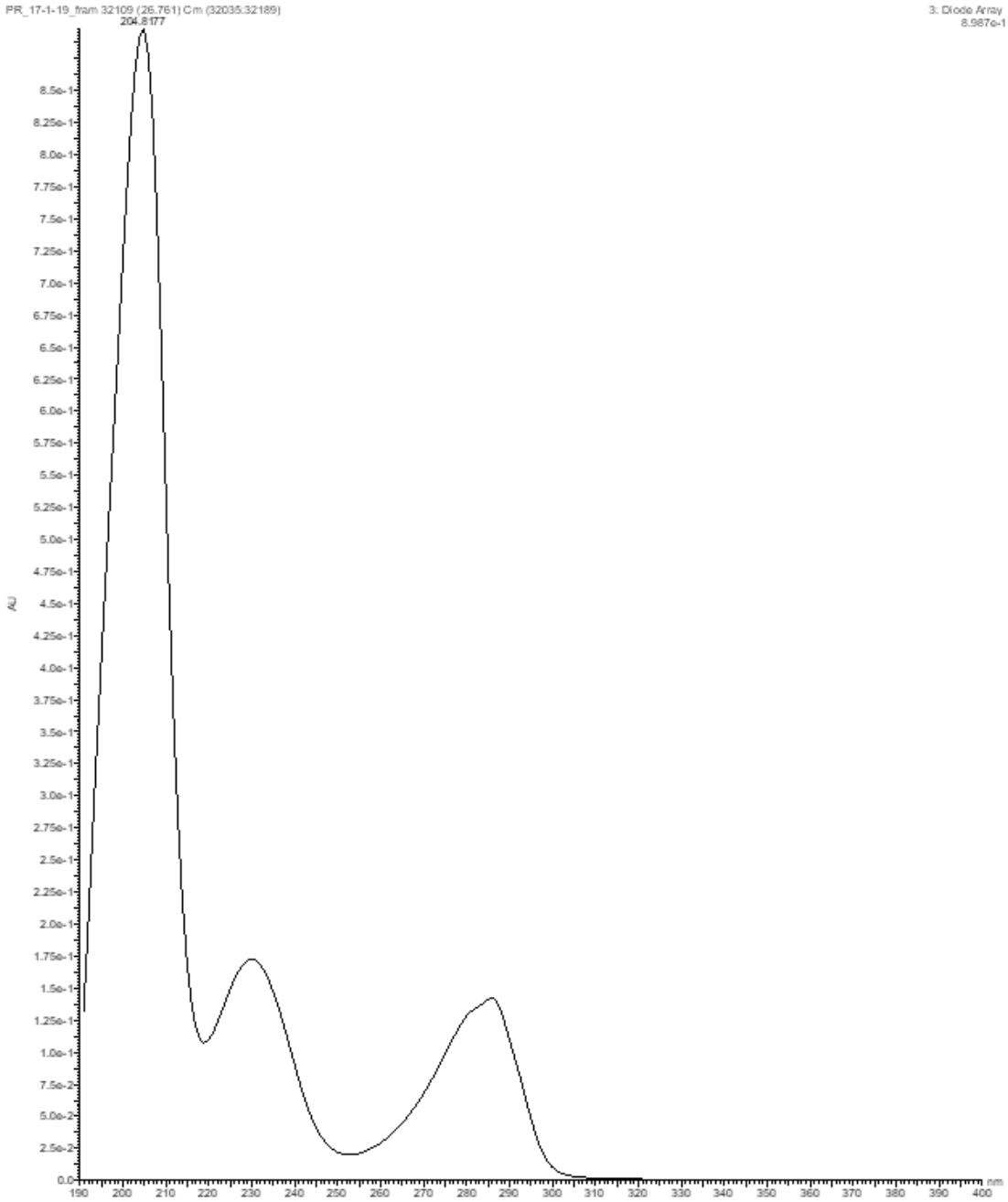
PR_17-1-19_fram 32109 (26.761) Cm (32035:32189)
204.8177
3: Diode Array
8.987e-1
AU
nm

- Guttiferone (RT = 54.06 min, λ_{max} = 252, 354 nm)

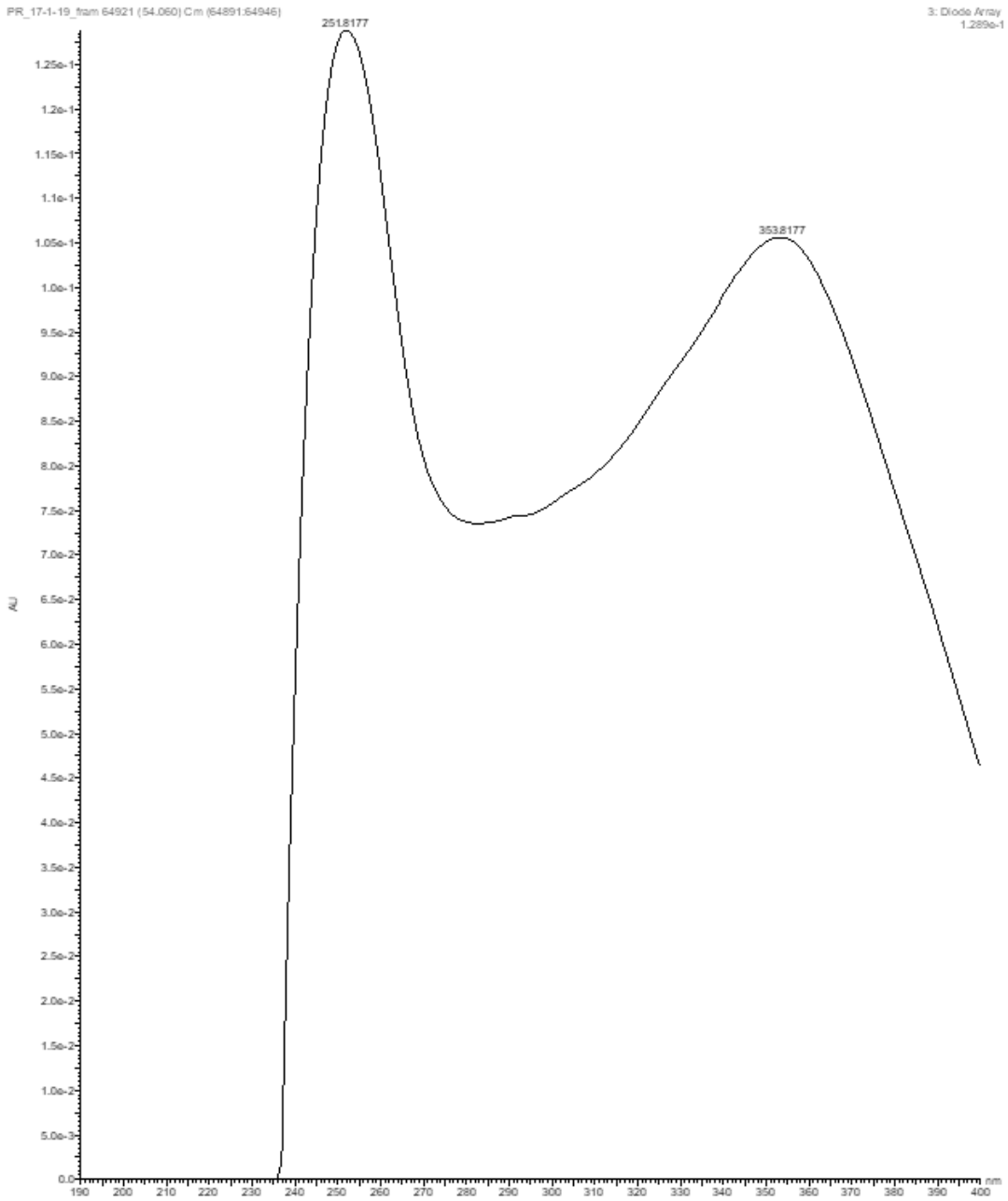

- Guttiferone (RT = 54.21, λ_{max} = 254, 345 nm)

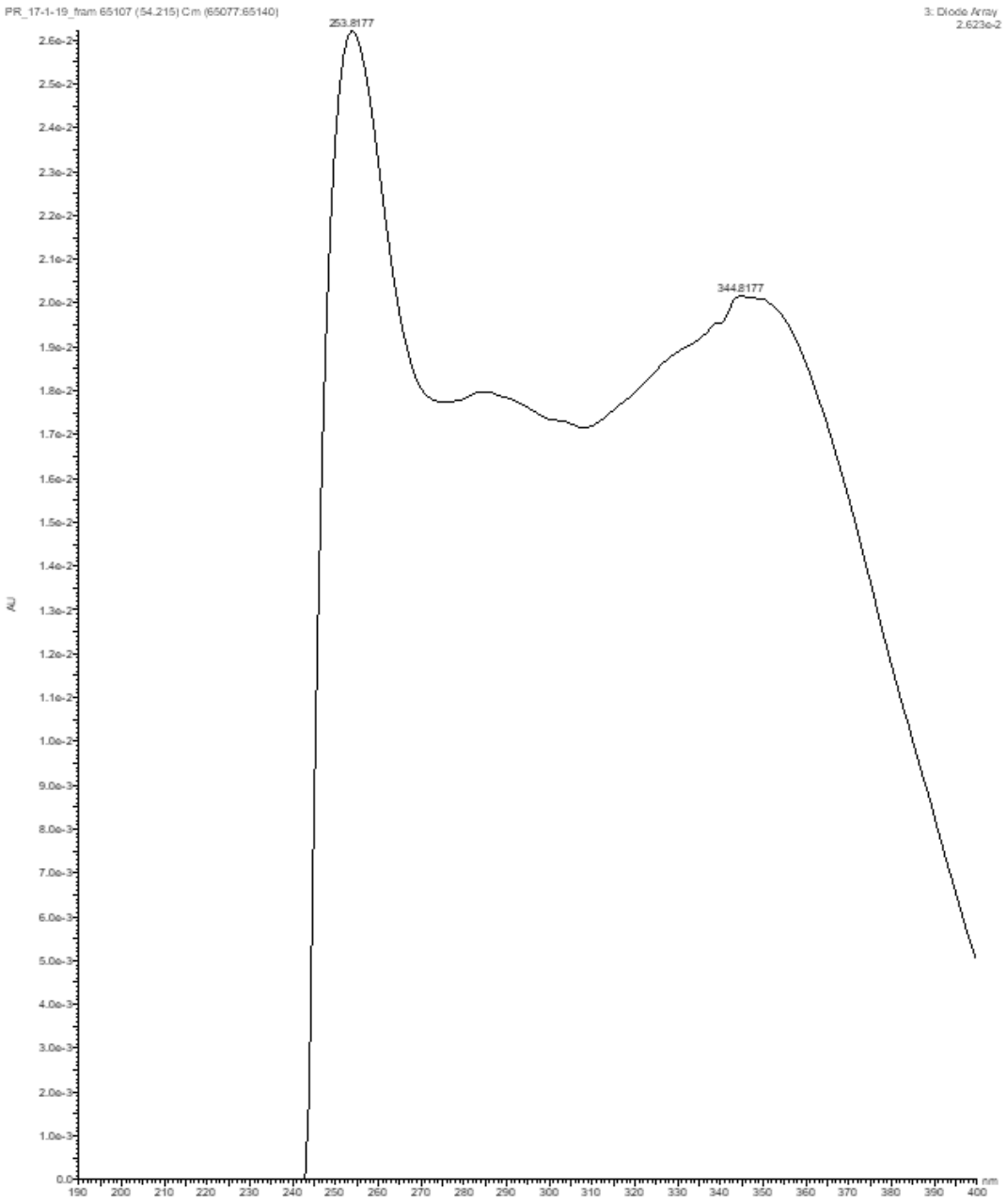

- Nemorosone (RT = 54.79 min, λ_{max} = 305 nm)

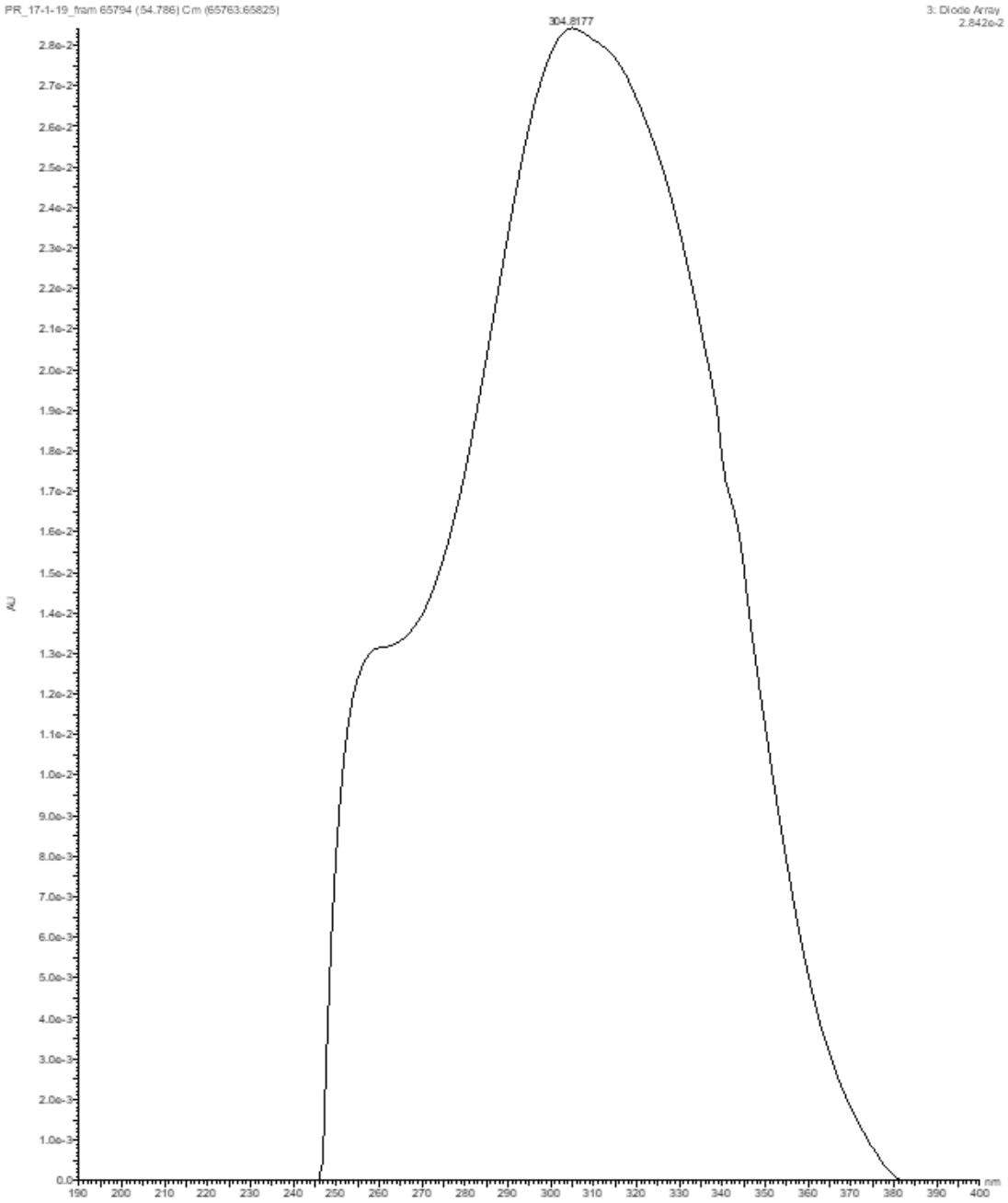

7 APPENDIX B

7.1 MS SPECTRA OF COMPOUNDS IDENTIFIED IN GREEN BRAZILIAN PROPOLIS THROUGH HPLC-ESI-HRMS ANALYSIS AND ELEMENTAL ANALYSIS

- *p*-coumaric acid (RT = 7.959 min, *m/z* 163.0395)

Monoisotopic Mass, Even Electron Ions
23 formula(e) evaluated with 1 results within limits (all results (up to 1000) for each mass)
Elements Used:
C: 0-100 H: 0-100 O: 0-20
PV_17-1-19 430 (7.959) Cm (429:434)

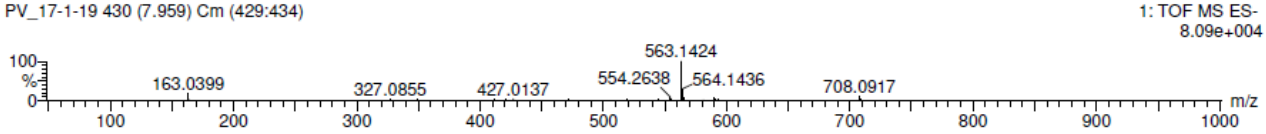

Minimum:				-1.5	
Maximum:		5.0	5.0	200.0	
Mass	**Calc. Mass**	**mDa**	**PPM**	**DBE**	**Formula**
163.0399	163.0395	0.4	2.5	6.5	C9 H7 O3

- Di-O-caffeoylquinic acid (RT = 12.457, *m/z* 515.1195)

PV_17-1-19 675 (12.457) AM2 (Ar,40000.0,0.00,0.00); Cm (672:676)

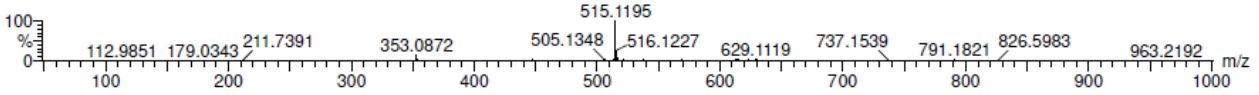

Minimum:				-1.5				
Maximum:		5.0	5.0	200.0				
Mass	**Calc. Mass**	**mDa**	**PPM**	**DBE**	**i-FIT**	**Norm**	**Conf(%)**	**Formula**
515.1195	515.1190	0.5	1.0	14.5	786.6	n/a	n/a	C25 H23 O12

- Di-O-caffeoylquinic acid (RT = 13.605, *m/z* 515.1190)

PV_17-1-19 737 (13.605) AM2 (Ar,40000.0,0.00,0.00); Cm (734:738)

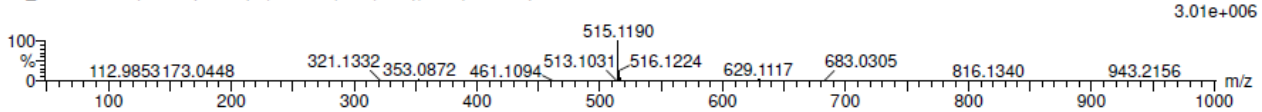

Minimum:				-1.5				
Maximum:		5.0	5.0	200.0				
Mass	**Calc. Mass**	**mDa**	**PPM**	**DBE**	**i-FIT**	**Norm**	**Conf(%)**	**Formula**
515.1190	515.1190	0.0	0.0	14.5	863.5	n/a	n/a	C25 H23 O12

- Drupanin (RT = 25.724, *m/z* 231.1029)

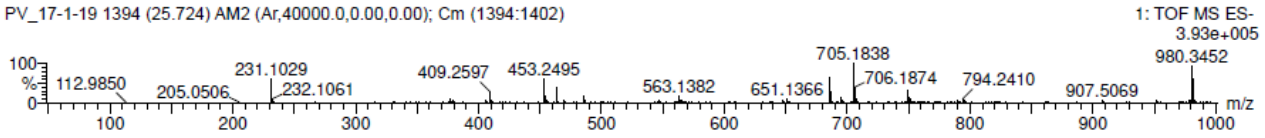

Minimum:				-1.5				
Maximum:		5.0	5.0	200.0				
Mass	Calc. Mass	mDa	PPM	DBE	i-FIT	Norm	Conf(%)	Formula
231.1029	231.1021	0.8	3.5	7.5	1338.0	n/a	n/a	C14 H15 O3

- Kaempferide (RT = 30.019, *m/z* 299.0554)

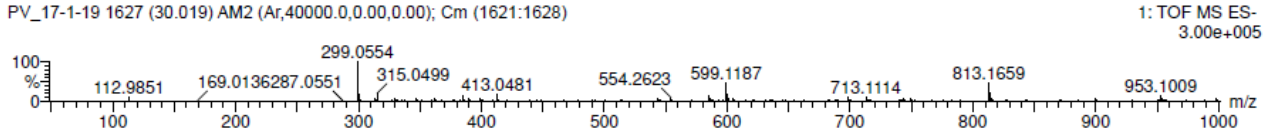

Minimum:				-1.5				
Maximum:		5.0	5.0	200.0				
Mass	Calc. Mass	mDa	PPM	DBE	i-FIT	Norm	Conf(%)	Formula
299.0554	299.0556	-0.2	-0.7	11.5	1044.6	n/a	n/a	C16 H11 O6

- Dimethylquercetin (RT = 30.684, *m/z* 329.0660)

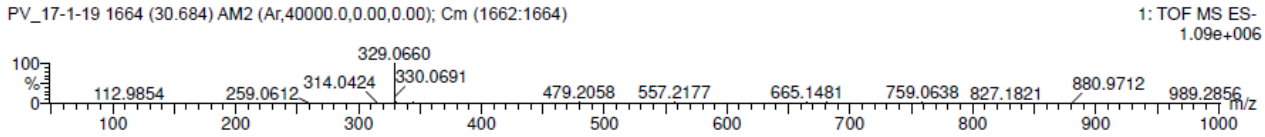

Minimum:				-1.5				
Maximum:		0.5	5.0	200.0				
Mass	Calc. Mass	mDa	PPM	DBE	i-FIT	Norm	Conf(%)	Formula
329.0660	329.0661	-0.1	-0.3	11.5	1735.6	n/a	n/a	C17 H13 O7

- Artepillin C (RT = 39.548, *m/z* 299.1633)

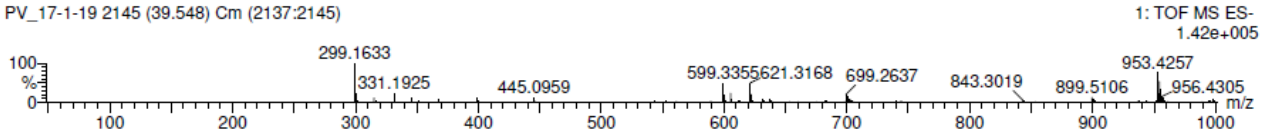

Minimum:				-1.5	
Maximum:		5.0	5.0	200.0	
Mass	Calc. Mass	mDa	PPM	DBE	Formula
299.1633	299.1647	-1.4	-4.7	8.5	C19 H23 O3

- Baccharin (RT = 45.659, *m/z* 363.1591)

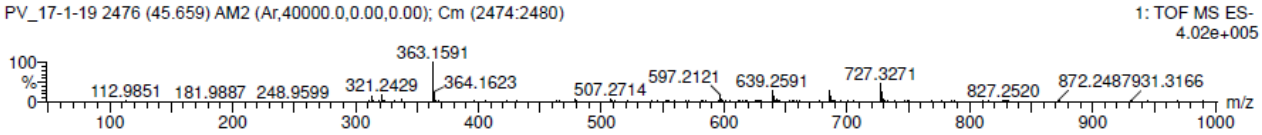

Minimum:				-1.5				
Maximum:		5.0	5.0	200.0				
Mass	Calc. Mass	mDa	PPM	DBE	i-FIT	Norm	Conf(%)	Formula
363.1591	363.1596	-0.5	-1.4	12.5	1014.2	n/a	n/a	C23 H23 O4

7.2 MS SPECTRA OF COMPOUNDS IDENTIFIED IN BRAZILIAN RED PROPOLIS THROUGH HPLC-ESI-HRMS ANALYSIS AND ELEMENTAL ANALYSIS

- Liquiritigenin/isoliquiritigenin (RT = 15.349, *m/z* 255.0657)

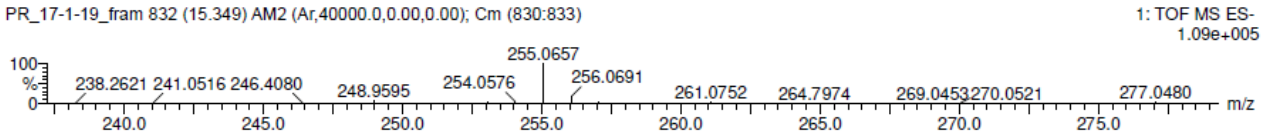

Minimum:				-1.5				
Maximum:		5.0	5.0	200.0				
Mass	Calc. Mass	mDa	PPM	DBE	i-FIT	Norm	Conf(%)	Formula
255.0657	255.0657	0.0	0.0	10.5	829.8	n/a	n/a	C15 H11 O4

- Formononetin/isoformononetin (RT = 23.701, *m/z* 267.0657)

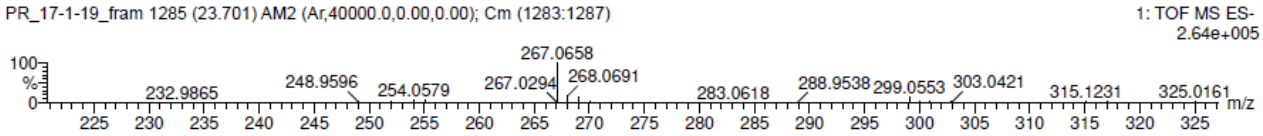

Minimum:				-1.5				
Maximum:		5.0	5.0	200.0				
Mass	Calc. Mass	mDa	PPM	DBE	i-FIT	Norm	Conf(%)	Formula
267.0658	267.0657	0.1	0.4	11.5	1041.1	n/a	n/a	C16 H11 O4

- Vestitol/neovestitol (RT =24.284, *m/z* 271.0974)

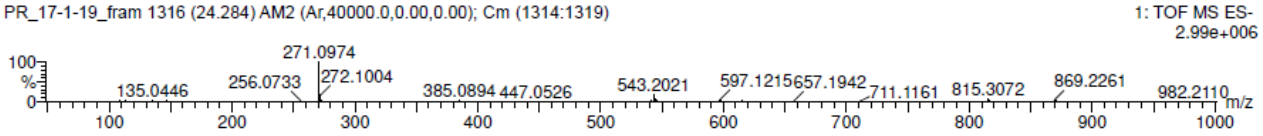

Minimum:				-1.5				
Maximum:		5.0	5.0	200.0				
Mass	Calc. Mass	mDa	PPM	DBE	i-FIT	Norm	Conf(%)	Formula
271.0974	271.0970	0.4	1.5	9.5	1501.2	0.011	98.95	C16 H15 O4

- Vestitol/neovestitol (RT =26.031, *m*/z 271.0972)

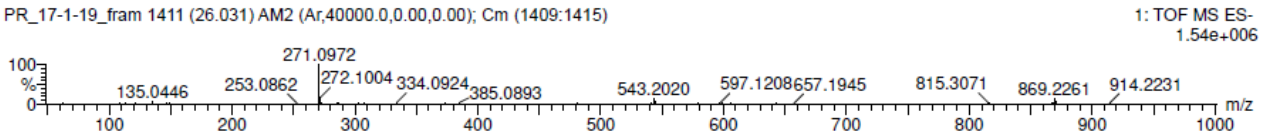

Minimum:				-1.5				
Maximum:		5.0	5.0	200.0				
Mass	Calc. Mass	mDa	PPM	DBE	i-FIT	Norm	Conf(%)	Formula
271.0972	271.0970	0.2	0.7	9.5	1305.1	0.001	99.95	C16 H15 O4

- Medicarpin (RT = 26.801, *m*/z 269.0813)

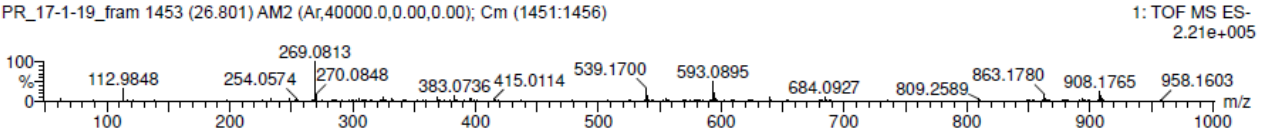

Minimum:				-1.5				
Maximum:		5.0	5.0	200.0				
Mass	Calc. Mass	mDa	PPM	DBE	i-FIT	Norm	Conf(%)	Formula
269.0813	269.0814	-0.1	-0.4	10.5	1118.5	n/a	n/a	C16 H13 O4

- Guttiferone (RT = 54.303, *m*/z 601.3531)

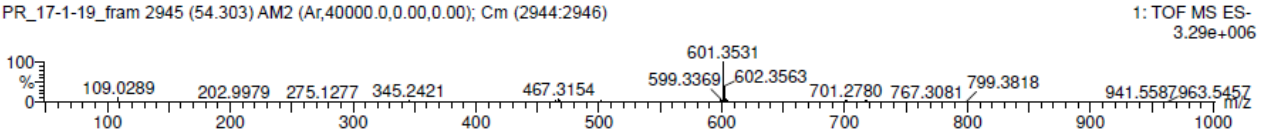

Minimum:				-1.5				
Maximum:		5.0	5.0	200.0				
Mass	Calc. Mass	mDa	PPM	DBE	i-FIT	Norm	Conf(%)	Formula
601.3531	601.3529	0.2	0.3	14.5	785.1	0.137	87.23	C38 H49 O6

- Guttiferone (RT = 54.883, *m*/z 601.3535)

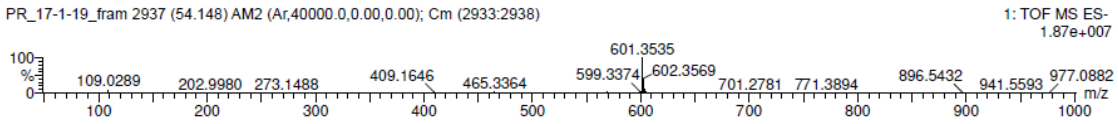

Minimum:				-1.5				
Maximum:		5.0	5.0	200.0				
Mass	Calc. Mass	mDa	PPM	DBE	i-FIT	Norm	Conf(%)	Formula
601.3535	601.3529	0.6	1.0	14.5	918.0	0.230	79.48	C38 H49 O6

- Nemorosone (RT = 54.883, *m*/z 501.3003)

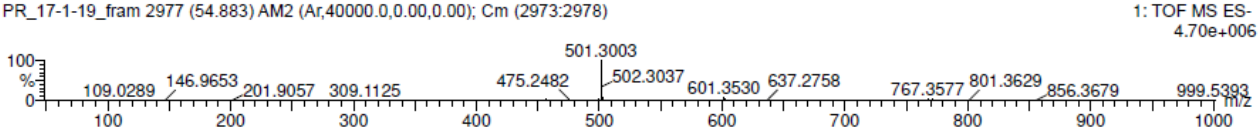

Minimum:				-1.5				
Maximum:		5.0	5.0	200.0				
Mass	Calc. Mass	mDa	PPM	DBE	i-FIT	Norm	Conf(%)	Formula
501.3003	501.3005	-0.2	-0.4	13.5	967.5	0.055	94.61	C33 H41 O4

8 REFERENCES

Ahangari, Z., Naseri, M., & Vatandoost, F. (2018). Propolis: Chemical Composition and Its Applications in Endodontics. *Iran Endod J, 13*(3), 285-292. doi:10.22037/iej.v13i3.20994

Ahn, M.-R., Kumazawa, S., Usui, Y., Nakamura, J., Matsuka, M., Zhu, F., & Nakayama, T. (2007). Antioxidant activity and constituents of propolis collected in various areas of China. *Food Chemistry, 101*, 1383-1392. doi:10.1016/j.foodchem.2006.03.045

Albuquerque-Júnior, R. L. C. d., Barreto, A. L. S., Pires, J. A., Reis, F. P., Lima, S. O., Ribeiro, M. A. G., & Cardoso, J. C. (2009). Effect of Bovine Type-I Collagen-Based Films Containing Red Propolis on Dermal Wound Healing in Rodent Model. *International Journal of Morphology, 27*, 1105-1110.

Alencar, S. M., Oldoni, T. L., Castro, M. L., Cabral, I. S., Costa-Neto, C. M., Cury, J. A., . . . Ikegaki, M. (2007). Chemical composition and biological activity of a new type of Brazilian propolis: red propolis. *J Ethnopharmacol, 113*(2), 278-283. doi:10.1016/j.jep.2007.06.005

Ali, Z. (2018). *Investigating mechanisms of angiogenesis in health and disease using zebrafish models*.

Anjum, S. I., Ullah, A., Khan, K. A., Attaullah, M., Khan, H., Ali, H., . . . Dash, C. K. (2019). Composition and functional properties of propolis (bee glue): A review. *Saudi J Biol Sci, 26*(7), 1695-1703. doi:10.1016/j.sjbs.2018.08.013

Bachiega, T. F., Orsatti, C. L., Pagliarone, A. C., & Sforcin, J. M. (2012). The effects of propolis and its isolated compounds on cytokine production by murine macrophages. *Phytother Res, 26*(9), 1308-1313. doi:10.1002/ptr.3731

Bankova, V. (2005a). Chemical diversity of propolis and the problem of standardization. *J Ethnopharmacol, 100*(1-2), 114-117. doi:10.1016/j.jep.2005.05.004

Bankova, V. (2005b). Recent trends and important developments in propolis research. *Evid Based Complement Alternat Med, 2*(1), 29-32. doi:10.1093/ecam/neh059

Bankova, V., Bertelli, D., Borba, R., Conti, B., da Silva Cunha, I. B., Danert, C., . . . Zampini, C. (2019). Standard methods for Apis mellifera propolis research. *Journal of Apicultural Research, 58*(2), 1-49. doi:10.1080/00218839.2016.1222661

Bankova, V., Boudourova-Krasteva, G., Sforcin, J. M., Frete, X., Kujumgiev, A., Maimoni-Rodella, R., & Popov, S. (1999). Phytochemical Evidence for the Plant Origin of Brazilian Propolis from São Paulo State. *Z Naturforsch C, 54*(5-6), 401-405. doi:10.1515/znc-1999-5-616

Bankova, V., de Castro, S., & Marcucci, M. (2000). Propolis: recent advances in chemistry and plant origin. *Apidologie, 31*(1), 3-15.

Bankova, V., Popova, M., Bogdanov, S., & Sabatini, A.-G. (2002). Chemical composition of European propolis: expected and unexpected results. *Zeitschrift fur Naturforschung. C, Journal of biosciences, 57*(5-6), 530-533. doi:10.1515/znc-2002-5-622

Bankova, V., Popova, M., & Trusheva, B. (2014). Propolis volatile compounds: chemical diversity and biological activity: a review. *Chem Cent J, 8*, 28. doi:10.1186/1752-153x-8-28

Bankova, V., Popova, M., & Trusheva, B. (2018). The phytochemistry of the honeybee. *Phytochemistry, 155*, 1-11. doi:10.1016/j.phytochem.2018.07.007

Banskota, A. H., Tezuka, Y., Midorikawa, K., Matsushige, K., & Kadota, S. (2000). Two novel cytotoxic benzofuran derivatives from Brazilian propolis. *J Nat Prod, 63*(9), 1277-1279. doi:10.1021/np000143z

Bartels, K., Grenz, A., & Eltzschig, H. K. (2013). Hypoxia and inflammation are two sides of the same coin. *Proc Natl Acad Sci U S A, 110*(46), 18351-18352. doi:10.1073/pnas.1318345110

Bartkova, J., Grøn, B., Dabelsteen, E., & Bartek, J. (2003). Cell-cycle regulatory proteins in human wound healing. *Arch Oral Biol, 48*(2), 125-132. doi:10.1016/s0003-9969(02)00202-9

Bastos, E. M., Santana, R. A., Calaça-Costa, A. G., & Thiago, P. S. (2011). Interaction between Apis mellifera L. and Baccharis dracunculifolia DC, that favours green propolis production in Minas Gerais. *Braz J Biol, 71*(3), 727-734. doi:10.1590/s1519-69842011000400018

Batista, C. M., Alves, A. V. F., Queiroz, L. A., Lima, B. S., Filho, R. N. P., Araújo, A. A. S., . . . Cardoso, J. C. (2018). The photoprotective and anti-inflammatory activity of red propolis extract in rats. *J Photochem Photobiol B, 180*, 198-207. doi:10.1016/j.jphotobiol.2018.01.028

Batista, L. L., Campesatto, E. A., Assis, M. L., Barbosa, A. P., Grillo, L. A., & Dornelas, C. B. (2012). Comparative study of topical green and red propolis in the repair of wounds induced in rats. *Rev Col Bras Cir, 39*(6), 515-520. doi:10.1590/s0100-69912012000600012

Berra, E., Benizri, E., Ginouvès, A., Volmat, V., Roux, D., & Pouysségur, J. (2003). HIF prolyl-hydroxylase 2 is the key oxygen sensor setting low steady-state levels of HIF-1alpha in normoxia. *Embo j, 22*(16), 4082-4090. doi:10.1093/emboj/cdg392

Berra, E., Roux, D., Richard, D. E., & Pouysségur, J. (2001). Hypoxia-inducible factor-1 alpha (HIF-1 alpha) escapes O(2)-driven proteasomal degradation irrespective of its subcellular localization: nucleus or cytoplasm. *EMBO Rep, 2*(7), 615-620. doi:10.1093/embo-reports/kve130

Berretta, A., Arruda, C., Miguel, F., Baptista, N., Nascimento, A., Marquele-Oliveira, F., . . . Ferreira, R. (2017). Functional Properties of Brazilian Propolis: From Chemical Composition Until the Market. In.

Berretta, A. A., Silveira, M. A. D., Cóndor Capcha, J. M., & De Jong, D. (2020). Propolis and its potential against SARS-CoV-2 infection mechanisms and COVID-19 disease: Running title: Propolis against SARS-CoV-2 infection and COVID-19. *Biomed Pharmacother, 131*, 110622. doi:10.1016/j.biopha.2020.110622

Boelsma, E., Verhoeven, M. C., & Ponec, M. (1999). Reconstruction of a human skin equivalent using a spontaneously transformed keratinocyte cell line (HaCaT). *J Invest Dermatol, 112*(4), 489-498. doi:10.1046/j.1523-1747.1999.00545.x

Bonham, C. A., Rodrigues, M., Galvez, M., Trotsyuk, A., Stern-Buchbinder, Z., Inayathullah, M., . . . Gurtner, G. C. (2018). Deferoxamine can prevent pressure ulcers and accelerate healing in aged mice. *Wound Repair Regen, 26*(3), 300-305. doi:10.1111/wrr.12667

Borrelli, F., Maffia, P., Pinto, L., Ianaro, A., Russo, A., Capasso, F., & Ialenti, A. (2002). Phytochemical compounds involved in the anti-inflammatory effect of propolis extract. *Fitoterapia, 73 Suppl 1*, S53-63. doi:10.1016/s0367-326x(02)00191-0

Botusan, I. R., Sunkari, V. G., Savu, O., Catrina, A. I., Grünler, J., Lindberg, S., . . . Catrina, S. B. (2008). Stabilization of HIF-1alpha is critical to improve wound healing in diabetic mice. *Proc Natl Acad Sci U S A, 105*(49), 19426-19431. doi:10.1073/pnas.0805230105

Boukamp, P., Petrussevska, R. T., Breitkreutz, D., Hornung, J., Markham, A., & Fusenig, N. E. (1988). Normal keratinization in a spontaneously immortalized aneuploid human keratinocyte cell line. *J Cell Biol, 106*(3), 761-771. doi:10.1083/jcb.106.3.761

Brandenburg, M. M., Rocha, F. G., Pawloski, P. L., Soley, B. D. S., Rockenbach, A., Scharf, D. R., . . . Otuki, M. F. (2020). Baccharis dracunculifolia (Asteraceae) essential oil displays anti-inflammatory activity in models of skin inflammation. *J Ethnopharmacol, 259*, 112840. doi:10.1016/j.jep.2020.112840

Bueno-Silva, B., Franchin, M., Alves, C. F., Denny, C., Colon, D. F., Cunha, T. M., . . . Rosalen, P. L. (2016). Main pathways of action of Brazilian red propolis on the modulation of neutrophils migration in the inflammatory process. *Phytomedicine, 23*(13), 1583-1590. doi:10.1016/j.phymed.2016.09.009

Bueno-Silva, B., Marsola, A., Ikegaki, M., Alencar, S. M., & Rosalen, P. L. (2017). The effect of seasons on Brazilian red propolis and its botanical source: chemical composition and antibacterial activity. *Nat Prod Res, 31*(11), 1318-1324. doi:10.1080/14786419.2016.1239088

Camargo, M. S., Prieto, A. M., Resende, F. A., Boldrin, P. K., Cardoso, C. R. P., Fernández, M. F., . . . Varanda, E. A. (2013). Evaluation of estrogenic, antiestrogenic and genotoxic activity of nemorosone, the major compound found in brown Cuban propolis. *BMC Complementary and Alternative Medicine, 13*(1), 201. doi:10.1186/1472-6882-13-201

Castro, M. L., do Nascimento, A. M., Ikegaki, M., Costa-Neto, C. M., Alencar, S. M., & Rosalen, P. L. (2009). Identification of a bioactive compound isolated from Brazilian propolis type 6. *Bioorg Med Chem, 17*(14), 5332-5335. doi:10.1016/j.bmc.2009.04.066

Chern, C. M., Lu, C. K., Liou, K. T., Wang, Y. H., Tsai, K. C., Chang, C. L., . . . Shen, Y. C. (2021). Medicarpin isolated from Radix Hedysari ameliorates brain injury in a murine model of cerebral ischemia. *J Food Drug Anal, 29*(4), 581-605. doi:10.38212/2224-6614.3377

Choi, D., Han, J., Lee, Y., Choi, J., Han, S., Hong, S., . . . Jung, Y. (2010). Caffeic acid phenethyl ester is a potent inhibitor of HIF prolyl hydroxylase: structural analysis and pharmacological implication. *J Nutr Biochem, 21*(9), 809-817. doi:10.1016/j.jnutbio.2009.06.002

Chylińska-Wrzos, P., Lis-Sochocka, M., & Jodłowska-Jędrych, B. (2017). Use of propolis in difficult to heal diabetic wounds. Short review. *Polish Journal of Public Health, 127*(4), 173-175. doi:doi:10.1515/pjph-2017-0037

Corrêa, F. R., Schanuel, F. S., Moura-Nunes, N., Monte-Alto-Costa, A., & Daleprane, J. B. (2017). Brazilian red propolis improves cutaneous wound healing suppressing inflammation-associated transcription factor NFκB. *Biomed Pharmacother, 86*, 162-171. doi:10.1016/j.biopha.2016.12.018

Corrêa, J. L., Veiga, F. F., Jarros, I. C., Costa, M. I., Castilho, P. F., de Oliveira, K. M. P., . . . Negri, M. (2020). Propolis extract has bioactivity on the wall and cell membrane of Candida albicans. *J Ethnopharmacol, 256*, 112791. doi:10.1016/j.jep.2020.112791

Costa, P., Somensi, L. B., da Silva, R., Mariano, L. N. B., Boeing, T., Longo, B., . . . da Silva, L. M. (2020). Role of the antioxidant properties in the gastroprotective and gastric healing activity promoted by Brazilian green propolis and the healing efficacy of Artepillin C. *Inflammopharmacology, 28*(4), 1009-1025. doi:10.1007/s10787-019-00649-7

Cottica, S., Sawaya, A., Eberlin, M. N., Franco, S., Zeoula, L., & Visentainer, J. (2011). Antioxidant Activity and Composition of Propolis Obtained by Different Methods of Extraction. *Journal of the Brazilian Chemical Society, 22*, 929-935. doi:10.1590/S0103-50532011000500016

Cushnie, T. P., & Lamb, A. J. (2005). Antimicrobial activity of flavonoids. *Int J Antimicrob Agents, 26*(5), 343-356. doi:10.1016/j.ijantimicag.2005.09.002

Cuvelier, M. E., Richard, H., & Berset, C. (1992). Comparison of the Antioxidative Activity of Some Acid-phenols: Structure-Activity Relationship. *Bioscience, Biotechnology, and Biochemistry, 56*(2), 324-325. doi:10.1271/bbb.56.324

Cvek, J., Medić-Šarić, M., Vitali, D., Vedrina-Dragojević, I., Šmit, Z., & Tomić, S. (2008). The content of essential and toxic elements in Croatian propolis samples and

their tinctures. *Journal of Apicultural Research, 47*(1), 35-45. doi:10.1080/00218839.2008.11101421

da Cruz Almeida, E. T., da Silva, M. C. D., Oliveira, J., Kamiya, R. U., Arruda, R., Vieira, D. A., . . . do Nascimento, T. G. (2017). Chemical and microbiological characterization of tinctures and microcapsules loaded with Brazilian red propolis extract. *J Pharm Anal, 7*(5), 280-287. doi:10.1016/j.jpha.2017.03.004

da Silva Filho, A. A., de Sousa, J. P., Soares, S., Furtado, N. A., Andrade e Silva, M. L., Cunha, W. R., . . . Bastos, J. K. (2008). Antimicrobial activity of the extract and isolated compounds from Baccharis dracunculifolia D. C. (Asteraceae). *Z Naturforsch C J Biosci, 63*(1-2), 40-46. doi:10.1515/znc-2008-1-208

da Silva, R. O., Andrade, V. M., Bullé Rêgo, E. S., Azevedo Dória, G. A., Santos Lima, B. D., da Silva, F. A., . . . Zanardo Gomes, M. (2015). Acute and sub-acute oral toxicity of Brazilian red propolis in rats. *J Ethnopharmacol, 170*, 66-71. doi:10.1016/j.jep.2015.05.009

Daleprane, J. B., & Abdalla, D. S. (2013). Emerging roles of propolis: antioxidant, cardioprotective, and antiangiogenic actions. *Evid Based Complement Alternat Med, 2013*, 175135. doi:10.1155/2013/175135

Daugsch, A., Moraes, C. S., Fort, P., & Park, Y. K. (2008). Brazilian red propolis--chemical composition and botanical origin. *Evid Based Complement Alternat Med, 5*(4), 435-441. doi:10.1093/ecam/nem057

Dávalos, A., Gómez-Cordovés, C., & Bartolomé, B. (2004). Extending applicability of the oxygen radical absorbance capacity (ORAC-fluorescein) assay. *J Agric Food Chem, 52*(1), 48-54. doi:10.1021/jf0305231

Dayan, F., Roux, D., Brahimi-Horn, M. C., Pouyssegur, J., & Mazure, N. M. (2006). The oxygen sensor factor-inhibiting hypoxia-inducible factor-1 controls expression of distinct genes through the bifunctional transcriptional character of hypoxia-inducible factor-1alpha. *Cancer Res, 66*(7), 3688-3698. doi:10.1158/0008-5472.Can-05-4564

de Almeida, E. B., Cordeiro Cardoso, J., Karla de Lima, A., de Oliveira, N. L., de Pontes-Filho, N. T., Oliveira Lima, S., . . . de Albuquerque-Júnior, R. L. (2013). The incorporation of Brazilian propolis into collagen-based dressing films improves dermal burn healing. *J Ethnopharmacol, 147*(2), 419-425. doi:10.1016/j.jep.2013.03.031

de Barros, M. P., Sousa, J. P., Bastos, J. K., & de Andrade, S. F. (2007). Effect of Brazilian green propolis on experimental gastric ulcers in rats. *J Ethnopharmacol, 110*(3), 567-571. doi:10.1016/j.jep.2006.10.022

de Carvalho, F. M. A., Schneider, J. K., de Jesus, C. V. F., de Andrade, L. N., Amaral, R. G., David, J. M., . . . de Albuquerque-Júnior, R. L. C. (2020). Brazilian Red Propolis: Extracts Production, Physicochemical Characterization, and Cytotoxicity Profile for Antitumor Activity. *Biomolecules, 10*(5). doi:10.3390/biom10050726

de Mendonça, I. C., Porto, I. C., do Nascimento, T. G., de Souza, N. S., Oliveira, J. M., Arruda, R. E., . . . Barreto, F. S. (2015). Brazilian red propolis: phytochemical screening, antioxidant activity and effect against cancer cells. *BMC Complement Altern Med, 15*, 357. doi:10.1186/s12906-015-0888-9

de Moura, S. A., Negri, G., Salatino, A., Lima, L. D., Dourado, L. P., Mendes, J. B., . . . Cara, D. C. (2011). Aqueous extract of brazilian green propolis: primary components, evaluation of inflammation and wound healing by using subcutaneous implanted sponges. *Evid Based Complement Alternat Med, 2011*, 748283. doi:10.1093/ecam/nep112

Demidova-Rice, T. N., Hamblin, M. R., & Herman, I. M. (2012). Acute and impaired wound healing: pathophysiology and current methods for drug delivery, part 1:

normal and chronic wounds: biology, causes, and approaches to care. *Adv Skin Wound Care, 25*(7), 304-314. doi:10.1097/01.ASW.0000416006.55218.d0

Denizot, F., & Lang, R. (1986). Rapid colorimetric assay for cell growth and survival. Modifications to the tetrazolium dye procedure giving improved sensitivity and reliability. *J Immunol Methods, 89*(2), 271-277. doi:10.1016/0022-1759(86)90368-6

Deodhar, A. K., & Rana, R. E. (1997). Surgical physiology of wound healing: a review. *J Postgrad Med, 43*(2), 52-56.

desJardins-Park, H. E., Mascharak, S., Chinta, M. S., Wan, D. C., & Longaker, M. T. (2019). The Spectrum of Scarring in Craniofacial Wound Repair. *Front Physiol, 10*, 322. doi:10.3389/fphys.2019.00322

Diaz-Carballo, D., Gustmann, S., Acikelli, A. H., Bardenheuer, W., Buehler, H., Jastrow, H., . . . Strumberg, D. (2012). 7-epi-nemorosone from Clusia rosea induces apoptosis, androgen receptor down-regulation and dysregulation of PSA levels in LNCaP prostate carcinoma cells. *Phytomedicine, 19*(14), 1298-1306. doi:10.1016/j.phymed.2012.08.004

Diaz-Carballo, D., Ueberla, K., Kleff, V., Ergun, S., Malak, S., Freistuehler, M., . . . Strumberg, D. (2010). Antiretroviral activity of two polyisoprenylated acylphloroglucinols, 7-epi-nemorosone and plukenetione A, isolated from Caribbean propolis. *Int J Clin Pharmacol Ther, 48*(10), 670-677. doi:10.5414/cpp48670

Diegelmann, R. F., & Evans, M. C. (2004). Wound healing: an overview of acute, fibrotic and delayed healing. *Front Biosci, 9*, 283-289. doi:10.2741/1184

Dos Santos, F. F., Morais-Urano, R. P., Cunha, W. R., de Almeida, S. G., Cavallari, P., Manuquian, H. A., . . . Amdrade, E. S. M. L. (2022). A review on the anti-inflammatory activities of Brazilian green, brown and red propolis. *J Food Biochem*, e14350. doi:10.1111/jfbc.14350

Duscher, D., Neofytou, E., Wong, V. W., Maan, Z. N., Rennert, R. C., Inayathullah, M., . . . Gurtner, G. C. (2015). Transdermal deferoxamine prevents pressure-induced diabetic ulcers. *Proc Natl Acad Sci U S A, 112*(1), 94-99. doi:10.1073/pnas.1413445112

Eichler, M. J., & Carlson, M. A. (2006). Modeling dermal granulation tissue with the linear fibroblast-populated collagen matrix: a comparison with the round matrix model. *J Dermatol Sci, 41*(2), 97-108. doi:10.1016/j.jdermsci.2005.09.002

Eltzschig, H. K., Sitkovsky, M. V., & Robson, S. C. (2012). Purinergic signaling during inflammation. *N Engl J Med, 367*(24), 2322-2333. doi:10.1056/NEJMra1205750

Emerling, B. M., Weinberg, F., Liu, J. L., Mak, T. W., & Chandel, N. S. (2008). PTEN regulates p300-dependent hypoxia-inducible factor 1 transcriptional activity through Forkhead transcription factor 3a (FOXO3a). *Proc Natl Acad Sci U S A, 105*(7), 2622-2627. doi:10.1073/pnas.0706790105

Endo, S., Hoshi, M., Matsunaga, T., Inoue, T., Ichihara, K., & Ikari, A. (2018). Autophagy inhibition enhances anticancer efficacy of artepillin C, a cinnamic acid derivative in Brazilian green propolis. *Biochem Biophys Res Commun, 497*(1), 437-443. doi:10.1016/j.bbrc.2018.02.105

Epstein, A. C., Gleadle, J. M., McNeill, L. A., Hewitson, K. S., O'Rourke, J., Mole, D. R., . . . Ratcliffe, P. J. (2001). C. elegans EGL-9 and mammalian homologs define a family of dioxygenases that regulate HIF by prolyl hydroxylation. *Cell, 107*(1), 43-54. doi:10.1016/s0092-8674(01)00507-4

Eroglu, N., Akkus, S., Yaman, M., Asci, B., & Silici, S. (2016). Amino Acid and Vitamin Content of Propolis Collected by Native Caucasican Honeybees. *Journal of Apicultural Science, 60*(2), 101-110. doi:doi:10.1515/jas-2016-0021

Espírito-Santo, M. M., Madeira, B. G., Neves, F. S., Faria, M. L., Fagundes, M., & Fernandes, G. W. (2003). Sexual differences in reproductive phenology and

their consequences for the demography of Baccharis dracunculifolia (Asteraceae), a dioecious tropical shrub. *Ann Bot, 91*(1), 13-19. doi:10.1093/aob/mcg001

Fonder, M. A., Lazarus, G. S., Cowan, D. A., Aronson-Cook, B., Kohli, A. R., & Mamelak, A. J. (2008). Treating the chronic wound: A practical approach to the care of nonhealing wounds and wound care dressings. *J Am Acad Dermatol, 58*(2), 185-206. doi:10.1016/j.jaad.2007.08.048

Fonseca Bezerra, C., de Alencar Júnior, J. G., de Lima Honorato, R., Dos Santos, A. T. L., Pereira da Silva, J. C., Silva, T. G. D., . . . da Silva, T. G. (2020). Antifungal Properties of Nerolidol-Containing Liposomes in Association with Fluconazole. *Membranes (Basel), 10*(9). doi:10.3390/membranes10090194

Fonseca, Y. M., Marquele-Oliveira, F., Vicentini, F. T., Furtado, N. A., Sousa, J. P., Lucisano-Valim, Y. M., & Fonseca, M. J. (2011). Evaluation of the Potential of Brazilian Propolis against UV-Induced Oxidative Stress. *Evid Based Complement Alternat Med, 2011*. doi:10.1155/2011/863917

Formenti, F., Constantin-Teodosiu, D., Emmanuel, Y., Cheeseman, J., Dorrington, K. L., Edwards, L. M., . . . Robbins, P. A. (2010). Regulation of human metabolism by hypoxia-inducible factor. *Proc Natl Acad Sci U S A, 107*(28), 12722-12727. doi:10.1073/pnas.1002339107

Forsythe, J. A., Jiang, B. H., Iyer, N. V., Agani, F., Leung, S. W., Koos, R. D., & Semenza, G. L. (1996). Activation of vascular endothelial growth factor gene transcription by hypoxia-inducible factor 1. *Mol Cell Biol, 16*(9), 4604-4613. doi:10.1128/mcb.16.9.4604

Franchin, M., Colón, D. F., da Cunha, M. G., Castanheira, F. V., Saraiva, A. L., Bueno-Silva, B., . . . Rosalen, P. L. (2016). Neovestitol, an isoflavonoid isolated from Brazilian red propolis, reduces acute and chronic inflammation: involvement of nitric oxide and IL-6. *Sci Rep, 6*, 36401. doi:10.1038/srep36401

Franchin, M., Freires, I. A., Lazarini, J. G., Nani, B. D., da Cunha, M. G., Colón, D. F., . . . Rosalen, P. L. (2018). The use of Brazilian propolis for discovery and development of novel anti-inflammatory drugs. *Eur J Med Chem, 153*, 49-55. doi:10.1016/j.ejmech.2017.06.050

Freires, I. A., Queiroz, V., Furletti, V. F., Ikegaki, M., de Alencar, S. M., Duarte, M. C. T., & Rosalen, P. L. (2016). Chemical composition and antifungal potential of Brazilian propolis against Candida spp. *J Mycol Med, 26*(2), 122-132. doi:10.1016/j.mycmed.2016.01.003

Goldman, R. (2004). Growth factors and chronic wound healing: past, present, and future. *Adv Skin Wound Care, 17*(1), 24-35. doi:10.1097/00129334-200401000-00012

Grange, J. M., & Davey, R. W. (1990). Antibacterial properties of propolis (bee glue). *J R Soc Med, 83*(3), 159-160.

Greenaway, W., Scaysbrook, T., & Whatley, F. R. (1990). The Composition and Plant Origins of Propolis: A Report of Work at Oxford. *Bee World, 71*(3), 107-118. doi:10.1080/0005772X.1990.11099047

Greenhalgh, D. G. (1998). The role of apoptosis in wound healing. *Int J Biochem Cell Biol, 30*(9), 1019-1030. doi:10.1016/s1357-2725(98)00058-2

Hämäläinen, M., Nieminen, R., Asmawi, M. Z., Vuorela, P., Vapaatalo, H., & Moilanen, E. (2011). Effects of flavonoids on prostaglandin E2 production and on COX-2 and mPGES-1 expressions in activated macrophages. *Planta Med, 77*(13), 1504-1511. doi:10.1055/s-0030-1270762

Hattori, H., Okuda, K., Murase, T., Shigetsura, Y., Narise, K., Semenza, G. L., & Nagasawa, H. (2011). Isolation, identification, and biological evaluation of HIF-

1-modulating compounds from Brazilian green propolis. *Bioorg Med Chem, 19*(18), 5392-5401. doi:10.1016/j.bmc.2011.07.060

Hennings, H., Kruszewski, F. H., Yuspa, S. H., & Tucker, R. W. (1989). Intracellular calcium alterations in response to increased external calcium in normal and neoplastic keratinocytes. *Carcinogenesis, 10*(4), 777-780. doi:10.1093/carcin/10.4.777

Hine, R. (2019). *A dictionary of biology*.

Hinz, B. (2006). Masters and servants of the force: the role of matrix adhesions in myofibroblast force perception and transmission. *Eur J Cell Biol, 85*(3-4), 175-181. doi:10.1016/j.ejcb.2005.09.004

Hirsilä, M., Koivunen, P., Günzler, V., Kivirikko, K. I., & Myllyharju, J. (2003). Characterization of the human prolyl 4-hydroxylases that modify the hypoxia-inducible factor. *J Biol Chem, 278*(33), 30772-30780. doi:10.1074/jbc.M304982200

Hon, W. C., Wilson, M. I., Harlos, K., Claridge, T. D., Schofield, C. J., Pugh, C. W., . . . Jones, E. Y. (2002). Structural basis for the recognition of hydroxyproline in HIF-1 alpha by pVHL. *Nature, 417*(6892), 975-978. doi:10.1038/nature00767

Hong, W. X., Hu, M. S., Esquivel, M., Liang, G. Y., Rennert, R. C., McArdle, A., . . . Longaker, M. T. (2014). The Role of Hypoxia-Inducible Factor in Wound Healing. *Adv Wound Care (New Rochelle), 3*(5), 390-399. doi:10.1089/wound.2013.0520

Hori, J. I., Zamboni, D. S., Carrão, D. B., Goldman, G. H., & Berretta, A. A. (2013). The Inhibition of Inflammasome by Brazilian Propolis (EPP-AF). *Evid Based Complement Alternat Med, 2013*, 418508. doi:10.1155/2013/418508

Hozzein, W. N., Badr, G., Al Ghamdi, A. A., Sayed, A., Al-Waili, N. S., & Garraud, O. (2015). Topical application of propolis enhances cutaneous wound healing by promoting TGF-beta/Smad-mediated collagen production in a streptozotocin-induced type I diabetic mouse model. *Cell Physiol Biochem, 37*(3), 940-954. doi:10.1159/000430221

Huang, S., Zhang, C. P., Wang, K., Li, G. Q., & Hu, F. L. (2014). Recent advances in the chemical composition of propolis. *Molecules, 19*(12), 19610-19632. doi:10.3390/molecules191219610

Huang, W. J., Huang, C. H., Wu, C. L., Lin, J. K., Chen, Y. W., Lin, C. L., . . . Chen, C. N. (2007). Propolin G, a prenylflavanone, isolated from Taiwanese propolis, induces caspase-dependent apoptosis in brain cancer cells. *J Agric Food Chem, 55*(18), 7366-7376. doi:10.1021/jf0710579

Iizuka, H. (1994). Epidermal turnover time. *J Dermatol Sci, 8*(3), 215-217. doi:10.1016/0923-1811(94)90057-4

Iocono, J. A., Colleran, K. R., Remick, D. G., Gillespie, B. W., Ehrlich, H. P., & Garner, W. L. (2000). Interleukin-8 levels and activity in delayed-healing human thermal wounds. *Wound Repair Regen, 8*(3), 216-225. doi:10.1046/j.1524-475x.2000.00216.x

Isidorov, V. A., Szczepaniak, L., & Bakier, S. (2014). Rapid GC/MS determination of botanical precursors of Eurasian propolis. *Food Chemistry, 142*, 101-106. doi:10.1016/j.foodchem.2013.07.032

Jacob, A., Parolia, A., Pau, A., & Davamani Amalraj, F. (2015). The effects of Malaysian propolis and Brazilian red propolis on connective tissue fibroblasts in the wound healing process. *BMC Complement Altern Med, 15*, 294. doi:10.1186/s12906-015-0814-1

Johnson, B. Z., Stevenson, A. W., Prêle, C. M., Fear, M. W., & Wood, F. M. (2020). The Role of IL-6 in Skin Fibrosis and Cutaneous Wound Healing. *Biomedicines, 8*(5). doi:10.3390/biomedicines8050101

Kalucka, J., Ettinger, A., Franke, K., Mamlouk, S., Singh, R. P., Farhat, K., . . . Wielockx, B. (2013). Loss of epithelial hypoxia-inducible factor prolyl hydroxylase 2

accelerates skin wound healing in mice. *Mol Cell Biol, 33*(17), 3426-3438. doi:10.1128/mcb.00609-13

Kimoto, T., Arai, S., Kohguchi, M., Aga, M., Nomura, Y., Micallef, M. J., . . . Mito, K. (1998). Apoptosis and suppression of tumor growth by artepillin C extracted from Brazilian propolis. *Cancer Detect Prev, 22*(6), 506-515. doi:10.1046/j.1525-1500.1998.00020.x

Klicks, J., Molitor, E., Ertongur-Fauth, T., Rudolf, R., & Hafner, M. (2017). In vitro skin three-dimensional models and their applications. *Journal of Computational Biology, 3*, 21-39.

Knodler, M., Conrad, J., Wenzig, E. M., Bauer, R., Lacorn, M., Beifuss, U., . . . Schieber, A. (2008). Anti-inflammatory 5-(11'Z-heptadecenyl)- and 5-(8'Z,11'Z-heptadecadienyl)-resorcinols from mango (Mangifera indica L.) peels. *Phytochemistry, 69*(4), 988-993. doi:10.1016/j.phytochem.2007.10.013

Koivunen, P., Hirsilä, M., Günzler, V., Kivirikko, K. I., & Myllyharju, J. (2004). Catalytic properties of the asparaginyl hydroxylase (FIH) in the oxygen sensing pathway are distinct from those of its prolyl 4-hydroxylases. *J Biol Chem, 279*(11), 9899-9904. doi:10.1074/jbc.M312254200

Koo, H., Hayacibara, M. F., Schobel, B. D., Cury, J. A., Rosalen, P. L., Park, Y. K., . . . Bowen, W. H. (2003). Inhibition of Streptococcus mutans biofilm accumulation and polysaccharide production by apigenin and tt-farnesol. *J Antimicrob Chemother, 52*(5), 782-789. doi:10.1093/jac/dkg449

Kujumgiev, A., Tsvetkova, I., Serkedjieva, Y., Bankova, V., Christov, R., & Popov, S. (1999). Antibacterial, antifungal and antiviral activity of propolis of different geographic origin. *J Ethnopharmacol, 64*(3), 235-240. doi:10.1016/s0378-8741(98)00131-7

Kumazawa, S., Nakamura, J., Murase, M., Miyagawa, M., Ahn, M. R., & Fukumoto, S. (2008). Plant origin of Okinawan propolis: honeybee behavior observation and phytochemical analysis. *Naturwissenschaften, 95*(8), 781-786. doi:10.1007/s00114-008-0383-y

Kumazawa, S., Yoneda, M., Shibata, I., Kanaeda, J., Hamasaka, T., & Nakayama, T. (2003). Direct evidence for the plant origin of Brazilian propolis by the observation of honeybee behavior and phytochemical analysis. *Chemical & pharmaceutical bulletin, 51*(6), 740-742. doi:10.1248/cpb.51.740

Kurek-Górecka, A., Walczyńska-Dragon, K., Felitti, R., Nitecka-Buchta, A., Baron, S., & Olczyk, P. (2021). The Influence of Propolis on Dental Plaque Reduction and the Correlation between Dental Plaque and Severity of COVID-19 Complications-A Literature Review. *Molecules, 26*(18). doi:10.3390/molecules26185516

Kuropatnicki, A. K., Szliszka, E., & Krol, W. (2013). Historical aspects of propolis research in modern times. *Evid Based Complement Alternat Med, 2013*, 964149. doi:10.1155/2013/964149

Lampe, M. A., Burlingame, A. L., Whitney, J., Williams, M. L., Brown, B. E., Roitman, E., & Elias, P. M. (1983). Human stratum corneum lipids: characterization and regional variations. *J Lipid Res, 24*(2), 120-130.

Lima, L. D., Andrade, S. P., Campos, P. P., Barcelos, L. S., Soriani, F. M., Moura, S. A., & Ferreira, M. A. (2014). Brazilian green propolis modulates inflammation, angiogenesis and fibrogenesis in intraperitoneal implant in mice. *BMC Complement Altern Med, 14*, 177. doi:10.1186/1472-6882-14-177

Lin, Z. Q., Kondo, T., Ishida, Y., Takayasu, T., & Mukaida, N. (2003). Essential involvement of IL-6 in the skin wound-healing process as evidenced by delayed wound healing in IL-6-deficient mice. *J Leukoc Biol, 73*(6), 713-721. doi:10.1189/jlb.0802397

Lisy, K., & Peet, D. J. (2008). Turn me on: regulating HIF transcriptional activity. *Cell Death Differ, 15*(4), 642-649. doi:10.1038/sj.cdd.4402315

Lopez, B. G., Schmidt, E. M., Eberlin, M. N., & Sawaya, A. C. (2014). Phytochemical markers of different types of red propolis. *Food Chem, 146*, 174-180. doi:10.1016/j.foodchem.2013.09.063

Lotti, C., Campo Fernandez, M., Piccinelli, A. L., Cuesta-Rubio, O., Márquez Hernández, I., & Rastrelli, L. (2010). Chemical Constituents of Red Mexican Propolis. *Journal of Agricultural and Food Chemistry, 58*(4), 2209-2213. doi:10.1021/jf100070w

Lourenço, A. P., Guidugli-Lazzarini, K. R., Freitas, F. C., Bitondi, M. M., & Simões, Z. L. (2013). Bacterial infection activates the immune system response and dysregulates microRNA expression in honey bees. *Insect Biochem Mol Biol, 43*(5), 474-482. doi:10.1016/j.ibmb.2013.03.001

Machado, B. A., Silva, R. P., Barreto Gde, A., Costa, S. S., Silva, D. F., Brandão, H. N., . . . Padilha, F. F. (2016). Chemical Composition and Biological Activity of Extracts Obtained by Supercritical Extraction and Ethanolic Extraction of Brown, Green and Red Propolis Derived from Different Geographic Regions in Brazil. *PLoS One, 11*(1), e0145954. doi:10.1371/journal.pone.0145954

Magnavacca, A., Sangiovanni, E., Racagni, G., & Dell'Agli, M. (2022). The antiviral and immunomodulatory activities of propolis: An update and future perspectives for respiratory diseases. *Med Res Rev, 42*(2), 897-945. doi:10.1002/med.21866

Marcucci, M. C. (1995). Propolis: chemical composition, biological properties and therapeutic activity. *Apidologie, 26*(2), 83-99.

Maróstica Junior, M. R., Daugsch, A., Moraes, C. S., Queiroga, C. L., Pastore, G. M., & Parki, Y. K. (2008). Comparison of volatile and polyphenolic compounds in Brazilian green propolis and its botanical origin Baccharis dracunculifolia. *Food Science and Technology, 28*(1), 178-181. doi:https://doi.org/10.1590/S0101-20612008000100026

Martin, P., & Leibovich, S. J. (2005). Inflammatory cells during wound repair: the good, the bad and the ugly. *Trends Cell Biol, 15*(11), 599-607. doi:10.1016/j.tcb.2005.09.002

Martinotti, S., & Ranzato, E. (2015). Propolis: a new frontier for wound healing? *Burns Trauma, 3*, 9. doi:10.1186/s41038-015-0010-z

Mast, B. A., & Schultz, G. S. (1996). Interactions of cytokines, growth factors, and proteases in acute and chronic wounds. *Wound Repair Regen, 4*(4), 411-420. doi:10.1046/j.1524-475X.1996.40404.x

Matsuda, A. H., & de Almeida-Muradian, L. B. (2008). Validated method for the quantification of artepillin-C in Brazilian propolis. *Phytochem Anal, 19*(2), 179-183. doi:10.1002/pca.1043

Mauro, T. M., Isseroff, R. R., Lasarow, R., & Pappone, P. A. (1993). Ion channels are linked to differentiation in keratinocytes. *J Membr Biol, 132*(3), 201-209. doi:10.1007/bf00235738

Mauro, T. M., Pappone, P. A., & Isseroff, R. R. (1990). Extracellular calcium affects the membrane currents of cultured human keratinocytes. *J Cell Physiol, 143*(1), 13-20. doi:10.1002/jcp.1041430103

Maxwell, P. H., Wiesener, M. S., Chang, G. W., Clifford, S. C., Vaux, E. C., Cockman, M. E., . . . Ratcliffe, P. J. (1999). The tumour suppressor protein VHL targets hypoxia-inducible factors for oxygen-dependent proteolysis. *Nature, 399*(6733), 271-275. doi:10.1038/20459

Midwood, K. S., Williams, L. V., & Schwarzbauer, J. E. (2004). Tissue repair and the dynamics of the extracellular matrix. *Int J Biochem Cell Biol, 36*(6), 1031-1037. doi:10.1016/j.biocel.2003.12.003

Militão, G. C., Dantas, I. N., Pessoa, C., Falcão, M. J., Silveira, E. R., Lima, M. A., . . . Costa-Lotufo, L. V. (2006). Induction of apoptosis by pterocarpans from Platymiscium floribundum in HL-60 human leukemia cells. *Life Sci, 78*(20), 2409-2417. doi:10.1016/j.lfs.2005.09.044

Mirastschijski, U., Haaksma, C. J., Tomasek, J. J., & Agren, M. S. (2004). Matrix metalloproteinase inhibitor GM 6001 attenuates keratinocyte migration, contraction and myofibroblast formation in skin wounds. *Exp Cell Res, 299*(2), 465-475. doi:10.1016/j.yexcr.2004.06.007

Mirzoeva, O. K., Grishanin, R. N., & Calder, P. C. (1997). Antimicrobial action of propolis and some of its components: the effects on growth, membrane potential and motility of bacteria. *Microbiol Res, 152*(3), 239-246. doi:10.1016/s0944-5013(97)80034-1

Moise, A. R., & Bobiş, O. (2020). Baccharis dracunculifolia and Dalbergia ecastophyllum, Main Plant Sources for Bioactive Properties in Green and Red Brazilian Propolis. *Plants (Basel), 9*(11). doi:10.3390/plants9111619

Moll, R., Divo, M., & Langbein, L. (2008). The human keratins: biology and pathology. *Histochem Cell Biol, 129*(6), 705-733. doi:10.1007/s00418-008-0435-6

Morton, L. M., & Phillips, T. J. (2016). Wound healing and treating wounds: Differential diagnosis and evaluation of chronic wounds. *J Am Acad Dermatol, 74*(4), 589-605; quiz 605-586. doi:10.1016/j.jaad.2015.08.068

Nagaraja, S., Wallqvist, A., Reifman, J., & Mitrophanov, A. Y. (2014). Computational approach to characterize causative factors and molecular indicators of chronic wound inflammation. *J Immunol, 192*(4), 1824-1834. doi:10.4049/jimmunol.1302481

Nani, B. D., Franchin, M., Lazarini, J. G., Freires, I. A., da Cunha, M. G., Bueno-Silva, B., . . . Rosalen, P. L. (2018). Isoflavonoids from Brazilian red propolis down-regulate the expression of cancer-related target proteins: A pharmacogenomic analysis. *Phytother Res, 32*(4), 750-754. doi:10.1002/ptr.6016

Newton, P. M., Watson, J. A., Wolowacz, R. G., & Wood, E. J. (2004). Macrophages restrain contraction of an in vitro wound healing model. *Inflammation, 28*(4), 207-214. doi:10.1023/b:ifla.0000049045.41784.59

Niehues, H., Bouwstra, J. A., El Ghalbzouri, A., Brandner, J. M., Zeeuwen, P., & van den Bogaard, E. H. (2018). 3D skin models for 3R research: The potential of 3D reconstructed skin models to study skin barrier function. *Exp Dermatol, 27*(5), 501-511. doi:10.1111/exd.13531

Nunan, R., Harding, K. G., & Martin, P. (2014). Clinical challenges of chronic wounds: searching for an optimal animal model to recapitulate their complexity. *Dis Model Mech, 7*(11), 1205-1213. doi:10.1242/dmm.016782

Nunes, C. A., & Guerreiro, M. C. (2012). Characterization of Brazilian green propolis throughout the seasons by headspace GC/MS and ESI-MS. *J Sci Food Agric,* 92(2), 433-438. doi:10.1002/jsfa.4596

O'Leary, R., Wood, E. J., & Guillou, P. J. (2002). Pathological scarring: strategic interventions. *Eur J Surg, 168*(10), 523-534.

Oldoni, T. L. C., Cabral, I. S. R., d'Arce, M. A. B. R., Rosalen, P. L., Ikegaki, M., Nascimento, A. M., & Alencar, S. M. (2011). Isolation and analysis of bioactive isoflavonoids and chalcone from a new type of Brazilian propolis. *Separation and Purification Technology, 77*(2), 208-213. doi:https://doi.org/10.1016/j.seppur.2010.12.007

Oryan, A., Alemzadeh, E., & Moshiri, A. (2018). Potential role of propolis in wound healing: Biological properties and therapeutic activities. *Biomed Pharmacother, 98*, 469-483. doi:10.1016/j.biopha.2017.12.069

Ovaere, P., Lippens, S., Vandenabeele, P., & Declercq, W. (2009). The emerging roles of serine protease cascades in the epidermis. *Trends Biochem Sci, 34*(9), 453-463. doi:10.1016/j.tibs.2009.08.001

Pahlavani, N., Malekahmadi, M., Firouzi, S., Rostami, D., Sedaghat, A., Moghaddam, A. B., . . . Ghayour-Mobarhan, M. (2020). Molecular and cellular mechanisms of the effects of Propolis in inflammation, oxidative stress and glycemic control in chronic diseases. *Nutr Metab (Lond), 17*, 65. doi:10.1186/s12986-020-00485-5

Papandreou, I., Cairns, R. A., Fontana, L., Lim, A. L., & Denko, N. C. (2006). HIF-1 mediates adaptation to hypoxia by actively downregulating mitochondrial oxygen consumption. *Cell Metab, 3*(3), 187-197. doi:10.1016/j.cmet.2006.01.012

Papp, Z., Bouchelaghem, S., Szekeres, A., Meszéna, R., Gyöngyi, Z., & Papp, G. (2021). The Scent of Antifungal Propolis. *Sensors (Basel), 21*(7). doi:10.3390/s21072334

Park, Y., Ikegaki, M., & Alencar, S. (2000). Classification of Brazilian propolis by physicochemical method and biological activity. *Mensagem Doce, 58*, 2-7.

Park, Y. K., Alencar Sm Fau - Aguiar, C. L., & Aguiar, C. L. (2002). Botanical origin and chemical composition of Brazilian propolis. (0021-8561 (Print)).

Pastar, I., Stojadinovic, O., Yin, N. C., Ramirez, H., Nusbaum, A. G., Sawaya, A., . . . Tomic-Canic, M. (2014). Epithelialization in Wound Healing: A Comprehensive Review. *Adv Wound Care (New Rochelle), 3*(7), 445-464. doi:10.1089/wound.2013.0473

Paulino, N., Abreu, S. R., Uto, Y., Koyama, D., Nagasawa, H., Hori, H., . . . Bretz, W. A. (2008). Anti-inflammatory effects of a bioavailable compound, Artepillin C, in Brazilian propolis. *Eur J Pharmacol, 587*(1-3), 296-301. doi:10.1016/j.ejphar.2008.02.067

Pellati, F., Orlandini, G., Pinetti, D., & Benvenuti, S. (2011). HPLC-DAD and HPLC-ESI-MS/MS methods for metabolite profiling of propolis extracts. *J Pharm Biomed Anal, 55*(5), 934-948. doi:10.1016/j.jpba.2011.03.024

Peng, L., Yang, S., Cheng, Y. J., Chen, F., Pan, S., & Fan, G. (2012). Antifungal activity and action mode of pinocembrin from propolis against Penicillium italicum. *Food Science and Biotechnology, 21*(6), 1533-1539. doi:10.1007/s10068-012-0204-0

Piccinelli, A. L., Lotti, C., Campone, L., Cuesta-Rubio, O., Campo Fernandez, M., & Rastrelli, L. (2011). Cuban and Brazilian red propolis: botanical origin and comparative analysis by high-performance liquid chromatography-photodiode array detection/electrospray ionization tandem mass spectrometry. *J Agric Food Chem, 59*(12), 6484-6491. doi:10.1021/jf201280z

Pillai, S., & Bikle, D. D. (1991). Role of intracellular-free calcium in the cornified envelope formation of keratinocytes: differences in the mode of action of extracellular calcium and 1,25 dihydroxyvitamin D3. *J Cell Physiol, 146*(1), 94-100. doi:10.1002/jcp.1041460113

Pobiega, K., Gniewosz, M., & Kraśniewska, K. (2017). Antimicrobial and antiviral properties of different types of propolis. *Zeszyty Problemowe Postępów Nauk Rolniczych, 2017*, 69-79. doi:10.22630/ZPPNR.2017.589.22

Popova, M., Trusheva, B., Cutajar, S., Antonova, D., Mifsud, D., Farrugia, C., & Bankova, V. (2012). Identification of the plant origin of the botanical biomarkers of Mediterranean type propolis. *Nat Prod Commun, 7*(5), 569-570.

Popova, M., Trusheva, B., Khismatullin, R., Gavrilova, N., Legotkina, G., Lyapunov, J., & Bankova, V. (2013). The Triple Botanical Origin of Russian Propolis from the Perm Region, Its Phenolic Content and Antimicrobial Activity. *Natural Product Communications, 8*, 617-620.

Popova, M. P., Graikou, K., Chinou, I., & Bankova, V. S. (2010). GC-MS profiling of diterpene compounds in Mediterranean propolis from Greece. *J Agric Food Chem, 58*(5), 3167-3176. doi:10.1021/jf903841k

Popravko, S. A., Sokolov, I. V., & Torgov, I. V. (1982). New natural phenolic triglycerides. *Chemistry of Natural Compounds, 18*(2), 153-157. doi:10.1007/BF00577181

Proksch, E., Brandner, J. M., & Jensen, J. M. (2008). The skin: an indispensable barrier. *Exp Dermatol, 17*(12), 1063-1072. doi:10.1111/j.1600-0625.2008.00786.x

Przybyłek, I., & Karpiński, T. M. (2019). Antibacterial Properties of Propolis. *Molecules, 24*(11). doi:10.3390/molecules24112047

Regueira, M. S. N., Tintino, S. R., da Silva, A. R. P., Costa, M. D. S., Boligon, A. A., Matias, E. F. F., . . . Melo Coutinho, H. D. (2017). Seasonal variation of Brazilian red propolis: Antibacterial activity, synergistic effect and phytochemical screening. *Food Chem Toxicol, 107*(Pt B), 572-580. doi:10.1016/j.fct.2017.03.052

Reijnders, C. M., van Lier, A., Roffel, S., Kramer, D., Scheper, R. J., & Gibbs, S. (2015). Development of a Full-Thickness Human Skin Equivalent In Vitro Model Derived from TERT-Immortalized Keratinocytes and Fibroblasts. *Tissue Eng Part A, 21*(17-18), 2448-2459. doi:10.1089/ten.TEA.2015.0139

Reinke, J. M., & Sorg, H. (2012). Wound repair and regeneration. *Eur Surg Res, 49*(1), 35-43. doi:10.1159/000339613

Reiss, M., Lipsey, L. R., & Zhou, Z. L. (1991). Extracellular calcium-dependent regulation of transmembrane calcium fluxes in murine keratinocytes. *J Cell Physiol, 147*(2), 281-291. doi:10.1002/jcp.1041470213

Repetto, G., del Peso, A., & Zurita, J. L. (2008). Neutral red uptake assay for the estimation of cell viability/cytotoxicity. *Nat Protoc, 3*(7), 1125-1131. doi:10.1038/nprot.2008.75

Rieger, S., Zhao, H., Martin, P., Abe, K., & Lisse, T. S. (2015). The role of nuclear hormone receptors in cutaneous wound repair. *Cell Biochem Funct, 33*(1), 1-13. doi:10.1002/cbf.3086

Rikken, G., Niehues, H., & van den Bogaard, E. H. (2020). Organotypic 3D Skin Models: Human Epidermal Equivalent Cultures from Primary Keratinocytes and Immortalized Keratinocyte Cell Lines. *Methods Mol Biol, 2154*, 45-61. doi:10.1007/978-1-0716-0648-3_5

Rodrigues, D. M., De Souza, M. C., Arruda, C., Pereira, R. A. S., & Bastos, J. K. (2020). The Role of Baccharis dracunculifolia and its Chemical Profile on Green Propolis Production by Apis mellifera. *J Chem Ecol, 46*(2), 150-162. doi:10.1007/s10886-019-01141-w

Rohloff, J. (2015). Analysis of phenolic and cyclic compounds in plants using derivatization techniques in combination with GC-MS-based metabolite profiling. *Molecules, 20*(2), 3431-3462. doi:10.3390/molecules20023431

Rook, A. B. T. (2010). Rook's textbook of dermatology.

Rosenberger, P., Schwab, J. M., Mirakaj, V., Masekowsky, E., Mager, A., Morote-Garcia, J. C., . . . Eltzschig, H. K. (2009). Hypoxia-inducible factor-dependent induction of netrin-1 dampens inflammation caused by hypoxia. *Nat Immunol, 10*(2), 195-202. doi:10.1038/ni.1683

Rufatto, L. C., Luchtenberg, P., Garcia, C., Thomassigny, C., Bouttier, S., Henriques, J. A. P., . . . Moura, S. (2018). Brazilian red propolis: Chemical composition and antibacterial activity determined using bioguided fractionation. *Microbiol Res, 214*, 74-82. doi:10.1016/j.micres.2018.05.003

Ruszczak, Z. (2003). Effect of collagen matrices on dermal wound healing. *Adv Drug Deliv Rev, 55*(12), 1595-1611. doi:10.1016/j.addr.2003.08.003

Saelao, P., Borba, R. S., Ricigliano, V., Spivak, M., & Simone-Finstrom, M. (2020). Honeybee microbiome is stabilized in the presence of propolis. *Biol Lett, 16*(5), 20200003. doi:10.1098/rsbl.2020.0003

Saito, Y., Tsuruma, K., Ichihara, K., Shimazawa, M., & Hara, H. (2015). Brazilian green propolis water extract up-regulates the early expression level of HO-1 and accelerates Nrf2 after UVA irradiation. *BMC Complement Altern Med, 15*(1), 421. doi:10.1186/s12906-015-0945-4

Salatino, A., Teixeira, E. W., Negri, G., & Message, D. (2005). Origin and Chemical Variation of Brazilian Propolis. *Evid Based Complement Alternat Med, 2*(1), 33-38. doi:10.1093/ecam/neh060

Sandilands, A., Sutherland, C., Irvine, A. D., & McLean, W. H. (2009). Filaggrin in the frontline: role in skin barrier function and disease. *J Cell Sci, 122*(Pt 9), 1285-1294. doi:10.1242/jcs.033969

Sang, N., Fang, J., Srinivas, V., Leshchinsky, I., & Caro, J. (2002). Carboxyl-terminal transactivation activity of hypoxia-inducible factor 1 alpha is governed by a von Hippel-Lindau protein-independent, hydroxylation-regulated association with p300/CBP. *Mol Cell Biol, 22*(9), 2984-2992. doi:10.1128/mcb.22.9.2984-2992.2002

Santoro, M. M., & Gaudino, G. (2005). Cellular and molecular facets of keratinocyte reepithelization during wound healing. *Exp Cell Res, 304*(1), 274-286. doi:10.1016/j.yexcr.2004.10.033

Santos, F. A., Bastos, E. M., Uzeda, M., Carvalho, M. A., Farias, L. M., Moreira, E. S., & Braga, F. C. (2002). Antibacterial activity of Brazilian propolis and fractions against oral anaerobic bacteria. *J Ethnopharmacol, 80*(1), 1-7. doi:10.1016/s0378-8741(02)00003-x

Scholz, C. C., Cavadas, M. A., Tambuwala, M. M., Hams, E., Rodríguez, J., von Kriegsheim, A., . . . Taylor, C. T. (2013). Regulation of IL-1β-induced NF-κB by hydroxylases links key hypoxic and inflammatory signaling pathways. *Proc Natl Acad Sci U S A, 110*(46), 18490-18495. doi:10.1073/pnas.1309718110

Schoop, V. M., Mirancea, N., & Fusenig, N. E. (1999). Epidermal organization and differentiation of HaCaT keratinocytes in organotypic coculture with human dermal fibroblasts. *J Invest Dermatol, 112*(3), 343-353. doi:10.1046/j.1523-1747.1999.00524.x

Semenza, G. L. (2007). Hypoxia-inducible factor 1 (HIF-1) pathway. *Sci STKE, 2007*(407), cm8. doi:10.1126/stke.4072007cm8

Semenza, G. L. (2010). HIF-1: upstream and downstream of cancer metabolism. *Curr Opin Genet Dev, 20*(1), 51-56. doi:10.1016/j.gde.2009.10.009

Semenza, G. L. (2014). Oxygen sensing, hypoxia-inducible factors, and disease pathophysiology. *Annu Rev Pathol, 9*, 47-71. doi:10.1146/annurev-pathol-012513-104720

Sen, C. K. (2009). Wound healing essentials: let there be oxygen. *Wound Repair Regen, 17*(1), 1-18. doi:10.1111/j.1524-475X.2008.00436.x

Sforcin, J. M. (2007). Propolis and the immune system: a review. *J Ethnopharmacol, 113*(1), 1-14. doi:10.1016/j.jep.2007.05.012

Sforcin, J. M., & Bankova, V. (2011). Propolis: is there a potential for the development of new drugs? *J Ethnopharmacol, 133*(2), 253-260. doi:10.1016/j.jep.2010.10.032

Shahinozzaman, M., Basak, B., Emran, R., Rozario, P., & Obanda, D. N. (2020). Artepillin C: A comprehensive review of its chemistry, bioavailability, and pharmacological properties. *Fitoterapia, 147*, 104775. doi:10.1016/j.fitote.2020.104775

Siheri, W., Alenezi, S., Tusiimire, J., & Watson, D. G. (2017). The Chemical and Biological Properties of Propolis. In J. M. Alvarez-Suarez (Ed.), *Bee Products - Chemical and Biological Properties* (pp. 137-178). Cham: Springer International Publishing.

Silva-Carvalho, R., Baltazar, F., & Almeida-Aguiar, C. (2015). Propolis: A Complex Natural Product with a Plethora of Biological Activities That Can Be Explored for Drug Development. *Evid Based Complement Alternat Med, 2015*, 206439. doi:10.1155/2015/206439

Silva, B. B., Rosalen, P. L., Cury, J. A., Ikegaki, M., Souza, V. C., Esteves, A., & Alencar, S. M. (2008). Chemical composition and botanical origin of red propolis, a new type of brazilian propolis. *Evid Based Complement Alternat Med, 5*(3), 313-316. doi:10.1093/ecam/nem059

Simões, L. M., Gregório, L. E., Da Silva Filho, A. A., de Souza, M. L., Azzolini, A. E., Bastos, J. K., & Lucisano-Valim, Y. M. (2004). Effect of Brazilian green propolis on the production of reactive oxygen species by stimulated neutrophils. *J Ethnopharmacol, 94*(1), 59-65. doi:10.1016/j.jep.2004.04.026

Simone, M., Evans, J. D., & Spivak, M. (2009). Resin collection and social immunity in honey bees. *Evolution, 63*(11), 3016-3022. doi:10.1111/j.1558-5646.2009.00772.x

Smith, S. M., Wunder, M. B., Norris, D. A., & Shellman, Y. G. (2011). A simple protocol for using a LDH-based cytotoxicity assay to assess the effects of death and growth inhibition at the same time. *PLoS One,* 6(11), e26908. doi:10.1371/journal.pone.0026908

Song, G., Nguyen, D. T., Pietramaggiori, G., Scherer, S., Chen, B., Zhan, Q., . . . Murphy, G. F. (2010). Use of the parabiotic model in studies of cutaneous wound healing to define the participation of circulating cells. *Wound Repair Regen, 18*(4), 426-432. doi:10.1111/j.1524-475X.2010.00595.x

Souto, E. B., Fangueiro, J., Rita Fernandes, A., Cano, A., Sánchez-López, E., García, M., . . . Silva, A. (2022). Physicochemical and biopharmaceutical aspects influencing skin permeation and role of SLN and NLC for skin drug delivery. *Heliyon, 8*, e08938. doi:10.1016/j.heliyon.2022.e08938

Stadelmann, W. K., Digenis, A. G., & Tobin, G. R. (1998). Physiology and healing dynamics of chronic cutaneous wounds. *Am J Surg, 176*(2A Suppl), 26s-38s. doi:10.1016/s0002-9610(98)00183-4

Stark, H. J., Szabowski, A., Fusenig, N. E., & Maas-Szabowski, N. (2004). Organotypic cocultures as skin equivalents: A complex and sophisticated in vitro system. *Biol Proced Online, 6*, 55-60. doi:10.1251/bpo72

Stojadinovic, A., Carlson, J. W., Schultz, G. S., Davis, T. A., & Elster, E. A. (2008). Topical advances in wound care. *Gynecol Oncol, 111*(2 Suppl), S70-80. doi:10.1016/j.ygyno.2008.07.042

Stojko, M., Wolny, D., & Włodarczyk, J. (2021). Nonwoven Releasing Propolis as a Potential New Wound Healing Method-A Review. *Molecules, 26*(18). doi:10.3390/molecules26185701

Strudwick, X., Lang, D., Smith, L., & Cowin, A. (2015). Combination of Low Calcium with Y-27632 Rock Inhibitor Increases the Proliferative Capacity, Expansion Potential and Lifespan of Primary Human Keratinocytes while Retaining Their Capacity to Differentiate into Stratified Epidermis in a 3D Skin Model. *PLoS One, 10*, e0123651. doi:10.1371/journal.pone.0123651

Stücker, M., Struk, A., Altmeyer, P., Herde, M., Baumgärtl, H., & Lübbers, D. W. (2002). The cutaneous uptake of atmospheric oxygen contributes significantly to the oxygen supply of human dermis and epidermis. *J Physiol, 538*(Pt 3), 985-994. doi:10.1113/jphysiol.2001.013067

Szliszka, E., Kucharska, A. Z., Sokół-Łętowska, A., Mertas, A., Czuba, Z. P., & Król, W. (2013). Chemical Composition and Anti-Inflammatory Effect of Ethanolic

Extract of Brazilian Green Propolis on Activated J774A.1 Macrophages. *Evid Based Complement Alternat Med, 2013*, 976415. doi:10.1155/2013/976415

Toledo-Pereyra, L. H., Lopez-Neblina, F., & Toledo, A. H. (2004). Reactive oxygen species and molecular biology of ischemia/reperfusion. *Ann Transplant, 9*(1), 81-83.

Toreti, V. C., Sato, H. H., Pastore, G. M., & Park, Y. K. (2013). Recent progress of propolis for its biological and chemical compositions and its botanical origin. *Evid Based Complement Alternat Med, 2013*, 697390. doi:10.1155/2013/697390

Trusheva, B., Popova, M., Bankova, V., Simova, S., Marcucci, M. C., Miorin, P. L., . . . Tsvetkova, I. (2006). Bioactive constituents of brazilian red propolis. *Evidence-based complementary and alternative medicine : eCAM, 3*(2), 249-254. doi:10.1093/ecam/nel006

Trusheva, B., Popova, M., Koendhori, E. B., Tsvetkova, I., Naydenski, C., & Bankova, V. (2011). Indonesian propolis: chemical composition, biological activity and botanical origin. *Nat Prod Res, 25*(6), 606-613. doi:10.1080/14786419.2010.488235

Tu, C. L., Oda, Y., & Bikle, D. D. (1999). Effects of a calcium receptor activator on the cellular response to calcium in human keratinocytes. *J Invest Dermatol, 113*(3), 340-345. doi:10.1046/j.1523-1747.1999.00698.x

Turcatto, A. P., Lourenço, A. P., & De Jong, D. (2018). Propolis consumption ramps up the immune response in honey bees infected with bacteria. *Apidologie, 49*(3), 287-296. doi:10.1007/s13592-017-0553-z

Versteeg, H. H., Heemskerk, J. W., Levi, M., & Reitsma, P. H. (2013). New fundamentals in hemostasis. *Physiol Rev, 93*(1), 327-358. doi:10.1152/physrev.00016.2011

Wagh, V. D. (2013). Propolis: a wonder bees product and its pharmacological potentials. *Adv Pharmacol Sci, 2013*, 308249. doi:10.1155/2013/308249

Walko, G., Castañón, M. J., & Wiche, G. (2015). Molecular architecture and function of the hemidesmosome. *Cell Tissue Res, 360*(3), 529-544. doi:10.1007/s00441-015-2216-6

Wang, G. L., Jiang, B. H., Rue, E. A., & Semenza, G. L. (1995). Hypoxia-inducible factor 1 is a basic-helix-loop-helix-PAS heterodimer regulated by cellular O2 tension. *Proc Natl Acad Sci U S A, 92*(12), 5510-5514. doi:10.1073/pnas.92.12.5510

Washio, K., Kobayashi, M., Saito, N., Amagasa, M., & Kitamura, H. (2015). Propolis Ethanol Extract Stimulates Cytokine and Chemokine Production through NF-κB Activation in C2C12 Myoblasts. *Evid Based Complement Alternat Med, 2015*, 349751. doi:10.1155/2015/349751

Weber, T. J., Smallwood, H. S., Kathmann, L. E., Markillie, L. M., Squier, T. C., & Thrall, B. D. (2006). Functional link between TNF biosynthesis and CaM-dependent activation of inducible nitric oxide synthase in RAW 264.7 macrophages. *Am J Physiol Cell Physiol, 290*(6), C1512-1520. doi:10.1152/ajpcell.00527.2005

Werner, S., & Grose, R. (2003). Regulation of wound healing by growth factors and cytokines. *Physiol Rev, 83*(3), 835-870. doi:10.1152/physrev.2003.83.3.835

Wilkins, S. E., Abboud, M. I., Hancock, R. L., & Schofield, C. J. (2016). Targeting Protein-Protein Interactions in the HIF System. *ChemMedChem, 11*(8), 773-786. doi:10.1002/cmdc.201600012

Wilson, M. B., Brinkman, D., Spivak, M., Gardner, G., & Cohen, J. D. (2015). Regional variation in composition and antimicrobial activity of US propolis against Paenibacillus larvae and Ascosphaera apis. *J Invertebr Pathol, 124*, 44-50. doi:10.1016/j.jip.2014.10.005

Witte, M. B., & Barbul, A. (2002). Role of nitric oxide in wound repair. *Am J Surg, 183*(4), 406-412. doi:10.1016/s0002-9610(02)00815-2

Xue, M., & Jackson, C. J. (2015). Extracellular Matrix Reorganization During Wound Healing and Its Impact on Abnormal Scarring. *Adv Wound Care (New Rochelle), 4*(3), 119-136. doi:10.1089/wound.2013.0485

Yang, J., Zhang, L., Erbel, P. J., Gardner, K. H., Ding, K., Garcia, J. A., & Bruick, R. K. (2005). Functions of the Per/ARNT/Sim domains of the hypoxia-inducible factor. *J Biol Chem, 280*(43), 36047-36054. doi:10.1074/jbc.M501755200

Yuan, Q., Bleiziffer, O., Boos, A. M., Sun, J., Brandl, A., Beier, J. P., . . . Horch, R. E. (2014). PHDs inhibitor DMOG promotes the vascularization process in the AV loop by HIF-1a up-regulation and the preliminary discussion on its kinetics in rat. *BMC Biotechnol, 14*, 112. doi:10.1186/s12896-014-0112-x

Zaccaria, V., Curti, V., Di Lorenzo, A., Baldi, A., Maccario, C., Sommatis, S., . . . Daglia, M. (2017). Effect of Green and Brown Propolis Extracts on the Expression Levels of microRNAs, mRNAs and Proteins, Related to Oxidative Stress and Inflammation. *Nutrients, 9*(10). doi:10.3390/nu9101090

Zhang, X., Yan, X., Cheng, L., Dai, J., Wang, C., Han, P., & Chai, Y. (2013). Wound healing improvement with PHD-2 silenced fibroblasts in diabetic mice. *PLoS One, 8*(12), e84548. doi:10.1371/journal.pone.0084548

Zhang, Y., Strehin, I., Bedelbaeva, K., Gourevitch, D., Clark, L., Leferovich, J., . . . Heber-Katz, E. (2015). Drug-induced regeneration in adult mice. *Sci Transl Med, 7*(290), 290ra292. doi:10.1126/scitranslmed.3010228

Zhang, Z., & Michniak-Kohn, B. B. (2012). Tissue engineered human skin equivalents. *Pharmaceutics, 4*(1), 26-41. doi:10.3390/pharmaceutics4010026

Zhang, Z., Yao, L., Yang, J., Wang, Z., & Du, G. (2018). PI3K/Akt and HIF-1 signaling pathway in hypoxia-ischemia (Review). *Mol Med Rep, 18*(4), 3547-3554. doi:10.3892/mmr.2018.9375

Zhao, R., Liang, H., Clarke, E., Jackson, C., & Xue, M. (2016). Inflammation in Chronic Wounds. *Int J Mol Sci, 17*(12). doi:10.3390/ijms17122085

Zulhendri, F., Chandrasekaran, K., Kowacz, M., Ravalia, M., Kripal, K., Fearnley, J., & Perera, C. O. (2021). Antiviral, Antibacterial, Antifungal, and Antiparasitic Properties of Propolis: A Review. *Foods, 10*(6). doi:10.3390/foods10061360